DEPARTAMENTO DE BIOQUÍMICA Y BIOLOGÍA MOLECULAR
FACULTAD DE FARMACIA
UNIVERSIDAD DE SEVILLA

EFECTOS DE LA ACUMULACIÓN DEL PÉPTIDO BETA AMILOIDE EN TEJIDO CEREBRAL DE RATONES PS1xAPP MODELOS DE LA ENFERMEDAD DE ALZHEIMER.

Memoria presentada por el Ldo. Sebastián Jiménez Muñoz, para optar al grado de Doctor por la Universidad de Sevilla.

Sevilla, 29 de Septiembre de 2015

UNIVERSIDAD DE SEVILLA

Departamento de Bioquímica y Biología Molecular
Facultad de Farmacia

C / Profesor García González, 2.
41012 Sevilla (España)
Teléfono: 954 55 67 55
Fax: 954 55 68 54

Dr. Javier Vitorica Ferrández, Catedrático de Universidad y **Dra. Mª Luisa Vizuete Chacón**, Profesora Titular de Universidad. Ambos asociados al Departamento de Bioquímica y Biología Molecular de la Universidad de Sevilla,

INFORMAN:

Que D. Sebastián Jiménez Muñoz, ha realizado bajo nuestra dirección el trabajo experimental que ha llevado a la redacción de la presente memoria de Tesis Doctoral, titulada **Efectos de la acumulación del péptido Beta amiloide en tejido cerebral de ratones PS1xAPP modelos de la Enfermedad de Alzheimer.** Considerando que constituye trabajo de tesis doctoral, autorizamos su presentación para optar al grado de Doctor.

Para que así conste y surta los efectos oportunos, firmamos el presente informe en Sevilla, a 28 de Septiembre de 2015.

Fdo. Javier Vitorica Ferrández

Fdo. María Luisa Vizuete Chacón

UNIVERSIDAD DE SEVILLA

Departamento de Bioquímica y Biología Molecular
Facultad de Farmacia

C / Profesor García González, 2.
41012 Sevilla (España)
Teléfono: 954 55 67 55
Fax: 954 55 68 54

Dr. Juan D. Bautista Palomas, Catedrático de Universidad y Director del Departamento de Bioquímica y Biología Molecular de la Universidad de Sevilla,

INFORMA:

Que D. Sebastián Jiménez Muñoz ha realizado el trabajo experimental que ha llevado a la redacción de la presente memoria de Tesis Doctoral bajo la dirección del Dr. Javier Vitorica Ferrández y la Dra. María Luisa Vizuete Chacón.

Para que así conste y surta los efectos oportunos, firmo el presente informe en Sevilla, a 28 de Septiembre de 2015.

FACULTAD DE FARMACIA
Departamento de Bioquímica
y Biología Molecular

Fdo. Dr. Juan D. Bautista Palomas

Servicio de Doctorado
DIRECCIÓN DEL SECRETARIADO DE DOCTORADO
VICERRECTORADO DE INVESTIGACIÓN

Sevilla, 23 de septiembre de 2015
Su referencia:
NUESTRA REFERENCIA: AMB/YD
ASUNTO:
AUTORIZACION TESIS POR COMPENDIO

DESTINATARIO:

Sebastián Jiménez Muñoz
Dpto. Bioquímica y Biología Molecular
Facultad de Farmacia
Universidad de Sevilla

Le comunico que el Director del Secretariado, actuando por delegación de la Comisión de Doctorado, por razones de urgencia, ha acordado el día 23 de septiembre de 2015, INFORMAR FAVORABLEMENTE su solicitud de presentación de tesis por compendio a la vista de la documentación presentada por Registro el 21/09/2015, ya que cumple con los requisitos exigidos en la Normativa Reguladora del Régimen de tesis doctoral (Acuerdo 9.1/ CG 19-04-2012).

EL DIRECTOR DEL SECRETARIADO

Fdo. : Antonio Delgado García

UNIVERSIDAD DE SEVILLA
REGISTRO GENERAL AUXILIAR
PABELLON DE BRASIL
SALIDA
Nº. 201500400016859
28/09/2015 08:32:58

α7nAChR: subunidad α7 del receptor nicotínico de acetilcolina
Aβ, Abeta: péptido β-amiloide
Aβi: péptido β-amiloide intracelular
AAC: Angiopatía amiloide cerebral.
ACE: Enzima convertidora de angiotensina.
Alzheimer's Disease
ADAM: del inglés A desintegrin and metalloprotease
ADDL: del inglés Amiloide-β Derived Diffusible Ligands).
DNA: Ácido desoxirribonucleico.
AICD: dominio intracelular del APP
ANOVA: análisis de la varianza (del inglés ANalysis Of VAriance)
AMPA: receptor del ácido α-amino-3-hidroxi-5-metilo-4-isoxazolpropiónico.
APOE: Apolipoproteína E
APH-1: del inglés pharynx-defective -1. Subunidad del complejo gamma secretasa.
APP: Proteína precursora del péptido β-amiloide.
Arg-1: Arginasa 1.
ARN: Ácido ribonucleico.
BACE: enzima de corte del APP en el sitio beta
BDNF: factor neurotrófico derivado del cerebro.
bFGF: Factor de crecimiento de fibroblastos básico.
BHE: Barrera hemato encefálica.
CA: Cuerno de Ammon
CD: del inglés cluster of differentiation
CDK5: Quinasa dependiente de ciclina 5.
cDNA: DNA complementario.
CE: Corteza entorrinal
CH3LI: del inglés Chitinase-3-like protein 1.
ChAT: colinacetiltransferasa.
CLU: Clusterina.
CTF: fragmento C-terminal
CX3CR1: del inglés CX3C chemokine receptor 1.
DAB: 3-3'-diaminobencidina tetrahidrochlorhídrico
DEPC: Dietilpirocarbonato
DN: densidad numérica
EA: dnfermedad de Alzheimer
ECE: Enzima convertidora de endotelina.
ELISA: del inglés Enzyme-Linked ImmunoSorbent Assay
ERK: del inglés extracellular-signal-regulated kinases
FAD: Alzheimer familiar (del inglés, Familial Alzheimer's Disease)
FAS-L: Ligando de FAS.
GABA: Ácido gamma amino butírico
GAPDH: del inglés glyceraldehyde-3-phosphate dehydrogenase
GD: giro dentado
GDNF: del inglés glial cell line-derived neurotrophic factor
GFAP: Proteína glial fibrilar ácida (del inglés glial
GSK-3: Quinasa glucógeno sintasa 3
h: hilio del giro dentado
HIPP: interneuronas del hilo asociadas a la vía perforante (del inglés hilar interneurons of performant pathway)
HMG-CoA: 3-hidroxi-3-metilglutaril-coenzima A
HSP: Proteína del choque térmico (del inglés Heat schok protein)
Iba1: del inglés ionized calcium binding adapter molecule 1
IDE: Enzima degradadora de insulina
IFN-γ: Interferón gamma Ig: Inmunoglobulina
IGF-1: Factor de crecimiento insulínico de tipo 1 (del inglés insulin-like growth factor-1)
IL: Interleuquina
iNOS: Sintasa del óxido nítrico inducible
KI: knock-in
KO: knockout
LAMP2: del inglés Lysosome-associated membrane protein 2
LC3: del inglés Light chain 3
LCR: Líquido cefaloraquídeo.
LDL: Lipoproteína de baja densidad. Del inglés Low density lipoprotein.
LDLR: Receptor de lipoproteína de baja densidad.
Li: Litio.
LMW-Aβ: del inglés low molecular weight Aβ
LPS: .Lipopolisacárido.
Lond; L: Mutación London de APP
LTD: depresión a largo plazo
LTP: potenciación a largo plazo
m: capa molecular del giro dentado
M1: estadio clásico de activación de los macrófagos
M2: estadio alternativo de activación de los macrófagos
MAP: Proteína de union a microtúbulos
MCI: del inglés Mild cognitive impairment
MHC: Complejo mayor de histocompatibilidad
MMP: Metaloproteasas de matriz
MRC: del inglés mannose receptor 1.
MSR-1: del inglés macrophage scavenger receptor 1.
MT: Microtúbulos
NADPH: Nicotinamida adenina dinucleótido fosfato.
ND: nummerical density
NEP: Neprelisina.
NF: Neurofilamento
NFs: Factores neurotróficos
NFTs: Ovillos neurofibrilares (del inglés neurofibrillary tangles)
NGF: Factor de crecimiento nervioso
NMDA: Ácido N-metil-D-aspártico
NO: óxido nítrico
NPY: Neuropéptido Y

NT: Neurotrofinas
oAbeta: péptido Aβ oligomérico.
O-LM: interneuronas del stratum oriens-lacunosomoleculare
OMS: Organización mundial de la salud.
p75NTR: Receptor de neurotrofinas p75
PAGE: Electroforesis en gel de poliacrilamida.
PB: Tampón fosfato
PBS: Tampón fosfato salino
PCR: Reacción en cadena de la polimerasa
PDPK: Quinasa dependiente de prolina.
PEN2: del inglés presenilin enhancer 2. Subunidad del complejo gamma secretasa.
PF: Protofibrillas.
PHF: filamentos apareados helicoidales
PI3K: Fosfoinositol 3 quinasa.
PICALM: del inglés phosphatidylinositol binding clathrin assembly protein
PKA: Proteína quinasa A.
PP: Proteínas fosfatasas
PPAR-γ: Del inglés peroxisome proliferatoractivated receptor-gamma
PrP: proteína priónica
PS: Presenilina
RE: retículo endoplasmático
RNA: Ácido ribonucleico.
ROS: especies reactivas de oxígeno
RT-PCR: Reacción en cadena de la polimerasa con transcriptasa inversa S,
sAPPα: Fracción APP alfa soluble
sAPPβ: Fracción APP beta soluble
SD: Standard deviation
SDS: Dodecilsulfato sódico
SiRPB-1: del inglés signal regulatory protein B-1.
SL: Mutaciones Swedish y London de APP
slm: stratum lacunosum-moleculare
SNC: Sistema nervioso central so: stratum oriens
so: stratum oriens.
SOM: Somatostatina
sp: stratum pyramidale
sr: stratum radiatum
Swe, S: mutación Swedish de la APP
Syn: sinaptofisina
Tg: transgénico
TGF-β: Factor de crecimiento transformante beta
Th: Linfocito T helper
Thio-S: Tioflavina S
TLR: del inglés Toll like receptor
TNF-α: Factor de necrosis tumoral α, del inglés Tumor necrosis factor
TPBS: Buffer PBS Tween 20
TRAIL: Ligando inductor de apoptosis relacionado con TNFα del inglés TNF-related apoptosis-inducing ligand.
TREM2: del inglés triggering receptor expressed on myeloid cells 2
TrkA: del inglés tropomyosin-related kinase A
Broca
VEGF: Factor de crecimiento endotelial vascular.
VGLUT: transportador vesicular de glutamato
VIM: Vimblastina.
VIP: Polipéptido intestinal vasoactivo
WB: Western blot
WT: genotipo salvaje (del inglés wild type)

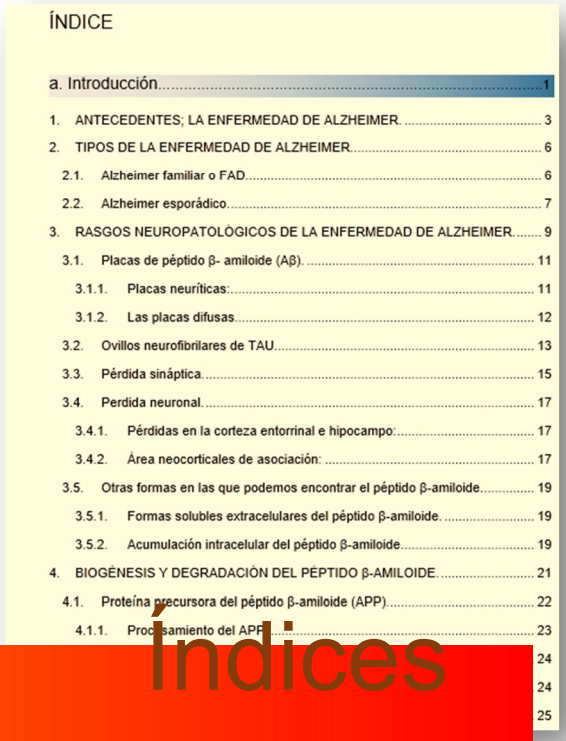

ÍNDICE

Índices

ÍNDICE

ÍNDICE DE FIGURAS.

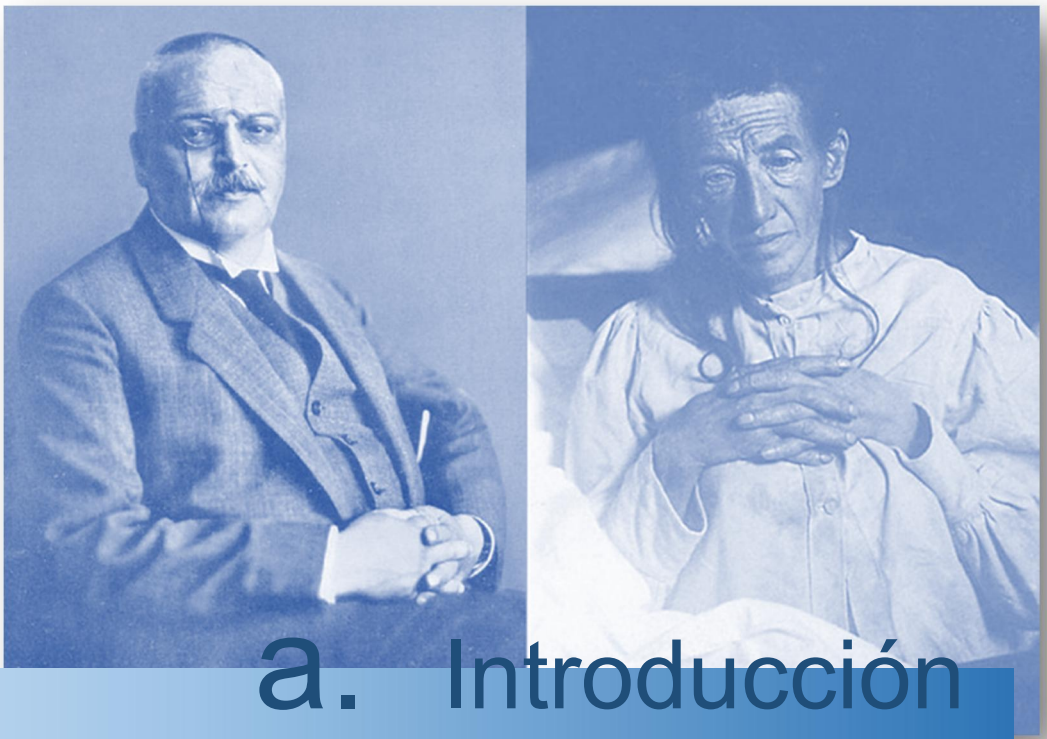

a. Introducción

1. ANTECEDENTES; LA ENFERMEDAD DE ALZHEIMER.

La enfermedad de Alzheimer (EA) fue descrita por primera vez en 1907 por el psiquiatra y neurólogo Alois Alzheimer (Alzheimer A., 1907). La primera paciente diagnosticada con esta enfermedad fue Auguste Deter de 51 años de edad, que murió cuatro años después en estado total de invalidez tras sufrir pérdida progresiva de memoria, desorientación espacio-temporal, cuadros graves de alucinaciones y delirios, paranoia y trastornos de la conducta y del lenguaje.

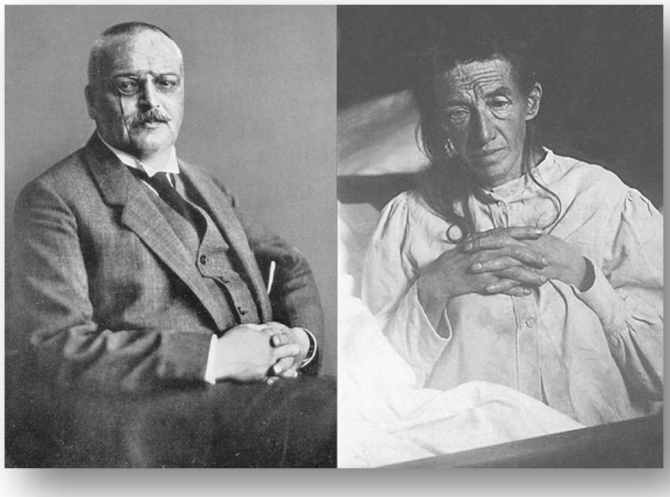

Figura 1.1. Alois Alzheimer y su paciente. El Dr. Alois Alzheimer (1864-1915) a la derecha y Auguste Deter (1850-1906) a la izquierda.

El análisis anatómico patológico del cerebro de esta paciente reveló la presencia de depósitos extracelulares (placas seniles) y agregados fibrilares intracelulares (ovillos) localizados principalmente en la corteza cerebral e hipocampo. Actualmente estas lesiones histopatológicas se usan como los principales marcadores de esta enfermedad. De hecho, la ausencia de marcadores biológicos para la enfermedad de Alzheimer, hace que el análisis neuropatológico post-mortem sea crucial para el diagnóstico definitivo de la enfermedad.

No fue hasta 1910 cuando el psiquiatra alemán Emil Kraepelin dio nombre a esta nueva entidad clínica y patológica, conocida actualmente como Enfermedad de Alzheimer (EA).

La EA se puede definir como un proceso neurodegenerativo progresivo e irreversible caracterizado por la pérdida de memoria, de habilidades intelectuales y de

razonamiento, así como por la presencia de desorientación espacio-temporal, cambios de humor, alteraciones conductuales, afasia (disminución progresiva de la capacidad del lenguaje), apraxia (alteración de los gestos e incapacidad de realizar tareas rutinarias) y agnosia (incapacidad de reconocimiento de personas o cosas) (Reiman y Caselli, 1999; Van Strien y col., 2009). Estas alteraciones se deben a daños selectivos en regiones cerebrales implicadas en estos procesos, tales como el hipocampo, la corteza entorrinal, la amígdala y el telencéfalo basal. El curso clínico de la EA suele durar 8-10 años, pudiendo llegar hasta los 25 (Gies y Lessick, 2009). La muerte del paciente suele atribuirse a enfermedades no relacionadas o indirectamente relacionadas, sólo un 20% de las muertes son directamente atribuibles a la demencia o a las complicaciones durante la fase terminal (Reiman y Caselli, 1999) como la malnutrición y la neumonía.

La EA representa hoy en día la forma más común de demencia entre las personas mayores de 65 años, así como una de las patologías neurodegenerativas más graves que afecta a este sector de la población. Los pacientes manifiestan un deterioro progresivo hasta perder la capacidad de desempeñar una vida autónoma e independiente, quedando en estado vegetativo durante los últimos meses, e incluso años, de su vida. Por ello, esta enfermedad es generalmente incapacitante y, en consecuencia, requiere de la ayuda de familiares o servicios especializados.

A nivel mundial hay aproximadamente 44,35 millones de personas que padecen demencia (World Alzheimer Report, 2013), entre estas la enfermedad de Alzheimer es la más común constituyendo el 60-70 % de los casos de demencia (OMS; 20012). (Fig. 1.2) entre las personas mayores de 65 años. La prevalencia de la enfermedad está por debajo del 1% en individuos menores de 65, pero muestra un incremento casi exponencial con la edad, y en personas de 85 años la incidencia es del 30% en el mundo occidental, ascendiendo al 63,9% en personas mayores de 90 años (Prince y col., 2013).

Estos datos hacen que la EA sea un grave problema de salud pública que se agravará en el futuro debido al aumento progresivo de la esperanza de vida actual, al envejecimiento de la población, y al elevado coste económico, sanitario y social que supone el cuidado de un enfermo de EA. Todo esto ha convertido a esta enfermedad en el tercer problema de salud más grave en los países desarrollados (detrás de los accidentes cardiovasculares y el cáncer). Existen alrededor de 800.000 enfermos diagnosticados en España y 35 millones a nivel mundial. Se calcula que en el año 2050, 115 millones de personas en el mundo se encontrarán afectadas por esta enfermedad. (Neugroschl y Sano, 2010; ver http://www.alz.org/downloads/facts_figures_2014.pdf)

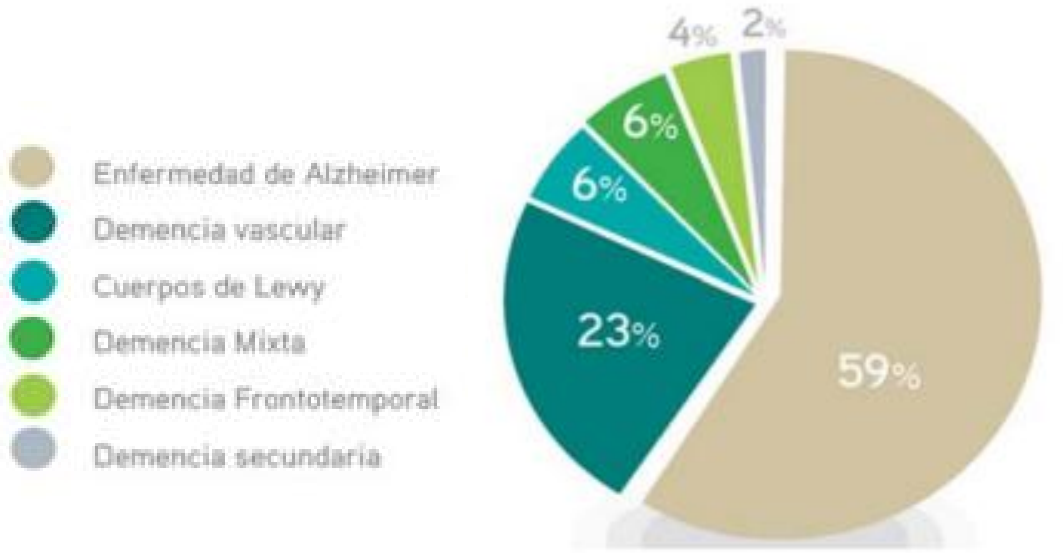

Figura 1.2. Distribución de los tipos de demencia. Estudio poblacional de prevalencia de demencias. Del informe: "Estado del arte de la enfermedad de Alzheimer en España". PWC (2013).

Actualmente la EA no tiene tratamiento farmacológico eficaz, es una enfermedad incurable debido en gran parte a la falta de dianas terapéuticas conocidas. Existen medicamentos que mejoran los síntomas, pero ninguno es totalmente efectivo. A mediados de los años 70 se estableció la hipótesis colinérgica de la EA, que consideraba que la mayoría de los síntomas de la enfermedad eran producidos por la pérdida de un gran número de neuronas colinérgicas (Whitehouse y col., 1981; Arendt y col., 1985). A raíz de estos hallazgos se empezaron a utilizar fármacos inhibidores de la acetilcolinesterasa para tratar la enfermedad, aunque más tarde se demostró que sólo en el 50% de los pacientes tratados con dichos fármacos se produce un retraso parcial en el déficit cognitivo. Por tanto el sistema colinérgico no es una buena diana terapéutica para combatir la sintomatología de la enfermedad. Un tratamiento eficaz debería evitar, o al menos retrasar, la pérdida de contactos sinápticos y la muerte neuronal progresiva que se produce en esta enfermedad, lo que mejoraría significativamente la calidad de vida del paciente y de sus familiares-cuidadores y reduciría enormemente los costes socio-sanitarios y asistenciales. Se hace necesario continuar con la investigación de las causas que inician esta patología y la búsqueda de posibles dianas terapéuticas que posibiliten el desarrollo de fármacos eficaces.

2. TIPOS DE LA ENFERMEDAD DE ALZHEIMER.

Se distinguen dos tipos de EA, el **Alzheimer familiar** (FAD del inglés *Familial Alzehimer Disease*) y el **Alzheimer esporádico**. Ambas formas de Alzheimer poseen los mismos síntomas y poseen las mismas lesiones histopatológicas, pero difieren en la edad de inicio, la incidencia y las causas por la que aparecen (ver revisiones Gomez-Isla y col., 2008; Perl 2010; Ballard y col., 2011; Bagyinszky y col., 2014).

2.1. **Alzheimer familiar o FAD.** Esta forma de la enfermedad se caracteriza por un comienzo temprano, generalmente antes de los 60 años, por eso también es conocido como presenil o de inicio temprano. Representa menos del 5% de los casos de EA. Este tipo de EA se transmite hereditariamente con carácter autosómico dominante. En la actualidad se conocen tres genes, cuyas mutaciones causan FAD; estos genes codifican para la Proteína Precursora Amiloide (APP), Presenilina 1 (PS1) y la Presenilina 2 (PS2) (ver revisiones O'Brien y Wong, 2011; Karch y col., 2014; Calero y col., 2015). Todas estas proteínas están implicas en el producción del péptido β-amiloide (Aβ), ya que la primera se trata de su precursor y la segunda y tercera forman parte del complejo gamma-secretasa que procesa el APP hasta Aβ. La alteración de cualquiera de estas proteínas lleva a una generación y acumulación no fisiológica de Aβ que se agregan para formar placas extracelulares de Aβ características de la EA. En la actualidad se han descrito 32 mutaciones en APP, 185 en PS1 y 13 en PS2 que generan FAD. (Cruts et al., 2012; http://www.molgen.vib-ua.be/ADMutations).

- **Proteína Precursora del Péptido Amiloide (APP):** Este gen está localizado en el cromosoma 21 (Goate y col., 1991). En él se describió la primera mutación relacionada con el Alzheimer, pero sólo afecta al 10% de los enfermos de FAD. Se han descubierto 32 mutaciones implicadas con esta versión presenil de la enfermedad. La implicación de este gen es tal, que su duplicación en los casos de trisomía del cromosoma 21 es suficiente para causar daños a edades tempranas como ocurre en los enfermos de Síndrome de Down que pueden desarrollar demencia (ver revisión Thinakaran y Koo, 2008).

- **Presenilina 1 (PS1):** Este gen está localizado en el cromosoma 14. Las mutaciones en este gen son la causa más frecuente de Alzheimer familiar, con un 70% del total de los casos (Sherrington y col., 1995). Se han descrito 185 mutaciones en este gen que están implicadas en casos de FAD.

- **Presenilina 2 (PS2):** Localizado en el cromosoma 1 (Rogaev y col., 1995). Se han descrito alrededor de 14 mutaciones en este gen asociadas con el Alzheimer familiar (Czech y col., 2000).

2.2. **Alzheimer esporádico**. Aparece a partir de los 60-65 años y representa el 95-98% de los casos. Es de origen multifactorial y el principal factor de riesgo es la edad. Afecta al 3-4% de personas con edades comprendidas entre los 60 y 65 años. Es a partir de aquí cuando la incidencia aumenta al doble cada cinco años, llegando a afectar a un 40% de la población a partir de los 80 años.

Esta forma de Alzheimer no tiene origen genético, pero se han descrito ciertos polimorfismos en genes que están asociados con un mayor riesgo de padecer EA (ver revisiones Karch y col., 2014; Calero y col., 2015). A continuación se enumeran los más importantes:

- **CLU** (Clusterina)**.** Codifica para parte de la cadena B de esta proteína (conocida como Apolipoproteína J). Su gen está localizado en el cromosoma 8. Esta proteína es secretada por astrocitos y forman complejos con el Aβ soluble generando complejos insolubles que atraviesan la barrera hematoencefálica (Boggs y col., 1996). Su expresión está incrementada en ciertas regiones cerebrales de pacientes de EA (Lambert y col., 2009).

- **PICALM** (*phosphatidyl inositol-binding clathrin assembly protein*). (Harold y col., 2009). Este gen está localizado en el cromosoma 11. Podría afectar a la autofagia (Moreau y col., 2013) y participar en el metabolismo de Aβ a través de la ruta endocítica.

- **APOE** (Apolipoproteína E). Gen localizado en el cromosoma 19 y presenta tres isoformas mayoritarias; ε2, ε3 (la más común) y ε4 (Strittmatter y

col.1993; Yu y col., 2014). La isoforma ε4 está considerado como el mayor factor de riesgo por asociación genética de Alzheimer esporádico ya que entre 65-80% de los enfermos de EA presentan al menos uno de los dos alelos APOEε4. La presencia de uno de los alelos incrementa el riesgo de padecer EA en tres veces, mientras que en los individuos homocigotos ε4 el riesto aumenta 15 veces (Eisenstein, 2011; Saunders y col., 1993; Farrer y col., 1997). Por otro lado hay pruebas de que la herencia del alelo ε2 puede conferir protección contra el desarrollo de la enfermedad de Alzheimer (Selkoe, 2001).

3. RASGOS NEUROPATOLÓGICOS DE LA ENFERMEDAD DE ALZHEIMER.

La EA se caracteriza por unos rasgos anatómico-patológicos distintivos (para revisión ver Perl, 2010; Claeysen y col., 2012). Estos cambios se pueden incluir en dos grandes grupos: los macroscópicos y los microscópicos.

Entre las principales **alteraciones macroscópicas** observadas en los pacientes de EA podemos encontrar atrofia cortical severa, adelgazamiento de las circunvoluciones y ensanchamiento de los surcos, engrosamiento de las meninges, dilatación de las cavidades ventriculares, disminución del bulbo olfatorio y pérdida de peso y volumen cerebral (Fig. 3.1.).

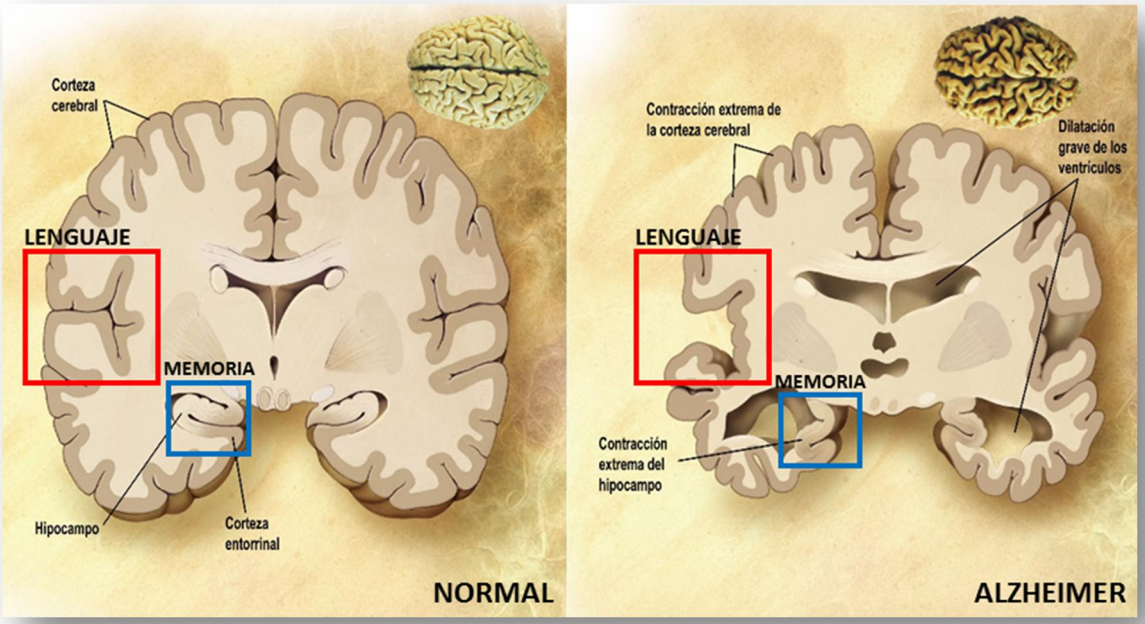

Figura 3.1. Esquema comparativo de un cerebro humano sano (izq.) y otro de un enfermo de EA (der.). El cerebro enfermo posee un menor volumen y unos ventrículos muy dilatados. La atrofia afecta a los lóbulos temporales, frontales, parietales y occipitales. Las regiones importantes para la memoria (en azul) y para el lenguaje (azul) son las más afectadas.

Esta atrofia cortical puede ser analizada por resonancia magnética, esta técnica no invasiva podría suponer un avance en el diagnóstico precoz de la EA y detectar estados iniciales donde el uso de los medicamentos pueda tener un mayor efecto evitando la progresión de la enfermedad. (Nasrallah y Wolk, 2014; Eskildsen y col., 2015).

Las principales **alteraciones microscópicas** características de la EA son los agregados proteícos extracelulares en forma de placa del péptido β-amiloide, los ovillos neurofibrilares intraneuronales de la proteína TAU hiperfosforilada, la disminución del número de sinápsis y la degeneración neuronal en las áreas cerebrales afectadas (ver revisiones en Gómez-Isla y col., 2008; Perl, 2010; Serrano-Pozo y col., 2011).

Estas lesiones aparecen principalmente en áreas cerebrales implicadas en los mecanismos de memoria, aprendizaje y en los procesos cognitivos focales. Inicialmente se manifiestan en la corteza entorrinal, progresando hacia el hipocampo, y finalmente afectando a las áreas neocorticales (Braak and Braak, 1991). (Fig.3.2.) Las cortezas motora y sensorial no se afectan, y si lo hacen, no es hasta estadios muy avanzados de la enfermedad.

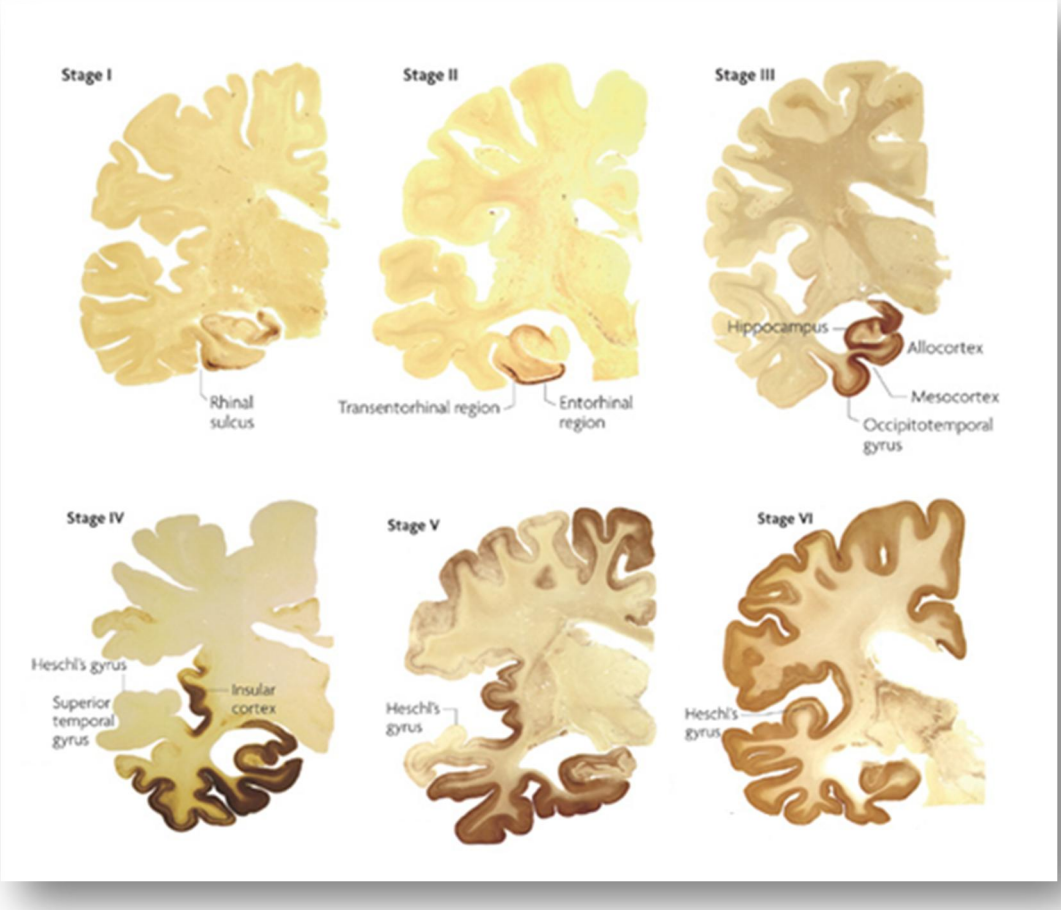

Figura 3.2. Estadios de Braak. Progresión propuesta para la patología neurofibrilar en la corteza cerebral. En los estadios I y II se encuentra en las cortezas transentorrinal y entorrinal; en los estadios III y IV se afecta el hipocampo, para finalmente, alcanzar en los estadios V y VI la isocorteza. Modificado de Hans Kretzschmar, 2009.

3.1. Placas de péptido β- amiloide (Aβ).

Son agregados proteícos insolubles extracelulares. Se depositan tanto en el parénquima cerebral como en la pared de los vasos sanguíneos cerebrales. El componente principal de las mismas es el péptido *β*-amiloide (Glenner and Wong, 1984; Masters et al., 1985), aunque también puede contener otras proteínas así como restos de neuronas y células gliales.

El péptido A*β* contiene entre 39 y 43 aminoácidos y es un producto derivado del metabolismo natural de la proteína precursora del péptido *β*-amiloide (APP) (De Strooper, 2010). *In vivo* existen dos formas mayoritarias del péptido A*β*: A*β*40 que termina en el aminoácido Val40, y A*β*42 que tiene dos aminoácidos adicionales, Ile41 y Ala42, que le confiere mayor hidrofobicidad y capacidad de agregación (Wolfe, 2007). Estas dos características son responsables de que el A*β*42 sea más abundante en las placas extracelulares que el A*β*40. Aunque se ha propuesto que las placas extracelulares de A*β* podrían ser el origen de la neurodegeneración observada en las zonas involucradas en la memoria y el control emocional (Van Gassen y Annaert, 2003), no parece existir correlación clara entre la acumulación de A*β* cerebral y las alteraciones cognitivas en pacientes de EA (Giannakopoulos y col., 2003; Ingelsson et al., 2004).

Las placas se dividen en **neuríticas** y **difusas**. Las neuríticas a su vez se pueden dividir en clásicas o primitivas (ver revisiones Selkoe, 2001; Perl, 2010):

3.1.1. Placas neuríticas: (por estar asociadas a neuritas distróficas), son depósitos extracelulares de aspecto filamentoso (Dickson, 1997). Como se ha dicho aparecen asociadas a neuritas distróficas (y son positivas al marcaje con Tau, APP, Ubiquitina o ChAT), también están asociadas a células de la microglía; en estas placas la astroglía se localiza en la periferia (Duyckaerts y col., 2009) (Fig.3.3.).

Atendiendo a su morfología estas placas **neuríticas** pueden ser:

a. Clásicas. Con un núcleo compacto central, formado por Aβ y células microgliales, rodeado por un halo que contiene especies del péptido β-amiloide. Estas placas normalmente están asociadas a los vasos.

b. Primitivas. Son esféricas y sin un núcleo compacto. Normalmente aparecen cercanas a axones y sinapsis.

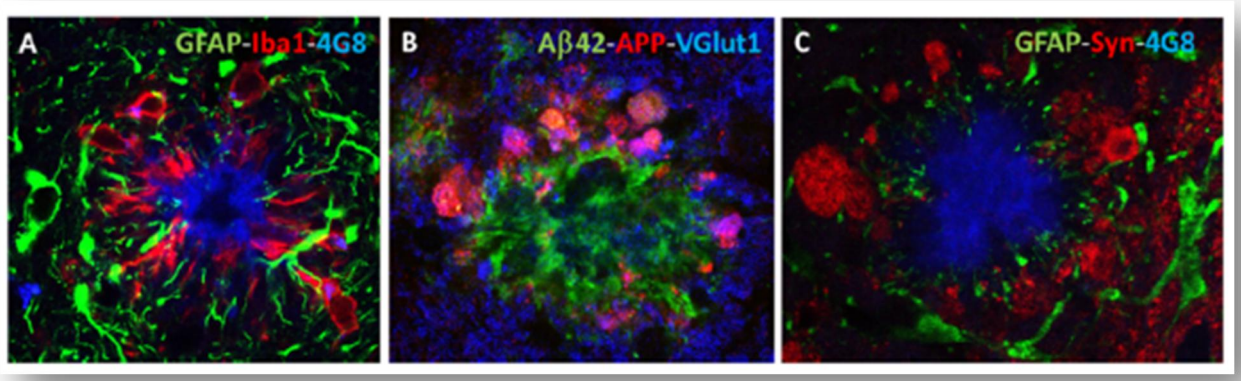

Figura 3.3. Placas neuríticas de un ratón transgénico de la EA. Imagen A: Triple inmunohistoquímica para GFAP (astroglía), Iba1 (microglía) y 4G8 (placas de Aβ), se observa el contacto íntimo de la microglía con la placa mientras que la astroglía se mantiene en la periferia. Imagen B: Triple inmunohistoquímica para Aβ42, APP y VGlut1 (ambos marcando neuritas distróficas). Imagen C: Triple inmunohistoquímica para GFAP (astroglía), Syn (Sinaptofisina, marcando neuritas distróficas) y 4G8 (marcando la placa de Aβ). Estas imágenes muestran la relación entre las células gliales, el Aβ y las distrofias existentes en las placas neuríticas. Imágenes cedidas por el grupo de la Dr. Antonia Gutiérrez.

3.1.2. Las **placas difusas** (no están asociadas a neuritas distróficas). Son depósitos extracelulares no fibrilares de Aβ (no congófilos). Como su nombre indica presentan una estructura difusa sin núcleo compacto apreciable y, a diferencia de las placas primitivas, no contienen ni neuritas distróficas, ni microglía asociada a ellas (Selkoe, 2001). Suelen aparecer en zonas cercanas a neuronas.

El proceso de formación de las placas extracelulares de A*β* es aún desconocido, aunque se atribuye en gran parte a la hidrofobicidad y capacidad de agregación del péptido A*β*42 (Chen and Glabe, 2006). Está claro que es importante en la formación de la placa el aumento en la producción extracelular de A*β* y la disminución en el aclaramiento del mismo. En cualquier caso, parece que la aparición de placas de A*β* tiene un importante componente cronológico que depende de la formación progresiva de ADDLs (Amiloide-*β* Derived Diffusible Ligands), fibras de A*β* y complejos A*β*-ApoE (Thal et al., 2006).

3.2. **Ovillos neurofibrilares de TAU.**

Son agregados intracelulares, formados por filamentos helicoidales emparejados y filamentos rectos cuyo componente mayoritario es la proteína Tau hiperfosforilada (Spillantini and Goerdert, 2013). Tau es una proteína asociada a microtúbulos (MAP: microtubule associated protein), cuya función es estabilizar los microtúbulos del citoesqueleto colaborando en la generación y mantenimiento de la estructura de los axones, siendo fundamental en el transporte axonal y en la regulación sináptica (Spires-Jones and Hyman, 2014).

Para formar los ovillos Tau se disocia de los microtúbulos, probablemente mediante su hiperfosforilación. Al ser insolubles tienden a agregarse formando pares de filamentos helicoidades (PHF) y pasan de tener una localización axonal a somatodendrítica, donde estos filamentos se unen formando los ovillos neurofibrilares intracelulares (NFTs) característicos de la EA (Morishima-Kawashima e Ihara, 2002). (Fig. 3.4.) Al fosforilarse tau y disociarse de los microtúbulos se produciría una pérdida de función de los mismos, con lo que se generan fallos en el transporte axonal y muerte neuronal (Gotz, 2001; Spires-Jones et al., 2009). Además, una extensa hiperfosforilación de Tau inhibe la actividad del proteasoma aumentando de esta forma el efecto negativo de la hiperfosforilación de Tau (Gendron y Petrucelli, 2009; Wang y col., 2013).

Podemos encontrar Tau hiperfosforilada acumulada en el cuerpo neuronal como NTFs, en las dendritas como *neuropil threads,* en los axones de las neuronas con degeneración neurofibrilar y las neuritas distróficas asociadas a los depósitos extracelulares de Aβ dando lugar a las placas neuríticas. (Duyckaerts y col., 2009).

La agregación de Tau también se ve potenciada por otras modificaciones postraduccionales como la glicosilación, acetilación y ubiquitinación entre otras (Iqbal y Grundke-Iqbal, 2008; Wang y col., 2013).

Debido a la presencia de estos NTFs intracelulares formados por la proteína Tau hiperfosforilada la EA es considerada una taupatía (Lee y col., 2001), término que agrupa a distintas enfermedades con depósito anormal de Tau hiperfosforilada en neuronas y células gliales. Existen unas 40 mutaciones de Tau ligadas a la demencia frontotemporal, mientras que ninguna ha sido descrita en casos de FAD.

Muchos investigadores sugieren que estas alteraciones en el citoesqueleto producen la patogénesis propia de EA, relacionando la muerte neuronal con la presencia de los ovillos neurofibrilares (Spires-Jones et al., 2009). Por otro lado, la aplicación de

métodos estereológicos en cerebros de enfermos de Alzheimer han revelado que el número de neuronas perdidas excede al número de neuronas que contienen ovillos, indicando que la perdida neuronal en la EA podría ser independiente de la formación de ovillos (Morishima-Kawashima and Ihara, 2002). De hecho, a pesar de las anormalidades en el citoesqueleto, las neuronas que contienen ovillos pueden sobrevivir durante años, aunque no estemos seguro de que mantengan su integra su función.

Datos recientes sugieren que son las formas solubles, tanto de Aβ como de Tau fosforilada pueden jugar un papel más importante que las placas y los ovillos (ambos insolubles) sobre el daño sináptico y la demencia (McDonald y col., 2012). Indicando que más que la formación de ovillos o placas es la acumulación anormal de formas solubles en las sinapsis la que puede estar más relacionada con la muerte neuronal (Perez-Nievas y col., 2013; Spires-Jones y Hyman, 2014). Además los niveles de Tau fosforilado en líquido cefalorraquídeo (LCR) se correlacionan de forma directa con los procesos neurodegenerativos producidos en la EA (Brunden y col., 2009; Matsuo y col., 1994).

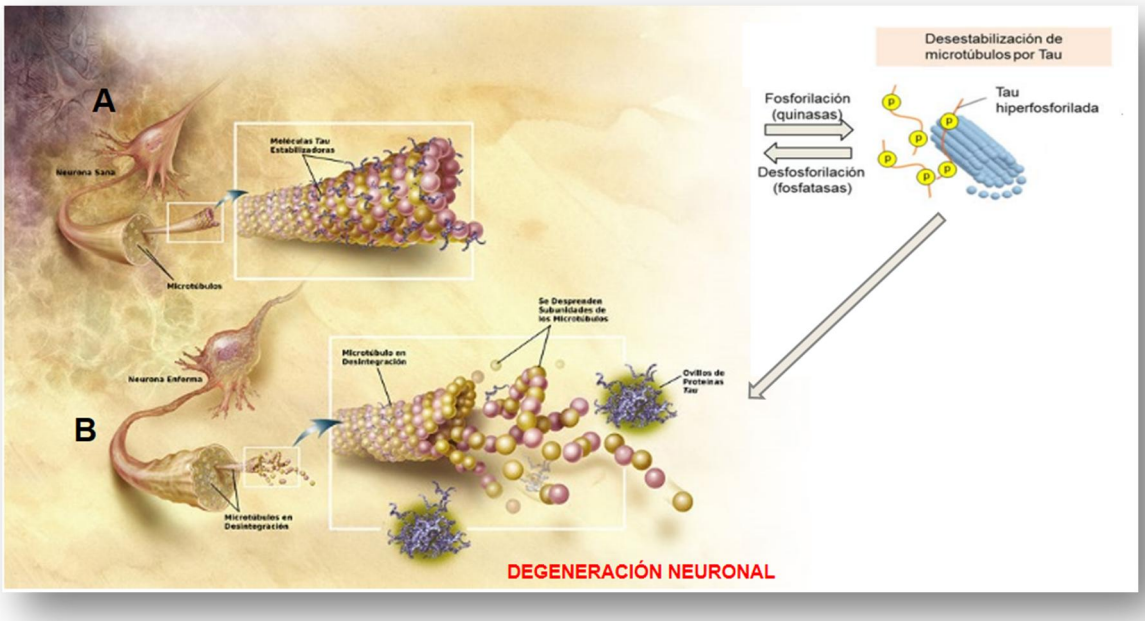

Figura 3.4. Formación de ovillos neurofibrilares. Tau está unida a microtúbulos estabilizándolos y con localización preferentemente axonal. Al hiperfosforilarse se separan de los microtúbulos desestabilizando a los mismos. En primer lugar forman los PHF que al unirse generan los NFTs, implicados en la degeneración neuronal. A. Indica como estaría Tau en el axón de una neurona sana, mientras que B representa la desorganización de los microtúbulos que desencadenaría un proceso de degeneración neuronal. (Modificado de Querfurth y LaFerla, 2010).

Como hemos visto en la Fig. 3.2 en los enfermos de Alzheimer existe un patrón de deposición de los ovillos, que comienza en la corteza entorrinal y avanza hacia el hipocampo y corteza asociativa, afectándose en estadios avanzados las áreas sensoriales primarias (Spires-Jones y Hyman, 2014).

3.3. Pérdida sináptica.

En la enfermedad de Alzheimer se produce una gran pérdida de conexiones sinápticas que producen los fallos en las funciones cognitivas y de memoria característicos de la enfermedad. Esta pérdida sináptica fue referida por primera vez a principio de los años 90 por varias investigaciones que describieron una disminución de las sinapsis y de proteínas implicadas en ellas en la corteza frontal, temporal y en giro dentado. En ellas se comprobaba que dicho hallazgo patológico correlacionaba mejor con la demencia asociada a EA (DeKosky y Scheff, 1990; DeKosky y col., 1996; Masliah y col., 1994; Terry y col., 1991). Se han reportado pérdidas de un 30% en la densidad sináptica (Davies y col., 1987) y la disminución de inmunorreactividad para sinaptofisina en hipocampo y corteza de personas que presentaban deterioro cognitivo leve o EA leve (Overk y Masliah, 2014). Estos datos pueden mostrar que anterior a la muerte neuronal existen fallos a nivel sináptico, y que son estas modificaciones las que mejor correlacionan con las deficiencias cognitivas de los pacientes (Tampellini y Gouras, 2010). En la actualidad se reconoce que son estos defectos a nivel sináptico la base del declive cognitivo que se produce en EA ya que afectan a la plasticidad sináptica de las neuronas, que no es otra cosa que la capacidad de realizar nuevas sinapsis con otras células para cambiar la intensidad de una señal y que son la fundamentales para los distintos tipos de memoria y aprendizaje.

La potenciación a largo plazo (LTP) y la depresión a largo plazo (LTD) participan de manera activa en la plasticidad sináptica y están mediadas principalmente por los receptores NMDA y AMPA de glutamato. En la respuesta LTP se produce una potenciación de la sinapsis que conlleva al aumento de receptores AMPA post sinápticos. La respuesta LTD, por el contrario, produce un debilitamiento de la respuesta sináptica con la consiguiente internalización de receptores AMPA y NMDA. La pérdida de integridad sináptica en aquellas zonas relacionadas con el aprendizaje y la formación de recuerdos, como son el hipocampo y la neocorteza, pueden ser la causa del síntoma inicial más importante de la EA: la pérdida de memoria. A lo largo de la evolución de la

patología se produce una alteración generalizada de la plasticidad sináptica, así como de todos los mecanismos implicados en su funcionamiento (Dudai and Morris, 2013).

Tanto Tau, como el péptido Aβ parecen tener un papel relevante en el correcto mantenimiento de las sinapsis en individuos sanos. Tau está claro que con su función estabilizadora de los microtúbulos está implicada en un correcto funcionamiento del transporte axonal. El péptido Aβ parece participar en el desarrollo natural de las sinapsis y en la plasticidad sináptica, aunque los mecanismos no están claros. Lo que está claro es que niveles elevados de este péptido disminuyen la excitabilidad neuronal, provocando la internalización de receptores AMPA. Esto provoca depresión sináptica y pérdida de espinas dendríticas, provocando la interrupción de la LTP imprescindible en la plasticidad sináptica asociada con los procesos de memoria y aprendizaje (Small, 2008). Además se ha demostrado que la presencia de Aβ oligomérico provoca una reducción de la densidad de espinas dendríticas y una pérdida de sinapsis electrofisiológicamente activas en cultivo de neuronas principales del hipocampo, mientras que la adición de monómeros no tiene el mismo efecto (Shankar y col., 2007). Referente a Tau, se ha descrito recientemente su implicación en la internalización de los receptores NMDA en la terminal postsináptica (Spires-Jones and Hyman, 2014).

Además, hay estudios que demuestran la posible implicación de Tau en la sinaptotoxicidad producida por Aβ (Ittner et al., 2010; Roberson et al., 2011). En este sentido varios autores han descrito que la degeneración sináptica es más específica en regiones con una previa desorganización de microtúbulos y han demostrado que el efecto de Aβ es menos tóxico en modelos que no sobre expresan Tau.

Al parecer son las formas solubles de estas proteínas, y no las formas fibrilares y agregadas, tanto de Tau fosforilada como de Aβ las causantes de la pérdida sináptica (revisado en Crimins et al., 2013).

3.4. Perdida neuronal.

En la EA se produce una extensa y selectiva degeneración neuronal que afecta a regiones y tipos celulares concretos (Duyckaerts y col., 2009). Las principales áreas afectadas son:

3.4.1. Pérdidas en la corteza entorrinal e hipocampo:

En los casos preclínicos de EA, caracterizados por la presencia de algunas placas amiloides y ovillos neurofibrilares y ausencia de demencia, la región CA1 del hipocampo y la corteza entorrinal no presentan una dismininucíón significativa en el número de neuronas (Giannakopoulos et al., 1998). Sin embargo a estos niveles las neuronas colinérgicas del telencéfalo basal (Whitehouse y col., 1981) y las noradrenérgicas del locus coeruleus (German y col., 1992) ya están afectadas. En la fase intermedia de EA se producen en la corteza entorrinal un pérdida neuronal del 32%, principalmente en las capas II y IV, con una disminución del 57% y 41% respectivamente. En la fase avanzada de la patología, la pérdida neuronal en la corteza entorrinal alcanza el 69%, y al igual que en los estadios moderados, afecta principalmente a las capas II y IV, con un 87% y un 69% de muerte respectivamente, mientras que la pérdida total del resto de las capas es del 63% (Gómez-Isla et al., 1996). En el caso de la capa CA1 del hipocampo la muerte neuronal sólo se produce en los estadios avanzados de la patología, aunque el 60% de las neuronas de la capa piramidal de CA1 parecen no afectarse (West et al., 1994; Von Gunten et al., 2006).

3.4.2. Área neocorticales de asociación:

El patrón de progresión de la EA en estas zonas es el siguiente: primero se afecta la corteza temporal, posteriormente la corteza frontal y, finalmente a la corteza somatosensorial. En los estadios tempranos de la enfermedad se produce una disminución bilateral del 15% de la sustancia gris en la corteza temporal y parietal, mientras que la corteza motora o sensorial primaria apenas se ven afectadas (<5%). Un año más tarde, imágenes de resonancia realizadas en un mismo individuo mostraron que la corteza frontal pasaba de tener una pérdida neuronal del 6% a más del 15%, mientras las áreas motoras y sensoriales permanecían sin daños (Thompson y col.,

2003). Por tanto, el lóbulo temporal es especialmente susceptible a la EA. La vulnerabilidad de estas áreas de asociación neocortical posiblemente se deba a la conexión funcional que tienen con las estructuras límbicas, zona de inicio de la patología.

El declive cognitivo se correlaciona estrechamente con la pérdida neuronal. Las causas y los mecanismos de muerte neuronal se desconocen, aunque poseen un papel importante la generación de especies reactivas de oxígeno, la sobre activación de receptores de aminoácidos excitadores como el glutamato y el incremento en la concentración citoplasmática de calcio.

Esta pérdida neuronal y los cambios sufridos a nivel sináptico que se observan con la progresión de la EA se pueden monitorizar mediante imágenes de resonancia magnética. Y esto ha permitido describir el patrón de progresión de la patología (Thompson y col., 2003). Se podría resumir como se expone a continuación**:**

- Se expande a través del cerebro con una secuencia temporal-frontal-sensomotora. La pérdida de sustancia gris se produce primero en las regiones temporal y parietal, siendo el hipocampo y la corteza entorrinal las zonas más tempranas y severamente afectadas. Más tarde, el déficit afecta a la corteza temporal y frontal, y finalmente, a las cortezas sensomotora y visual.

- El hemisferio cerebral izquierdo pierde sustancia gris más rápidamente que el derecho, consistente con una afectación más severa de este hemisferio en la EA.

- Hay regiones cerebrales, como la corteza sensomotora, donde no aparece daño hasta muy avanzada la enfermedad.

3.5. Otras formas en las que podemos encontrar el péptido β-amiloide.

El péptido Aβ además de estar formando parte de las placas extracelulares insolubles que hemos mencionado anteriormente se pueden encontrar en otros estados, como por ejemplo en formas solubles tanto dentro de las células como por el parénquima cerebral.

3.5.1. Formas solubles extracelulares del péptido β-amiloide.

En la actualidad se piensa que la presencia de la placas extracelulares de Aβ no son la causa principal de los problemas sinápticos, de pérdida neuronal y respuesta inflamatoria que nos podemos encontrar en EA (esto no se corresponde con lo defendido hasta el momento en la Hipótesis de la cascada amiloide), ya que no siempre correlaciona el número de placas extracelulares de Aβ con la severidad de la patología (Mucke y col., 2000). El péptido Aβ no sólo se puede encontrar en forma insoluble, se han descrito formas tóxicas solubles de Aβ oligomérico (ADDLs) que pueden difundir por el parénquima cerebral provocando activación de la respuesta inflamatoria, pérdida sináptica y fallos cognitivos en las fases tempranas de la EA (Haass y Selkoe, 2007; Benilova y col., 2012; Viola y Klein, 2015).

En cuanto al proceso de oligomerización-fibrilización, distintos estudios sugieren que las proteínas amiloides se agregan formando distintos intermediarios (ver revisión Sakono y Zako, 2010) de entre 8 KDa (dímeros) y 100 kDa (Shankar y col., 2008).

Brevemente, en primer lugar, la asociación de pequeños n-oligómeros solubles (LMW-Aβ, del inglés *Low Molecular Weight*), resultaría en ensamblajes de peso molecular más alto, incluyéndose en este grupo a las estructuras anulares, paranúcleos, ligandos difusibles derivados del Aβ (ADDLs, del inglés *A*β*-derived difusible ligands*, cuyos niveles correlacionan bien con los fallos cognitivos y pueden inhibir la LTP en el hipocampo) (Lambert y col., 1998; Haass y Selkoe, 2007), Aβ*56 (Lesné y col., 2006), amiloesferoides (Noguchi y col., 2009), y las protofibrillas (PFs; Walsh y col., 1997). Éstas excederían los límites de solubilidad y se depositarían como fibrillas amiloides en conformación de hoja β plegada (ver revisión Goldsbury y col., 2005). Los mecanismos por los cuales se producen estos ensamblajes no están claramente definidos.

3.5.2. Acumulación intracelular del péptido β-amiloide.

El péptido β-amiloide también se puede encontrar a nivel intracelular (Aβi) aunque sea mayoritaria su acumulación en las placas extracelulares. La presencia de

Aβi es frecuente en neuronas que contienen ovillos neurofibrilares lo que puede indicar que ambas patologías estén relacionadas (Blurton-Jones y LaFerla, 2006).
La acumulación puede darse por una falta de liberación tras la generación de Aβ a partir del APP que se puede encontrar en distintos compartimentos celulares. Los endosomas son un sitio probable de generación de Aβ, ya que su pH ácido es idóneo para la actividad de BACE-1. APP podría ser internalizada por endocitosis y mediante proteólisis generar Aβ, si se bloquea dicha internalización se reducen los niveles de Aβ (revisión LaFerla y col., 2007). Pero esta acumulación de Aβi también podría producirse por una captación del Aβ extracelular captado por receptores específicos para Aβ, algunos ejemplos son: la subunidad α7 del receptor nicotínico (α7nAChR; Wang y col., 2000), el receptor LDLR de APOE (Zerbinatti y col., 2006) o los receptores NMDA (Bi y col., 2002).

El Aβi se acumula predominantemente en los cuerpos multi vesiculares de las neuronas, donde se asocia con la patología sináptica (Takahashi y col., 2002). Estos cuerpos se pueden fusionar con la membrana plasmática liberando el Aβ al espacio extracelular.

Podríamos estar frente a un acontecimiento temprano en la EA (Bayer y Wirths, 2010), ya que aparece en las células piramidales del hipocampo y la corteza entorrinal (regiones con afecciones patológicas más evidentes) de pacientes con defectos cognitivos leves y los niveles parecen descender con la formación de las placas. Esta acumulación intracelular se da, incluso, en individuos sanos (ver revisión LaFerla y col., 2007).

No se conoce el efecto que puede tener este Aβi, aunque puede afectar a la función mitocondrial y del proteasoma, provocar problemas sinápticos, y potenciar la hiperfosforilación de Tau (LaFerla y col., 2007), provocar déficits en la LTP (Billings y col., 2005) e incluso muerte neuronal (Li y col., 2009b; ver revisión Bayer y Wirths, 2010). La liberación al medio puede actuar como semillas de inicio de la formación de placas, e incluso constituir una forma de propagar el péptido β-amiloide a través de distintas zonas del cerebro (Rajendran y Annaert, 2012).

4. BIOGÉNESIS Y DEGRADACIÓN DEL PÉPTIDO β-AMILOIDE.

El péptido A*β* contiene entre 39 y 43 aminoácidos y es un producto derivado del metabolismo natural de la proteína precursora del péptido *β*-amiloide (APP) (De Strooper, 2010). Este péptido se origina a partir de la una región de APP localizada tanto en el dominio extracelular como en el transmembrana (Fig. 4.1), es precisamente ésta la que le confiere propiedades agregativas. La producción del péptido *β*-amiloide no es un proceso patológico, sino que se genera de forma natural apareciendo tanto en plasma como en el líquido cefalorraquídeo de individuos sanos. Incluso durante el envejecimiento normal estos péptidos de Aβ insolubles se depositan en el parénquima cerebral y en la pared de los vasos sanguíneos cerebrales (Selkoe, 2004; Gomez-Isla y col., 2008).

Se están realizando trabajos para intentar aclarar cuál es el papel fisiológico del Aβ. Se sugiere que podría tener un papel importante en el mantenimiento de la tasa basal y en la regulación de la liberación de vesículas desde terminales presinápticos excitatorios (Abramov y col., 2009). Además, se le atribuye un papel como regulador negativo a niveles postsinápticos cuando se encuentra a altas concentraciones (ver revisión Palop y Mucke, 2010). De hecho, se ha descrito que concentraciones picomolares de Aβ mejoran la plasticidad sináptica y la memoria (Puzzo y col., 2008; Morley y col., 2010). Por otro lado, los monómeros de Aβ42 parecen ejercer un papel neuroprotector (Giuffrida y col., 2009). Todos estos datos apuntan a una posible pérdida de función del Aβ como otra causa posible del inicio de la patología de la EA.

La isoforma más frecuente es la de 40 aminoácidos (Aβ40) con Val40 en el extremo C-terminal, la de 42 aminoácidos (Aβ42) sólo constituye el 10% del total. Estos dos aminoácidos lo hacen más hidrofóbico, por lo que tiene mayor tendencia a agregarse y formar fibras. Las mutaciones descritas en FAD actúan aumentando la producción relativa de Aβ42 frente al Aβ40 (Ashe y Zahs, 2010).

El proceso de formación de la placa no se conoce en la actualidad. A pesar de esto se consideran factores importantes el aumento de la producción extracelular de Aβ (especialmente de la isoforma Aβ42) y la disminución en el aclaramiento del mismo. Además de depender de la formación progresiva de ADDLs (Amiloide-β Derived Diffusible Ligands), de fibras de Aβ y de complejos ApoE-Aβ (Thal et al., 2006). Por esto es fundamental conocer el proceso mediante el cual se genera el péptido Aβ y los mecanismos que pueden eliminarlo. A continuación vamos a hablar de las proteínas que están implicadas en la biogénesis de las distintas isoformas de péptido β-amiloide, y también en su degradación-aclaramiento.

4.1. Proteína precursora del péptido β-amiloide (APP).

Esta proteína pertenece a una familia de proteínas transmembrana tipo I altamente conservada tanto en vertebrados como en invertebrados. Aunque podemos encontrar distintas isoformas y variantes dependiendo de la especie animal todas comparten una misma estructura: un largo dominio globular extracelular (con el extremo N-terminal), un segmento transmembrana y un corto dominio citosólico donde se encuentra el extremo C-terminal. (Gralle and Ferreira, 2007). El gen de APP se localiza en el cromosoma 21, y puede generar 10 isoformas alternativas, aunque tres son las más frecuentes APP695, APP751 y APP770 (Tanzi y col., 1988; revisado en Yamada y Nabeshima, 2000), con 695, 751 y 770 aminoácidos respectivamente. La proteína APP se expresa en la mayoría de células del organismo pero las isoformas 751 (APP751) y 770 (APP770) aminoácidos se expresan principalmente en células no neurales, mientras que la isoforma de 695 aminoácidos (APP695) se expresa predominantemente en neuronas (Haass et al., 1991).

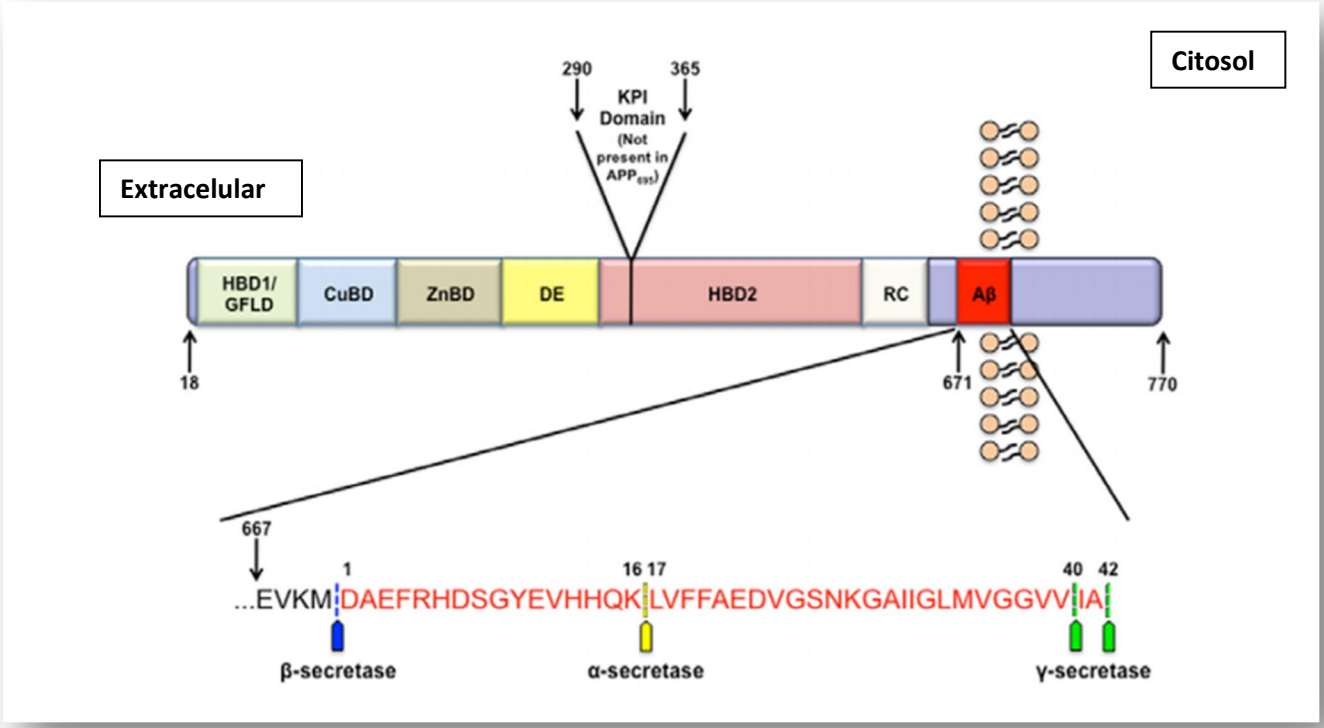

Figura 4.1. Esquema estructural de la Proteína Precursora del péptido β-amiloide (APP). Presenta tres dominios principales. Un dominio extracelular N-terminal, un dominio transmembrana y un dominio citosólico. El dominio extracelular contiene a su vez una serie de dominios funcionales, una región de estructura plegada al azar y el dominio β-amiloide (Aβ), que presenta parte de su estructura en el dominio extracelular y parte transmembrana. La imagen muestra la secuencia del péptido β-amiloide humano, indicando los puntos de corte de las diferentes enzimas implicadas en el procesamiento de APP. Figura tomada de Lazarov et al., 2012.

Esta proteína una vez sintetizada en el retículo endoplásmico (RE), es extensamente modificada por glucosilaciones (N- u O- glucosilaciones), además de por fosforilación y sulfatación; que tienen lugar durante su viaje hacia la membrana plasmática en la vía secretora (Walter y col., 1997).

4.1.1. Procesamiento del APP.

Existen dos vías alternativas para el procesamiento postraduccional de esta proteína (ver revisiones Zhang y col., 2011; Rajendran y Annaert, 2012) (Fig.4.2.). Durante la secreción e internalización a través de la vía secretora, APP puede sufrir diversas escisiones proteolíticas por las actividades de tres secretasas (α, β y γ secretasas). Según qué enzima lleve a cabo el corte la proteína APP será procesada por la **vía amiloidogénica** o por al **vía no amiloidogénica**. El péptido Aβ se genera únicamente por la ruta amiloidogénica, aunque durante el envejecimiento normal se genera Aβ, y esta generación está acusada en la EA.

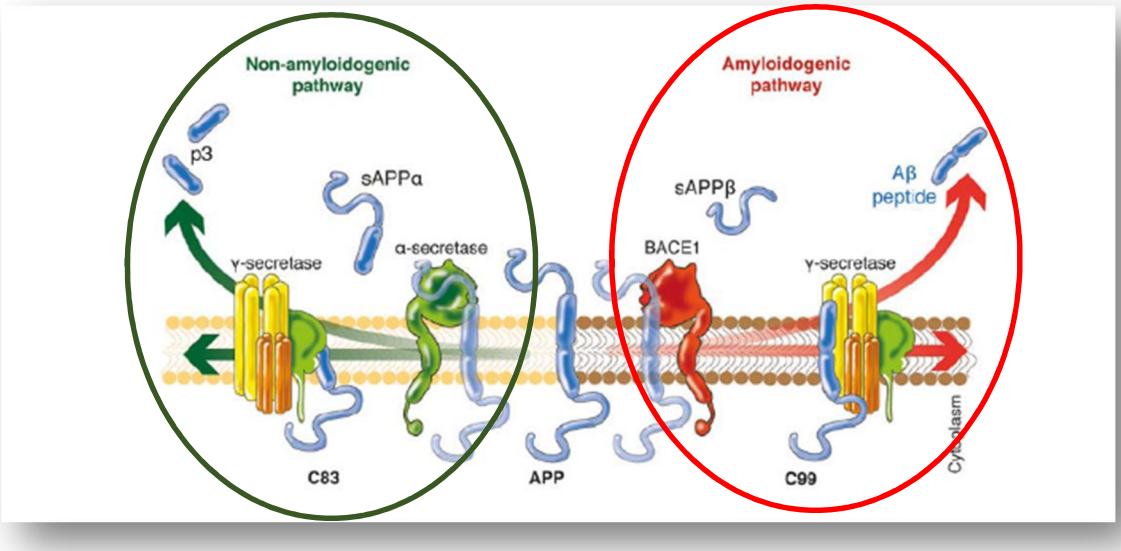

Figura 4.2. Procesamiento de la Proteína Precursora del péptido β-Amiloide (APP). Esquema explicativo de la ruta amiloidogénica y no amiloidogénica. A través de la ruta amiloidogénica se genera el péptido Aβ, que se acumula en el medio extracelular y forma las placas seniles características de la EA (Figura adaptada de Zolezzi et al., 2014).

4.1.2. Ruta no amiloidogénica.

En esta ruta no se genera péptido β-amiloide y es la predominante en la mayoría de las células. El proceso ocurre mayoritariamente en la membrana plasmática y en ella se produce en primer lugar la fragmentación de APP por el corte de la α-secretasa (perteneciente a la familia de las desintegrinas y metaloproteasas (ADAM)) generándose el fragmento sAPPα, que es un fragmento soluble que es liberado dentro del lumen vesicular o al espacio extracelular y que contiene el extremo N-terminal.

Por otro lado en el extremo C-terminal se genera un fragmento carboxi-terminal (APP-CTF) de 83 aminoácidos (C83) que queda anclado en la membrana y que es sustrato del complejo ɣ-secretasa. El fragmento C83 es cortado por este complejo enzimático, del que forma parte la presenilina, entre los aminoácidos 711 y 713, originando los péptidos P3 (Aβ 17-40 y Aβ17-42) que se libera al espacio extracelular o vesicular, y un dominio AICD (dominio intracelular de la proteína precursora amiloide, también llamado p7) que como su nombre indica queda en el citosol. AICD forma parte, junto a FE65 y FE60, de un complejo que regula la transcripción de varios de genes. (De Strooper, 2010). En esta ruta no se genera péptido Aβ, e incluso a los fragmentos generados se le atribuyen propiedades neurotróficas y neuroprotectoras, como es el caso del sAPPα, que actúa a través de receptores de insulina (Hiltunen y col., 2009). P3 puede aparecer formando parte de las placas pero en principio no es tóxico. (De Strooper, 2010).

4.1.3. Ruta amiloidogénica.

En esta ruta se genera péptido β-amiloide (de 39-43 aminoácidos) por la actuación consecutiva de la β-secretasa y del complejo ɣ- secretasa sobre APP (ver revisión Rajendran y Annaert, 2012). El primer corte es realizado por la β-secretasa, actividad que ha sido atribuida a la enzima BACE-1 (β-site APP cleaving enzime 1) (Vassar y col., 2009). Esta primera escisión se producen entre los aminoácidos Met671 y Asp672 dando lugar a un fragmento sAPPβ soluble que contiene el extremo N-terminal. También se genera un fragmento carboxi-terminal (CTF-APP) con 99 aminoácidos, conocido como C99, y que queda anclado en la membrana para ser procesado por el complejo de la ɣ-secretasa, que corta a C99 por los aminoácidos 711 y 713 generando el péptido β-amiloide (Aβ) que se libera al medio extracelular, y un ectodomino intracelular AICD (Takami et al., 2009).

Este procesamiento, que a excepción de las neuronas es minoritario en la mayoría de los tipos celulares, ocurre de forma mayoritaria en los compartimentos subcelulares. APP puede llegar a estos compartimentos al ser re-internalizada desde la membrana plasmática en un compartimento endosomal que contiene las proteasas BACE-1 y el complejo ɣ-secretasa; o bien pasa a dicho compartimento desde la red trans del Golgi a lo largo del sistema Golgi-endosoma-lisosoma. Estos sistemas membranosos son los posibles puntos de generación del Aβ (Greenfield y col., 1999; Thinakaran y Koo., 2008; Zhang y col., 2011). Este modelo de generación de Aβ se apoya en el hecho de que evitando la endocitosis de APP desde la superficie celular se bloquea la liberación del 80% del Aβ. (ver revisión O'Brien y Wong, 2011). También se han propuesto las llamadas balsas lipídicas (*lipid rafts*) como un posible lugar donde se genera el péptido Aβ (ver revisión Selkoe, 2008).

4.1.3.1. Enzimas implicadas en la ruta amiloidogénica (generando Aβ).

- **Enzima β-secretasa (BACE-1).**

Se trata de una aspartil proteasa transmembrana de tipo 1, localizada principalmente en compartimentos intracelulares. Estudios con modelos en los que se elimina la expresión de BACE-1 provoca la desaparición del Aβ cerebral, señalándola como la principal proteína con actividad β-secretasa a nivel cerebral (revisado por De Strooper et al., 2010).

Tras su síntesis en el RE como una pro-proteína sufre una serie de modificaciones post-traduccionales en su camino hacia el Golgi alcanzando con ellas su maduración final y su máxima actividad catalítica (revisado por Hunt and Turner 2009). La enzima madura es transportada a la superficie celular y desde allí es internalizada formando endosomas y vesículas asociadas al aparato de Golgi. Es aquí donde coinciden APP y BACE-1 y tiene lugar el procesamiento β-secretasa, generando el Aβ que posteriormente será secretado mediante exocitosis.

BACE-1 no sólo actúa sobre APP, tiene otros sustratos, esto supone un inconveniente para usarla como posible diana terapéutica ya que una actuación sobre su actividad produce una alteración sobre el resto de sustratos de la enzima (De Strooper, 2010; Hunt and Turner, 2009). Se han desarrollado varias moléculas que inhiben el procesamiento *in vitro* de APP por BACE-1, pero aún no se dispone de una molécula de vida media adecuada, capaz de atravesar la barrera hemato encefálica e inhibir de forma selectiva a BACE-1 sin afectar a otras aspartil-proteasas, pero se están realizando avances al respecto (De Strooper, 2010; Sankaranarayanan y col., 2009).

- **Complejo ɣ-secretasa.**

Se trata de un complejo aspartil-proteasa que procesa a APP dentro de la región transmembrana. Contiene cuatro subunidades diferentes: un núcleo catalítico y tres proteínas accesorias. La actividad aspartil proteasa la posee la presenilina 1 (PS1) o presenilina 2 (PS2), mientras que nicastrina, APH-1 (pharynx-defective-1) y PEN2 (presenilin enhancer 2) son necesarias para la maduración, la estabilidad y actividad del complejo (De Strooper, 2003; Wolfe and Kopan, 2004; Takasugi y col., 2003; Edbauer y col., 2003).

Al igual que BACE-1 el complejo ɣ-secretasa es considerado una posible diana terapeútica en el tratamiento de EA. No existe en la actualidad ninguna molécula capaz de inhibir selectivamente su actividad, además su inhibición normalmente se acompaña de una disminución en el procesamiento de otros sustratos que son necesarios para la supervivencia neuronal. Entre ellos podemos encontrar Nectina-1α, CD44, N-Caderinas, Receptores de LDL, Nav*β*2 y Notch, y participa en numerosas funciones celulares esenciales para la supervivencia (Wakabayashi y De Strooper, 2008; Parent y Thinakaran, 2010).

En este sentido, teniendo en cuenta el gran número de proteínas que pueden ser procesadas por el complejo ɣ-secretasa, se plantea como un objetivo complicado el obtener un inhibidor específico del procesamiento de APP, aunque en la actualidad se han obtenido compuestos capaces de inhibir el procesamiento de APP sin afectar al de Notch (De Strooper y col., 2010).

4.1.3.1.1. Enzimas implicadas en la degradación del péptido Aβ.

La acumulación defectuosa de cualquier proteína se debe a un desbalance entre su producción y los mecanismos de eliminación-aclaramiento de la misma. Evidentemente esto ocurre también en el caso de la acumulación del péptido β-amiloide (ver revisiones Evin y Weidemann, 2002; Thal y col., 2006; Duyckaerts y col., 2009). En los casos de FAD existe un aumento en la producción de Aβ, pero en los casos de Alzheimer esporádico no se muestran signos de un aumento en la producción, por lo que se ha sugerido que una disminución en su degradación y una reducción en el drenaje perivascular, implicado en el aclaramiento del mismo, podría explicar el aumento de la cantidad de Aβ en estos pacientes (Miners y col., 2014).

Existen varias enzimas que están implicadas en la degradación de las distintas formas que este péptido puede presentar. Entre ellas la neprelisina (NEP), plasmina, la enzima degradadora de insulina (IDE), la enzimas que procesan a endotelina (ECE-1,

ECE-2), la enzima que procesa angiotensina (ACE), distintas metalo-proteasas de matriz (MMPs) y las catepsina B y D (De Strooper., 2010). Estas enzimas están presentes en el parénquima cerebral o en las paredes vasculares, y la mayoría se expresan en neuronas, como es el caso de IDE, ECE, ACE, plasmina y NEP.

- **Neprelisina (NEP)**.

Se trata de una zinc-metalopeptidasa que se encuentra anclada a la membrana plasmática. Tiene capacidad de degradar Aβ monomérico y oligomérico (Kanemitsu y col., 2003). Los niveles de neprelisina disminuyen con el envejecimiento (Farris y col., 2007) y esto podría provocar un aumento de Aβ.

- **Enzima degradadora de Insulina (IDE).**

Es una tiol-metalopeptidasa que reconoce sustratos con estructura en hoja β-plegada. Degrada además del Aβ monomérico otros péptidos como la insulina, glucagón, TGF-α, amilina, IGF-1 e IGF-2. Se encuentra principalmente soluble en el citosol, aunque también puede detectarse en la superficie celular y en membranas intracelulares.

- **Enzimas que procesan a endotelina (ECEs).**

Son metalo-endopeptidadas dependientes de zinc tipo II que se encuentran ampliamente distribuidas por todo el endotelio vascular. Mientras que ECE-1 se expresa mayoritariamente en las células endoteliales, ECE-2 lo hace en el medio intracelular de las neuronas piramidales del hipocampo. Aunque se ha descrito que ECE-1 y ECE-2 están implicados en la degradación de A*β* (Eckman y col., 2001; Eckman y col., 2003; Eckman y col., 2006), en humanos no está del todo claro. Diversos estudios proponen aumentar la expresión de ECE-1 como factor protector de la EA (Funalot y col., 2004).

- **Plasmina.**

Se trata de una serin-proteasa que puede cortar al péptido Aβ por distintos sitios, además de evitar que adopte la conformación de hoja plegada β. En casos de EA existe una pérdida de expresión de esta enzima, especialmente en aquellos pacientes que presentan el alelo ε4 del gen APOE. Lo mismo ocurre con la expresión y/o actividad de NEP e IDE. Esta es una explicación más que razonable a la mayor predisposición de padecer EA que presenta aquellas personas con el alelo ε4 (Miners y col.,2008).

- **Metaloproteasas de matriz (MMPs).**

Son endopeptidasas dependientes de zinc y calcio que se expresan en neuronas, células gliales y vasculares. MMP-2, -3 y -9 tiene actividad catalítica sobre el péptido Aβ, y tienen la capacidad de procesar agregados de Aβ fibrilar (Miners et al.,2008).

- **Catepsinas**.

Son cistein-proteasas encargadas de degradar proteínas que han entrado en la vía endo-lisosomal. Esta enzima participa en la degradación de oligómeros y fibras de Aβ42 produciendo especies de Aβ con menor capacidad de agregación y mayor afinidad por IDE y NEP (Mueller-Steiner et al., 2006).

Algunas de estas enzimas actúan intracelularmente vía autofágica (Nixon, 2007; Mizushima y Komatsu, 2011; Nixon y Yang, 2011; Friedman y col., 2015) o vía lisosomal como es el caso de las catepsinas mencionadas anteriormente.

Pero aquí no acaban los mecanismos de aclaramiento del péptido Aβ, también en este proceso se han implicado a las células gliales que gracias a su capacidad fagocítica y de su capacidad de secreción de enzimas proteolíticas como NEP e IDE pueden eliminar el péptido del parénquima cerebral (Lee y Landreth, 2010).Este hecho está abriendo una nueva vía terapeútica mediatne protocolos de inmunización que puedan potenciar la capacidad fagocítica de estas células (Sokolowski y Mandell, 2011).

5. PROTEÍNA TAU: ESTRUCTURA, FUNCIÓN Y FOSFORILACIÓN.

5.1. Estructura de Tau.

Tau pertenece a la familia de las proteínas asociadas a microtúbulos: MAPs (Microtubule associated proteins), expresándose de forma predominante en las neuronas. Está codificada en el gen MAPT localizado en el cromosoma 17 (Neve y col., 1986). En el cerebro humano el procesamiento alternativo de su ARNm puede generar 6 isoformas. (ver revisiones Duyckaerts y col., 2009; Wang y col., 2013). Cada isoforma se caracteriza por la presencia o ausencia de fragmentos (N) de 29 ó 58 aminoácidos en el extremo amino-terminal, y de una secuencia de 31-32 aminoácidos que se repite 3 ó 4 veces en el extremo carboxilo-terminal (R), que constituye el "dominio de unión a microtúbulos". (Fig. 5.1). Durante el desarrollo neuronal Tau va cambiando de isoforma y de localización, de forma que durante el desarrollo fetal esta proteína se encuentra por todo el citosol celular (tanto en soma como en el axón) pero a medida que la neurona madura pasa a localizarse de forma casi exclusiva a lo largo del axón neuronal.

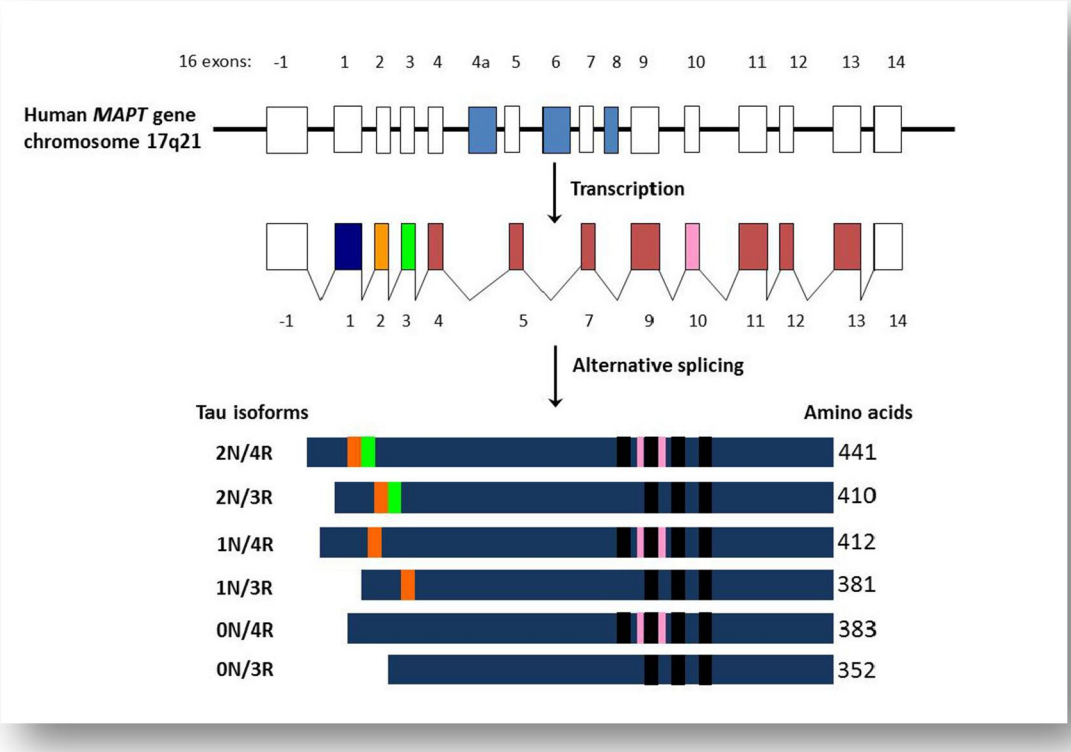

Figura 5.1. Esquema del gen MAPT y de las diferentes isoformas de Tau. El gen MAPT puede dar lugar a 6 isoformas de Tau tras el procesamiento alternativo de su ARNm. Figura modificada de Luna-Muñoz et al., 2013.

5.2. Función de la proteína Tau.

Su función es estabilizar los microtúbulos (MTs) del citoesqueleto y favorecer su polimerización (ver revisión Scholz y Mandelkow, 2014), por lo que es crítica para la supervivencia celular, ayudando a mantener la estructura interna de la célula y siendo fundamental en el transporte axonal y en la regulación sináptica (Spires-Jones and Hyman, 2014).

En condiciones fisiológicas Tau se asocia a los microtúbulos través del dominio de unión a microtúbulos y los estabiliza promoviendo su ensamblaje. Tras su unión a microtúbulos el extremos amino-terminal de Tau queda libre pudiendo interaccionar con distintas proteínas del citoesqueleto, proteínas de membrana o proteínas kinasas (revisado por Scholz and Mandelkow, 2014).También se han atribuido a Tau distintas funciones en procesos de señalización y de organización del citoesqueleto, que parecen depender del estado de fosforilación en las repeticiones del dominio de unión a microtúbulos (Morris et al., 2011).

Al fosforilarse tau y disociarse de los microtúbulos se produciría una pérdida de función de los mismos, con lo que se generan fallos en el transporte axonal y muerte neuronal (Gotz, 2001; Spires-Jones et al., 2009). Además, la agregación de Tau inhibe la actividad del proteasoma aumentando de esta forma el efecto negativo de la hiperfosforilación de Tau (Gendron y Petrucelli, 2009; Wang y col., 2013).

La agregación de Tau también se ve potenciada por otras modificaciones postraduccionales, como glicosilación, acetilación y ubiquitanación entre otras (Iqbal y Grundke-Iqbal, 2008; Wang y col., 2013).

5.3. Fosforilación de Tau.

El estado de fosforilación de cualquier proteína depende de la actividad de las enzimas quinasas y fosfatasas que actúan sobre ella. Hay más de 20 quinasas que pueden fosforilar a Tau y que se pueden dividir en 4 grupos: PDPKs (quinasas dependientes de prolina), no-PDPKs, quinasas que fosforilan residuos de tirosina y quinasas que fosforilan residuos de serina o treonina. De estas, las más estudiadas son la proteína quinasa dependiente de ciclina (CDK-5) y la quinasa glucógeno sintasa 3β (GSK-3) (Kimura y col., 2014), ambas son PDKs.

- **GSK-3β.**

Esta enzima pertenece al grupo de la PDPKs, y fosforila residuos localizados en las regiones de tau que están implicadas en la unión a microtúbulos. Esta enzima también interacciona con la presenilina 1 (PS1) participando por tanto en la producción de Aβ (Corbo y Alonso, 2011).

- **Cdk-5.**

También pertenece al grupo de las PDPKs y está formada por una subunidad catalítica (que es la propia Cdk-5) y el polipéptido p25 o p35 que actúa como unidad reguladora. El péptido p25 procede del procesamiento N-terminal de un péptido de mayor tamaño p35 llevado a cabo por la enzima calpaina proteasa dependiente de calcio. Fueron los estudios de Imahori y Uchida en 1997, los que pusieron de manifiesto la participación de Cdk5 en la enfermedad de Alzheimer al comprobar que las hiperfosforilaciones de Tau se producían en los mismos residuos sobre los que actuaba esta quinasa, y al reportar una acumulación de p25 en enfermos de AD. Varios estudios han descrito una mayor actividad enzimática del complejo formado por Cdk5-p25 que el Cdk5-p35 (revisado por Kimura et al., 2014).

La existencia de grandes cantidades de Aβ o estrés oxidativo en las células, puede provocar una desregulación en la actividad de las quinasas de Tau, provocando su hiperfosforilación. Además, se ha propuesto que el metabolismo de APP regula la proteostasis de Tau (Moore y col., 2015).

Tau tiene 80 residuos de serina o treonina además de 5 de tirosina con posibilidad de ser fosforilados. Esto residuos se encuentran la mayoría rodeando el dominio de unión a microtúbulos. La hiperfosforilación anómala de Tau produce un cambio conformacional que dificulta su unión a microtúbulos y desestabiliza la estructura axonal, formando agregados que interrumpen el transporte axonal (Scholz and Mandelkow, 2014). Cuando se desorganizan los microtúbulos, Tau al ser insoluble, tiende a agregarse formando los conocidos NTFs característicos de la patología de EA.

El estado de fosforilación de tau es regulado por diversas fosfatasas. En el cerebro humano, las fosfatasas más abundantes son PP2A y PP1 (Liu C. y col., 2013). A su vez PP2A regula la actividad de varias kinasas, entre ellas CaM-kinasa II, PKA y ERK1/2. Se ha observado que la actividad de PP2A está reducida en los cerebros de pacientes con EA.

6. RESPUESTA INFLAMATORIA. NEUROINFLAMACIÓN.

La inflamación se desencadena frente a diversos estímulos tras ponerse en marcha los mecanismos moleculares y celulares de la respuesta inmune innata. La respuesta inflamatoria es necesaria para la defensa del organismo y es beneficiosa si está regulada y se resuelve en un periodo de tiempo adecuado. El problema es cuando esta respuesta se vuelve crónica, excesiva o inapropiada, es entonces cuando pasa de ser beneficiosa a convertirse en patológica.

El sistema nervioso central (SNC) ha sido considerado durante muchos años un sistema inmunoprivilegiado, ya que la barrera hemato encefálica (BHE) restringe el acceso de mediadores y células inmunes al tejido cerebral (Glezer et al., 2007). Actualmente se sabe que, al igual que en el resto del organismo, un patógeno/lesión en el SNC es capaz de activar una respuesta inmune innata y desarrollar una respuesta inflamatoria que en este caso llamaremos **neuroinflamación**.

Como la BHE restringe el acceso de células del sistema inmune periférico al interior del cerebro, el SNC tiene la capacidad *per se* de generar una respuesta inmune innata ante cualquier tipo de lesión/daño, y/o infección. Para ello la células microgliales (fagocitos mononucleares residentes) liberan, en respuesta al antígeno, una serie de citoquinas y quimioquinas proinflamatorias, fagocíticas, citotóxicas y reguladoras de linfocitos T. Además de la microglía, los astrocitos también tienen un papel importante en el desarrollo de la respuesta neuroinflamatoria.

Mediante la liberación de citoquinas y quimioquinas, la microglía y los astrocitos participan en el reclutamiento de células del sistema inmune periférico (macrófagos, células dendríticas, linfocitos, etc.) al SNC (Kielian 2006).

Si el proceso neuroinflamatorio sobreactivado podría generar parte del daño celular y producir la pérdida de la función neuronal observado en la EA (Heneka y O'Banion, 2007; Perry y col., 2010; Heneka y col., 2015b; Heppner y col., 2015), al igual que ocurre en otras enfermedades neurodegenerativas, como el Parkinson (Mena y García de Yebenes, 2008).

De forma general se puede clasificar la respuesta inmune en **innata** o **adaptativa**. La respuesta inflamatoria que caracteriza a la mayoría de las enfermedades neurodegenerativas, incluida la EA, implica la activación de componentes de la respuesta inmune innata (a través de la microglía y astroglía; Heneka y col., 2015a), mientras que la respuesta inmune adaptativa y la infiltración de linfocitos T se da en menor grado.

Aunque la neuroinflamación no sea la principal causante de la neurodegeneración que se produce en la EA, existen múltiples evidencias que sugieren que desempeña un papel importante en la patogénesis de la misma (Nuzzo et al., 2014). Numerosos investigadores piensan que la neurodegeneración observada en los pacientes de EA está mediada por una respuesta inflamatoria crónica de las células de la glía activadas por los depósitos de *β*-amiloide (Butovsky y col., 2005; Sastre y col., 2006). Estos depósitos extracelulares de Aβ generan una activación de la microglía y la aparición de astrocitos reactivos, que pueden generar productos tóxicos que provoquen la muerte neuronal, tales como citoquinas inflamatorias, aminoácidos excitadores y ROS (Mrak y Griffin, 2005). Si fuese este Aβ el que inicia el proceso inflamatorio, serían las zonas en las que más Aβ se deposita, como el hipocampo, el subículo y la corteza entorrinal, las que muestran mayor activación microglial. Además, este proceso se ha asociado con la formación de placas de Aβ y ovillos neurofibrilares, ya que un ambiente inflamatorio puede activar las quinasas de Tau (ver revisión McNaull y col., 2010). En la actualidad aún se desconoce si la neuroinflamación es una consecuencia secundaria al proceso de neurodegeneración en la EA o es al contrario, siendo la inflamación una de las causas que provocan su aparición y desarrollo al generar muerte neuronal (Wyss-Coray, 2006; Glass y col., 2010).

El SNC posee un sistema inmune endógeno coordinado por células inmunocompetentes (Shie y Woltjer, 2007; Rogers y col., 2007; Deane y Zlokovic, 2007; Eikelenboom y col., 2006). Los responsables de la neuroinflamación pueden dividirse en:

- Componentes celulares del SNC: microglía, células dendríticas, astrocitos y neuronas.
- Mediadores inflamatorios: citoquinas liberadas por los componentes celulares anteriores.

6.1. Componentes celulares del sistema inmune del SNC.

6.1.1. Microglía.

Son células mieloides residentes en el SNC. La microglía representa entre un 0.5 y un 16.6% del total de células presentes en el cerebro humano, esta gran variabilidad es debida a una elevada diferencia en la distribución regional, presentando en general una mayor densidad en la sustancia blanca que en la sustancia gris (Mittelbronn et al., 2001).

Aunque aún no se conocen todas sus funciones en el SNC las células microgliales se consideran los "macrófagos del cerebro" (Ginhoux et al., 2010) constituyendo un claro agente protector. Entre sus funciones conocidas, destaca su participación en el sistema inmune innato como primera línea de defensa del SNC. La microglía tiene la capacidad de detectar y fagocitar patógenos, a la vez que activa la respuesta inflamatoria y recluta al resto de células inmunomoduladoras. También actúa sobre la proliferación, motilidad, migración, comunicación entre células y proteostasis.

En un cerebro adulto y sano, las células de la microglía se encuentran en un estado quiescente, con una morfología ramificada y una escasa expresión de moléculas asociadas a la función de macrófagos. Sin embargo, estudios recientes han revelado que la microglía residente posee procesos o ramificaciones altamente móviles, por lo que no se encuentran en estado de reposo, sino en una situación de escaneo o inspección continuo del entorno, sondeando su medio para detectar la posible llegada de algún tipo de daño. De esta forma, mientras que el soma permanece siempre en la misma posición las prolongaciones son capaces de barrer todo el entorno que las rodea. Cuando estas prolongaciones detectan una alteración la célula microglial cambia a un estado inflamatorio en el que su principal función es neutralizar al agente causante del daño. De esta forma rodea al patógeno/lesión con sus prolongaciones y se activan una serie de vías de señalización en el interior de la celular que ponen en marcha la liberación de citoquinas inflamatorias con el fin de activar al resto de células implicadas en la respuesta inmune (Gomez-Nicola and Perry, 2015).

La capacidad fagocítica de la microglía le permite limpiar el entorno de células muertas y de restos celulares que en el caso de quedarse en el parénquima podrían desencadenar una respuesta pro-inflamatoria. Desde este punto de vista, esta función fagocítica se puede considerar beneficiosa, sin embargo la microglía también fagocita células dañadas que aún no han muerto, produciendo una alteración en la sinapsis que puede llegar a ser neuropatológica, aunque por otro lado, una función importante de la microglia es su participación en la saneamiento y remodelación de las sinapsis tras la muerte de neuronas y células gliales que ocurre de manera fisiológica durante el desarrollo cerebral postnatal (Gomez-Nicola and Perry, 2015).

El efecto del envejecimiento sobre la microglía no conlleva necesariamente la pérdida de estas funciones, sino que implica una disfunción de las mismas y una respuesta hiperreactiva (Gomez-Nicola y Perry, 2015). De hecho, se ha observado que la microglía muestra cambios morfológicos y moleculares con el envejecimiento y

progresión de la EA, una mayor capacidad proliferativa y la presencia de microglía distrófica", caracterizada por la fragmentación, pérdida de prolongaciones, etc. (Baron y col., 2014; Mosher y Wyss-Coray,2014; Streit y col., 2014), algo que también se ha observado en modelos de la EA.

En la AD se produce una activación de la respuesta inmune innata microglial previa a la manifestación de la patología (Cribbs et al., 2012). Esta respuesta inflamatoria se mantiene a lo largo de la enfermedad y puede adoptar distintos fenotipos. A día de hoy existen dudas sobre si la microglía adopta estrictamente un solo fenotipo o puede modificarlo, y sobre los factores que hacen que la microglía cambie de un fenotipo a otro (Gómez-Nicola and Perry, 2015). Atendiendo a sus funciones y a las citoquinas liberadas, la microglia activada se clasifica en dos fenotipos: El **fenotipo clásico** (M1), típico de una respuesta proinflamatoria y citotóxica, que produce citoquinas y quimioquinas proinflamatorias, y el **fenotipo alternativo** (M2), que genera una respuesta inflamatoria contenida, pro-supervivencia, regeneradora y antiinflamatoria, liberando citoquinas anti-inflamatorias y factores tróficos.

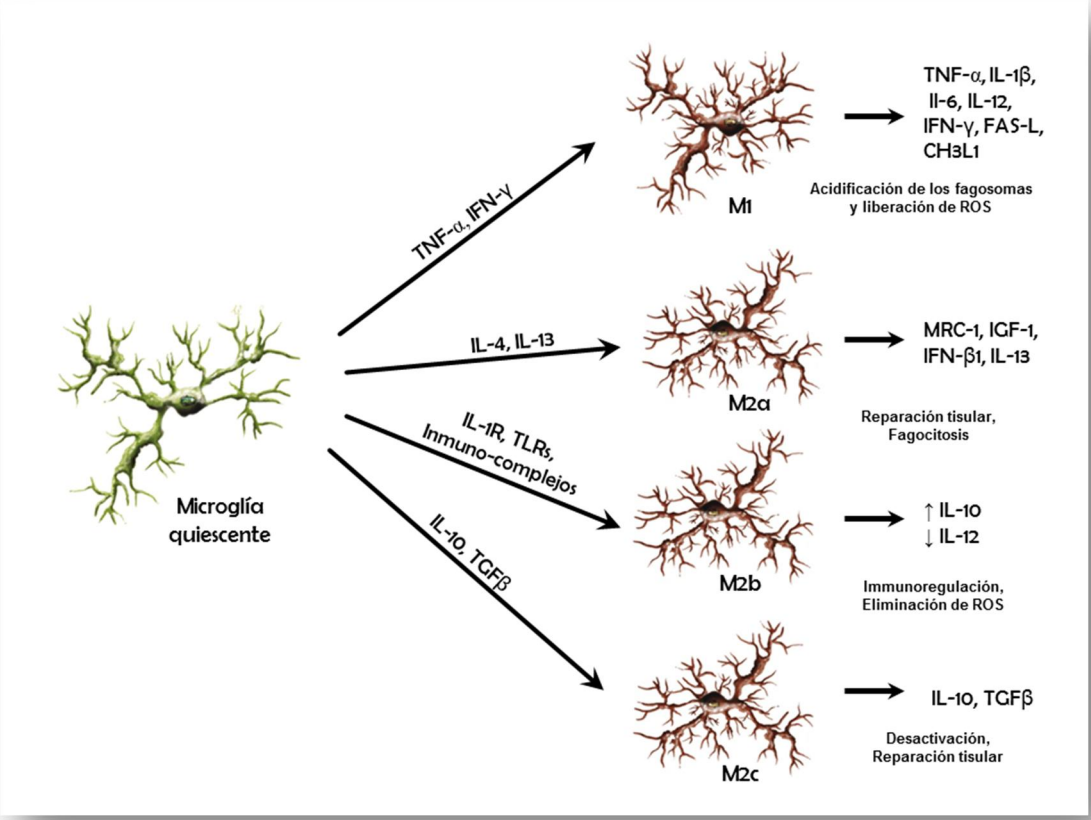

Figura 9. Fenotipos de Activación microglial. Fenotipo M1, Respuesta Inflamatoria Clásica. Fenotipo M2a, Respuesta Inflamatoria Alternativa: Protectora y antiinflamatoria. Fenotipo M2b, Respuesta Inflamatoria Alternativa: Regeneradora. Fenotipo M2c, Respuesta Inflamatoria Alternativa: Inmunomoduladora. Figura modificada de Kraft-Terry et al., 2009

6.1.1.1. Fenotipo Clásico o M1.

Se produce tras la exposición a IFN-ɣ, TNF-α, y/o ligandos de los receptores TLRs (toll like receptor). Como consecuencia, las células microgliales producen la liberación de una serie de factores neurotóxicos, que incluye especies reactivas de oxígeno (ROS) y nitrógeno, óxido nítrico, citoquinas y quimioquinas, entre ellas TNF-α, IL-1*β*, IL-6, IL-12, IFN-γ, IFN-*β*1, FAS-L, TRAIL y CH3L1 (Varnum and Ikezu, 2012), Todos estos factores tienen como finalidad la activación y mantenimiento de una respuesta inflamatoria tóxica que proteja al SNC del agente dañino. Sin embargo, si dicha respuesta inflamatoria se descontrola puede provocar daño celular y neurodegeneración debido a la presencia de esos factores citotóxicos.

La respuesta microglial M1 es similar a la activación de linfocitos Th1, y en ambas se produce un ciclo de activación entre las distintas células implicadas, creando un círculo vicioso de potenciación de la respuesta proinflamatoria (Cherry y col., 2014).

Como ya hemos mencionado, el fenotipo M1 tiene como objetivo presentar y eliminar al patógeno, y ello implica el aumento de expresión de ciertas proteínas, como MHC-II, la enzima óxido nítrico sintasa inducible (iNOS) o el receptor CD86 entre otras. Aunque generalmente la microglía activa M1 implica un aumento en la expresión de marcadores proinflamatorios y una disminución de proteínas antiinflamatorias (Cherry y col., 2014), hay autores que describen que dicha microglía puede expresar tanto marcadores clásicos como alternativos (Weekman y col., 2014).

6.1.1.2. Respuesta inflamatoria Alternativa o M2.

La respuesta alternativa inhibe la activación clásica de las células inmunes y promueve la reparación del tejido y la recuperación de la homeostasis, mediante la liberación de citoquinas y receptores antiinflamatorios y factores de crecimiento (Imai y col., 2007; Chhor y col., 2013).

El fenotipo M2 se clasifica a su vez en tres subtipos según los mediadores responsables de su activación (Fig. 6.1.) y los marcadores característicos que expresan (Colton y col., 2006).

A pesar de estar dividido en tres grupos, el fenotipo M2 tiene una función conjunta que es neutralizar al agente causante de la lesión sin dañar al tejido cerebral (Cherry y col., 2014).

- **M2a.**

  Esta respuesta se induce por IL4 e Il13 a través de los receptores TLRs. Se observa un aumento en la expresión de genes que tienen como objetivo evitar que se genere mayor respuesta inflamatoria y mantener un entorno neuroprotector. Entre ellos está Arginasa-1 (Arg-1) que disminuye la producción de NO; IGF-1 (Insulin growth factor-1), IL4, IL13 y MRC-1 (Mannose Receptor 1). Este estado de activación presenta capacidad fagocítica, necesaria para la eliminación del patógeno y de los restos celulares que hayan quedado como resultado de la respuesta inflamatoria citotóxica. Algunos de los receptores implicados en la fagocitosis son MSR-1 (macrophage scavenger receptor-1), SiRPβ-1 (Signal Regulatory Protein *β*-1) y CD36. TREM-2 y CD33 son dos receptores, implicados en la fagocitosis de A*β*, que han sido descritos como factores de riesgo de la EA.

- **M2b.**

  Este fenotipo es el menos conocido. La activación de este fenotipo es dependiente del inmuno-complejo, los TLRs y/o el receptor IL-1R (revisado por Boche et al., 2013). Se caracteriza por la falta de expresión de marcadores típicos M2, aunque presentan una expresión alta de IL-10 y baja de IL-12, característico de una polarización M2 (Mosser y Edwards, 2008). Este fenotipo, además, se ha relacionado con la activación de linfocitos Th2.

- **M2c**.

  Esta polarización tiene lugar gracias a la estimulación de IL-10 y TGF-*β*, dos potentes citoquinas antiinflamatorias. La actividad de estas células podría asociarse a una función regeneradora y reguladora de la respuesta inmune, que se pone en marcha una vez que las células polarizadas a M1 han hecho su función. TGF-*β* además se ha asociado a una mayor capacidad fagocítica de la microglía.

6.1.1.3. Papel de la microglia en la patología de la enfermedad de Alzheimer.

La implicación de la microglía en el desarrollo de la EA no se conoce con exactitud, y su papel debe ser entendido como dual y muy complejo, esto es lo nos hace pensar los datos que se tienen en la actualidad. Algunas de sus actuaciones son beneficiosas, pero otras, directa o indirectamente, pueden generar un ambiente citotóxico perjudicial para las neuronas.

Está claro que el péptido Aβ puede atraer y activar a la microglía (Malm y col., 2005; Meyer-Luehmann y col., 2008). Las prolongaciones de la microglía rodeando a la placa podrían constituir una barrera para evitar su expansión y contener la toxicidad de la misma. Es un hecho que las áreas de placas no cubiertas por microglía son menos compactas y están asociadas con una distrofia axonal más severa (Condello y col., 2015). La protección no queda en esta barrera física constituida por las prolongaciones celulares, ya que la fagocitosis activa del Aβ oligomérico (Frautschy y col., 1992; Mandrekar y col., 2009), y la actividad proteolítica de las enzimas que pueden secretar la microglía (Yang y col., 2011), no sólo actuarían reduciendo la polimerización del Aβ, sino que también tendría efecto sobre el posible crecimiento de la placa (Simard y col., 2006; Bolmont y col., 2008).

Todo esto se apoya por la presencia de receptores en las células microgliales que reconocen al péptido Aβ (Yu y Ye, 2015) y de enzimas, como la neprelisina, que son capaces de degradarlo.

Si la microglía desempeña un papel importante en el aclaramiento de A*β* en la EA, sería lógico pensar que la acumulación de dicho péptido en los estadios avanzados de la enfermedad puede ser indicativo de una deficiente actividad fagocítica microglial. Aunque en la actualidad no está claro si la microglía tiene la capacidad de degradar intracelularmente el Aβ internalizado o si esta capacidad se encuentra disminuida con el envejecimiento y progresión de la enfermedad.

Son distintos estudios los que involucran a la microglía con la EA, por ejemplo correlacionando ciertas variaciones genéticas en TREM2 (Triggering receptor expressed on myeloid cells 2), proteína reguladora de la fagocitosis en microglía y macrófagos, con un mayor riesgo para la EA (Guerreiro y col., 2013; Jonsson y col., 2013). También existen pruebas del papel del receptor microglial de quimocinas CX3CR1 (la unión de CX3CL1 neuronal a este receptor inhibe la activación clásica) en la pérdida neuronal, un ratón *knockout* para éste, no muestra muerte neuronal y presenta una menor carga amiloide (Fuhrmann y col., 2010; Liu y col., 2010; Cho y col., 2011).

Por otro lado, la microglía puede intervenir en el mantenimiento de la red neuronal (Kettenmann y col., 2013), lo que explicaría que la disminución en la complejidad de sus prolongaciones asociadas a la presencia de placas de Aβ fuese un factor clave en el deterioro cognitivo observado en algunos modelos de EA (Baron y col., 2014). Datos que junto al hecho de que la disminución microglial en ratones ocasiona un déficit cognitivo y una reducción en la actividad motora dependiente de formación de sinapsis dentro de la corteza motora (Parkhurst y col., 2013). Todos estos datos apoyan el papel activo que juega la microglía en el desarrollo y la evolución de la EA.

Por otro lado, la microglía podría causar neurotoxicidad debido a su capacidad de secretar citoquinas y especies reactivas de oxígeno (McGeer y McGeer, 2010).

Como hemos visto la microglía activada pueda generar mediadores proinflamatorios pero también es capaz de secretar citoquinas antiinflamatorias (Butovsky y col., 2006) y factores neuroprotectores (Streit, 2005). El posible papel neuroprotector de la inflamación en la EA está cobrando fuerza actualmente y, en apoyo a esta idea, está el estudio en el que la ausencia de microglía en un modelo animal provoca un incremento en la formación de placas y la muerte neuronal (El Khoury y col., 2007). Además en humanos y en animales transgénicos se ha observado la existencia de distintos tipos de activación microglial, pudiendo ocurrir un cambio durante la progresión de la enfermedad (Colton y col., 2006; Jiménez y col., 2008).

Queda por dilucidar si la función microglial juega un papel beneficioso o perjudicial en general, además se puede proponer la regulación de la actividad microglial como una nueva diana terapéutica para la EA (Condello y col., 2015).

6.1.2. Astroglia.

Son las células más numerosas del cerebro humano. Morfológicamente se caracterizan por presentar una estructura estrellada con múltiples prolongaciones que pueden conectar con vasos sanguíneos, neuronas, oligodendrocitos, microglía y otros astrocitos. Las proteínas más abundantemente expresadas en los astrocitos son GFAP (Glial fibrilary acidic protein) y vimentina (Vim). Los astrocitos reaccionan frente a agresiones físicas o químicas mediante un aumento en la producción de GFAP y vimentina en un proceso conocido como **astrogliosis**. Los dos grupos principales de astrocitos son los astrocitos protoplasmáticos que conectan con neuronas, y astrocitos fibrosos que conectan con los oligodendrocitos y los nódulos de Ranvier.

Los astrocitos desarrollan multiples funciones que son fundamentales para el correcto mantenimiento del SNC. Los protoplasmáticos generan una red de

comunicación entre neuronas y células vasculares que se extiende por todo el parénquima cerebral y que es fundamental para el mantenimiento de la actividad neuronal y del flujo sanguíneo cerebral (Fu y Jhamandas, 2014). Los astrocitos forman junto con las células del endotelio capilar y los pericitos vasculares la BHE que regula el paso de sustancias hacia el SNC (Ota y col., 2013). También intervienen en el mantenimiento de la homeostasis general del cerebro; la regulación del tono vascular; la liberación de factores tróficos como VEGF (Vascular endotelial growth factor), GDNF (glial cell line-derived neurotrophic factor) o bFGF (Basic fibroblastic growth factor), imprescindibles para el crecimiento y mantenimiento de la BHE y de las neuronas; la liberación de factores quimiotáxicos; el mantenimiento de la concentración de potasio y del pH; la liberación de gliotransmisores y glutamato; y la eliminación de neurotransmisores como GABA, glutamato y dopamina (Cabezas et al., 2014). Además, protegen a las neuronas del daño oxidativo, ya que poseen una alta actividad de la enzima superóxido dismutasa (Pertusa y col., 2007).

6.1.2.1. Papel de la Astroglía en la patología de la enfermedad de Alzheimer.

En la EA se produce una alteración de la red de astrocitos (ver revisión Oberheim y col., 2012), pudiendo afectar a cualquiera de sus funciones básicas. De forma que en tejidos post mortem de la EA y en el de ratones transgénicos modelos de la enfermedad se observa una reactividad astrocitaria generalizada (ver revisión Verkhratsky y col., 2010; Fu y Jhamandas, 2014).

La implicación de los astrocitos en la AD fue descrita por primera vez por Aloïs Alzheimer, que describió como los astrocitos se encontraban rodeando las placas de Aβ y en contacto con las neuronas dañadas. Esta relación íntima con la placa permite la fagocitosis del péptido Aβ, habiéndose observado Aβ en el interior de estas células de la astroglía (Nagele y col., 2003), sugiriendo su implicación activa en la síntesis o fagocitosis de Aβ, siendo más probable esta última opción, ya que se ha determinado la capacidad fagocítica *in vitro* e *in vivo* de los astrocitos (Wyss-Coray y col., 2003). Esta capacidad fagocítica permite el aclaramiento de las placas amiloides.

Ante cualquier daño en el SNC los astrocitos responden pasando a un estado de activación que puede ser tanto beneficioso como dañino (Sofroniew and Vinters, 2010). Los astrocitos reactivos se pueden concentrar en las regiones de placas de Aβ, no sólo fagocitando Aβ, sino también secretando moléculas proinflamatorias al ser activados por éstas. Estas moléculas pueden generar daños celulares (Johnstone y

col., 1999; Tuppo y Arias, 2005). Además, los astrocitos son capaces de producir NO (Simic y col., 2000) y expresan receptores para citoquinas inflamatorias como IL-1β y TNF-α (ver revisión Morales y col., 2014).

Todo esto está apoyado por estudios en los que se exponen astrocitos a Aβ, esto produce una activación caracterizada por la producción de citoquinas proinflamatorias, que son responsables a su vez, de una respuesta tóxica en la neurona y de una amplificación de la activación astroglial (Zhang y col., 2010; Scuderi y col., 2011).

Esta astrogliosis se observa también en los modelos animales de EA, aunque hay diferencias según la región estudiada, siendo mayor en el hipocampo que en la corteza entorrinal y prefrontal, de acuerdo con la diferente vulnerabilidad regional a la patología (revisado por Lim y col., 2014).

Las alteraciones cerebrovasculares, relacionadas con daños en la BHE, son un aspecto importante en la patología de EA (Kalaria, 2000; Kalaria, 1999). Estudios en pacientes humanos han demostrado que la disminución en la perfusión sanguínea y la hipoxia parecen aumentar el riesgo de padecer Alzheimer (Vermeer y col., 2003). En concreto se ha descrito que pacientes de EA presentan alteraciones del flujo sanguíneo en la corteza frontal temporal e hipocampo, y que aquellos pacientes con MCI (Mild Cognitive Impairment), con hipoperfusión en el giro parahipocampal, han terminado desarrollando la enfermedad (Park y col., 2011; Tang y col., 2012).

En la enfermedad de Alzheimer se produce la deposición de Aβ sobre la vasculatura cerebral provocando la obstrucción de los propios vasos. Como consecuencia se producen alteraciones en el intercambio de metabolitos y sustancias tóxicas, pérdida del flujo sanguíneo cerebral y la consecuente degeneración de neuronas y células gliales. La neuroinflamación característica de la EA, cursa con activación de células inmunocompetentes, entre las cuales se incluyen los astrocitos. Esta activación produce un cambio morfológico que afecta a los pies de los astrocitos, lo que puede producir alteraciones en la integridad de la BHE, provocando micro hemorragias cerebrales típicas en enfermos de EA (revisado por Avila-Muñoz y Arias, 2014).

Por otra parte, recientemente se ha sugerido que los astrocitos pueden desempeñar un papel relevante en el denominado "sistema glinfático" (Nedergaard, 2013), encargado de generar flujos de líquido intersticial, proveniente del espacio perivascular, desde las ramas arteriales hasta las ramas venosas. Este flujo "glinfático" estaría encargado de drenar el exceso de proteínas extracelulares, como

el Aβ evitando su acumulación. El papel activo en el aclaramiento es tal que la eliminación de la expresión de GFAP y vimentina en un modelo APP/PS1 de la EA, provoca una exacerbación de la carga amiloide, que es independiente del procesamiento de APP y de la producción de Aβ (Kraft y col., 2013), lo que sugiere que los astrocitos son importantes en la eliminación de este péptido.

A día de hoy el potencial patológico o neuroprotector de los astrocitos en la progresión de la EA no es bien conocido, siendo fundamental caracterizar a nivel funcional la astroglía reactiva.

6.2. Citoquinas y radicales libres.

Las citoquinas son moléculas de comunicación intercelular capaces de regular funciones celulares tan diversas como la proliferación, diferenciación, producción de otras moléculas y el proceso inflamatorio. En el proceso neuroinflamatorio están implicadas las células del sistema inmune, pero también estas moléculas de comunicación que aumentan el rendimiento de la respuesta inflamatoria. Estas moléculas son producidas, principalmente, por linfocitos y macrófagos en su estado activado. La mayoría de los mediadores inflamatorios tienen una expresión muy baja en el SNC sano y su efecto es muy limitado. Sin embargo, cuando se produce un daño se estimula la producción de estos mediadores, lo que desencadena la activación de otras células inflamatorias, el reclutamiento de células del sistema inmune o la inducción de otros mediadores de la respuesta inflamatoria (Rothwell y Luheshi, 2000). En el cerebro de pacientes de EA aparecen en niveles elevados, tanto las de la naturaleza pro- como antiinflamatoria, entre ellas las interleuquinas (IL-1, IL-4, IL-6, IL-10), TNF-α y TGF-β (Henekay O'Banion, 2007).

Los radicales libres intervienen en la respuesta inflamatoria que se da en la EA, ya que el Aβ puede activar directamente el complejo NADPH oxidasa (Mosher y WyssCoray, 2014). Entre ellos se encuentran las ROS, que pueden generar estrés oxidativo, y especies nitrogenadas, como el NO (Heneka y O'Banion, 2007). Los radicales libres pueden ser producidos tanto por las neuronas afectadas como por la microglía y astroglía activadas.

7. HIPÓTESIS DE LA ENFERMEDAD DE ALZHEIMER.

Existen diversas hipótesis sobre las causas que inician el desarrollo de la enfermedad de Alzheimer, a continuación vamos a realizar un pequeño resumen de las que tienen mayor peso en la actualidad (ver revisión De la Torre, 2011). Todas ellas tienen puntos en común, aunque se diferencian por la causa inicial que desencadena todo el proceso.

7.1. Hipótesis de la cascada amiloide.

Esta hipótesis establece que es la acumulación del péptido β-amiloide la causa inicial para el desarrollo de la enfermedad de Alzheimer (Hardy y Higgins, 1992).

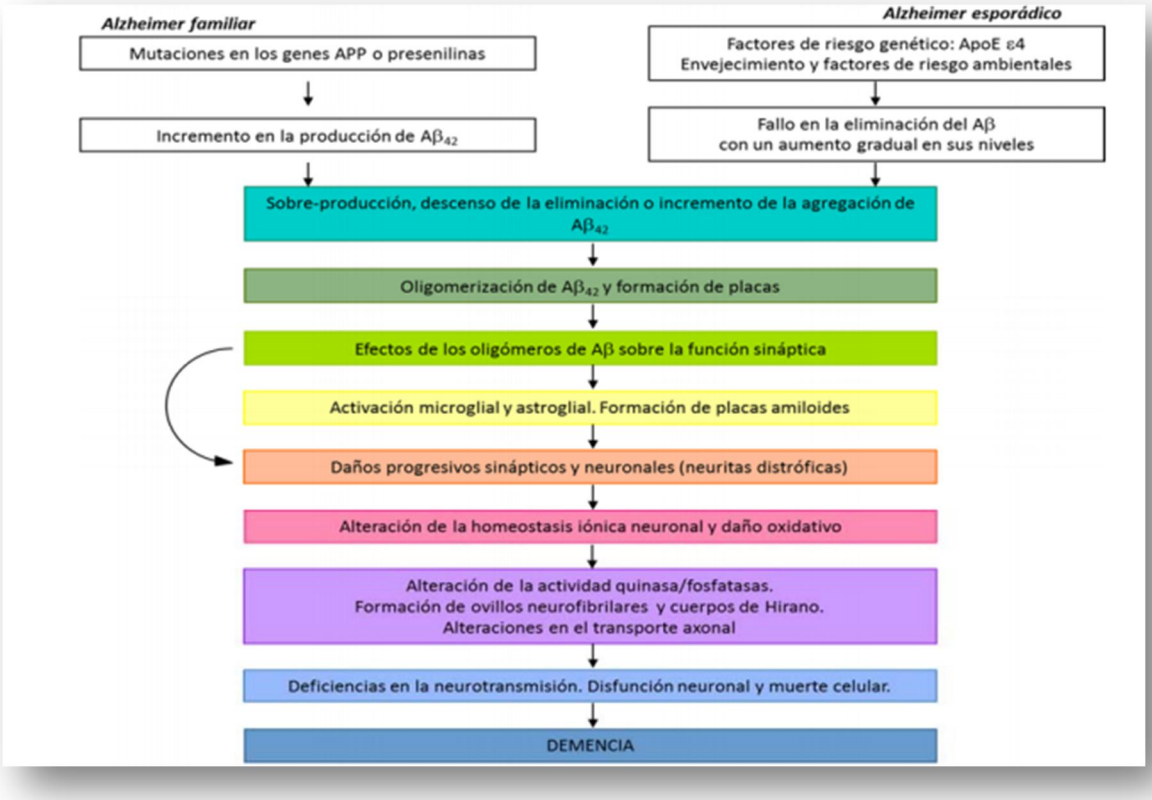

Figura 7.1. Posible sucesión de eventos que conforman la hipótesis de la cascada amiloide. Según esta hipótesis todo comienza con el depósito de Aβ. Este provoca la formación de NFTs, la muerte celular y la demencia. Se han identificado numerosos mecanismos por los que el péptido Aβ ejerce su efecto neurotoxico (ver Crews y Masliah, 2010). (Modificado de Haass y Selkoe, 2007).

Según esta hipótesis (Fig. 7.1) todo comienza con un cambio en el metabolismo de la proteína precursora del péptido β-amiloide que produce un incremento en la producción de Aβ, especialmente de la isoforma Aβ42 que tiene mayor tendencia a agregar. Esto da lugar a problemas en la función sináptica, generándose neuritas distróficas. La deposición de este Aβ en placas extracelulares provoca, además, una activación de la glía alrededor de las mismas. Esta activación mantenida en el tiempo genera estrés oxidativo afectando a la homeostasis neuronal.

Todos estos cambios provocan alteraciones en el transporte axonal y una alteración en el equilibrio de la actividad de las quinasas y las fosfatasas, desequilibrio que conduce a una hiperfosforilación de Tau con la consecuente formación de NTFs, que generan daños mayores en la organización de los axones y el transporte que por el él se desarrolla. La consecuencia final es una muerte neuronal masiva que conduce a un deterioro cognitivo progresivo que desencadena en demencia.

Está claro que el péptido Aβ tiene un papel relevante en el desarrollo y progresión de la EA, existen muchas evidencias que apoyan esta hipótesis, aunque también existen investigaciones que no apoyan esta secuencia tan directa entre el aumento de Aβ y el desarrollo de demencia.

El principal apoyo que tiene esta hipótesis es que las mutaciones implicadas en los casos de FAD se encuentran en los genes implicados en el metabolismo de Aβ, y que estas conducen a un aumento en la generación y acumulación del Aβ42. Es más, las personas con síndrome de Down (trisomía del par cromosómico 21, donde se localiza el gen APP) desarrollan placas a edades tempranas (Rovelet-Lecrux y col., 2006), lo que demuestra una relación directa entre la carga de APP y la acumulación del Aβ en placas.

Sin embargo, no todas las evidencias están a favor de esta hipótesis (Herrup, 2015), así podemos encontrar que haya animales transgénicos que sobreexpresan mutaciones en APP y no desarrollen la secuencia completa de eventos de esta cascada. Además, la aparición de placas y ovillos se produce en momentos y regiones diferentes (Armstrong, 2006). Por último, hay estudios que han mostrado una falta de correlación entre la carga amiloide y el daño cognitivo, y la ausencia de mejora cognitiva en los individuos inmunizados contra Aβ42 a pesar de la disminución de la carga amiloide observada (Karran y col., 2011; Musiek y Holtzman, 2015).

Para paliar estas contradicciones se ha propuesto que la neurodegeneración se produce debido a las formas oligoméricas tóxicas que desde la placa se pueden liberar al medio, considerando de esta forma a las mismas como entes más dinámicos. Esto conduciría a la reconciliación entre la hipótesis clásica y la oligomérica (Hardy y Selkoe, 2002; Walsh y Selkoe, 2007), ya que las formas oligoméricas de Aβ pueden

difundir a través del parénquima cerebral causando toxicidad neuronal incluso en aquellas zonas libres de placas.

7.2. Hipótesis de la neurodegeneración del citoesqueleto de las neuronas.

Según ésta todo comienza con la hiperfosforilación de la proteína Tau dando lugar a los NTFs. La desorganización de los microtúbulos produciría fallos en el transporte axonal que conduciría a la muerte neuronal con la liberación de Tau. Esta liberación anómala de Tau podría promover la agregación de Aβ continuando la cascada (ver revisión Gendron y Petrucelli, 2009).

7.3. Hipótesis colinérgica.

Gracias a esta hipótesis se han desarrollado los inhibidores de la acetilcolinesterasa (Bartus, 2000), uno de los pocos medicamentos usados en el tratamiento de la EA. Estos medicamentos son incapaces de parar la progresión de la enfermedad y sólo producen ciertas mejoras en la sintomatología inicial. Este fracaso constituye las principales razones para invalidar esta hipótesis que se propuso al observar una disminución de la actividad de la enzima de síntesis de este neurotransmisor en la corteza cerebral e hipocampo de pacientes, que correlacionaba con el daño cognitivo (Coyle y col., 1983), y una degeneración de neuronas colinérgicas en el telencéfalo basal (Whitehouse y col., 1982). Además la acetilcolina es uno de los principales neurotransmisores del SNC y periférico, implicado en el aprendizaje y la memoria. El sistema colinérgico está implicado también en la modulación de la expresión de factores neurotróficos importantes en la supervivencia neuronal (Craig y col., 2011).

7.4. Hipótesis neurovascular.

La hipoperfusión cerebral aparece durante el envejecimiento con una disminución del flujo sanguíneo de aproximadamente 0,5% por año, y ésta puede ser crítica para la supervivencia neuronal (Iadecola, 2004). La hipótesis neurovascular considera central el papel de enfermedades cerebrovasculares en el desarrollo de la EA, y se basa en estudios epidemiológicos que ligan los problemas vasculares con ésta (Deschaintre y col., 2009), en el solapamiento de los síntomas e histopatología de la demencia vascular y la EA (Kalaria, 2002), y en el hecho de que la EA suele aparecer asociada con una extensa angiopatía amiloide cerebral o ACC (deposiciones de Aβ en los vasos sanguíneos; Jiang y col., 2008).

7.5. Hipótesis inflamatoria.

Propone que la inflamación contribuye a la patogénesis inicial de la EA, ya que en los pacientes se han observado niveles altos de citoquinas proinflamatorias y un incremento de células microgliales activas alrededor de las placas. Dos estudios muestran una correlación negativa entre la función cognitiva y la activación de la microglía (Edison y col., 2008; Yokokura y col., 2011), aunque los resultados no son concluyentes (ver revisión Varnum e Ikezu, 2012). Además, esta hipótesis también se apoya en el hecho de que pacientes tratados con drogas antiinflamatorias presentan una menor incidencia de la EA (Morales y col., 2014).

7.6. Otras hipótesis de la EA.

Recientemente se han propuesto otras hipótesis explicativas, como la hipótesis **calpaína-catepsina** (Yamashima, 2013) o la del **estrés oxidativo** (Padurariu y col., 2013). Sin embargo, las teorías basadas en un único factor propuestas no se adecuan a los síntomas clínicos y neuropatológicos. McDonald (2002) ha propuesto un **modelo basado en cofactores**. Este modelo propone que son una combinación de diferentes de factores de riesgo de la EA (estrés, disfunción colinérgica, dieta, etc.) los que producen las variantes de la enfermedad. Una de las fortalezas de este modelo es que puede explicar las diferencias individuales observadas entre los pacientes y la diferente respuesta al tratamiento.

8. MODELOS ANIMALES DE LA ENFEMEDAD DE ALZHEIMER.

El desarrollo de estos modelos es fundamental en las investigaciones que se realizan sobre la EA. Por un lado permiten estudiar la evolución temporal de la enfermedad desde los estadios más tempranos, y por otro, son una herramienta necesaria para probar el efecto *in vivo* de posibles terapias desarrolladas para combatir la EA. (Yamada y Nabeshima, 2000; Webster y col., 2014).

En los últimos años se están desarrollando multitud de modelos de la EA, ninguno de ellos reproduce todos los efectos que la misma tiene en humanos, pero sí que están proporcionando una valiosa información sobre su patogénesis. Existen desde modelos espontáneos como monos viejos (Voytko y Tinkler, 2004), perros (Cummings y col., 1996) o ratones con senescencia acelerada; modelos invertebrados, como *Saccharomyces cerevisiae, Caenorhabditis elegans* (Alexander y col., 2014), *Drosophila melanogaster* (Crowther y col., 2004), o vertebrados como el pez cebra (Newman y col., 2014); modelos *in vitro*; modelos inducidos químicamente (Kausahl y col., 2013); aunque los más empleados para el estudio de esta enfermedad son los modelos transgénicos (Tg.) murinos, que portan las mutaciones encontradas en los pacientes de la EA familiar (ver revisiones Duyckaerts y col., 2008, Ashe y Zahs, 2010; Elder y col., 2010b; Bilkei-Gorzo, 2014; Neha y col., 2014; Webster y col., 2014).

Estos modelos, difieren en el fondo genético de los animales utilizados, en la mutación seleccionada, en el promotor utilizado, y en la técnica empleada para su obtención, por lo que existen grandes diferencias en las características neuropatológicas que manifiestan.

Los principales modelos desarrollados son:

8.1. Ratones transgénicos PS1.

Estos ratones sobre-expresan una forma mutada de la PS1 humana. Como consecuencia presentan una razón de Aβ42/Aβ40 incrementada, pero no desarrollan placas extracelulares del péptido β-amiloide (Borchelt y col., 1997), esto puede ser debido a que el Aβ murino presenta propiedades de agregación distintas al humano (Jankowsky y col., 2007).

Debido a la falta de patología de placas, los ratones transgénicos PS1 han sido menos utilizados que los APP. No obstante, estos modelos muestran pérdida neuronal y sináptica relacionada con la edad, así como patología vascular y déficits en la neurogénesis hipocampal (ver revisión Elder y col., 2010a). En este sentido, Chui y col.

(1999), fueron los primeros en describir un fenotipo neurodegenerativo en el ratón transgénico PS1L286V, mostrando una pérdida neuronal en el hipocampo y la neocorteza. Además, se ha mostrado una pérdida sináptica en modelos con la mutación M146L (Rutten y col., 2005) y A246E (Priller y col., 2007). Se ha propuesto que las mutaciones en PS incrementan la susceptibilidad neuronal al daño excitotóxico, ya que las neuronas con mutaciones en PS1 liberan una cantidad excesiva de calcio desde el RE (Small, 2009). Por otro lado, se ha observado una reducción en la fosforilación del residuo Ser9 de GSK-3β que se relaciona con un incremento en su actividad enzimática, en modelos PS1 (Tanemura y col., 2006; Dewachter y col., 2008), dando lugar a la hiperfosforilación de Tau. Además, se ha mostrado un incremento en el estrés oxidativo y la peroxidación lipídica y proteica en ratones PS1. Por último, se han detectado déficits de aprendizaje y memoria en modelos trasngénicos para PS, aunque son sutiles (ver revsión Elder y col., 2010a).

8.2. Ratones transgénicos APP.

Estos ratones sobre-expresan la forma mutada y/o no mutada de esta proteína. En la actualidad existen más de 40 tipos diferentes de animales transgénicos APP y más de 20 que expresan APP junto con otros genes relacionados, como PS1 y TAU (www.alzforum.org).

Nos vamos a centrar en el análisis de uno de estos ratones transgénicos, el modelo **APP23** que sobre-expresa la isoforma humana APP751 con la doble mutación *Swedish* bajo control del promotor Thy-1 murino (Sturchler-Pierrat y col., 1997). Este modelo presenta depósitos de Aβ a los 6 meses y déficits cognitivos desde los 3 meses de edad (Prut y col., 2007). También presenta activación de la glía (Bornemann y col., 2001), pérdida sináptica, hiperfosforilación de Tau (aunque no aparecen ovillos) y neuritas distróficas (Sturchler-Pierrat y Staufenbiel, 2000). La pérdida neuronal es moderada en la neocorteza y el hipocampo (Bondolfi y col., 2002), pero acusada en el *locus coeruleus* (Heneka y col., 2006). Además, este modelo muestra una prominente angiopatía amiloide (Beckmann y col., 2003). Sin lugar a dudas estos modelos transgénicos son mejores que los PS1 al compartir más rasgos (aunque no todos) con la patología observada en los humanos.

8.3. Ratones transgénicos bigénicos PS1/APP.

Estos modelos sobre-expresan ambas proteínas humanas mutadas. En este caso las manifestaciones patológicas de la enfermedad aparecen a edades comprendidas entre los 4 y 6 meses, lo que los convierte en modelos más interesantes. Por ejemplo desarrollan depósitos de Aβ mucho antes que los animales de la misma edad que expresan sólo uno de los genes mutados (Borchelt y col., 1996; Matarin y col., 2015). Sin embargo siguen sin reproducir totalmente la patología de la EA, ya que no presentan ni ovillos neurorfiblilares, ni muerte neuronal masiva. Vamos a hablar a continuación de dos de estos modelos.

El modelo doble transgénico **$PS1_{M146L}$/APP_{SL}** (que sobre-expresa PS1M146L, bajo el promotor HMG-CoA reductasa, junto con la isoforma 751 del APP con la doble mutación *Swedish* y la mutación *London*), generado por el grupo de Blanchard y col., (2003), presenta muerte neuronal en hipocampo y corteza entorrinal (Ramos y col., 2006; Moreno-González y col., 2009; Baglietto-Vargas y col., 2010). En este modelo aparecen las placas extracelulares a partir de los 3-4 meses, y presenta activación de la glía desde edades muy tempranas (Jiménez y col., 2008). Aunque no presenta ovillos neurofibrilares.

El modelo **$PS1_{dE9}$/APP_{SWE}**, bajo elpromotor PrP en un única inserción genómica, presenta déficits cognitivos a los 3 meses (Jankowsky y col., 2001) con fallos en el laberinto acuático de Morris a los 12 (Lalonde y col., 2005). Las placas de Aβ están presente desde las 6-8 semanas, muestra una intensa activación de la glía (Ruan y col., 2009) y neuritas positivas para Tau (Kurt y col., 2003). No obstante, no presenta una pérdida neuronal masiva, aunque algunas poblaciones presentan déficits significativos, como las neuronas catecolaminérgicas del *locus coeruleus* (O'Neil y col., 2007) y las interneuronas del hipocampo (Popovic y col., 2008).

El modelo **5xFAD**, fue descrito por Oakley y col. (2006) y presenta la doble mutación sueca y las mutaciones Florida (I716V) y *London* (V717I) en el gen APP, y dos mutaciones en PS1 (M146L+L286V). Desarrolla déficits cognitivos a los 3 meses de edad (Ohno y col., 2006) y Aβ intracelular a los 1,5 meses, con deposición extracelular a partir de los 2 meses. Además, presenta pérdida neuronal a partir de los 9 meses, que afecta a las neuronas noradrenérgicas (Kalinin y col., 2012) y colinérgicas (Devi y Ohno, 2010), así como de células piramidales en la corteza cerebral y el subículo (Oakley y col., 2006).

8.4. Ratones transgénicos basados en Tau.

Estos ratones sobre-expresan la proteína humana componente principal de los NTFs. Sin embargo, al sobre-expresar tau silvestre, sólo se ha conseguido desarrollar ovillos en un modelo y a partir de los 24 meses (Gotz, 2001). A pesar que no se identificado ninguna mutación en Tau en los pacientes de Alzheimer, los ovillos neurofibrilares sólo se encuentran en animales transgénicos que sobre-expresan la forma humana mutada de TAU. Al igual que ocurre en los transgénicos APP y PS1xAPP, los transgénicos tau tampoco desarrollan pérdida neuronal masiva.

Por lo tanto, ninguno de estos modelos reproducen al completo todas las manifestaciones patológicas que caracterizan a la enfermedad de Alzheimer.

8.5. Ratones transgénicos tri-génicos PS1/APP/Tau.

Para intentar conseguir la manifestación conjunta de placas de Aβ y ovillos neurofibrilares se desarrolló un modelo triple transgénico, **3xTg-AD**, con mutaciones en los genes para APP (APPSWE), Tau (P301L) y PS1 (M146L), bajo el promotor Thy-1.2 de ratón (Oddo y col., 2003). Este modelo muestra daños cognitivos a los 3-5 meses (Webster y col., 2014). En este modelo la progresión de la patología es comienza con la acumulación de Aβ intracelular, seguido de la hiperfosforilación de Tau, deposición de Aβ extracelular y aparición de NFTs (Oddo y col., 2003; Mastrangelo y Bowers, 2008).

Además presenta una pérdida noradrenérgica (Manaye y col., 2013) y colinérgica (Girao da Cruz y col., 2012), y activación microglial. Sin embargo, no hay una pérdida neuronal en el hipocampo, aunque si presenta disfunción sináptica. Este modelo ofrece la posibilidad de probar la interacción entre Aβ y Tau (Oddo y col., 2007), aunque la expresión de los tres genes a la vez, no permite analizar la implicación patológica de cada uno en la EA. Un año después, Boutajangout y col. (2004), desarrollaron otro animal triple transgénico sin mutaciones en TAU (PS1M146L, APP751SL, hTAu3R), que muestra placas a partir de los 2,5 meses, acumulación somato-dendrítica de Tau, neuritas distróficas con Tau hiperfosforilado. Sin embargo, no existen NFTs ni a los 18 meses.

b. Objetivos Generales

1. Estudio de la respuesta inflamatoria en hipocampo del doble transgénico, modelo de la Enfermedad de Alzheimer, $PS1_{M146L}/APP_{751SL}$. Evaluación de la misma con el transcurso de la edad del animal, y caracterización del cambio fenotípico sufrido en la activación de la microglial.

2. Evaluación del efecto tóxico producido por la acumulación de formas oligoméricas solubles a edades avanzadas en el modelo transgénico murino $PS1_{M146L}/APP_{751SL}$ de la enfermedad de Alzheimer. Estudio de la modulación de la ruta PI3K/Akt-GSK-3β mediada por la fracción soluble extracelular S1 obtenidas en ratones dobles transgénicos jóvenes (6 meses de edad) y viejos (18 meses de edad).

3. Efecto del tratamiento crónico mediante la ingesta oral de Litio en los ratones $PS1_{M146L}/APP_{751SL}$ modelos de la enfermedad de Alzheimer. Caracterización de cambios sufridos en la patología propia de la enfermedad de Alzheimer observado en este modelo animal transgénico.

4. Evaluación del contenido de Aβ en la fracción soluble en muestras post mortem de hipocampo de enfermos de EA y ratones transgénicos modelo de EA. Análisis de la posible repercusión, sobre el contenido de formas solubles de Aβ, del protocolo inicial de homogeneización del tejido usado en la preparación de las fracciones solubles S1. Estudio *in vitro* del efecto de estas fracciones S1 obtenidas mediante distintos protocolos de homogeneización.

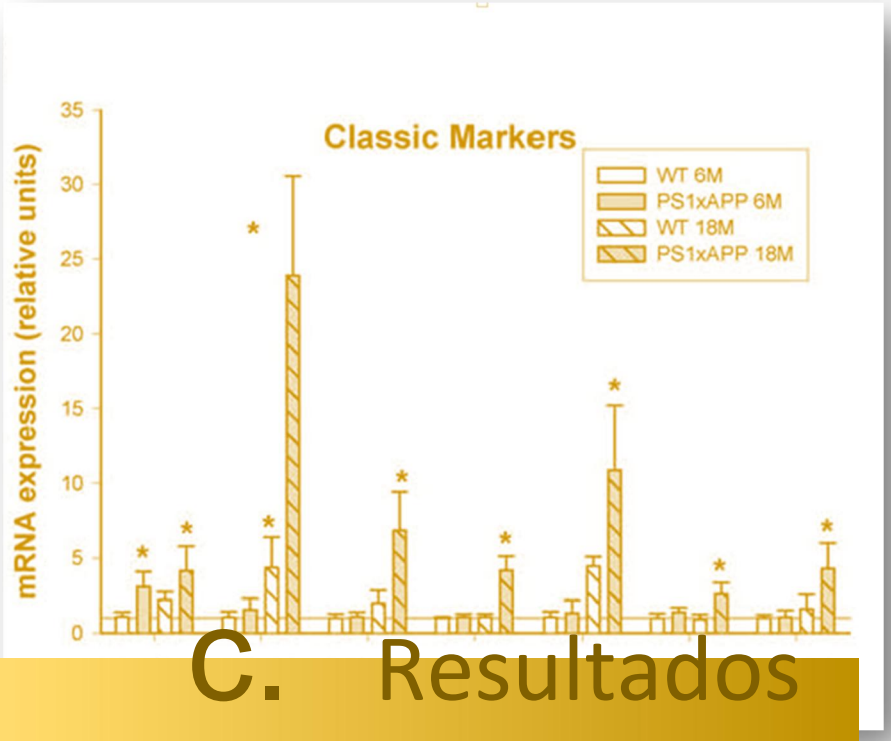

C. Resultados

Resultados: Capitulo I.

11650 • The Journal of Neuroscience, November 5, 2008 • 28(45):11650–11661

Neurobiology of Disease

Inflammatory Response in the Hippocampus of $PS1_{M146L}/APP_{751SL}$ Mouse Model of Alzheimer's Disease: Age-Dependent Switch in the Microglial Phenotype from Alternative to Classic

Sebastian Jimenez,[1,3,4]* David Baglietto-Vargas,[2,3]* Cristina Caballero,[1,3,4]* Ines Moreno-Gonzalez,[2,3] Manuel Torres,[1,3,4] Raquel Sanchez-Varo,[2,3] Diego Ruano,[1,3,4] Marisa Vizuete,[1,3,4] Antonia Gutierrez,[2,3] and Javier Vitorica[1,3,4]

[1]Department Bioquímica, Bromatologia, Toxicología y Medicina Legal, Facultad de Farmacia, Universidad de Sevilla, 41012 Sevilla, Spain, [2]Department Biologia Celular, Genetica y Fisiologia. Facultad de Ciencias, Universidad de Málaga, 29071 Málaga, Spain, [3]Centro de Investigación Biomédica en Red sobre Enfermedades Neurodegenerativas (CIBERNED) 41013 Sevilla, Spain, [4]Instituto de Biomedicina de Sevilla (IBiS)–Hospital Universitario Virgen del Rocío/CSIC/Universidad de Sevilla, 41013 Sevilla, Spain

Although the microglial activation is concomitant to the Alzheimer's disease, its precise role (neuroprotection vs neurodegeneration) has not yet been resolved. Here, we show the existence of an age-dependent phenotypic change of microglial activation in the hippocampus of *PS1xAPP* model, from an alternative activation state with Aβ phagocytic capabilities (at 6 months) to a classic cytotoxic phenotype (expressing TNF-α and related factors) at 18 months of age. This switch was coincident with high levels of soluble Aβ oligomers and a significant pyramidal neurodegeneration. *In vitro* assays, using astromicroglial cultures, demonstrated that oligomeric Aβ42 and soluble extracts from 18-month-old *PS1xAPP* hippocampus produced a potent TNF-α induction whereas monomeric Aβ42 and soluble extract from 6- or 18-month-old control and 6-month-old *PS1xAPP* hippocampi produced no stimulation. This stimulatory effect was avoided by immunodepletion using 6E10 or A11. In conclusion, our results show evidence of a switch in the activated microglia phenotype from alternative, at the beginning of Aβ pathology, to a classical at advanced stage of the disease in this model. This change was induced, at least in part, by the age-dependent accumulation of extracellular soluble Aβ oligomers. Finally, these cytotoxic activated microglial cells could participate in the neuronal lost observed in AD.

Key words: Alzheimer; transgenic model; neuroinflammation; hippocampus Aβ plaques; oligomers; hippocampus

Objetivos I

Estudio de la respuesta inflamatoria que tiene lugar en hipocampo del doble transgénico, modelo de la Enfermedad de Alzheimer, **$PS1_{M146L}$/APP_{751SL}.** Evaluación de la misma con el transcurso de la edad del animal, y caracterización del cambio fenotípico sufrido en la activación de la microglía.

a. Caracterización del estado de activación (alternativo y clásico) de las células microgliales en los ratones **$PS1_{M146L}$/APP_{751SL}** a los 6 y 18 meses de edad.

b. Estudio de la posible infiltración de linfocitos T (CD3+) en el parénquima de hipocampo de estos ratones transgénicos modelos de la EA y su vinculación con la activación de la microglía.

c. Cambios en la producción/acumulación de las formas solubles oligoméricas del péptido Aβ a los 6 y 18 meses de edad, y su implicación en la activación de las células microgliales.

Este trabajo se presenta como artículo.

11650 • The Journal of Neuroscience, November 5, 2008 • 28(45):11650–11661

Neurobiology of Disease

Inflammatory Response in the Hippocampus of $PS1_{M146L}/APP_{751SL}$ Mouse Model of Alzheimer's Disease: Age-Dependent Switch in the Microglial Phenotype from Alternative to Classic

Sebastian Jimenez,[1,3,4]* David Baglietto-Vargas,[2,3]* Cristina Caballero,[1,3,4]* Ines Moreno-Gonzalez,[2,3] Manuel Torres,[1,3,4] Raquel Sanchez-Varo,[2,3] Diego Ruano,[1,3,4] Marisa Vizuete,[1,3,4] Antonia Gutierrez,[2,3] and Javier Vitorica[1,3,4]

[1]Department Bioquímica, Bromatologia, Toxicología y Medicina Legal, Facultad de Farmacia, Universidad de Sevilla, 41012 Sevilla, Spain, [2]Department Biologia Celular, Genetica y Fisiologia. Facultad de Ciencias, Universidad de Málaga, 29071 Málaga, Spain, [3]Centro de Investigación Biomédica en Red sobre Enfermedades Neurodegenerativas (CIBERNED) 41013 Sevilla, Spain, [4]Instituto de Biomedicina de Sevilla (IBiS)–Hospital Universitario Virgen del Rocío/CSIC/Universidad de Sevilla, 41013 Sevilla, Spain

Although the microglial activation is concomitant to the Alzheimer's disease, its precise role (neuroprotection vs neurodegeneration) has not yet been resolved. Here, we show the existence of an age-dependent phenotypic change of microglial activation in the hippocampus of *PS1xAPP* model, from an alternative activation state with Aβ phagocytic capabilities (at 6 months) to a classic cytotoxic phenotype (expressing TNF-α and related factors) at 18 months of age. This switch was coincident with high levels of soluble Aβ oligomers and a significant pyramidal neurodegeneration. *In vitro* assays, using astromicroglial cultures, demonstrated that oligomeric Aβ42 and soluble extracts from 18-month-old *PS1xAPP* hippocampus produced a potent TNF-α induction whereas monomeric Aβ42 and soluble extract from 6- or 18-month-old control and 6-month-old *PS1xAPP* hippocampi produced no stimulation. This stimulatory effect was avoided by immunodepletion using 6E10 or A11. In conclusion, our results show evidence of a switch in the activated microglia phenotype from alternative, at the beginning of Aβ pathology, to a classical at advanced stage of the disease in this model. This change was induced, at least in part, by the age-dependent accumulation of extracellular soluble Aβ oligomers. Finally, these cytotoxic activated microglial cells could participate in the neuronal lost observed in AD.

Key words: Alzheimer; transgenic model; neuroinflammation; hippocampus Aβ plaques; oligomers; hippocampus

Introduction

As proposed by the inflammation hypothesis of Alzheimer's disease (AD), the neurodegenerative process could be exacerbated by a chronic inflammatory response to β-amyloid (Aβ) peptides (for review, see Griffin et al., 1998; Wyss-Coray, 2006; Heneka and O'Banion, 2007). Secondary to Aβ accumulation, there is an inflammatory response characterized by activated microglia and reactive astrocytes. Activated inflammatory cells could mediate neuronal damage by producing toxic products, such as inflammatory cytokines, excitatory amino acids, reactive oxygen intermediates and other factors (Mrak and Griffin, 2005; Craft et al., 2006; Ralay Ranaivo et al., 2006; Zipp and Aktas, 2006). This potential cytotoxic effect was further emphasized by clinical studies demonstrating that the symptoms of AD could be attenuated by nonsteroidal antiinflammatory drugs (Aisen, 2000; McGeer and McGeer, 2007). However, recent trials have not confirmed this positive effect (Aisen et al., 2003; Reines et al., 2004).

Although a deleterious inflammatory reaction could indeed mediate the neurodegeneration in AD, a completely different possibility is just beginning to be considered, supporting a trophic, proregenerative role of the inflammatory response. Activated glial cells are also capable to secrete anti-inflammatory cytokines (Butovsky et al., 2006), as well as neuroprotective factors that may protect against AD pathology (Streit, 2005). In this sense, vaccination against the Aβ peptides led to activation of microglia and successfully decreased amyloid load (Wilcock et al., 2003, 2004a,b). Similarly, stimulating the immune system with lypopolisaccharide (LPS) led to a reduction in Aβ plaques (DiCarlo et al., 2001; Herber et al., 2004). Nevertheless, at present little information is known about the balance between procytotoxic and anticytotoxic events occurring in AD or about the cellular and temporal induction of inflammatory cascade by Aβ.

Received June 30, 2008; revised Sept. 18, 2008; accepted Sept. 27, 2008.

This work was supported by Fondo de Investigadón Sanitaria (FIS) from Instituto de Salud Carlos III of Spain through Grants PI060567 (J.V.), PI060556 (A.G.), and PI060781 (D.R.), and by Junta de Andalucia, Proyecto de Excelencia CVI-902. S.J. and I.M.-G. are the recipients of a contract from CIBERNED. D.B.-V. and M.T. were recipients of PhD fellowships from Junta de Andalucia and R.S.-V. and C.C. from Ministerio de Educación y Ciencia (MEC) of Spain. We thank Dr. I. Torres-Aleman for his valuable critical reading of this manuscript, Drs. W. Klein and M. Lambert for their generous gift of Nu-1 antibody, and Dr. D. Pozo for his help with tissue culture experiments.

*S.J., D.B.-V., and C.C. contributed equally to this work.

Correspondence should be addressed to Javier Vitorica, Department Bioquímica, Bromatologia, Toxicologia y Medicina Legal, Facultad de Farmacia. Universidad de Sevilla, C/ Prof. García Gonzalez 2, 41012 Sevilla, Spain. E-mail: vitorica@us.es.

DOI:10.1523/JNEUROSCI.3024-08.2008

 0270-6474/08/2811650-12$15.00/0

Transgenic (tg) mice models are widely used to study AD pathology. We have previously characterized a double PS1xAPP tg mouse. These transgenic mice developed early (3–4 months) hippocampal Aβ plaques (Blanchard et al., 2003; Ramos et al., 2006; Caballero et al., 2007). In parallel with Aβ deposition, we also demonstrated the existence of degeneration of a particular subset of hippocampal GABAergic neurons (O-LM and HIPP cells; Ramos et al., 2006). However, despite the age-dependent accumulation of extracellular Aβ (Blanchard et al., 2003; Ramos et al., 2006; Caballero et al., 2007), no significant pyramidal degeneration was detected until 17–18 months of age (Schmitz et al., 2004; Ramos et al., 2006; unpublished results). Thus, it is possible that in the AD tg models the Aβ pathology could be attenuated until relatively old ages. In this work, we determined the *in vivo* inflammatory response in the hippocampus of *PS1xAPP* tg mice from a wide age range (from 2 to 18 months). At early ages (6 months), we have observed the activation of the microglial cells to an alternative phenotype, exclusively, surrounding the Aβ plaques. However, at 18 months of age, expanded microglial activation throughout all hippocampal layers displaying a classic cytotoxic phenotype was observed. Finally, we also investigated the reasons that could determine this age-dependent microglial phenotypic change.

Materials and Methods

Transgenic mice. The generation and initial characterization of the $PS1_{M146L}$ (PS1) and PS1xAPP751sl (*PS1xAPP*) tg mice have been reported previously (Blanchard et al., 2003). PS1 tg mice (C57BL/6 background) overexpressed the mutated PS1M146L form under the control of the HMGCoA-reductase promoter. *PS1xAPP* double tg mice (C57BL/6 background) were generated by crossing homozygotic PS1 tg mice with heterozygotic Thy1-APP751SL mice (all tg mice were provided by Transgenic Alliance-IFFA-Credo). Mice represented filial generation 10–15 (F10–F15) offspring of heterozygous tg mice. Only male mice were used in this work. Age-matched non-transgenic male mice of the same genetic background (C57BL/6) were used as controls (WT).

Anesthetized mice were killed by decapitation, and both hippocampi were dissected, frozen in liquid N_2, and stored at −80°C until use. All animal experiments were performed in accordance with the guidelines of the Committee of Animal Research of the University of Seville (Spain) and the European Union Regulations.

RNA and total protein extraction. Total RNA was extracted using the Tripure Isolation Reagent (Roche) as described previously (Ramos et al., 2006; Caballero et al., 2007). The contaminating DNA in the RNA samples was removed by incubation with DNAase (Sigma-Aldrich) and confirmed by PCR analysis of total RNA samples prior reverse transcription (RT). After isolation, the integrity of the RNA samples was assessed by agarose gel electrophoresis. The yield of total RNA was determined by measuring the absorbance (260 of 280 nm) of ethanol-precipitated aliquots of the samples. The recovery of RNA was comparable in all groups (1.2–1.5 μg/mg tissue).

The protein pellets, obtained using the Tripure Isolation Reagent, were resuspended in 4% SDS and 8 M urea in 40 mM Tris-HCl, pH 7.4, and rotated overnight at room temperature (Ramos et al., 2006; Caballero et al., 2007).

Retrotranscription and real-time RT-PCR. The retrotranscription was done using random hexamers, 3 μg of total RNA as template and High-Capacity cDNA Archive Kit (Applied Biosystems) following the manufacturer recommendations (Ramos et al., 2006; Caballero et al., 2007). For real time RT-PCR, each specific gene product was amplified using commercial Taqman probes, following the instruction of the manufacturer (Applied Biosystems), using an ABI Prism 7000 sequence detector (Applied Biosystems). For each assay, a standard curve was first constructed, using increasing amounts of cDNA. In all cases, the slope of the curves indicated optimal PCR conditions (slope 3.2–3.4). The cDNA levels of the different mice were determined using two different housekeepers [i.e., glyceraldehyde-3-phosphate dehydrogenase (GAPDH) and β-actin]. The amplification of the housekeepers was done in parallel with the gene to be analyzed. Similar results were obtained using both housekeepers. Thus, the results were normalized using only the GAPDH expression.

Independently of the gene analyzed, the results were always expressed using the comparative Ct method, after the Bulleting number 2 from Applied Biosystems. As a control condition, we selected 6-month-old WT mice. In consequence, the expression of all tested genes, for all ages and mice types, was referenced to the expression levels observed in 6-month-old WT mice.

Peptide preparation. To prepare the Aβ42 peptides, we allowed synthetic lyophilized Aβ1–42 peptide (human sequence; AnaSpec) to equilibrate, at 20–23°C, for 30 min before it was resuspended and diluted to 1 mM in 1,1′,1″,3,3′,3″-hexafluoro-2-propanol. After evaporation, peptide films were dried in a Speed Vacuum and stored at −40°C. Peptide films were resuspended to 5 mM in dimethyl sulfoxide (DMSO) for 10 min. To form the ADDLs (Lambert et al., 2001), we diluted the 5 mM DMSO solution to 100 μM in cold PBS, vortexed for 30 s, and incubated overnight at 4°C. Before use, the Aβ-PBS solution was further diluted in culture media. The presence of ADDLs was tested by Western blots using 6E10 (data not shown).

To form the monomers, immediately before use, we diluted the 5 mM DMSO solution in PBS (to a final concentration of 100 μM), followed by ultrafiltration through 5 kDa cutoff device (Vivaspin 2; Sartorius Biolab Products). The presence of the monomeric Aβ42 peptide (Mr 4.5 kDa) was verified by Western blots (data not shown).

Soluble protein extraction. The soluble fractions (S1) were obtained by ultracentrifugation of the homogenates as described previously (Kayed et al., 2003). Briefly, tissue samples were homogenized (using a Teflon-glass homogenizer) in cold PBS [containing a mixture of protease inhibitors (Sigma-Aldrich)] and ultracentrifuged (Optima MAX Preparative Ultracentrifuge; Beckman Coulter) at 120,000 × g, 4°C, during 60 min. Immediately after centrifugation, the samples were aliquoted and stored at −81°C until use. The protein content in the soluble fractions was determined by Lowry.

Western blot and dot blot. Western blots were performed as described previously (Araujo et al., 1996). Briefly, 20 μg of protein from the different samples were loaded on 16% SDS-Tris-Tricine-PAGE and transferred to nitrocellulose (Hybond-C Extra; Amersham). After blocking, the membranes were incubated overnight, at 4°C, with the appropriate antibody (monoclonal 6E10, Sigma-Aldrich; dilution 1:2000). The membranes were then incubated with anti-mouse horseradish-peroxidase-conjugated secondary antibody (Dako) at a dilution of 1:8000. The blots were developed using the ECL-plus detection method (Amersham).

Dot-blots were done as described previously (Araujo et al., 1996; Lambert et al., 2007). One microgram of protein from the different soluble fractions was directly applied to dry nitrocellulose in a final volume of 2 μl. Blots were air-dried, blocked for 1 h, and incubated overnight at 4°C, with either Nu-1 (courtesy of Dr. W. Klein, Northwestern University, Evanston, IL; 1 μg/ml) or A11 (1:5000 dilution; Biosource) antibodies. After the incubation, the blots were washed and visualized as described above. For quantification, the scanned (Epson 3200) images were analyzed using PCBAS program. In each experiment, the intensity of dots from WT mice were averaged and considered as background of the corresponding age group. Data were always normalized by the specific signal observed in 6-month-old *PS1xAPP* group.

Tissue preparation. After deep anesthesia with sodium pentobarbital (60 mg/kg), 2-, 4-, 6-, 12-, and 18-month-old WT and *PS1xAPP* tg male mice were perfused transcardially with 0.1M PBS, pH 7.4 followed by 4% paraformaldehyde, 75 mM lysine, 10 mM sodium metaperiodate in 0.1 M phosphate buffer (PB), pH 7.4. Brains were then removed, postfixed overnight in the same fixative at 4°C, cryoprotected in 30% sucrose, sectioned at 40 μm thickness in the coronal plane on a freezing microtome and serially collected in wells containing cold PBS and 0.02% sodium azide. Each experiment was composed of 3–6 sets of animals (each one containing one WT and one *PS1xAPP* tg mice). All animal experiments were approved by the Committee of Animal Use for Re-

search of the Malaga University (Spain) and the European Union Regulations.

Immunohistochemistry. Coronal free-floating sections (40 μm thick) from WT and *PS1xAPP* hippocampus were first treated with 3% H_2O_2/3% methanol in PBS and with avidin-biotin Blocking Kit (Vector Labs). For single immunolabeling, sections were incubated overnight at room temperature with one of the following primary antibodies: mouse monoclonal anti-Aβ 6E10 (1:1500 dilution; Sigma), rat monoclonal anti-CD11b (1:150,000; Serotec), chicken polyclonal anti-GFAP (1:10,000; Dako), hamster monoclonal anti-CD3 (1:100; BD PharMingen), rat monoclonal anti-TNFalpha (1:100; Abcam), rabbit polyclonal anti-iNOS (1:1000; Transduction Laboratories), goat polyclonal anti-IL4 (1:250 dilution; SantaCruz), and goat polyclonal anti-AMCase (YM-1; 1:100 dilution; SantaCruz). The tissue-bound primary antibody was detected by incubating with the corresponding biotinylated secondary antibody (1:500 dilution; Vector Laboratories), and then followed by streptavidin-conjugated horseradish peroxidase (Sigma-Aldrich), diluted 1:2000. The peroxidase reaction was visualized with 0.05% 3-3′-diaminobenzidine tetrahydrochloride (DAB, Sigma-Aldrich), 0.03% nickel ammonium sulfate, and 0.01% hydrogen peroxide in PBS. Some immunolabeled sections were then incubated for 3 min in a solution of 20% Congo red. Sections were then mounted on gelatin-coated slides, air dried, dehydrated in graded ethanols, cleared in xylene and coverslipped with DPX (BDH) mounting medium. Specificity of the immune reactions was controlled by omitting the primary antiserum.

For double immunofluorescence labeling (GFAP-6E10, GFAP-iNOS, GFAP-IL4, or CD3-IL4), sections were first sequentially incubated with the primaries antibodies (see antibodies above listed), followed by the corresponding Alexa488/Alexa568-conjugated secondary antibodies (1:1000 dilution, Invitrogen) or by biotinylated secondary antibody (1:500; Vector Laboratories) and streptavidin-conjugated Alexa488/568 (1:2000 dilution; Invitrogen). For double CD11b-Thioflavin-S, YM1-Tomato lectin, 6E10-Tomato lectin or IL4-Tomato lectin, fluorescence labeling, sections were first incubated with the primary antibody followed by Alexa568 or Alexa488 conjugated secondary antibody. Then, sections were washed and processed for thioflavin-S staining (see below) or incubated for 1 h with a solution of 5 μg/ml biotinylated Tomato lectin (Sigma) followed by streptavidin-conjugated Alexa 568 (1:1000; Invitrogen). Sections were mounted onto gelatin-coated slides, coverslipped with 0.01 M PBS containing 50% glycerin and 2.5% triethylenediamine and then examined under a confocal laser microscope (Leica TCS-NT).

Thioflavin S staining. Free-floating sections were incubated for 5 min with 0.015% Thio-S (Sigma) in 50% ethanol, and then washed in 50% ethanol, mounted onto gelatin-coated slides and coverslipped with 0.01M PBS containing 50% glycerin and 2.5% triethylenediamine.

Plaque loading and plaque size distribution. Hippocampal 6E10 immunostaining from 2-, 4-, 6-, 12-, and 18-month-old *PS1xAPP* mice was observed under a Nikon Eclipse 50i microscope using a 4× objective and images acquired with a Nikon DS-5M high-resolution digital camera. The camera settings were adjusted at the start of the experiment and maintained for uniformity. Digital images (seven sections per mouse and six mice per age group) were analyzed using Visilog 6.3 analysis program (Noesis). The plaque area within the hippocampus was identified by bright-level threshold, the level of which was maintained throughout the experiment for uniformity. The gray-scale image was converted to a binary image with plaque and hippocampal field areas identified. Plaque loading was defined as percentage of total hippocampal area stained for Aβ, excluding principal cell layers intracellular labeling that was removed by manual editing. The hippocampal area in each 4×image was manually outlined. The plaque loading (percentage) for each tg mouse was estimated and defined as (sum plaque area measured/sum hippocampal area analyzed) ×100. The sums were taken over all slides sampled and a single plaque burden was computed for each mouse. The mean and SD of the plaque loading were determined using all the available data. Quantitative comparisons were performed on sections processed at the same time.

For β-amyloid plaque morphometric analysis (surface area), three coronal sections immunostained with 6E10 from 6- ($n = 3$), 12 ($n = 3$) and 18-month-old ($n = 3$) *PS1xAPP* mice were analyzed using the nucleator method with isotropic probes by the NewCast software package from Olympus sterological system. Hippocampal CA1 subfield (9 sections per age) was analyzed using a counting frame of 7154.7 μm^2 and step lengths of 299.55 × 225.54 μm. For individual plaque measurement we used the 40× objective. Number of plaques/mm^2 falling into four surface categories (ranging from <200 μm^2 to >2000 μm^2) was calculated. Each analysis was done by a single examiner blinded to sample identities.

Stereology. Cresyl-violet stained CA1 principal cell nuclei belonging to 6-, 12-, and 18-month-old WT and *PS1xAPP* mice ($n = 6$/group/age; 10–15 sections per animal) were quantified according to the optical fractionator method, using an Olympus BX51 microscope (Olympus), interfaced with a computer and a color JVC digital videocamera. The CAST-Grid software package (Olympus) generated sampling frames with a known area (a_{frame}) and directed the motorized X-Y stage (Prior Proscan; Prior Scientific Instruments), and a microcator (MT12; Heidenheim), which monitored the movements in the *z*-axis with a resolution of 0.5 μm. The number of neurons was quantified in every seventh section (with a distance of 280 μm) through the entire anteroposterior extent of the hippocampus (between −0.94 mm anterior and 3.64 mm posterior to Bregman according to the atlas of Paxinos and Watson). This selection criteria prevented counting neurons from contiguous sections. CA1 subfield was defined using a 10× objective and the number of principal cells was counted using a 100×/1.35 objective. Each counting frame was 2342.8 μm^2. We used the optical 3 μm from the upper surfaces as look-up, and those 3–13 μm from the surfaces as reference sections. The software calculated the estimated total number of cresyl-violet stained nuclei in the CA1 region using the optical fractionator formula (West et al., 1991; Schmitz and Hof, 2005), $N = 1/bsf.1/ssf.1/asf.1/hsf.\Sigma Q^-$, where bsf is the block sampling fraction, ssf represents the section sampling fraction, asf is the area sampling fraction, which is calculated by dividing the area sampled with the total area of the layer, hsf stands for the height sampling fraction, which is calculated by dividing the height sampled (10 μm in this study) with the section thickness, and ΣQ^- is the total count of nuclei sampled for the entire layer. The precision of the individual estimations is expressed by the coefficient of error (CE) (Gundersen et al., 1999) and here we have estimated the total CE (CE group value) that was calculated using the CEs in each individual animal. The CEs ranged between 0.03 and 0.07.

The numerical density (Nv) of activated microglial cells (number of cells per mm^3) was determined in the CA1 subfield using the NewCast Grid Stereological System from Olympus. For each animal from 6- ($n = 3$) and 18- ($n = 3$) month-old *PS1xAPP*, activated microglial cells were quantified with the optical dissector method in two slices immunostained with anti-CD11b at −1.82 mm and 2.30 mm from the Bregman according to the atlas of Paxinos and Watson. Each section was analyzed using a systematically random manner, the counting frame was 29,031 μm^2 and step lengths of 121.06 × 91.15 μm. CA1 subfield was defined using a 4× objective and the number of activated microglia cells was counted using a 100×/1.35 objective. We used the optical 3 μm from the upper surfaces as look-up, and that 3–13 μm from the surface as references sections and optical dissector height was 10 μm. The Nv of microglial cells per mm^3 was calculated by using the following equation: $Nv = \Sigma Q/\Sigma a \times h$. Where Q is the number of activated microglial cells per counting box, a is the area of the counting frame, and h is the height of the optical dissector. The average number of cells per mm^3 was derived for each section. Animal means were derived by averaging the Nv from two sections from each animal in the CA1 subfield.

Astro-microglial cultures. Mixed astromicroglial primary cultures were prepared from newborn C57BL/6 mice (1–3 d). Briefly, dissected brains were treated, for 5 min, with trypsin-DMEM-EDTA medium (Biowhittaker, Cambrex). The treatment was stopped using complete DMEM-F12 plus 10% FBS and the cells were mechanically dissociated. After mechanical dissociation, the debris were eliminated by filtration (40 μm; BD Falcon) and the cells were seeded (at a density of 250.000 cells/ml) in DMEM-F12 plus 10% FBS medium (containing glutamine, nonessential amino acids, 1% penicillin-streptomycin and gentamycin) on poly-D-lysine (Sigma-Aldrich) -treated Nunc 12-well plates. The cells were cultured at 37°C, in humidified 5% CO_2/95% atmosphere. Medium was replaced every 4 d. After 13–15 d in culture, the mixed glial cultures were

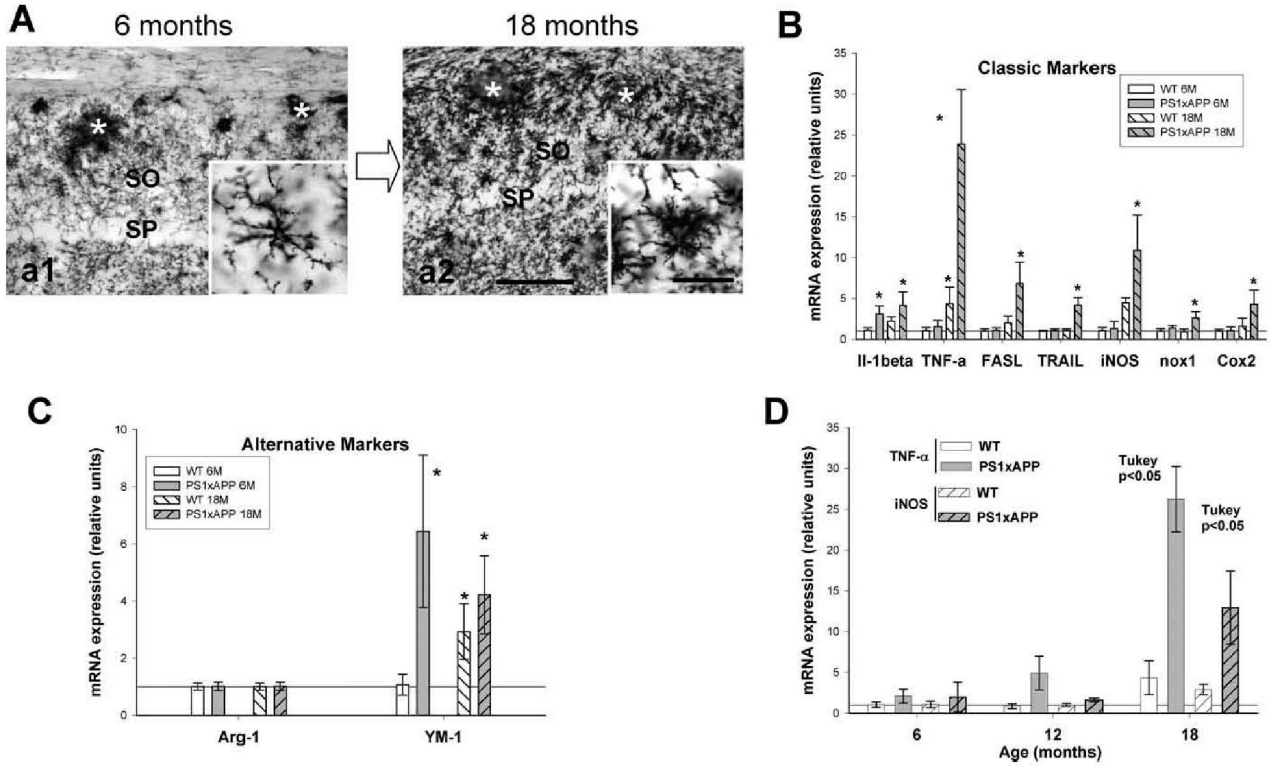

Figure 1. Phenotypic characterization of the activated microglial cells in *PS1xAPP* mice hippocampus at 6 and 18 months of age. ***A***, High magnification of CD11b positive microglial cell in 6 (***a1***) and 18 month (***a2***) *PS1xAPP* mice. At 6 months of age (***a1***), the activated microglial cells were mostly restricted to the Aβ plaques (asterisks) whereas the interplaque microglia displayed a resting morphology (***a1***, inset). At 18 months of age (***a2***), both plaque-associated and interplaque microglia displayed an activated morphology. The inset displays an interplaque activated microglial cell. ***B***, ***C***, The expression of classic (***B***) activation markers of microglial cells and the mRNA expression of genes considered markers of the alternative activation (***C***) were quantitatively determined (by real time RT-PCR) in 6- and 18-month-old WT and *PS1xAPP* mice (10 mice per mice group and age). The expression of the different genes was normalized by GAPDH or β-actin with identical results. Data are expressed in reference to 6-month-old WT mice. Significance was analyzed by one-way ANOVA followed by Tukey's test (*$p < 0.05$). ***D***, The mRNA expression levels of TNF-α and iNOS were quantitatively determined in 6-, 12-, and 18-month-old WT and *PS1xAPP* hippocampi. For each age and mice group, 10 animals were used. Data (mean ± SD) between mice groups (WT and *PS1xAPP*) and ages were compared by one-way ANOVA (TNF-α, $F_{(5,54)} = 91.42$; $p < 0.0001$; iNOS $F_{(5,54)} = 57.03$, $p < 0.0001$) followed by Tukey's test. Significance ($p < 0.05$) was indicated in the figure. Scale bars: ***a1***, ***a2***, 100 μm; insets, 20 μm.

treated with different concentrations (ranging from 1 to 50 μM) of ADDLs or monomeric Aβ42, prepared as described above. The cells were then incubated for 3 h. Control cultures (two wells per plate) were treated with equivalent volume of sterilized PBS (negative control) or 1 μg/ml LPS (*E. coli* O26:B6; Sigma-Aldrich) as positive control. The S1 from the different mice and ages were thawed immediately before use, diluted with DMEM-F12 (without FBS), sterilized by filtration (through 0.22 μm filters; Millipore), and added to the cultures (ranging from 5 to 100 μg of protein). For each experiment, duplicate wells were stimulated under the same experimental condition.

The immunodepletion experiments were done basically as described previously (Araujo et al., 1996). Briefly, 10 μg of protein from S1 fractions from 18-month-old *PS1xAPP* mice ($n = 3$) were subjected to three sequential incubations (8–12 h at 4°C) with either 6E10 (2 μg)-Protein G-Sepharose or A11(2 μg)-Protein-A-Sepahrose immunocomplexes. After immunodepletion, the S1 fractions were treated as above. As control, the different S1 fractions were sequentially incubated with either Protein G-Sepharose or Protein A-Sepharose and tested, in parallel experiments, with the immunodepleted samples.

After incubation, the cultures were treated with Tripure and RNA was isolated and retrotranscribed as described above.

Statistical analysis. Data were expressed as mean ± SD. The comparison between two mice groups (WT and *PS1xAPP* tg mice) was done by two-tailed *t* test. For comparison between several age groups, we used one-way ANOVA followed by Tukey's *post hoc* multiple comparisons test (Statgraphics plus 3.1). The significance was set at 95% of confidence.

Results

Phenotypic characterization of microglial cells in 6- and 18-month-old *PS1xAPP*

Coincident with the apparition of the extracellular Aβ plaques (4 months of age; data not shown), we observed a remarkable microglial activation in the hippocampus of *PS1xAPP* mice (supplemental Fig. 1, available at www.jneurosci.org as supplemental material). Numerous CD11b-positive activated microglial cells, showing a marked cellular hypertrophy and thicker and shorter processes, were concentrated surrounding and infiltrating the Aβ plaques (Fig. 1*A*; supplemental Figs. 1*C*, 2, available at www.jneurosci.org as supplemental material). However, at these early ages (4–6 months) most microglial cells no associated to Aβ plaques, which were also CD11b-positive, displayed a quiescent or resting morphology, with small compact somata bearing many long thin ramified processes (Fig. 1*A*, *a*1, inset).

Microglia could adopt several different phenotypes. The microglial activation by Aβ peptides has been associated with the production of proinflammatory and potentially toxic cytokines (Heneka and O'Banion, 2007). Thus, we quantitatively determined the mRNA expression of proinflammatory factors, including Il-1β; TNF-α and TNF-α related factors (TRAIL and FASL); iNOS; Cox2 and Nox1. As shown (Fig. 1*B*), in 6-month-old *PS1xAPP* mice, none of the classic proinflammatory and cyto-

toxic markers were significantly altered. Only the expression of Il-1β was moderately increased at this age. This absence of induction in the expression of cytotoxic factors occurred despite clear microglial activation (Fig. 1*A*, *a*1; supplemental Fig. 1, available at www.jneurosci.org as supplemental material). Thus, we next tested whether these early activated microglial cells could display a different phenotype. We determined the expression of YM-1 and Arg-1 genes, considered markers of the alternative differentiation in peripheral macrophages (Edwards et al., 2006). Results (Fig. 1*C*) demonstrated the existence of a clear induction in the expression of YM-1 mRNA at 6 months of age. The YM-1 positive cells were exclusively located surrounding and infiltrating the Aβ plaques (supplemental Fig. 2*A*, *a*1, available at www.jneurosci.org as supplemental material) and were identified as microglial cells, demonstrated by its colocalization with Tomato Lectin (supplemental Fig. 2*A*, *a*3–5, available at www.jneurosci.org as supplemental material). However, the expression of Arg-1 was not altered at any age (Fig. 1*C*).

However, at this early age, confocal laser microscopy demonstrated the existence of Aβ phagocytosis, as judged by the presence of intracellular 6E10 immunostaining in Tomato Lectin positive cells, surrounding the Aβ plaques (supplemental Fig. 2*B*, *b*1–3, available at www.jneurosci.org as supplemental material). Pseudo-3D reconstruction of 6E10-Tomato Lectin labeled confocal images confirmed this observation (supplemental Fig. 2*B*, *b*4, available at www.jneurosci.org as supplemental material).

A complete different scenario was observed in 18-month-old *PS1xAPP* hippocampus (Fig. 1*A*). At this old age, we have observed a patent further increase in the expression and density of activated CD11b-positive cells (supplemental Fig. 1*A*,*C*, available at www.jneurosci.org as supplemental material). These CD11b positive cells showed a widespread distribution, around plaques and also in areas free of Aβ plaques (Fig. 1*A*, *a*2; supplemental Fig. 1*C*, *c*3,*c*6, available at www.jneurosci.org as supplemental material). Importantly, these inter-Aβ plaques microglial cells also exhibited an activated morphology with marked cellular hypertrophy and thicker and shorter processes (Fig. 1*A*, compare *a*2, inset, *a*1, inset). This widespread interplaque microglial activation was also verified by quantifying (using stereology) the activated CD11b-positive microglia (morphologically discriminated) in 6 and 18 month *PS1xAPP* CA1 region. As expected, few interplaque activated microglial cells were detected at 6 months of age whereas, at 18 months, a highly significant increase was observed (199.80 ± 54.60 cell/mm^3 vs 1020.51 ± 143.22 cell/mm^3, $n = 3$, for 6- and 18-month-old, respectively; $p < 0.05$). Furthermore, this widespread activation of microglial cells was coincident with a prominent increase in the expression of TNF-α and TNF-α related factors (TRAIL and FASL), compared with 6-month-old *Ps1xAPP* mice. Similarly, the expression of iNOS mRNA and, more attenuated Cox2 and Nox1 mRNAs, was also significantly increased at this advanced age (Fig. 1*B*). However, the expression of the alternative marker YM-1 remained elevated in 18-month-old tg mice (Fig. 1*C*) and YM-1 positive microglia could be observed surrounding the Aβ plaques at this old age (supplemental Fig. 2*A*, *a*2, available at www.jneurosci.org as supplemental material).

The expression of TNF-α and iNOS was also quantified in 6-, 12- and 18-month-old *PS1xAPP*, to more precisely determine the age of the microglial phenotypic switch. As shown (Fig. 1*D*), the expression of TNF-α and iNOS was not significantly altered (compared with WT) in 6- and 12-month-old tg mice (although at 12 months a moderate increase in the TNF-α expression was observed). However, a remarkable induction in the expression of both TNF-α and iNOS was detected in 18-month-old *PS1xAPP* mice (Fig. 1*D*). Thus, the classic microglial activation seemed to be predominantly restricted to old ages.

The cellular origin of TNF-α, in 18-month-old *PS1xAPP*, was then determined by immunocytochemistry (Fig. 2*A*, *a*2; compare *a*4, *a*1,*a*3). TNF-α positive cells, displaying a clear microglial morphology (Fig. 2*A*, *a*5), were located in all hippocampal layers except in the vicinity of Aβ plaques, that appeared clearly immunonegative (Fig. 2*A*, *a*2). In fact, as shown in Figure 2*A–a*6, Congo red positive plaques were surrounded by a TNF-α immunonegative perimeter. As described in Figure 1 and supplemental Fig. 1*C–c*6 (available at www.jneurosci.org as supplemental material), there was a cluster of activated microglial cells in close contact with Aβ plaques; however, TNF-α positive microglia was mainly nonassociated to the amyloid plaques. This suggests the existence of, at least, two different activated microglial populations in aged *PS1xAPP* mice. To test this proposition, we performed Tomato Lectin labeling on sections previously immunostained for TNF-α and Congo Red. In this particular case, we did not use confocal microscopy because of the high tissue autofluorescence in aged animals. In any case, as shown (Fig. 2*A*, *a*7), the Congo Red stained plaques, as well as cells immediately in contact with the plaques, were TNF-α-negative. However, these TNF-α negative cells surrounding plaques were stained with Tomato Lectin, demonstrated their microglial origin (Fig. 2*A*, *a*8). Furthermore, a close inspection of the Congo Red-TNF-α double labeled sections revealed the absence of TNF-α immunopositive processes infiltrating the Aβ plaques (Fig. 2*A*, *a*7) whereas the same plaque, counterstained with Tomato Lectin displayed a clear infiltration by microglial prolongations (Fig. 2*A*, *a*8). Similar results were obtained using YM-1 (data not shown)

Concerning to iNOS expression, immunohistochemical experiments demonstrated the existence of few iNOS immunopositive cells in 6-month-old *PS1xAPP* hippocampus, restricted to certain areas, such as stratum oriens and hilus (Fig. 2*B*, *b*1,*b*2). The number of iNOS immunopositive cells increased markedly at 18 months, compared with age-matched WT (Fig. 2*B*, compare *b*3, *b*4, *b*6) or 6 month WT (Fig. 2, *b*5) or *PS1xAPP* mice (Fig. 2*B*, *b*1,*b*2). As also shown in Figure 2*B*, the iNOS-positive cells displayed an astroglial appearance. The astroglial origin of iNOS was confirmed by double GFAP-iNOS labeling and confocal microscopy (Fig. 2*B*, *b*7–*b*9). Furthermore, at 18 months of age, iNOS containing astroglial cells were widely distributed in all layers of the hippocampus and not restricted to the Aβ plaques (Fig. 2*B*, *b*3). The induction of iNOS expression by astrocytes, because of TNF-α and/or TRAIL, has been previously reported (Akama and Van Eldik, 2000; Cantarella et al., 2008).

Together, our data demonstrated that the apparition of the Aβ plaques (at early ages in this model) determined the microglial activation restricted to the Aβ plaques. These active microglial cells adopted a, perhaps incomplete, alternative phenotype (YM-1 positive) and were TNF-α negative. This alternative activated microglial cells displayed Aβ phagocytic capabilities. However, at 18 months of age, microglial activation was expanded into hippocampal areas free of plaques showing, in this case, a classic proinflammatory phenotype, with the expression of potential cytotoxic factors. This cytotoxic environment was also coincident with a significant loss of pyramidal cells in this model (supplemental Fig. 3, available at www.jneurosci.org as supplemental material). Nevertheless, the microglia surrounding plaques seemed to keep expressing the alternative phenotype. The possible Aβ phagocytosis, at old ages, was not assessed because of the high tissue autofluorescence in these animals. However, we also

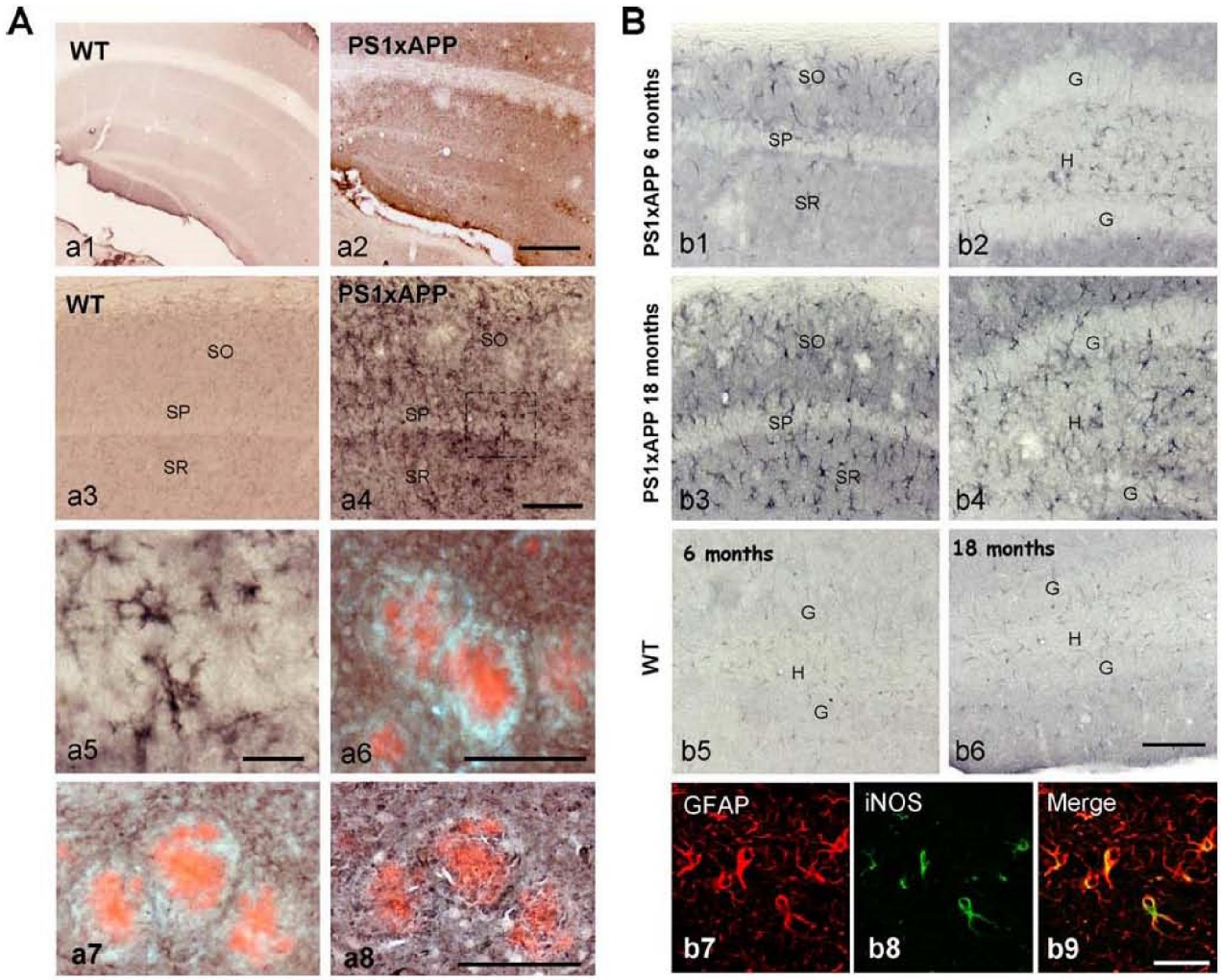

Figure 2. Expression of TNF-α and iNOS in 18-month-old *PS1xAPP* hippocampus. ***A***, The expression of TNF-α, in 18-month-old WT and *PS1xAPP* mice, was assessed by immunohistochemistry. TNF-α immunoreactivity was low in WT mice (***a1***, ***a3***), whereas a prominent immunoreactivity was observed in *PS1xAPP* (***a2***, ***a4***). The TNF-α positive cells displayed a microglial phenotype (***a5***). Importantly, the TNF-α immunoreactivity was widespread found in all layers of the hippocampus; however, the Aβ plaques border zone appeared immunonegative for TNF-α (***a6***). Sections from 18-month-old *PS1xAPP* mice were first immunostained with anti-TNF-α antibody followed by Congo Red staining (***a7***). These double labeled sections were photographed and then counterstained with Tomato Lectin (***a8***). As shown, the Aβ plaques (stained by Congo-red) were surrounded and infiltrated by TNF-α immunonegative and Tomato-lectin immunopositive microglia cells (***a8***). Scale bars: ***a1***, ***a2***, 500 μm; ***a3***, ***a4***, 100 μm; ***a5***, 20 μm; ***a6–a8***, 100 μm. ***B***, Immunostaining of iNOS expressing cells in 6- (***b1***, ***b2***) and 18-month-old (***b3***, ***b4***) *PS1xAPP* mice. At 6 months of age, a limited expression, restricted to stratus oriens and hilus, was observed. In 18-month-old *PS1xAPP*, the iNOS positive cells were observed in all hippocampal layers. A faint immunostaining was observed in WT mice of 6 months and, relatively more intense, 18 months of age (***b5***, ***b6***). Double iNOS-GFAP immunofluorescence labeling and confocal laser microscopy (***b7–b9***) demonstrated the localization of iNOS in astroglial cells. Scale bars: ***b1–b6***, 100 μm; ***b7–b9***, 20 μm.

observed an age-dependent increase in both the number and size of Aβ plaques (supplemental Fig. 1*E*, available at www.jneurosci.org as supplemental material). This increase in the plaque size might reflect a diminution in the microglial phagocytic capability.

Infiltration of CD3 positive T-cells in aged *PS1xAPP* mice

We next investigated the possible cause(s) that determine the microglial activation at old ages. The generalized glial activation, observed at 18 months of age in this AD model, could be attributable to the infiltration of peripheral T-cells into the hippocampal parenchyma. The recruitment of CD4+ Th1-cells in experimental autoimmune encephalomyelitis (EAE; a disease similar to human multiple sclerosis) induced the production of, among other cytotoxic factors, TNF-α (Dhib-Jalbut et al., 2006; Weaver et al., 2007). In consequence, we first determined the possible infiltration of T cells in *PS1xAPP* mice by examining the presence CD3-positive cells. As shown (Fig. 3*A*, *a3*) in 6-month-old *PS1xAPP* mice few CD3-positive cells were observed. On the contrary, in 18-month-old *PS1xAPP*, numerous CD3 immunopositive cells were clearly detected (Fig. 3*A*, *a2*). The presence of CD3-positive cells was observed in all layers of the hippocampus, although they were more abundant around some plaques and close to the hippocampal fissure (Fig. 3*A*, *a2*,*a4*). However, in WT mice very few CD3-positive cells were observed even at advanced ages (Fig. 3*A*, *a1*).

Because the T-cells could modify the microglial phenotype, as it was observed in 18-month-old *PS1xAPP* mice, we also determined the mRNA expression of interleukins, or key factors, implicated in the different polarization linage of the T cells. In this sense, we have quantified the expression of IL-12p35 and IFN-gamma (proinflammatory Th1 cells); IL-23 and IL-17 (proin-

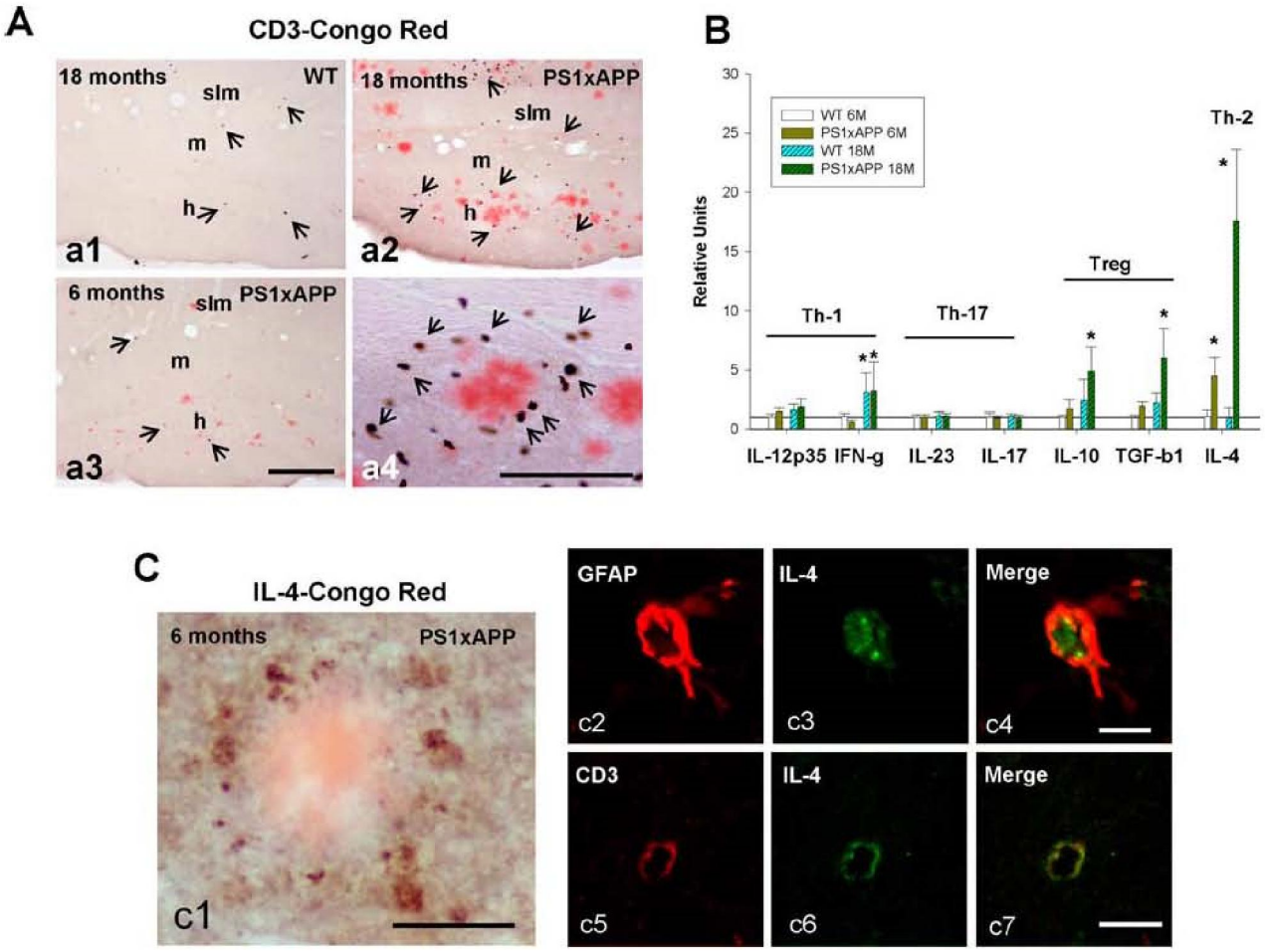

Figure 3. Infiltrated CD3 positive cells in 18-month-old *PS1xAPP* hippocampus predominantly developed a Th2 response. ***A***, Double labeling for anti-CD3 and Congo Red immunohistochemistry demonstrated the infiltration of CD3-positive cells in hippocampus of 18 month *PS1xAPP* mice (***a2***, ***a4***), whereas the presence of CD3 cells was scarce in 18 month WT (***a1***) or in 6 month *PS1xAPP* mice (***a3***). The infiltrated CD3 cells were preferential, but not exclusively located around some Aβ plaques (***a4***). ***B***, The expression of different interleukin mediators, IFN-gamma and TGF-β1, considered representative of the different adaptive T-mediated immune responses, were determined in 6- and 18-month-old WT and *PS1xAPP* mice ($n = 10$ per group). Compared with WT (using one-way ANOVA), only the expression of IL-10, TGF-β and, more prominently, IL-4 were significantly induced in *PS1xAPP* mice. Interestingly, the expression of IL-4 also displayed a significant increased in 6-month-old *PS1xAPP*. ***C***, At 6 months of age (***c1***), IL-4 punctate immunostaining was concentrated around Aβ plaques. Double GFAP-IL4 immunolabeling and confocal laser microscopy (***c2–c4***) revealed that activated astroglial cells expressed this interleukin. In 12-month-old *PS1xAPP* mice, all infiltrating CD3-positive cells were also immunoreactive for anti-IL4 (***c5–c7***). Scale bars: ***a1–a3***, 200 μm; ***a4***, 100 μm; ***c1***, 25 μm; ***c2–c4***, 5 μm; ***c5-c7***, 5 μm.

flammatory Th17 cells); IL-10 and TGF-β1 (Treg) and IL-4 (characteristic of anti-inflammatory Th2 response). Unexpectedly (Fig. 3*B*), absolutely no differences (compared with WT mice) were observed in the mRNA expression of any of the Th1/Th17 cell response interleukins. However, the expression of IL-10, TGF-β-1 and, more patently, IL-4 was highly increased in *PS1xAPP* mice. This response, in conjunction with the moderate increase in the expression of IL-10 and TGF-β1 could represent a strong adaptive anti-inflammatory response (Th2 and Treg). Thus, it is unlikely that this response could mediate the induction in the expression of cytotoxic factors by the activated microglial cells. It is noteworthy that the expression of IL-4 mRNA was also upregulated in 6-month-old *PS1xAPP* mice.

The expression of IL4 was further studied, by immunohistochemistry, in 6- and 18-month-old *PS1xAPP* mice. At 6 months of age (Fig. 3*C*, *c*1), IL-4-positive punctated structures were localized predominantly around amyloid deposits whereas, in 18-month-old tg mice (data not shown), IL-4 positive cells were located around plaques and as isolated small rounded cells. Double immunofluorescence and confocal laser microscopy, in 6-month-old *PS1xAPP* mice, determined that neither activated microglia surrounding plaques or APP positive principal cells expressed IL-4 (data not shown). Instead the IL-4 immunoreactivity colocalized with GFAP positive (Fig. 3*C*, *c*2–*c*4) and reactive (as judged by the hypertrophic cell body and prolongations) astroglial cells. These reactive astrocytes were located in close association with Aβ deposits (data not shown).

Concerning to the CD3 infiltration observed at older ages (18 months), we cannot directly assess the coexpression with IL-4 by confocal microscopy. However, we have indeed identified CD3-IL-4 coexpressing cells in 12-month-old *PS1xAPP* mice (Fig. 3*C*, *c*5–*c*7). In these middle age tg mice, the infiltration of CD3 positive cells was lower than that observed at 18 months (data not shown). However, and despite this limitation, all identified CD3-positive cells infiltrating the hippocampal parenchyma were also IL-4 positive.

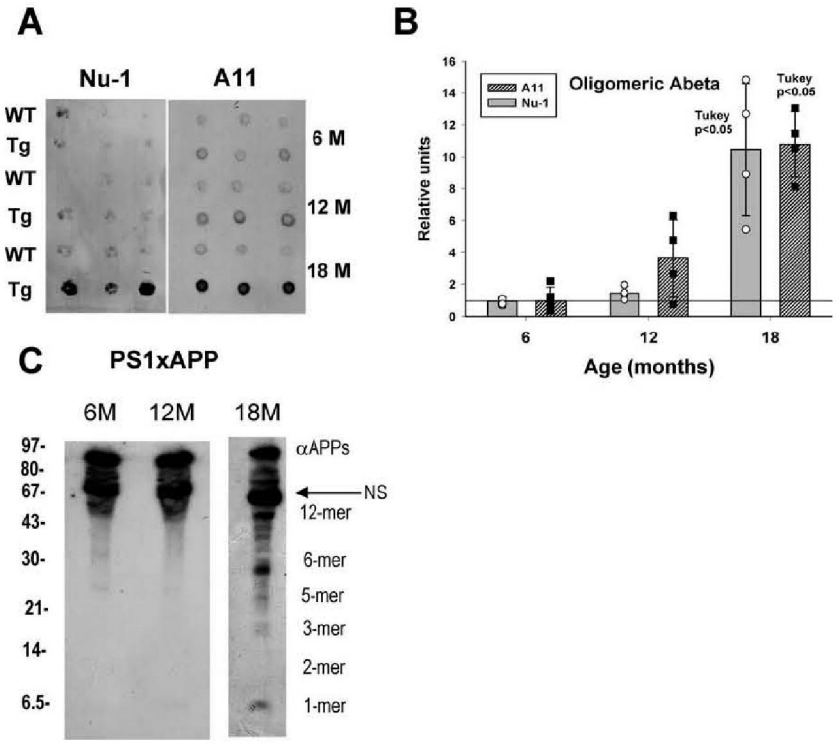

Figure 4. The increase in the soluble oligomeric Aβ, in 18 month *PS1xAPP* hippocampus. ***A***, Representative dot blots demonstrating the presence of oligomeric Aβ in the soluble fractions. In these experiments we used the conformational-specific antibodies Nu-1 and A11. For each blot, the soluble extracts form the different age and group (WT and *PS1xAPP*) mice ($n = 4$ per age and group) were used in different combinations. These experiments were repeated twice. ***B***, Quantitative analysis of *PS1xAPP* dot blots using Nu-1 and A11. The immunoreactivity of the different *PS1xAPP* mice was normalized by 6-month-old *PS1xAPP* mice and displayed individually or as mean ± SD. ***C***, Representative Western blot, using 6E10, of the different soluble fractions from 6-, 12-, and 18-month-old *PS1xAPP* mice. These experiments were repeated three times with similar results.

Soluble oligomeric Aβ could be responsible for the generalized microglial activation at advanced ages

Finally, we investigated the presence of extracellular soluble Aβ species [monomers or amyloid–beta-derived diffusible ligands (ADDLs)/oligomers] as putative inductors of the age-dependent glial generalized activation. We have first determined, by sandwich ELISA, the Aβ42 content in the soluble fractions (S1 fractions, see Materials and Methods). The Aβ42 levels in 6-month-old *PS1xAPP* hippocampus was maintained at very low levels (6.7 ± 1.3 pmol/mg protein, $n = 4$), despite abundant Aβ deposits in this model (Fig. 1*A*; supplemental Fig. 1*C*,*D*, available at www.jneurosci.org as supplemental material). However, at 18 months we observed a dramatic increase in the Aβ42 content. In fact, this soluble Aβ42 increased 15-fold (86.9 ± 54.2 pmol/mg protein, $n = 4$; $p < 0.05$), in average, compared with 6-month-old *PS1xAPP*. This increase was notably higher than the twofold increase in the plaque loading, observed between 6- and 18-month-old *PS1xAPP* (supplemental Fig. 1*D*, available at www.jneurosci.org as supplemental material).

We next tested the presence of Aβ oligomeric forms in the extracellular, soluble fractions. It is well known that diffusible aggregated Aβ forms (ADDLs/oligomers) are highly toxic (De Felice et al., 2007). Thus, we determined the presence of these Aβ forms using the specific monoclonal antibody Nu-1 in dot blots (Lambert et al., 2007). As shown in Figure 4*A*, quantitatively in Figure 4*B*, the presence of soluble ADDLs was barely detectable in 6- and 12-month-old *PS1xAPP* mice, as well as in WT mice. However, at 18 months, the soluble extracts displayed an intense immunoreactivity with Nu-1. Although it was difficult to quantify this age-dependent increase, because of the low specific signal observed at 6 and 12 months, our estimative quantification indicated the existence of 10-folds of increase at 18 months of age. Moreover, we also used A11 to corroborate the presence of oligomeric Aβ in these soluble extracts. As shown in Figure 4*A* and quantitatively in Figure 4*B*, the soluble extract from these 18 month *PS1xAPP* mice displayed a clear immunoreactivity with A11, compared with age-matched WT mice or 6 and 12 month *PS1xAPP*. It is also interesting that, using A11, we detected a small increase (although nonsignificant) in the oligomeric content in 12-month-old *PS1xAPP*. In conclusion, the amount of Nu-1 and A11 immunopositive oligomeric Aβ displayed a clear age-dependent increase in the soluble extract of *PS1xAPP* mice. At 18 months of age, the presence of these immunopositive Nu-1 and A11 oligomers was clearly patent.

Although SDS-PAGE is a reductive technique and as such cannot provide an accurate reflection of the noncovalently associated Aβ oligomers (Hepler et al., 2006), the presence of the soluble oligomeric Aβ forms was also assayed in Western blots using 6E10. As shown (Fig. 4*C*), a prominent αAPPs band was clearly detected in 6-, 12-, and 18-month-old *PS1xAPP* mice. At 6 and 12 months, very small amount of low-n aggregated Aβ was detected, under the conditions used for these experiments. A faint band, corresponding to 5- or 6-mer Aβ could be barely observed in 6- and 12-month-old *PS1xAPP* mice. However, as expected from the dot blot analysis, in 18 month *PS1xAPP* mice multiple Aβ forms were clearly distinguished. The observed 6E10-positive bands corresponded with the reported Mr for the oligomeric Aβ forms, detected by Western blots (see Lambert et al., 2007), and also similar to soluble oligomers identified in other aged tg models (Lesné et al., 2006). In fact, according with the Mr, three predominant Aβ forms were identified in the soluble extracts; monomer, 6-mer and 12-mer. Although the 12-mer could also be present, in lower amount, in 6 and 12 month mice (Fig. 4*C*), these low Mr oligomers were barely detectable in the soluble extract from 6- and 12-month-old *PS1xAPP*. We cannot discard that other high molecular weight forms were also increased in 18-month-old tg mice. Independently of the oligomeric state of Aβ, these data clearly demonstrated the existence of a marked increase in the soluble Aβ forms in our 18-month-old *PS1xAPP* mice population. Therefore, the presence of these ADDLs/oligomeric Aβ forms could be implicated in the classic microglial activation, observed in our 18-month-old *PS1xAPP* cohort.

To validate this hypothesis, we next tested, *in vitro* using astromicroglial cultures, the effect of monomeric and oligomeric Aβ42 forms in the expression of TNF-α. LPS was used as a positive control. The results (Fig. 5*A*) demonstrated that LPS and, dose-dependently, the oligomeric Aβ42 strongly stimulated the expression of the proinflammatory TNF-α. Interestingly, equiv-

alent concentrations of monomeric Aβ42 were totally ineffective stimulating the TNF-α expression in these cultures. Based on these data, we predicted that the soluble extracts from 18-month-old *PS1xAPP* mice should also stimulate the expression of TNF-α in the glial cultures. Thus, we tested the stimulatory effect of increasing amounts of soluble proteins (ranging from 5 to 100 μg of protein), obtained from 6- and 18-month-old WT and *PS1xAPP* mice. As shown, the soluble fractions from young WT and *PS1xAPP* mice produced no apparent effect on the expression of TNF-α (Fig. 5*B*). Similarly, the soluble fractions from 18-month-old WT mice were also ineffective stimulating the TNF-α production. However, the soluble fractions derived from 18-month-old *PS1xAPP* mice produced a potent dose-dependent stimulation in the expression of TNF-α in these astromicroglial cultures (Fig. 5*B*).

Finally, if the soluble oligomeric Aβ in the S1 fractions was indeed the causative agent of the TNF-α stimulation, this effect should be avoided by immunodepletion of the supernatant using specific antibodies. To test this point, the Aβ content of the S1 fractions, derived from 18-month-old *PS1xAPP* mice ($n = 3$), was immunodepleted by three sequential immunoprecipitations using either the mAb 6E10 (that should recognized the total soluble Aβ) or the conformation specific polyclonal A11 (specific of the oligomeric Aβ). As shown (Fig. 5*C*), after immunodepletion using 6E10, the induction in the TNF-α expression by these immunodepleted S1 fractions was deeply reduced (from 94.60 ± 6.02–2.87 ± 0.90, $n = 3$, before and after immunodepletion, relative units normalized by PBS effect, 1.01 ± 0.24; $p < 0.05$, Tukey's test). Moreover, the immunodepletion of the oligomeric Aβ using A11 (Fig. 5*C*), also produced an almost completed reduction in the TNF-α induction by the S1 fractions (2.33 ± 0.45, $n = 3$, after immunodepletion; $p < 0.05$, Tukey's test).

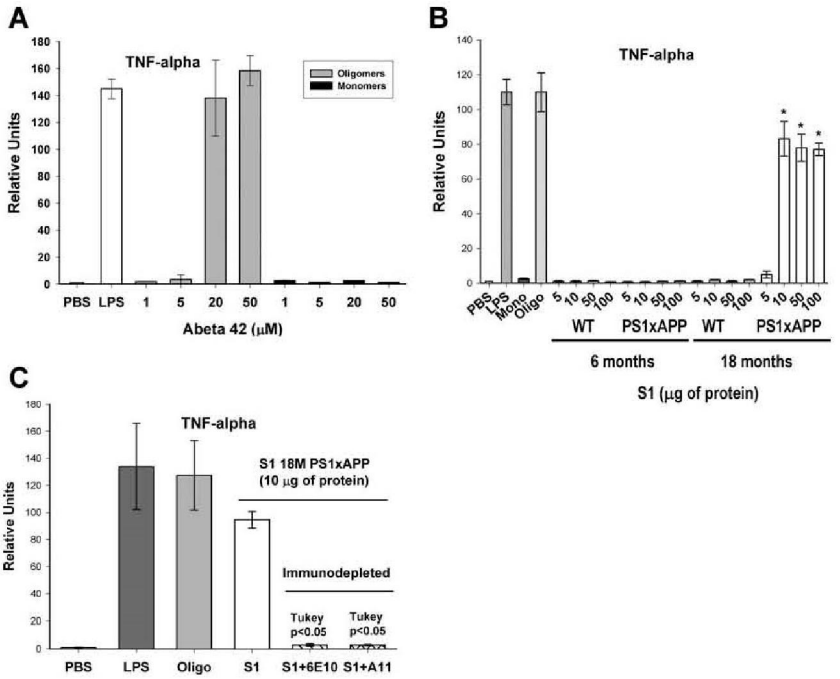

Figure 5. The oligomeric Aβ induced the TNF-α expression in glial primary cultures. ***A***, Dose–response stimulation of the TNF-α expression by oligomeric and monomeric Aβ42 assessed *in vitro* in astromicroglial cultures. PBS and LPS (1 μg/ml) were used as negative and positive controls, respectively. Data are mean ± SD from three independent cultures and Aβ42 preparations. ***B***, Stimulation of the glial cultures using the S1 soluble fractions. Increasing protein amounts (from 5 to 100 μg) of the different S1 fractions (6 and 18 months of age; WT and *PS1xAPP*; $n = 3$ per age and group) was added to the cultures. In parallel, PBS, monomeric (20 μM), oligomeric Aβ42 (20 μM) and LPS (1 μg/ml) were included as negative and positive controls, respectively. For each experiment, duplicate culture wells were used. This experiment was repeated twice, using independent cultures. Only the soluble extract from 18-month-old *PS1xAPP* produced the stimulation of the TNF-α expression in these experiments (asterisk; $p < 0.05$, Tukey's test). ***C***, Immunodepletion experiments. In these experiments, the Aβ content from the S1 fractions (10 μg of protein) of three different 18-month-old *PS1xAPP* mice was immunodepleted by three sequential immunoprecipitations using either 6E10-Protein G-Sepharose or A11-Protein A-Sepharose complexes. After immunodepletion, the S1 fractions were used in stimulation experiments. In parallel, the different S1 fractions were treated with Protein G-Sepharose or Protein A-Sepharose. We observed no differences in the TNF-α stimulation between these control S1 fractions and the results were pooled. The immunodepletion of Aβ, by any of the antibodies used, precluded the stimulatory effect of the S1 fractions. PBS, oligomeric Aβ42 (20 μM) and LPS (1 μg/ml) were included as negative and positive controls, respectively.

Discussion

Neuroinflammation is a key feature of AD pathology (Meda et al., 2001; Dudal et al., 2004; Craft et al., 2006). However, its role is still conflictive. Here, we have analyzed the microglial response associated to the age-dependent amyloid pathological progression in the hippocampus of $PS1^{M146L}$xAPP^{751SL} mice. The principal findings are as follows. (1) At early ages (4–6 months), activated microglia was restricted to Aβ deposits and characterized by the absence of induction of cytotoxic factors and by the expression of one alternative marker (YM-1). (2) In 18-month-old, microglial activation was expanded throughout the hippocampus, displaying a classical potentially cytotoxic phenotype (expressing TNF-α, FASL, TRAIL, Cox2 and Nox1). The expression of iNOS was restricted to astrocytes. (3) Although a clear hippocampal T-cell infiltration was detected at 18 months, these T-cells were polarized to Th2 phenotype. (4) There was an age-dependent increase in extracellular soluble Aβ oligomers, which were potent microglial stimulators as assessed by *in vitro* studies.

We observed a close spatial and temporal parallelism between Aβ deposits and microglial activation (Simard et al., 2006). At early ages, activated microglia was concentrated in clusters surrounding and infiltrating Aβ plaques. In fact, few extra-plaque microglial activation was observed. Thus, according with recent *in vivo* observations (Meyer-Luehmann et al., 2008), plaques attracted and stimulated microglial cells. However, activated microglia could adopt different phenotypes. Our data demonstrated that plaque-associated microglia displayed an alternative state. In peripheral macrophages, this phenotype was characterized by the absence of expression of cytotoxic factors and the expression of alternative markers (YM-1 and Arg-1) (Edwards et al., 2006). Although we have not observed the induction in Arg-1, the YM-1 expression was highly elevated in microglia surrounding plaques. These results, together with the absence of significant TNF-α, TRAIL, FASL or iNOS expression led us to conclude that the activated microglia could adopt an incomplete alternative phenotype. Furthermore, this alternative phenotype, associated to Aβ plaques, seemed to be maintained also at relative old ages. In fact, at 18-months, the microglia surrounding Aβ plaques was TNF-α negative and YM-1 positive. Therefore, activated micro-

glia in direct apposition with Aβ plaques adopted an alternative phenotype, regardless of the age of the animal. This proposition was consistent with the increased expression of IL-4. Multiple *in vitro* reports have probed the influence of IL-4 in the development of a non-proinflammatory alternative phenotype (Iribarren et al., 2005; Butovsky et al., 2005; Ponomarev et al., 2007; Lyons et al., 2007a,b). Furthermore, at early ages, the expression of this interleukin was restricted to reactive astrocytes, closely associated to Aβ plaques. Similarly, at 18 months, plaques were also surrounded by IL-4 positive astrocytes and, probably, CD3 cells. In consequence, we proposed that the alternative phenotype, associated to Aβ plaques, could be because of the expression of IL-4 by activated astrocytes and, when present, CD3-cells. We cannot discard that Aβ plaques could directly produce this microglial differentiation. The factor(s) that determine the astroglial activation remains to be investigated.

Concerning to the physiological role, the alternative activated microglia could exert a neuroprotective function. In presence of IL-4, microglia produces growth factors (i.e., IGF-1) (Butovsky et al., 2006; Zhao et al., 2006). The IL-4 reduced Aβ toxicity, *in vitro* and *in vivo* (Butovsky et al., 2005, 2006; Iribarren et al., 2005; Lyons et al., 2007a,b) and enhanced Aβ phagocytosis (Koenigsknecht-Talboo and Landreth, 2005). In agreement, we also observed the expression of IGF-1, in the vicinity of Aβ deposits (our unpublished results) and Aβ phagocytosis by microglia surrounding plaques (supplemental Fig. 2*B*, available at www.jneurosci.org as supplemental material). In this sense, Bolmont et al. (2008) have recently demonstrated the internalization of Aβ peptides by plaque-associated microglia and proposed an active role in the maintenance of plaque size. Furthermore, the decrease in the early recruitment of the microglial cells, by genetic ablation of either TLR2 receptor, in a PS1/APP model (Richard et al., 2008) or CCR2 in Tg2576 (El Khoury et al., 2007), increased Aβ42 levels, accelerated memory impairments and increased vascular amyloid pathology. Thus, we propose that the plaque-associated alternative activated microglia could limit Aβ toxicity directly, by phagocytosis (see also Simard et al., 2006), maintaining low extracellular Aβ levels. In fact, our data demonstrated low levels of soluble Aβ42 and oligomeric forms until advanced ages.

Furthermore, this alternative activated microglia could also indirectly exert a neuroprotective role by releasing growth factors, such as IGF-1. This proposition is also consistent with the positive effects of vaccination with the Th2 adjuvant glatiramer acetate, the concomitant increase in IL-4 expressing cells and the reduction of Aβ plaques (Butovsky et al., 2006).

At 18 months of age, microglia located between, not in direct contact with Aβ plaques, was clearly activated. Furthermore, these interplaque microglial cells expressed TNF-α (and probably other TNF-α related factors), whereas the microglia closely associated to Aβ plaques remained TNF-α negative and YM-1 positive. Thus, at old age, two functionally different activated microglial populations should coexist, indicating the existence of different microglial activators. In this sense, even at this old age, there was a clear IL-4 expression surrounding plaques. Thus, and similar to the situation observed in 6-month-old *PS1xAPP* mice, plaques (directly and/or indirectly through IL-4) might stimulate microglia to a noncytotoxic phenotype. This observation let us to propose that the generalized microglial activation should be induced by a diffusible agent.

As mentioned, the general microglial activation could reflect a Th1/Th17 CD3-mediated response. According with previous reports in AD and AD models (Itagaki et al., 1988; Togo et al., 2002; Stalder et al., 2005) we observed CD3-cells in 18-month-old *PS1xAPP* hippocampus. However, the expression of IL-12, IL-17 and IL-23 was unchanged, compared with age-matched WT. Instead, we observed a considerable induction of IL-4 and IL-10 expression. Moreover, these CD3-cells also expressed IL-4. Together, data strongly suggest that the infiltrated T-cells were predominantly polarized to Th2 and/or Treg states. These anti-inflammatory Th2/Treg cells could explain the absence of encephalitis signs in AD models (Stalder et al., 2005). Thus, the Th2 polarization could limit the potential neurotoxic effect of the activated microglia and it is highly unlikely that CD3 infiltration mediated the expanded microglial activation, observed in this model.

Multiple evidences suggested that diffusible Aβ oligomers (ADDLs) were the toxic agents in AD. These ADDLs were exclusively present in AD patients (Gong et al., 2003; Lacor et al., 2004) and their content increased with the disease severity (Lambert et al., 2007). In fact, our results demonstrated the increase in soluble Aβ42 in 18-month-old *PS1xAPP*. Furthermore, our data also probed the presence of Nu-1 and A11 immunopostive oligomers in these soluble fractions (barely detectable at early ages). Thus, we hypothesized that the oligomeric Aβ was also the causative agent of the generalized microglial response at 18 months. Our *in vitro* experiments strongly supported this proposal. In fact, oligomeric Aβ42 highly stimulated the TNF-α expression in cultures, whereas monomeric Aβ42 was ineffective. More relevant, the soluble S1 fractions from 6-month-old WT and *PS1xAPP* mice and 18-month-old WT, that lack detectable levels of oligomers, were also ineffective stimulating TNF-α production in culture. However, S1 fractions from 18-month-old *PS1xAPP* produced a strong TNF-α induction. Moreover, the immunodepletion of Aβ, using 6E10 or A11, completely abolished the stimulatory effect of the S1 fractions. In consequence, we proposed that the generalized microglial activation with a classic and potentially cytotoxic phenotype, observed at 18 months, could be because of the accumulation of soluble oligomeric Aβ in the hippocampal parenchyma. Furthermore, it has been reported that aging and/or Aβ could decrease the neuronal expression of microglial inhibitory factors, such as CD200, fractalkine or neurotransmitters (Acetylcholine or noradrenaline) (Cardona et al., 2006; Chitnis et al., 2007; Heneka and O'Banion, 2007; Lyons et al., 2007a; Duan et al., 2008). Furthermore, damaged neurons could release microglial stimulants, such as ATP, UDP or CCL21 (de Jong et al., 2005; Inoue et al., 2007). Therefore, it is possible that the classic microglial activation in our model could reflect a synergic effect of Aβ oligomers, acting directly on microglia and, indirectly, by affecting neuronal-microglial interplay.

The role of the classical microglial activation was unknown. The neuronal toxicity to TNF-α, TNF-α related factors and iNOS has been extensively probed (Cantarella et al., 2003; Lee et al., 2004; Li et al., 2004; Medeiros et al., 2007; Uberti et al., 2007). Indeed, in our model, we (supplemental Fig. 3, available at www.jneurosci.org as supplemental material) and others (Schmitz et al., 2004) have observed a significant decrease in pyramidal cell number, coincident with the classical microglial activation (17–18 months). Although present results do not allow establishing a direct relationship between these events, the production of TNF-α, TRAIL, FASL and NO derivates, together with the presence of soluble Aβ oligomers, could directly contribute to the observed pyramidal degeneration.

In conclusion, at early ages in our AD model, the apparition of Aβ plaques determined the microglia activation to an alternative phenotype with, apparently, a neuroprotective role. At older ages,

the accumulation of extracellular oligomeric Aβ produced marked widespread microglial activation toward a classic phenotype and the production of cytotoxic factors. The reasons that determined this age-dependent increase in the ADDL/oligomers content remained unknown.

References

Aisen PS (2000) Anti-inflammatory therapy for Alzheimer's disease. Neurobiol Aging 21:447–448.

Aisen PS, Schafer KA, Grudman M, Pfeiffer E, Sano M, Davis KL, Farlow MR, Jin S, Thomas RG, Thal LJ (2003) Effects of rofecoxib or naproxen vs placebo on Alzheimer disease progression: a randomized controlled trial. JAMA 289:2819–2826.

Akama KT, Van Eldik LJ (2000) Beta-amyloid stimulation of inducible nitric-oxide synthase in astrocytes is interleukin-1beta- and tumor necrosis factor-alpha (TNFalpha)-dependent, and involves a TNFalpha receptor-associated factor- and NFkappa B-inducing kinase-dependent signaling mechanism. J Biol Chem 275:7918–7924.

Araujo F, Tan S, Ruano D, Schoemaker H, Benavides J, Vitorica J (1996) Molecular and pharmacological characterization of native cortical gamma-aminobutyric acid(A) receptors containing both alpha(1) and alpha(3) subunits. J Biol Chem 271:27902–27911.

Blanchard V, Moussaoui S, Czech C, Touchet N, Bonici B, Planche M, Canton T, Jedidi I, Gohin M, Wirths O, Bayer TA, Langui D, Duyckaerts C, Tremp G, Pradier L (2003) Time sequence of maturation of dystrophic neurites associated with Abeta deposits in APP/PS1 transgenic mice. Exp Neurol 184:247–263.

Bolmont T, Haiss F, Eicke D, Radde R, Mathis CA, Klunk WE, Kohsaka S, Jucker M, Calhoun ME (2008) Dynamics of the microglial/amyloid interaction indicate a role in plaque maintenance. J Neurosci 28:4283–4292.

Butovsky O, Talpalar AE, Ben-Yaakov K, Schwartz M (2005) Activation of microglia by aggregated beta-amyloid or lipopolysaccharide impairs MHC-II expression and renders them cytotoxic whereas IFN-gamma and IL-4 render them protective. Mol Cell Neurosci 29:381–393.

Butovsky O, Koronyo-Hamaoui M, Kunis G, Ophir E, Landa G, Cohen H, Schwartz M (2006) Glatiramer acetate fights against Alzheimer's disease by inducing dendritic-like microglia expressing insulin-like growth factor 1. Proc Natl Acad Sci U S A 103:11784–11789.

Caballero C, Jimenez S, Moreno-Gonzalez I, Baglietto-Vargas D, Sanchez-Varo R, Gavilan MP, Ramos B, Del Rio JC, Vizuete M, Gutierrez A, Ruano D, Vitorica J (2007) Inter-individual variability in the expression of the mutated form of hPS1M146L determined the production of Abeta peptides in the PS1xAPP transgenic mice. J Neurosci Res 85:787–797.

Cantarella G, Uberti D, Carsana T, Lombardo G, Bernardini R, Memo M (2003) Neutralization of TRAIL death pathway protects human neuronal cell line from beta-amyloid toxicity. Cell Death Differ 10:134–141.

Cantarella G, Di Benedetto G, Pezzino S, Risuglia N, Bernardini R (2008) TRAIL-related neurotoxicity implies interaction with the Wnt pathway in human neuronal cells in vitro. J Neurochem 105:1915–1923.

Cardona AE, Pioro EP, Sasse ME, Kostenko V, Cardona SM, Dijkstra IM, Huang D, Kidd G, Dombrowski S, Dutta R, Lee JC, Cook DN, Jung S, Lira SA, Littman DR, Ransohoff RM (2006) Control of microglial neurotoxicity by the fractalkine receptor. Nat Neurosci 9:917–924.

Chitnis T, Imitola J, Wang Y, Elyaman W, Chawla P, Sharuk M, Raddassi K, Bronson RT, Khoury SJ (2007) Elevated neuronal expression of CD200 protects Wlds mice from inflammation-mediated neurodegeneration. Am J Pathol 170:1695–1712.

Craft JM, Watterson DM, Van Eldik LJ (2006) Human amyloid beta-induced neuroinflammation is an early event in neurodegeneration. Glia 53:484–490.

De Felice FG, Velasco PT, Lambert MP, Viola K, Fernandez SJ, Ferreira ST, Klein WL (2007) Abeta oligomers induce neuronal oxidative stress through an N-methyl-D-aspartate receptor-dependent mechanism that is blocked by the Alzheimer drug memantine. J Biol Chem 282:11590–11601.

de Jong EK, Dijkstra IM, Hensens M, Brouwer N, van Amerongen M, Liem RS, Boddeke HW, Biber K (2005) Vesicle-mediated transport and release of CCL21 in endangered neurons: a possible explanation for microglia activation remote from a primary lesion. J Neurosci 25:7548–7557.

Dhib-Jalbut S, Arnold DL, Cleveland DW, Fisher M, Friedlander RM, Mouradian MM, Przedborski SA, Trapp BD, Wyss-Coray T, Yong VW (2006) Neurodegeneration and neuroprotection in multiple sclerosis and other neurodegenerative diseases. J Neuroimmunol 176:198–215.

DiCarlo G, Wilcock D, Henderson D, Gordon M, Morgan D (2001) Intrahippocampal LPS injections reduce Abeta load in APP+PS1 transgenic mice. Neurobiol Aging 22:1007–1012.

Duan RS, Yang X, Chen ZG, Lu MO, Morris C, Winbland B, Zhu J (2008) Decreased fractalkine and increased IP-10 expression in aged brain of APP(swe) transgenic mice. Neurochem Res 33:1085–1089.

Dudal S, Krzywkowski P, Paquette J, Morissette C, Lacombe D, Tremblay P, Gervais F (2004) Inflammation occurs early during the Abeta deposition process in TgCRND8 mice. Neurobiol Aging 25:861–871.

Edwards JP, Zhang X, Frauwirth KA, Mosser DM (2006) Biochemical and functional characterization of three activated macrophage populations. J Leukoc Biol 80:1298–1307.

El Khoury J, Toft M, Hickman SE, Means TK, Terada K, Geula C, Luster AD (2007) Ccr2 deficiency impairs microglial accumulation and accelerates progression of Alzheimer-like disease. Nat Med 13:432–438.

Gong Y, Chang L, Viola KL, Lacor PN, Lambert MP, Finch CE, Krafft GA, Klein WL (2003) Alzheimer's disease-affected brain: presence of oligomeric Abeta ligands (ADDLs) suggests a molecular basis for reversible memory loss. Proc Natl Acad Sci U S A 100:10417–10422.

Griffin WS, Sheng JG, Royston MC, Gentleman SM, McKenzie J, Graham DI, Roberts GW, Mrak RE (1998) Glial-neuronal interactions in Alzheimer's disease: the potential role of a 'cytokine cycle' in disease progression. Brain Pathol 8:65–72.

Gundersen HJ, Jensen EB, Kiêu K, Nielsen J (1999) The efficiency of systematic sampling in stereology–reconsidered. J Microsc 193:199–211.

Heneka MT, O'Banion MK (2007) Inflammatory processes in Alzheimer's disease. J Neuroimmunol 184:69–91.

Hepler RW, Grimm KM, Nahas DD, Breese R, Dodson EC, Acton P, Keller PM, Yeager M, Wang H, Shughrue P, Kinney G, Joyce JG (2006) Solution state characterization of amyloid beta-derived diffusible ligands. Biochemistry 45:15157–15167.

Herber DL, Roth LM, Wilson D, Wilson N, Mason JE, Morgan D, Gordon MN (2004) Time-dependent reduction in A[beta] levels after intracranial LPS administration in APP transgenic mice. Exp Neurol 190:245–253.

Inoue K, Koizumi S, Tsuda M (2007) The role of nucleotides in the neuron-glia communication responsible for the brain functions. J Neurochem 102:1447–1458.

Iribarren P, Chen K, Hu J, Zhang X, Gong W, Wang JM (2005) IL-4 inhibits the expression of mouse formyl peptide receptor 2, a receptor for amyloid beta1–42, in TNF-alpha-activated microglia. J Immunol 175:6100–6106.

Itagaki S, McGeer PL, Akiyama H (1988) Presence of T-cytotoxic suppressor and leucocyte common antigen positive cells in Alzheimer's disease brain tissue. Neurosci Lett 91:259–264.

Kayed R, Head E, Thompson JL, McIntire TM, Milton SC, Cotman CW, Glabe CG (2003) Common structure of soluble amyloid oligomers implies common mechanism of pathogenesis. Science 300:486–489.

Koenigsknecht-Talboo J, Landreth GE (2005) Microglial phagocytosis induced by fibrillar beta-amyloid and IgGs are differentially regulated by proinflammatory cytokines. J Neurosci 25:8240–8249.

Lacor PN, Buniel MC, Chang L, Fernandez SJ, Gong Y, Viola KL, Lambert MP, Velasco PT, Bigio EH, Finch CE, Krafft GA, Klein WL (2004) Synaptic targeting by Alzheimer's-related amyloid beta oligomers. J Neurosci 24:10191–10200.

Lambert MP, Viola KL, Chromy BA, Chang L, Morgan TE, Yu J, Venton DL, Krafft GA, Finch CE, Klein WL (2001) Vaccination with soluble Abeta oligomers generates toxicity-neutralizing antibodies. J Neurochem 79:595–605.

Lambert MP, Velasco PT, Chang L, Viola KL, Fernandez S, Lacor PN, Khuon D, Gong Y, Bigio EH, Shaw P, De Felice FG, Krafft GA, Klein WL (2007) Monoclonal antibodies that target pathological assemblies of Abeta. J Neurochem 100:23–35.

Lee SM, Yune TY, Kim SJ, Kim YC, Oh YJ, Markelonis GJ, Oh TH (2004) Minocycline inhibits apoptotic cell death via attenuation of TNF-alpha expression following iNOS/NO induction by lipopolysaccharide in neuron/glia co-cultures. J Neurochem 91:568–578.

Lesné S, Koh MT, Kotilinek L, Kayed R, Glabe CG, Yang A, Gallagher M, Ashe KH (2006) A specific amyloid-beta protein assembly in the brain impairs memory. Nature 440:352–357.

Li R, Yang L, Lindholm K, Konishi Y, Yue X, Hampel H, Zhang D, Shen Y

(2004) Tumor necrosis factor death receptor signaling cascade is required for amyloid-beta protein-induced neuron death. J Neurosci 24:1760–1771.

Lyons A, Downer EJ, Crotty S, Nolan YM, Mills KH, Lynch MA (2007a) CD200 Ligand receptor interaction modulates microglial activation *in vivo* and *in vitro*: a role for IL-4. J Neurosci 27:8309–8313.

Lyons A, Griffin RJ, Costelloe CE, Clarke RM, Lynch MA (2007b) IL-4 attenuates the neuroinflammation induced by amyloid-beta in vivo and in vitro. J Neurochem 101:771–781.

McGeer PL, McGeer EG (2007) NSAIDs and Alzheimer disease: Epidemiological, animal model and clinical studies. Neurobiol Aging 28:639–647.

Meda L, Baron P, Scarlato G (2001) Glial activation in Alzheimer's disease: the role of Abeta and its associated proteins. Neurobiol Aging 22:885–893.

Medeiros R, Prediger RD, Passos GF, Pandolfo P, Duarte FS, Franco JL, Dafre AL, Di Giunta G, Figueiredo CP, Takahashi RN, Campos MM, Calixto JB (2007) Connecting TNF-{alpha} Signaling Pathways to iNOS Expression in a Mouse Model of Alzheimer's Disease: Relevance for the Behavioral and Synaptic Deficits Induced by Amyloid- beta Protein. J Neurosci 27:5394–5404.

Meyer-Luehmann M, Spires-Jones TL, Prada C, Garcia-Alloza M, de Calignon A, Rozkalne A, Koenigsknecht-Talboo J, Holtzman DM, Bacskai BJ, Hyman BT (2008) Rapid appearance and local toxicity of amyloid-plaques in a mouse model of Alzheimer/'s disease. Nature 451:720–724.

Mrak RE, Griffin WS (2005) Glia and their cytokines in progression of neurodegeneration. Neurobiol Aging 26:349–354.

Ponomarev ED, Maresz K, Tan Y, Dittel BN (2007) CNS-derived interleukin-4 is essential for the regulation of autoimmune inflammation and induces a state of alternative activation in microglial cells. J Neurosci 27:10714–10721.

Ramos B, Baglietto-Vargas D, del Rio JC, Moreno-Gonzalez I, Santa-Maria C, Jimenez S, Caballero C, Lopez-Tellez JF, Khan ZU, Ruano D, Gutierrez A, Vitorica J (2006) Early neuropathology of somatostatin/NPY GABAergic cells in the hippocampus of a PS1 x APP transgenic model of Alzheimer's disease. Neurobiol Aging 27:1658–1672.

Ralay Ranaivo H, Craft JM, Hu W, Guo L, Wing LK, Van Eldik LJ, Watterson DM (2006) Glia as a therapeutic target: selective suppression of human amyloid-beta-induced upregulation of brain proinflammatory cytokine production attenuates neurodegeneration. J Neurosci 26:662–670.

Reines SA, Block GA, Morris JC, Liu G, Nessly ML, Lines CR, Norman BA, Baranak CC (2004) Rofecoxib: No effect on Alzheimer's disease in a 1-year, randomized, blinded, controlled study. Neurology 62:66–71.

Richard KL, Filali M, Préfontaine P, Rivest S (2008) Toll-like receptor 2 acts as a natural innate immune receptor to clear amyloid beta1–42 and delay the cognitive decline in a mouse model of Alzheimer's disease. J Neurosci 28:5784–5793.

Schmitz C, Hof PR (2005) Design-based stereology in neuroscience. Neuroscience 130:813–831.

Schmitz C, Rutten BP, Pielen A, Schäfer S, Wirths O, Tremp G, Czech C, Blanchard V, Multhaup G, Rezaie P, Korr H, Steinbusch HW, Pradier L, Bayer TA (2004) Hippocampal Neuron Loss Exceeds Amyloid Plaque Load in a Transgenic Mouse Model of Alzheimer's Disease. Am J Pathol 164:1495–1502.

Simard AR, Soulet D, Gowing G, Julien JP, Rivest S (2006) Bone marrow-derived microglia play a critical role in restricting senile plaque formation in Alzheimer's disease. Neuron 49:489–502.

Stalder AK, Ermini F, Bondolfi L, Krenger W, Burbach GJ, Deller T, Coomaraswamy J, Staufenbiel M, Landmann R, Jucker M (2005) Invasion of hematopoietic cells into the brain of amyloid precursor protein transgenic mice. J Neurosci 25:11125–11132.

Streit WJ (2005) Microglia and neuroprotection: implications for Alzheimer's disease. Brain Res Rev 48:234–239.

Togo T, Akiyama H, Iseki E, Kondo H, Ikeda K, Kato M, Oda T, Tsuchiya K, Kosaka K (2002) Occurrence of T cells in the brain of Alzheimer's disease and other neurological diseases. J Neuroimmunol 124:83–92.

Uberti D, Ferrari-Toninelli G, Bonini SA, Sarnico I, Benarese M, Pizzi M, Benussi L, Ghidoni R, Binetti G, Spano P, Facchetti F, Memo M (2007) Blockade of the tumor necrosis factor-related apoptosis inducing ligand death receptor DR5 prevents beta-amyloid neurotoxicity. Neuropsychopharmacology 32:872–880.

Weaver CT, Hatton RD, Mangan PR, Harrington LE (2007) IL-17 family cytokines and the expanding diversity of effector T cell lineages. Annu Rev Immunol 25:821–852.

West MJ, Slomianka L, Gundersen HJ (1991) Unbiased stereological estimation of the total number of neurons in the subdivisions of the rat hippocampus using the optical fractionator. Anat Rec 231:482–497.

Wilcock DM, DiCarlo G, Henderson D, Jackson J, Clarke K, Ugen KE, Gordon MN, Morgan D (2003) Intracranially administered anti-Abeta antibodies reduce beta-amyloid deposition by mechanisms both independent of and associated with microglial activation. J Neurosci 23:3745–3751.

Wilcock DM, Munireddy SK, Rosenthal A, Ugen KE, Gordon MN, Morgan D (2004a) Microglial activation facilitates Abeta plaque removal following intracranial anti-A[beta] antibody administration. Neurobiol Disease 15:11–20.

Wilcock DM, Rojiani A, Rosenthal A, Levkowitz G, Subbarao S, Alamed J, Wilson D, Wilson N, Freeman MJ, Gordon MN, Morgan D (2004b) Passive amyloid immunotherapy clears amyloid and transiently activates microglia in a transgenic mouse model of amyloid deposition. J Neurosci 24:6144–6151.

Wyss-Coray T (2006) Inflammation in Alzheimer disease: driving force, bystander or beneficial response? Nat Med 12:1005–1015.

Zhao W, Xie W, Xiao Q, Beers DR, Appel SH (2006) Protective effects of an anti-inflammatory cytokine, interleukin-4, on motoneuron toxicity induced by activated microglia. J Neurochem 99:1176–1187.

Zipp F, Aktas O (2006) The brain as a target of inflammation: common pathways link inflammatory and neurodegenerative diseases. Trends in Neurosciences 29:518–527.

RESUMEN I

La neuroinflamación es clave en la patología de EA (Edison y col., 2008; Yokokura y col., 2011). Sin embargo su papel no está aún claro (ver revisión Varnum e Ikezu, 2012). Por ello hemos estudiado la respuesta microglial asociada a la progresión de la patología de Aβ con la edad en el ratón transgénico modelo de la enfermedad de Alzheimer **$PS1_{M146L}$/APP_{751SL}**, y su relación con la acumulación de las distintas especies de Aβ, tanto en placas insolubles extracelulares como en formas oligoméricas solubles.

A modo de resumen podemos decir que los principales hallazgos al respecto han sido:

1. A edades tempranas, hasta los 6 meses de edad, la microglía activa se restringe a las zonas de contacto con los depósitos de Aβ. Esta activación se caracteriza por la ausencia de inducción de factores citotóxicos y por la expresión de genes que son considerados marcadores de la activación microglial alternativa (YM-1).

2. A los 18 meses de edad, la activación de la microglía se extiende por todo el parénquima y por todo el hipocampo. Presenta un fenotipo de activación clásico que es potencialmente citotóxico. Produciéndose un incremento en la expresión de TNF-α, FASL, TRAIL, Cox2 y Nox1. La expresión de iNOS se restringe a los astrocitos.

3. Se detecta una clara infiltración de Linfocitos T hacia el parénquima hipocampal a los 18 meses, aunque están polarizados hacia un fenotipo Th2, por lo que la activación generalizada no puede ser debida a la presencia de los mismos.

4. Existe un claro aumento, edad dependiente, en el Aβ soluble oligomérico extracelular, el cual es un potente activador de la microglía según estudios realizados *in vitro*.

Resultados: Capitulo II.

THE JOURNAL OF BIOLOGICAL CHEMISTRY VOL. 286, NO. 21, pp. 18414–18425, May 27, 2011

Age-dependent Accumulation of Soluble Amyloid β (Aβ) Oligomers Reverses the Neuroprotective Effect of Soluble Amyloid Precursor Protein-α (sAPPα) by Modulating Phosphatidylinositol 3-Kinase (PI3K)/Akt-GSK-3β Pathway in Alzheimer Mouse Model[*S]

Received for publication, December 8, 2010, and in revised form, March 4, 2011 Published, JBC Papers in Press, April 1, 2011, DOI 10.1074/jbc.M110.209718

Sebastian Jimenez[‡§¶1,2], Manuel Torres[‡§¶1,2], Marisa Vizuete[‡§¶], Raquel Sanchez-Varo[§‖2], Elisabeth Sanchez-Mejias[§‖3], Laura Trujillo-Estrada[§‖3], Irene Carmona-Cuenca[‡§¶], Cristina Caballero[‡§¶], Diego Ruano[‡§¶], Antonia Gutierrez[§‖], and Javier Vitorica[‡§¶4]

From the [‡]Departamento Bioquímica y Biología Molecular, Facultad de Farmacia, Universidad de Sevilla, 41012 Sevilla, the [‖]Departamento Biología Celular, Genética y Fisiología, Facultad de Ciencias, Universidad de Málaga, 29071 Málaga, the [§]Centro de Investigación Biomédica en Red Sobre Enfermedades Neurodegenerativas, 41013 Sevilla, and the [¶]Instituto de Biomedicina de Sevilla-Hospital Universitario Virgen del Rocío/Consejo Superior de Investigaciones Científicas/Universidad de Sevilla, 41013 Sevilla, Spain

Neurotrophins, activating the PI3K/Akt signaling pathway, control neuronal survival and plasticity. Alterations in NGF, BDNF, IGF-1, or insulin signaling are implicated in the pathogenesis of Alzheimer disease. We have previously characterized a bigenic PS1×APP transgenic mouse displaying early hippocampal Aβ deposition (3 to 4 months) but late (17 to 18 months) neurodegeneration of pyramidal cells, paralleled to the accumulation of soluble Aβ oligomers. We hypothesized that PI3K/Akt/GSK-3β signaling pathway could be involved in this apparent age-dependent neuroprotective/neurodegenerative status. In fact, our data demonstrated that, as compared with age-matched nontransgenic controls, the Ser-9 phosphorylation of GSK-3β was increased in the 6-month PS1×APP hippocampus, whereas in aged PS1×APP animals (18 months), GSK-3β phosphorylation levels displayed a marked decrease. Using N2a and primary neuronal cell cultures, we demonstrated that soluble amyloid precursor protein-α (sAPPα), the predominant APP-derived fragment in young PS1×APP mice, acting through IGF-1 and/or insulin receptors, activated the PI3K/Akt pathway, phosphorylated the GSK-3β activity, and in consequence, exerted a neuroprotective action. On the contrary, several oligomeric Aβ forms, present in the soluble fractions of aged PS1×APP mice, inhibited the induced phosphorylation of Akt/GSK-3β and decreased the neuronal survival. Furthermore, synthetic Aβ oligomers blocked the effect mediated by different neurotrophins (NGF, BDNF, insulin, and IGF-1) and sAPPα, displaying high selectivity for NGF. In conclusion, the age-dependent appearance of APP-derived soluble factors modulated the PI3K/Akt/GSK-3β signaling pathway through the major neurotrophin receptors. sAPPα stimulated and Aβ oligomers blocked the prosurvival signaling. Our data might provide insights into the selective vulnerability of specific neuronal groups in Alzheimer disease.

OBJETIVOS II

Evaluación del efecto tóxico producido por la acumulación de formas oligoméricas solubles a edades avanzadas en el modelo transgénico murino **$PS1_{M146L}$/APP_{751SL}** de la enfermedad de Alzheimer. Estudio de la modulación de la ruta PI3K/Akt-GSK-3β mediada por la fracción soluble extracelular S1 obtenidas en ratones dobles transgénicos jóvenes (6 meses de edad) y viejos (18 meses de edad).

a. Estudio de posibles cambios, edad dependiente, en la fosforilación de GSK3β en nuestro modelo transgénico.

b. Estudio del efecto de los oligómeros solubles de Aβ sobre la ruta de señalización PI3K/Akt-GSK3β.

c. Análisis del efecto del sAPPα sobre la ruta PI3K/Akt-GSK3β a edades tempranas y tardías en presencia y ausencia de las formas oligómericas solubles de Ab.

El trabajo se presenta como artículo.

THE JOURNAL OF BIOLOGICAL CHEMISTRY VOL. 286, NO. 21, pp. 18414–18425, May 27, 2011

Age-dependent Accumulation of Soluble Amyloid β (Aβ) Oligomers Reverses the Neuroprotective Effect of Soluble Amyloid Precursor Protein-α (sAPPα) by Modulating Phosphatidylinositol 3-Kinase (PI3K)/Akt-GSK-3β Pathway in Alzheimer Mouse Model*[S]

Received for publication, December 8, 2010, and in revised form, March 4, 2011 Published, JBC Papers in Press, April 1, 2011, DOI 10.1074/jbc.M110.209718

Sebastian Jimenez[‡§¶1,2], Manuel Torres[‡§¶1,2], Marisa Vizuete[‡§¶], Raquel Sanchez-Varo[§‖2], Elisabeth Sanchez-Mejias[§‖3], Laura Trujillo-Estrada[§‖3], Irene Carmona-Cuenca[‡§¶], Cristina Caballero[‡§¶], Diego Ruano[‡§¶], Antonia Gutierrez[§‖], and Javier Vitorica[‡§¶4]

From the [‡]Departamento Bioquímica y Biología Molecular, Facultad de Farmacia, Universidad de Sevilla, 41012 Sevilla, the [‖]Departamento Biología Celular, Genética y Fisiología, Facultad de Ciencias, Universidad de Málaga, 29071 Málaga, the [§]Centro de Investigación Biomédica en Red Sobre Enfermedades Neurodegenerativas, 41013 Sevilla, and the [¶]Instituto de Biomedicina de Sevilla-Hospital Universitario Virgen del Rocío/Consejo Superior de Investigaciones Científicas/Universidad de Sevilla, 41013 Sevilla, Spain

Neurotrophins, activating the PI3K/Akt signaling pathway, control neuronal survival and plasticity. Alterations in NGF, BDNF, IGF-1, or insulin signaling are implicated in the pathogenesis of Alzheimer disease. We have previously characterized a bigenic PS1×APP transgenic mouse displaying early hippocampal Aβ deposition (3 to 4 months) but late (17 to 18 months) neurodegeneration of pyramidal cells, paralleled to the accumulation of soluble Aβ oligomers. We hypothesized that PI3K/Akt/GSK-3β signaling pathway could be involved in this apparent age-dependent neuroprotective/neurodegenerative status. In fact, our data demonstrated that, as compared with age-matched nontransgenic controls, the Ser-9 phosphorylation of GSK-3β was increased in the 6-month PS1×APP hippocampus, whereas in aged PS1×APP animals (18 months), GSK-3β phosphorylation levels displayed a marked decrease. Using N2a and primary neuronal cell cultures, we demonstrated that soluble amyloid precursor protein-α (sAPPα), the predominant APP-derived fragment in young PS1×APP mice, acting through IGF-1 and/or insulin receptors, activated the PI3K/Akt pathway, phosphorylated the GSK-3β activity, and in consequence, exerted a neuroprotective action. On the contrary, several oligomeric Aβ forms, present in the soluble fractions of aged PS1×APP mice, inhibited the induced phosphorylation of Akt/GSK-3β and decreased the neuronal survival. Furthermore, synthetic Aβ oligomers blocked the effect mediated by different neurotrophins (NGF, BDNF, insulin, and IGF-1) and sAPPα, displaying high selectivity for NGF. In conclusion, the age-dependent appearance of APP-derived soluble factors modulated the PI3K/Akt/GSK-3β signaling pathway through the major neurotrophin receptors. sAPPα stimulated and Aβ oligomers blocked the prosurvival signaling. Our data might provide insights into the selective vulnerability of specific neuronal groups in Alzheimer disease.

The molecular mechanisms underlying the selective neurodegeneration in Alzheimer disease (AD)[5] remain unclear. Amyloid-β (Aβ) peptides, proteolytically excised from the amyloid precursor protein (APP), are considered the primary pathological agents in AD. However, their precise modes of action, toxic conformational forms, and molecular targets are still controversial (for review see Ref. 1). Transgenic mouse models, overexpressing mutated forms of human APP, are widely used to study AD pathogenesis. These models develop extensive Aβ deposition in the disease-vulnerable brain regions (such as hippocampus); however, neurons are well protected until late ages. The factors and pathways maintaining neuronal integrity at young/middle ages in these AD models and those inducing neurodegeneration in the aged animals remains to be defined.

NGF, BDNF, IGF-1, and insulin are trophic factors critical for neuronal survival and plasticity, underlying memory, and learning (2–4) and could be implicated in AD development. Changes in growth factor expression and distribution, as well in their receptors (TrkA, TrkB, p75NTR, IGF-1R, and insulin-R), have been reported in AD and AD models (5). In fact, it has been suggested that the imbalance between NGF, its precursor pro-NGF, and the high (TrkA) and low (p75NTR) affinity NGF receptors seems to be a crucial factor underlying neurodegen-

* This work was supported in part by Grants PS09/00151 (to J. V.), PS09/00099 (to A. G.), and PS09/00848 (to D. R.) from the Fondo de Investigación Sanitaria (Instituto de Salud Carlos III, Spain) and by Grants CTS-4795 (to J. V.) and SAS PI-0496/2009 (to A. G.) from Junta de Andalucía (Spain).

[S] The on-line version of this article (available at http://www.jbc.org) contains supplemental Figs. 1–4.

[1] Both authors contributed equally to this work.

[2] Recipient of a contract from the Centro de Investigación Biomédica en Red Sobre Enfermedades Neurodegenerativas.

[3] Recipient of a Ph.D. fellowship from the Formación de Profesorado Universitario (FPU) Program (Spain).

[4] To whom correspondence should be addressed: Dept. of Bioquímica y Biología Molecular, Facultad de Farmacia, Universidad de Sevilla, 41012 Sevilla, Spain. Tel.: 34-954556670; E-mail: vitorica@us.es.

[5] The abbreviations used are: AD, Alzheimer disease; APP, amyloid precursor protein; sAPP, soluble APP; Aβ, amyloid β-protein; tg, transgenic; Tricine, *N*-[2-hydroxy-1,1-bis(hydroxymethyl)ethyl]glycine; ADDL, Aβ-derived diffusible ligand.

eration in AD (6, 7). Furthermore, defects in IGF-1R and insulin-R signaling are associated with amyloid plaque and neurofibrillary tangle pathology (8). In this sense, it has been reported that insulin resistance, central to type II diabetes, was implicated in the pathogenesis of AD. Alterations in IGF-1R, insulin-R, and IRS-1/2 in AD are implicated in insulin resistance (9). In fact, AD has been considered as a brain-specific "type III diabetes" (10, 11). Insulin administration facilitates memory in patients with AD (12), and IGF-1 is protective against the development of Aβ pathology (13). However, the mechanisms implicated in the Aβ-mediated insulin resistance are still unknown.

Trophic factors promote neuronal survival largely through the PI3K/Akt signaling pathway (14). After activation, phospho-Akt phosphorylates and inhibits the glycogen synthase kinase-3β (GSK-3β). The "GSK3 hypothesis of AD" (15) proposed that the overactivity of GSK-3β accounts for several features of this pathology such as memory impairment, Tau phosphorylation, increased amyloid production, microglia-mediated inflammation, and neuronal death. In fact, GSK-3β mediates the hyper-phosphorylation of Tau (16) and produces impairments in learning and memory by preventing the induction of long term potentiation (17). GSK-3β activity also is critical for inflammatory cell differentiation, migration, and secretion of pro-inflammatory cytokines (18), so it could potentially heighten microglia-mediated inflammatory responses in the local vicinity of Aβ plaques. Moreover, GSK-3β modulates key steps of the major apoptotic signaling pathways (the mitochondrial intrinsic apoptotic and the death receptor-mediated extrinsic apoptotic pathways) (19).

Increasing evidence suggests that the PI3K/Akt/GSK-3β signaling pathway is directly impacted by Aβ exposure and is altered in AD brains. In this sense, soluble (or diffusible) Aβ oligomers (putative toxic agents in AD) (20, 21) have been associated with Tau hyperphosphorylation (22), inhibition of long term potentiation, disruption of memory, loss of dendritic spine density (23), neuronal death (24, 25), and neurotoxic inflammatory response (26). Furthermore, Aβ oligomers have been shown to modulate the expression and density of insulin receptors through the modulation of the PI3K/Akt pathway (27), and alterations in the levels of phosphorylated Akt substrates have been reported in AD patients (28).

In this study, we have addressed the possible age-dependent variations in the GSK-3β phosphorylation in our PS1×APP tg model. This model developed early Aβ (3 to 4 months) plaques (29–31) but late (17 to 18 months) hippocampal neuronal degeneration, paralleled with the accumulation of soluble Aβ oligomers (26). The molecular changes that drive to this apparent age-dependent protective/degenerative neuronal condition are still unresolved. We hypothesized that the PI3K/Akt/GSK-3β signaling pathway could be involved. Using *in vivo* and *in vitro* assays, we report that natural and synthetic Aβ oligomers, acting through growth factor receptors, inhibit the prosurvival signaling PI3K/Akt/GSK-3β. Moreover, at early ages, despite the Aβ plaques, soluble APPα, acting through IGF-1 and insulin receptors, activated the prosurvival PI3K-Akt-GSK-3β pathway that might account for the lack of neurodegeneration in most transgenic models at these ages.

EXPERIMENTAL PROCEDURES

Antibodies—A11 and 6E10 antibodies were purchased from Invitrogen and Signet Laboratories, respectively. Anti-soluble APPα was provided by Immuno-Biological Laboratories. Anti-phospho-GSK-3β (Ser-9); phospho-Akt (Ser-473); phospho-Akt (Thr-308); phospho-IGF1 receptor β (Tyr-1135/1136); pTrkA-B (TrkA, Tyr-674/675; TrkB, Tyr-706/707) were from Cell Signaling Laboratory. Anti-phospho-insulin receptor (Tyr-1150/1151) was purchased from Millipore. Monoclonal anti-human PHF-Tau (Clone AT100) was purchased from Innogenetics. Anti-phospho- and total β-catenin antibodies were from Cell Signaling Laboratory and Abcam, respectively. Anti-β-actin was purchased from Sigma.

Transgenic Mice—The generation and initial characterization of the $PS1_{M146L}$×APP_{751sl} (PS1×APP) tg mice has been reported previously (29). This double tg mice (C57BL/6 background) were generated by crossing homozygotic $PS1_{M146L}$ mice with heterozygotic Thy1-APP751SL mice (all tg mice were provided by Transgenic Alliance, IFFA Credo, Lyon, France). Mice represented F10–F15 offspring of heterozygous tg mice. Only male mice were used in this work. Age-matched $PS1_{M146L}$ and nontransgenic (WT) male mice of the same genetic background (C57BL/6) were used as controls.

For glucose determination, the anesthetized (sodium pentobarbital; 60 mg/kg) animals were bled (50 μl) from the tail. The glucose levels were similar between ages and genotypes (in mM: 6.4 ± 1.4, 5.4 ± 1.2; 7.3 ± 1.2 and 6.5 ± 1.4, $n = 7$, for 6 or 18 months, WT and PS1×APP, respectively). After bleeding, the mice were killed by decapitation, and both hippocampi were dissected, frozen in liquid N_2, and stored at −80 °C until use. All animal experiments were performed in accordance with the guidelines of the Committee of Animal Research of the University of Seville (Spain) and the European Union Regulations.

RNA and Total Protein Extraction—Total RNA was extracted using the Tripure™ isolation reagent (Roche Applied Science) as described previously (30, 31).

The contaminating DNA in the RNA samples was removed by incubation with DNase (Sigma) and confirmed by PCR analysis of total RNA samples prior to reverse transcription (RT). After isolation, the integrity of the RNA samples was assessed by agarose gel electrophoresis. The yield of total RNA was determined by measuring the absorbance (260/280 nm) of ethanol-precipitated aliquots of the samples. The recovery of RNA was comparable in all groups (1.2–1.5 μg/mg of tissue). The protein pellets, obtained using the Tripure™ isolation reagent, were resuspended in 4% SDS and 8 M urea in 40 mM Tris-HCl, pH 7.4, and rotated overnight at room temperature (30, 31).

Retrotranscription and Real Time RT-PCR—The retrotranscription (RT) was done using random hexamers, and 3 μg of total RNA as template and high capacity cDNA archive kit (Applied Biosystems) following the manufacturer recommendations (30, 31). For real time RT-PCR, each specific gene product was amplified using commercial TaqMan™ probes, following the instructions of the manufactured (Applied Biosystems), using an ABI Prism 7000 sequence detector (Applied Biosystems). For each assay, a standard curve was first constructed, using increasing amounts of cDNA. In all cases, the

slope of the curves indicated optimal PCR conditions (slope 3.2–3.4). The cDNA levels of the different mice were determined using two different housekeepers (*i.e.* GAPDH and β-actin). The amplification of the housekeepers was done in parallel with the gene to be analyzed. Similar results were obtained using both housekeepers. Thus, the results were normalized using only the GAPDH expression.

Independently of the gene analyzed, the results were always expressed using the comparative *Ct* method, following Bulletin 2 from Applied Biosystems. As a control condition, we selected 6-month-old WT mice. In consequence, the expression of all tested genes, for all ages and mouse types, was referenced to the expression levels observed in 6-month-old WT mice.

Aβ42 Peptide Preparation—To prepare the Aβ42 peptides, we allowed synthetic lyophilized Aβ(1–42) peptide (human sequence, Anaspec) to equilibrate, at 20–23 °C, for 30 min before it was resuspended and diluted to 1 mM in hexafluoro-2-propanol. After evaporation, peptide films were dried in a Speed vacuum and stored at −40 °C. Peptide films were resuspended to 5 mM in dimethyl sulfoxide (DMSO) for 10 min. To form the ADDLs (32), we diluted the 5 mM DMSO solution to 100 μM in cold PBS, vortexed for 30 s, and incubated overnight at 4 °C. Before use, the Aβ/PBS solution was further diluted in culture media. The presence of ADDLs was tested by Western blots using 6E10 (data not shown).

To form the monomers, immediately before use, we diluted the 5 mM DMSO solution in PBS (to a final concentration of 100 μM), following by ultrafiltration through 5-kDa cutoff device (Vivaspin 2, Sartorius Biolab Products). The presence of the monomeric Aβ42 peptide (4.5 kDa) was verified by Western blots (data not shown).

Soluble Protein Extraction (Soluble Fractions) and Immunoprecipitation—The soluble fractions were obtained by ultracentrifugation of the homogenates as described previously (26, 33). Briefly, tissue samples were homogenized (using a Dounce homogenizer) in cold isotonic buffer (0.32 M sucrose, 1 mM EDTA, 1 mM EGTA, 20 mM Tris-HCl, pH 7.5, containing a mixture of protease and phosphatase inhibitors, Sigma) and ultracentrifuged (Optima™ MAX Preparative Ultracentrifuge, Beckman Coulter) at 120,000 × *g*, 4 °C, during 60 min. Immediately after centrifugation, the samples were aliquoted and stored at −81 °C until use. The protein content in the soluble fractions was determined by Lowry. To diminish the potential inter-individual variability, the S1 fractions from four different mice, for each age and genotype, were pooled.

For immunoprecipitation experiments, 50 μg of soluble proteins were incubated, overnight at 4 °C with continuous shaking, with A11 antibody, previously adsorbed to protein G-Sepharose or protein A-Sepharose beads (Sigma) (2 μg of purified antibody/20 μg of protein G- or A-Sepharose) in the presence of protease inhibitors (Roche Applied Science) in a final volume of 500 μl of TBS. Immunobeads were isolated by centrifugation and washed three times in cold TBS. Finally, the immunoprecipitated proteins were eluted using 20 μl of Laemmli's buffer and analyzed by Western blots.

For *in vitro* experiments, the soluble fractions from the different mice and ages were thawed immediately before use, diluted with DMEM (without FBS), sterilized by filtration (through 0.22-μm filters, Millipore), and added to cell cultures. For each experiment, duplicate wells were stimulated under the same experimental conditions.

The immunodepletion experiments were done basically as described previously (26, 34). Briefly, 50 μg of protein from soluble fractions from 6- and 18-month-old PS1×APP mice (n = 3/age) were subjected to three sequential incubations (8–12 h at 4 °C) with either 6E10 (5 μg) protein G-Sepharose or A11 (5 μg) protein A-Sepharose immunocomplexes. After immunodepletion, the soluble fractions were used for *in vitro* stimulation (see below). As control, the different soluble fractions were sequentially incubated with either protein G-Sepharose or protein A-Sepharose and tested, in parallel experiments, with the immunodepleted samples.

Western Blot and Dot Blot—Western blots were performed as described previously (34). Briefly, 10–20 μg of protein from the different samples were loaded on 16% SDS-Tris-Tricine-PAGE and transferred to nitrocellulose (Hybond-C Extra, Amersham Biosciences). Alternatively, the immunoprecipitated samples were electrophoresed on 12% SDS-Tris glycine.

After blocking, the membranes were incubated overnight, at 4 °C, with the appropriate antibody. The membranes were then incubated with anti-mouse horseradish peroxidase-conjugated secondary antibody (Dako, Denmark) at a dilution of 1:8000. The blots were developed using the ECL-plus detection method (Amersham Biosciences).

Dot blots were done as described previously (26, 34). One μg of protein from the different soluble fractions were directly applied to dry nitrocellulose in a final volume of 2 μl. Blots were air-dried, blocked for 1 h, and incubated overnight at 4 °C, with either Nu-1 (courtesy of Dr. W. Klein; 1 μg/ml) or A11 (1:5000 dilution, BIOSOURCE) antibodies. After the incubation, the blots were washed and visualized as described above.

For quantification, the scanned (Epson 3200) images were analyzed using the PCBAS program. In each experiment, the intensity of bands from WT mice and/or experimental conditions were averaged and considered as 1 relative unit. Data were always normalized by the specific signal observed in 6-month-old WT group or negative control for "*in vitro*" experiments.

Tissue Preparation—After deep anesthesia with sodium pentobarbital (60 mg/kg), 6- and 18-month-old control (WT) and PS1×APP tg male mice (n = 4/age/genotype) were perfused transcardially with 0.1 M phosphate-buffered saline (PBS), pH 7.4, followed by 4% paraformaldehyde, 75 mM lysine, 10 mM sodium metaperiodate in 0.1 M phosphate buffer (PB), pH 7.4. Brains were then removed, post-fixed overnight in the same fixative at 4 °C, cryoprotected in 30% sucrose, sectioned at 40 μm thickness in the coronal plane on a freezing microtome, and serially collected in wells containing cold PBS and 0.02% sodium azide. All animal experiments were approved by the Committee of Animal Use for Research of the Malaga University (Spain) and the European Union Regulations.

Immunohistochemistry—Coronal free-floating brain sections (40 μm thick) from 6-and 18 month-old control (WT) and PS1×APP mice were processed simultaneously for phospho-GSK-3β immunolabeling in the same solutions and conditions to prevent processing variables. Sections were first treated with 3% H_2O_2, 3% methanol in PBS and with

avidin-biotin blocking kit (Vector Laboratories, Burlingame, CA) and then incubated overnight at room temperature with rabbit anti-GSK-3β (phospho-Ser-9) antibody (dilution 1:100, Abcam ab30619).

The tissue-bound primary antibody was detected by incubating with the corresponding biotinylated secondary antibody (1:500 dilution, Vector Laboratories) and then followed by streptavidin-conjugated peroxidase (Sigma) diluted 1:2000. The reaction was visualized with 0.05% 3,3′-diaminobenzidine tetrahydrochloride (Sigma), 0.03% nickel ammonium sulfate, and 0.01% hydrogen peroxide in PBS. Sections were then mounted on gelatin-coated slides, air-dried, dehydrated in graded ethanols, cleared in xylene, and coverslipped with DPX (BDH) mounting medium. Specificity of the immune reaction was controlled by omitting the primary antiserum.

N2a and Primary Neuronal Cultures—N2a cells were plated at 25,000 cells/cm^2 and cultured in high glucose DMEM/OptiMEM (50–50%) supplemented with 2 mM glutamine and 5% fetal bovine serum (PPA Co.) in the presence of penicillin and streptomycin (100 units/ml and 0.01 mg/ml, respectively). For stimulation experiments, the medium was change to high glucose DMEM and serum-deprived for 12 h. The cells were stimulated using 5% fetal bovine serum, 100 nM IGF-1 (Sigma), 100 nM insulin (Sigma), 10 nM NGF-β (Sigma), or 25 nM sAPPα (Sigma) in the presence or absence of ADDLs (ranging from 0.01 to 2 μM; estimated from the initial Aβ42 concentration used for oligomerization; we are aware that the ADDL concentration could be underestimated). After stimulation, the proteins were isolated and analyzed as described above.

Primary neuronal cultures were done essentially as described previously (27). Briefly, embryonic E18–20 or postnatal P1 brains were dissected and treated, for 5 min, with trypsin/DMEM/EDTA medium (BioWhittaker, Cambrex, Belgium). The treatment was stopped using complete DMEM plus 10% FBS, and the cells were mechanically dissociated. After mechanical dissociation, the debris was eliminated by filtration (40 μm, Falcon), and the cells were seeded (at a density of 60,000 cells/ml) in Neurobasal medium plus B27 supplemental (containing glutamine, 1% penicillin/streptomycin and gentamycin) on poly-D-lysine (Sigma)-treated Nunc 12- or 96-well plates. The cells were cultured at 37 °C, in humidified 5% CO_2, 95% atmosphere. Medium was half-replaced every 4 days. After 13–15 days in culture, the cultures were treated with different concentrations (ranging from 0.01 to 2 μM) of ADDLs (prepared as described above) or different concentrations (ranging from 0.27 to 54 nM) of sAPPα. The cells were then incubated for 30 min and rinsed with cold PBS, and the proteins were extracted as above. The neuronal survival was assayed using MTS (Promega) following the manufacturer's indications.

Statistical Analysis—Data were expressed as means ± S.D. The comparison between two mouse groups (WT and PS1×APP tg mice) was done by two-tailed *t* test. For comparison between several age groups, we used one-way analysis of variance followed by Tukey post hoc multiple comparisons test (Statgraphics plus 3.1). The significance was set at 95% of confidence.

RESULTS

Age-dependent Modifications on the GSK-3β Activity in PS1×APP Mouse Hippocampus—The GSK-3β activity could play a central role controlling apoptosis and the development of Alzheimer disease. Because GSK-3β activity was inhibited by phosphorylation on Ser-9, we have first quantified, by Western blots, the Ser-9 phospho-GSK-3β levels in our PS1×APP tg model. We used two different ages, 6 and 18 months, before and after pyramidal neurodegeneration, respectively (26, 30). Western blot analysis demonstrated the existence of a clear age-dependent variation of the Ser-9 phosphorylation levels in PS1×APP mice (Fig. 1*A*, *panels a1* and *a2*). As compared with 6-month-old WT mice, the levels of Ser-9 phospho-GSK-3β were elevated in young PS1×APP hippocampus, whereas the 18-month-old PS1×APP mice displayed a significant decrease. In fact, the Ser-9 phosphorylation level, at 18 months, represented a decrease of 5.66 ± 0.46 times over 6-month-old PS1×APP mice. This observation was also confirmed using immunohistochemistry. As shown in Fig. 1*B*, the phospho-Ser-9 GSK-3β immunoreactivity was mainly located in the somata of hippocampal neuronal cells. As also shown (Fig. 1*B*, *panels b1* and *b2*), a marked increase in the immunoreactivity was observed in the hippocampus of 6-month-old PS1×APP tg mice, as compared with WT. This increase was evident in both pyramidal and interneuronal cell somata and their proximal dendrites. In parallel experiments, GSK-3β phosphorylation immunostaining was clearly decreased in aged PS1×APP tg mice (Fig. 1*B*, *panels b3* and *b4*).

The GSK-3β activity could modulate the intrinsic apoptotic pathway by modifying, directly and/or indirectly, the expression of pro- and anti-apoptotic Bcl-2 family proteins (35–37). Thus, we have determined the possible variations in the expression of mRNAs coding for Bcl-2 proteins in 6- and 18-month-old WT and PS1×APP tg mice. According to the phosphorylation of the GSK-3β (38), in 6-month-old PS1×APP mice the expression of *bcl-2* was increased (Fig. 1*C*). On the contrary, in 18- month-old PS1×APP animals, the expression of *bcl-2* was not different from WT, whereas *bim* and *bad* expression increased exclusively in transgenic animals. These data could indirectly reflect the activation of GSK-3β in aged PS1×APP mice. Additionally, the possible age-dependent activation of the GSK-3β was also tested by determining the protein level and phosphorylation status of β-catenin (39). Although the phosphorylated *versus* total β-catenin ratio was not altered in 6-month-old PS1×APP mice (Fig. 1*D*), we did observed an increase in the steady-state levels of both β-catenin forms. These data were consistent with a reduced GSK-3β activity. More relevant and also consistent with the proposed age-dependent increase in the GSK-3β activity, the total and phosphorylated β-catenin contents were dramatically reduced in 18-month-old PS1×APP mice (Fig. 1*D*). Furthermore, the ratio of phospho/total β-catenin displayed a considerable increase in these aged PS1×APP mice, suggesting a hyperphosphorylation status of the β-catenin.

These data demonstrated the existence of an age-dependent change in the phosphorylation of the GSK-3β in our PS1×APP tg model. Whereas at early ages the GSK-3β seemed to be

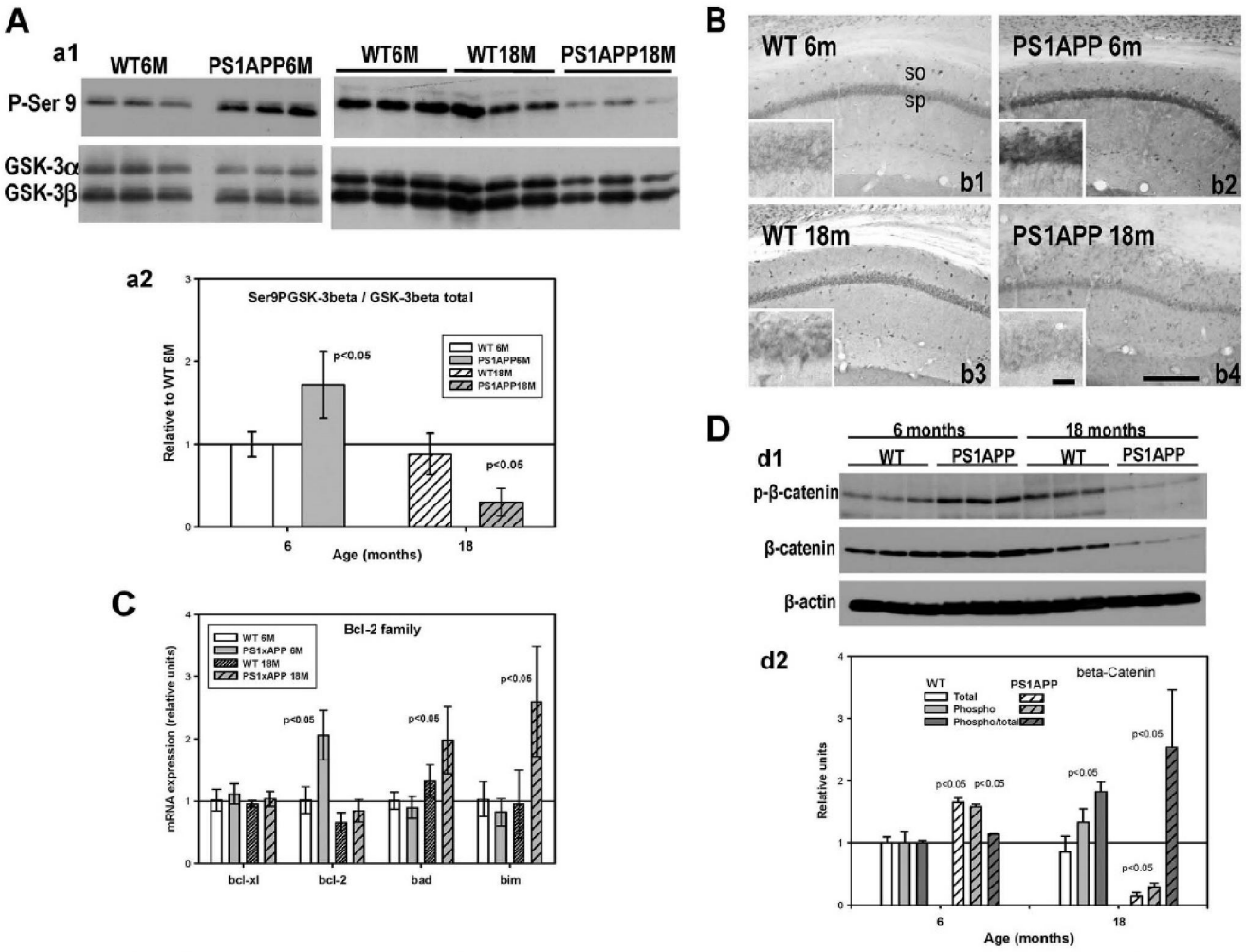

FIGURE 1. **Age-dependent decrease on GSK-3β phosphorylation (Ser-9) in PS1×APP hippocampus.** *A*, relative phosphorylation levels of Ser-9 GSK-3β (*panel a1, upper panel*) were determined, by Western blots, in 6- and 18-month-old WT and PS1×APP hippocampi. The Western blots were then reprobed for total GSK-3β (*a1, lower panel*). In these experiments, 10 μg of proteins from WT and PS1×APP mice were electrophoresed in parallel, using different distributions. In each gel, a minimum of three WT and three PS1×APP samples were run together. The experiment was repeated three times using different sample combinations. Quantitative analysis of the Western blots is shown in *panel a2*. The Western blots were scanned, and the ratio between phosphorylated/total expression was calculated. In each experiment, the phosphorylation/total ratio was normalized by 6-month-old WT value. The total protein loading was also tested by anti-β-actin antibody (data not shown). *B*, hippocampal (CA1) light microscopy images of phospho-Ser-9-GSK-3β immunohistochemistry from 6- (*panels b1* and *b2*) and 18-month-old (*panels b3* and *b4*) WT (*panels b1* and *b3*) and PS1×APP (*panels b2* and *b4*) mice. For these experiments, serial sections of 6- and 18 month-old WT and PS1×APP brains were processed in parallel. Thus, both WT and PS1×APP slices were equally developed. The image shown is representative of four different WT and PS1×APP mice. *Insets* show higher magnifications of stratum pyramidale. *C*, expression of different *bcl-2* family protein mRNAs was analyzed by quantitative RT-PCR. In each case, the results ($n = 7$) were corrected by the GAPDH expression and normalized by 6-month-old WT mice. *D*, total and phosphorylated β-catenin levels were assessed by Western blots (*panel d1*). Quantitative data are shown in *panel d2*. As shown, the total and phosphorylated β-catenin increased in samples from 6-month-old PS1×APP, and there was a dramatic decrease in both levels in samples from 18-month-old PS1×APP mice. Furthermore, the phosphorylated/total ratio also increased at this old age. Significance difference between the different samples was determined by analysis of variance followed by Tukey test. *so*, stratum oriens; *sp*, stratum pyramidale. *Scale bars*, 50 μm.

inhibited by Ser-9 phosphorylation (probably exerting a neuroprotective action), in aged PS1×APP mice the activation of GSK-3β was increased.

Young and Aged PS1×APP Hippocampus-derived Soluble Factors Increased or Inhibited, Respectively, the Akt-dependent Phosphorylation of GSK-3β—We next investigated the possibility that soluble APP-derived factors were involved in the modulation of GSK-3β phosphorylation in both young (6 months) and aged (18 months) PS1×APP mice. In this sense, it has been recently reported that monomeric Aβ42 mediated the activation of the PI3K-Akt pathway (40), whereas Aβ oligomers (ADDLs) induced an impairment of insulin receptors (27).

We have first determined *in vitro* using N2a cell cultures the effect of soluble brain extracts, derived from 6- and 18-month-old WT, PS1 (data not shown), and PS1×APP mice on the Ser-9 phosphorylation of GSK-3β. As shown (Fig. 2*A*, and quantitatively in Fig. 2*C*), the addition of the soluble fractions obtained from 6-month-old PS1×APP mice produced a clear induction in the GSK-3β phosphorylation over basal values (serum deprivation). This increase was mediated by the activation of the PI3K/Akt pathway because Akt was phosphorylated at both Thr-308 and Ser-473 residues (Fig. 2*A*), and the effect was abolished by the addition of LY294002 (data not shown). This activation of the PI3K/Akt pathway seemed to be mediated by at

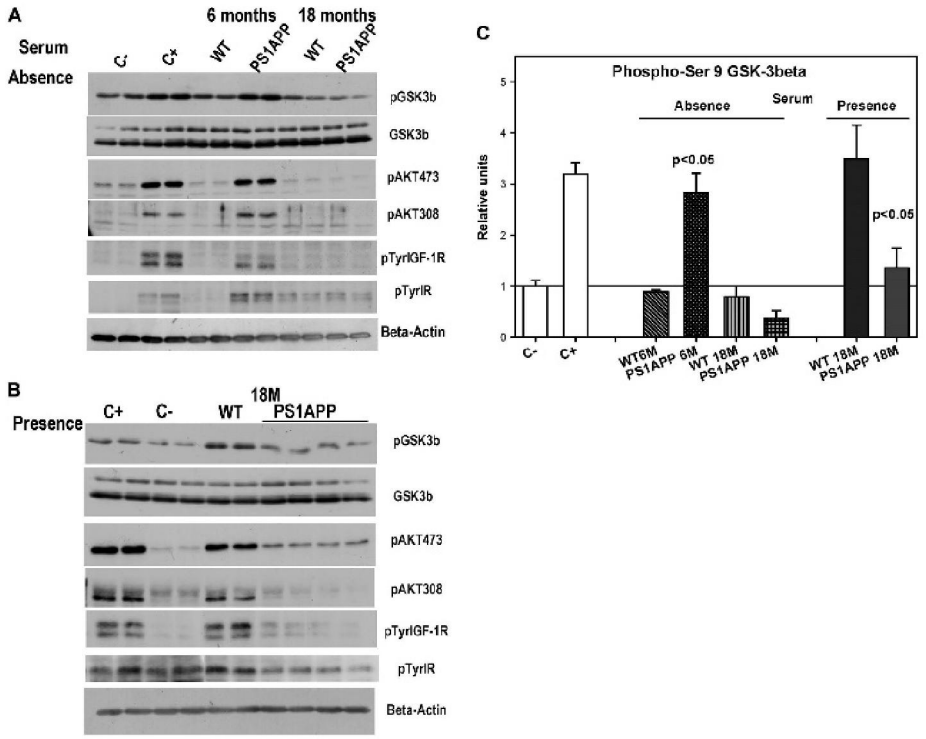

FIGURE 2. **Soluble fractions, derived from 6- or 18-month-old PS1×APP mice, produced the stimulation or inhibition of Akt-GSK-3β phosphorylation.** *A*, N2a cultures were serum-deprived for 12 h and treated with 50 μg of soluble proteins derived from young (6 months) or old (18 months) WT and PS1×APP mice. After treatment, the phosphorylation levels of GSK-3β (Ser-9), Akt (Ser-473 or Thr-308), IGF-1R (phospho-Tyr-1135/1136), or IR (phospho-Tyr-1150/1151) were determined by Western blots. As shown, the S1 fractions from 6-month-old PS1×APP produced a clear induction of the phosphorylation levels of all protein tested. *B*, possible inhibitory effect of 18-month-old PS1×APP S1 fractions (50 μg of protein) was assessed in serum-stimulated Akt-GSK-3β pathways. For each condition, two culture wells were treated in parallel, and the experiments were repeated at least three times. *C*, quantitative analysis of experiments shown in *A* and *B*. The results are mean ± S.D. of three independent experiments. Data were normalized by negative controls (*C*−). Negative (*C*−) and positive (*C*+) controls represented control experiments in the absence (12 h) or presence of serum, respectively. The protein loading was tested by total GSK-3 and β-actin.

least the IGF-1 and/or insulin receptors. In fact, both receptors were activated (Tyr-phosphorylated) in the presence of these soluble extracts. The activation of the Akt and phosphorylation of GSK-3β were specific for the factors present in PS1×APP mice because the addition of a similar amount of soluble proteins from WT or PS1 transgenic mice (data not shown) was devoid of any effect.

In parallel experiments, we have also tested the effect of soluble extracts from 18-month-old PS1×APP mice (Fig. 2, *A* and *C*). In contrast to that observed using young PS1×APP, 18-month-derived soluble fraction did not induce the phosphorylation of Akt-GSK-3β in serum-deprived cultures. In fact, a small inhibition, over control values, was observed (Fig. 2*C*). The soluble extracts from 18-month-old WT mice displayed no intrinsic effect.

The possible inhibitory action of the soluble fractions from aged transgenic mice was tested by analyzing their effect on the serum-stimulated Akt-GSK-3β phosphorylation. As shown (Fig. 2*B*), the treatment of N2a cells with fractions derived from 18-month-old PS1×APP mice produced a practically complete inhibition of the serum-induced GSK-3β phosphorylation (see also Fig. 2*C*). This inhibition was paralleled by a decrease in Akt473 and Akt308 phosphorylation and was also paralleled by a decrease in the Tyr phosphorylation of IGF-1R and insulin receptor. The soluble fractions from aged WT or PS1 (data not shown) mice showed no apparent effect.

In addition, we have also examined the effect of 6- and 18-month-derived soluble fractions on neuronal survival assays. For these experiments, primary neurons were subjected to deprivation and supplemented with 6- or 18-month soluble fractions. As expected (see supplemental Fig. 1), the soluble extract from 6-month-old PS1×APP avoided the decrease in neuronal survival due to growth factor deprivation. As also expected, the soluble fraction from 18 months did not protect or even produce a small decrease on the neuronal survival. In this sense, we also tested the possible neurotoxic effect of these 18-month PS1×APP-soluble fractions. After 24 h of incubation, in the presence of B27 supplement, these soluble fractions produced a significant decrease in the neuronal survival (100.0 ± 7.7% *versus* 80.19 ± 2.6%, $n = 3$; $p < 0.05$). The WT-derived soluble fractions displayed no intrinsic effect. These data demonstrated that soluble factors present exclusively in PS1×APP-derived brain fractions modulated (positively or negatively) the GSK-3β phosphorylation and neuronal survival.

Characterization of APP-derived Fragments from Young and Aged PS1×APP Mice—As mentioned above, APP-derived proteins could modulate the GSK-3β phosphorylation. In consequence, we have next analyzed, by Western blots using the mAb 6E10 (Fig. 3*A*), the presence of APP-derived soluble fragments in these fractions. As shown, the soluble fractions from 6-month-old PS1×APP mice exhibited a single specific (as compared with WT) band of high apparent molecular weight

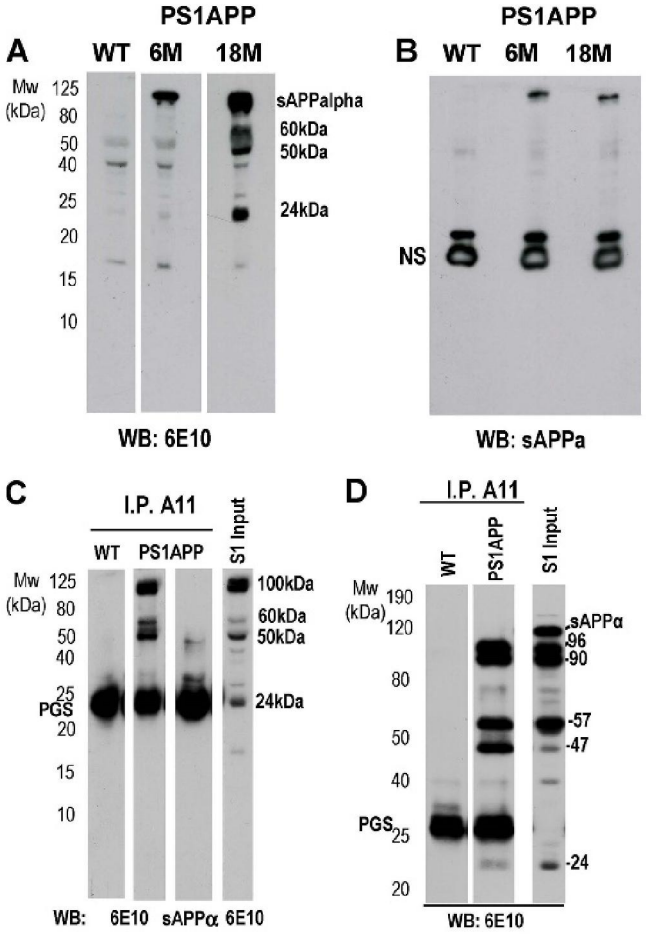

FIGURE 3. **Aβ oligomeric forms in soluble extracts from 18-month PS1×APP.** *A*, S1 fractions from 6 month-old WT and PS1×APP or 18-month PS1×APP were first analyzed by Western blot (16% SDS-Tris-Tricine-PAGE) using mAb 6E10. Results showed an age-dependent increase of soluble SDS-resistant oligomeric species of approximately 24, 50, 60, and 90 kDa in PS1×APP animals. No significant amounts of mono-, di-, or trimers were detected under these experimental conditions. *B*, Western blots (*WB*) were re-tested using anti-sAPPα antibody. Only a high molecular weight specific band (~90 kDa) was observed. No significant (*NS*) age-dependent changes could be appreciated in this band. *C*, immunoprecipitation (*I.P.*) experiments using A11 antibody were addressed for selective recognition of the Aβ oligomers in 18-month PS1×APP-soluble extracts. The S1 fractions obtained from 18-month-old WT or PS1×APP were incubated with A11-protein G-Sepharose immunocomplexes and analyzed by 16% SDS-Tris-Tricine-PAGE and Western blots using 6E10. As shown, the pattern of immunoisolated Aβ oligomers was similar to that observed in the crude S1 fraction. Anti-sAPPα antibody displayed no specific staining in these immunoprecipitated samples. *D*, A11 immunoisolated oligomers were resolved using 12%-SDS-Tris glycine-PAGE and blotted as in *C*. Using this approach, at least five different Aβ oligomeric forms were identified. Western blots are representative of at least four replicated experiments with similar results.

(Fig. 3*A*). Interestingly, no monomeric Aβ was detected by this assay, even after longer exposures (data not shown). Because mAb 6E10 recognized both Aβ peptides and sAPPα, we retested the Western blots using an anti-sAPPα antibody. As shown (Fig. 3*B*), a band of similar relative molecular weight (M_r) was also observed with this antibody. Therefore, sAPPα was the predominant APP-derived fragment (detected with 6E10) in young PS1×APP mouse hippocampi.

However, the analysis of the soluble fractions from 18-month-old PS1×APP mouse hippocampi demonstrated the presence of several oligomeric Aβ forms. Based on the calculated M_r (24, 50, and 60–70 kDa), these Aβ oligomers were compatible with the presence of 6- and 12–16-mer, SDS-resistant aggregates. As expected, these oligomers were immunopositive for A11 and Nu-1 antibodies in dot blots (data not shown but see Ref. 26). It is also interesting the absence of monomeric Aβ in these fractions. It is of note that the presence of a relatively abundant band localized in the high molecular weight range. This band probably corresponded to a different highly aggregated Aβ oligomer because, as probed by Western blots using anti-sAPPα antibody, this soluble fragment did not increase in aged PS1×APP mice (see Fig. 2*B*).

To further characterize these Aβ oligomers, we used the conformation-dependent anti-oligomeric A11 antibody in immunoprecipitation assays. As shown (Fig. 3*C*), three different high molecular weight Aβ oligomers (50, 60–70, and 90–100 kDa) were immunoprecipitated by A11 antibody. The 24-kDa oligomer was occluded by the presence of a prominent band corresponding to the protein G-Sepharose. This putative 6-mer oligomer was clearly visualized using A11-protein A-Sepharose immunocomplexes (data not shown but see below). Furthermore, as expected, A11 antibody did not immunoprecipitate the sAPPα (Fig. 3*C*).

To better resolve these relatively high molecular weight Aβ oligomers, the A11-immunoprecipitated proteins were also analyzed in 12% Tris glycine gels (Fig. 3*D*). As shown, at least five different putative Aβ oligomers (detected by 6E10) of 24, 47, 57, 90, and 96 kDa were identified in these experiments. As also shown, the sAPPα (110-kDa band), present in the soluble fraction, was not immunoprecipitated by A11. Therefore, the aggregated forms presented in the soluble fractions from 18-month-old PS1×APP mice were compatible with the presence of Aβ oligomers of 6-, 10-, 12-, 20- and 22-mers.

Opposite Actions of Synthetic sAPPα (Stimulation) and ADDLs (Inhibition) on the Akt Prosurvival Pathway—Based on the observed soluble fraction composition, we next characterized the effect of synthetic sAPPα and Aβ oligomers on the Akt-GSK-3β phosphorylation (Fig. 4) using N2a cell cultures.

The soluble APPα (Fig. 4*A*, *panel a1*, and quantitatively in *panel a2*) produced a dose-dependent increase in the phosphorylation levels of Ser-9 GSK-3β and Akt (at Thr-308 and Ser-473 residues), whereas the soluble APPβ, probed in parallel experiments, produced no effect in this *in vitro* phosphorylation assay (Fig. 4*A*, *panel a2*). Interestingly, the sAPPα displayed a quite high potency in the low nanomolar range (EC_{50} = 2.30 ± 0.93 nM, n = 4; Fig. 4*A*, *panel a2*) coincident with the estimated concentration (by Western blots using commercial sAPPα as standard) of the sAPPα in the soluble fraction of the 6-month-old PS1×APP mice (19.9 ± 4.11 nM). This stimulatory effect was also replicated using primary cortical cultures (supplemental Fig. 3*A*). As expected, sAPPα seemed to exert its effect acting through IGF-1R and insulin receptor (see Fig. 4*A*, *panel a1*) and, in consequence, was inhibited by LY294002, AG1024, and picropodophyllin (supplemental Fig. 2*A*).

These data indicated that in this *in vitro* model the sAPPα behaved like an agonist, acting at least through IGF-1R and insulin receptors, activating the PI3K/Akt pathway and, in consequence, phosphorylating and inhibiting the GSK-3β activity.

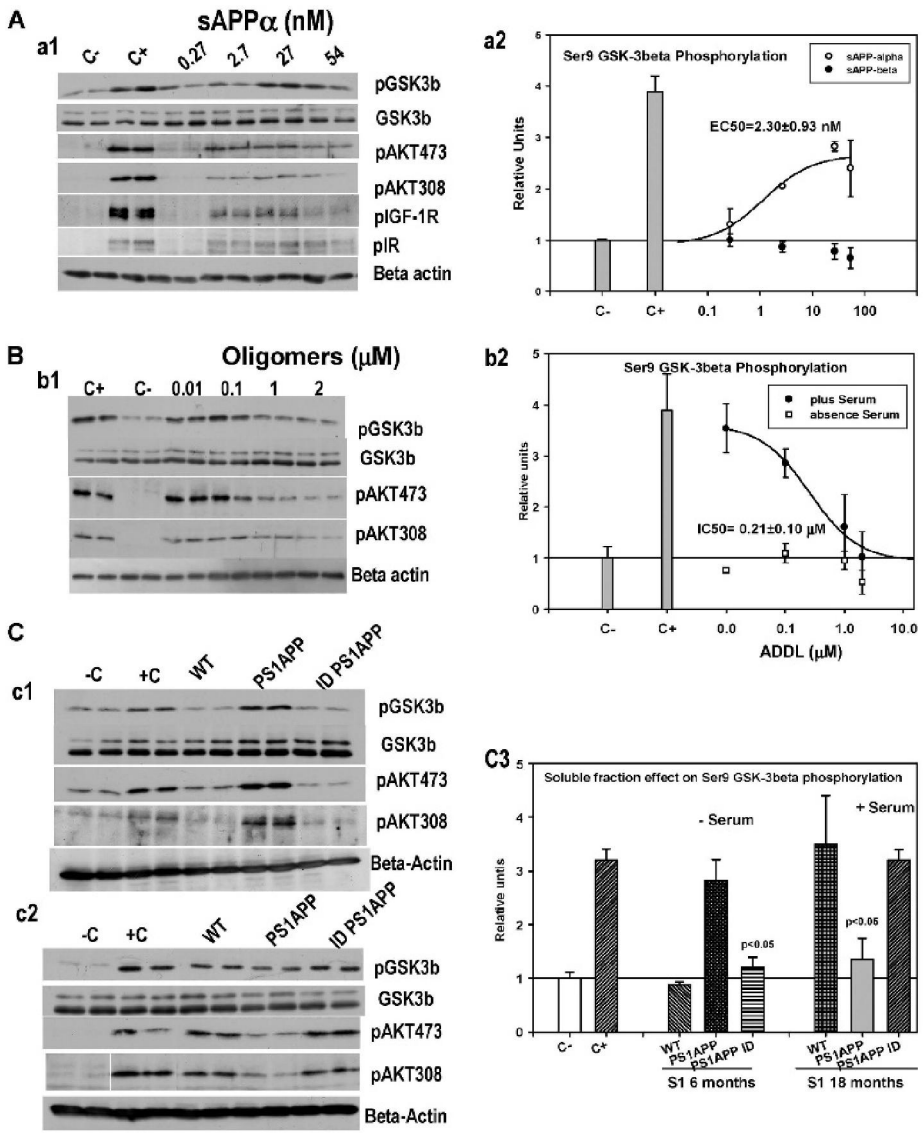

FIGURE 4. **Synthetic sAPPα and Aβ oligomers (ADDLs) stimulated or inhibited the Akt-GSK-3β phosphorylation in N2a cultures.** *A*, sAPPα activated the IGF-1R/IR Akt GSK-3β pathway. Serum-deprived N2a cultures were treated with increasing concentrations of synthetic sAPPα or sAPPβ (data not shown), and the phosphorylations of Ser-9 GSK-3β, Akt (473 and 308), IGF-1R (Tyr-1135/1136), and IR (Tyr-1150/1151) were analyzed by Western blots (*panel a1*). *Panel a2*, quantitative analysis of Western blots normalized by negative control (*C−*). *B*, inhibitory effect of increased concentrations of ADDLs on Akt-GSK-3β phosphorylation was assessed in N2a maintained in the presence of serum. Western blots (*panel b1*) and quantitative analysis of the data (*panel b2*) are illustrated. *C*, immunodepletion experiments. The S1 fractions, derived from 6- (*panel c1*) or 18-month-old (*panel c2*) PS1×APP mice, were immunodepleted using 6E10 or A11, and the samples were tested for stimulation experiments (as above) in the absence (*panel c1*) or presence of serum (*panel c2*). *Panel c3*, quantitative analysis of the Western blots. Data were normalized by the corresponding negative control and are means ± S.D. of three independent experiments. Data (mean ± S.D.) presented in *panels a2* and *b2* were fitted to a logistic four-parameter equation as described previously (34, 62). The protein loading was tested by total GSK-3β and β-actin.

In addition, saturating concentrations of sAPPα promoted neuronal survival in a deprivation assay (supplemental Fig. 2*B*).

Aiming to test the possible inhibitory effect of oligomeric Aβ, we have used synthetic Aβ oligomers (ADDLs) (41). Similar to natural Aβ oligomers, the synthetic ADDLs displayed no intrinsic effect in the absence of serum (data not shown). Also similar to natural oligomers, in the presence of serum, ADDLs displayed a dose-dependent inhibition of the GSK-3β phosphorylation (Fig. 4*B*, *panel b1*) with a calculated IC_{50} of 0.21 ± 0.10 μM ($n = 4$) (Fig. 4*B*, *panel b2*). As expected from our previous data, this inhibitory effect was paralleled by an inhibition of the serum-stimulated Akt activation (pAkt473 and -308) (Fig. 4*B*, *panel b1*). This inhibitory effect was also replicated in primary neuronal cultures (supplemental Fig. 3*B*).

In addition, we have tested the possible neuroprotective effect of sAPPα and 6-month PS1×APP-soluble fractions on ADDL (2 μM) toxicity (supplemental Fig. 3*C*). As shown, the sAPPα and 6-month PS1×APP soluble fractions avoided (partially and fully, respectively) the ADDL-induced neuronal toxicity.

Based on these observations, we postulated that if the stimulation (at 6 months) or inhibition (18 months) of the Akt-

GSK-3β phosphorylation was indeed mediated by sAPPα, at 6 months, or Aβ oligomers, at 18 months, their effect should be avoided by immunodepletion using 6E10 (for sAPPα) or A11 (for Aβ oligomers). Therefore, we tested the stimulation or inhibition of Akt-GSK-3β phosphorylation after three sequential immunodepletions of the soluble fractions with either 6E10 (for 6 months) or A11 (18 months). The results are shown in Fig. 4*C* (and quantitatively in Fig. 4*C*, *panel c3*). As expected, after immunodepletion with 6E10, the stimulatory action of the 6-month-derived fractions was completely avoided (Fig. 4*C*, *panel c1*). Neither GSK-3β nor Akt 473/308 was phosphorylated after 6E10 immunodepletion. Conversely, the inhibitory effect of the 18-month-derived fraction was completely reversed by A11 immunodepletion (Fig. 4*C*, *panel c2*). As shown, the serum-induced GSK-3β and Akt473/308 phosphorylation was almost completely re-established after A11 treatment.

Therefore, at young ages in our PS1×APP model, the production of sAPPα determined the activation of Akt and the phosphorylation of Ser-9-GSK-3β (throughout at least IGF-1 and/or insulin receptors), whereas the age-dependent appearance of soluble oligomeric forms of Aβ determined the inhibition of this pro-survival pathway.

Synthetic Aβ Oligomers Inhibit the Activation of Prosurvival Receptors—Because of the relevance of the inhibition of the pro-survival pathways in the development of AD, we have further evaluated the inhibitory properties of the oligomeric Aβ using *in vitro* assays. It has been suggested that Aβ oligomers could inhibit the prosurvival Akt-GSK-3β phosphorylation by direct interaction with at least insulin receptors (42) and/or produced insulin resistance (27, 43). To ascertain the possible specificity in the ADDL inhibition, we determined the effect of two different concentrations of ADDLs (0.2 and 2 μM) on the stimulatory effect of IGF-1, insulin, BDNF, NGF, and sAPPα (Fig. 5*A*, *panels a1* and *a2*). As expected, the addition of the different factors produced the phosphorylation of the GSK-3β, demonstrating the presence of functional receptors in the N2a cells. As also shown in Fig. 5*A*, ADDLs inhibited the induced GSK-3β phosphorylation for all factors tested. Importantly, the effect of ADDLs displayed a clear selectivity on the inhibitory action. As shown, the NGF stimulation of GSK-3β phosphorylation seemed to be preferentially inhibited. In fact, 0.2 μM ADDLs completely blocked the NGF stimulation. In contrast, BDNF stimulation displayed low sensitivity to the ADDL effect. Only a minor inhibition could be observed at the highest dose used (2 μM). Insulin, IGF-1. and sAPPα presented intermediated sensitivity.

This selectivity could indicate that ADDLs might interact directly with the different trophic receptors. Theoretically, if both ligands exert their action through the same receptor, the ADDL inhibition should be reverted by increasing the trophic factor concentration. In fact, the inhibitory effect of submaximal doses of ADDLs (20 nM) was totally reverted by increasing concentrations of NGF (Fig. 5*B*, *panels b2* and *b2*). Similar results were observed using IGF-1 or insulin (data not shown). Based on these data, we cannot discriminate between a direct inhibition or a negative allosteric effect of ADDLs. However, these data indicated that the inhibitory action of Aβ oligomers was, at least in part, mediated by a direct interaction with different prosurvival receptors. In fact, ADDLs inhibited the Tyr phosphorylation of IGF-1, insulin, and Trk-A receptors (supplemental Fig. 4). The results indicated that for all three receptors the addition of ADDLs prevented the Tyr phosphorylation and, consequently, the receptor activation. This effect was particularly evident for IGF-1R. Therefore, the ADDLs seemed to be acting primordially at the activation level of the different receptors tested.

DISCUSSION

Multiple APP-based transgenic mouse models have been developed to evaluate the neurological deficiencies observed in AD. However, none of them displayed all pathological signs of the disease. The most relevant discrepancies between AD and the transgenic models were the absence of Tau phosphorylation and late, if any, neuronal degeneration, even in the presence of large Aβ accumulation since early ages. This apparent age-dependent neuroprotective/neurodegenerative status has not yet been fully addressed. Here, using *in vivo* and *in vitro* assays, we demonstrated the following. 1) sAPPα acting through IGF-1R and insulin receptors activated the prosurvival PI3K-Akt-GSK-3β pathway, which might explain the lack of neuronal death in most transgenic models at early/middle ages. 2) The age-dependent increase in soluble Aβ oligomers blocked the neurotrophin (including sAPPα)-mediated prosurvival pathway, explaining the observed late neuronal vulnerability.

It has been postulated that GSK-3β activity might exert a central role in the development of AD. GSK-3β activity was implicated in Tau phosphorylation, APP processing, Aβ production, and neurodegeneration (15). Overexpression of GSK-3β in a conditional transgenic model produced Tau hyperphosphorylation and neuronal death (16, 44). Furthermore, pharmacological inhibition of the GSK-3β activity by lithium decreased Aβ production and plaque accumulation (45), improved performance in memory tests, preserved the dendritic structure, and reduced the Tau-dependent pathology in AD tg models (46, 47).

Therefore, in this study we have first determined the Ser-9 phosphorylation levels in young/middle (6 months) and aged (18 months) PS1×APP mice, before and after pyramidal cell neurodegeneration in hippocampus, respectively (26). Accordingly, with a putative neuroprotective environment at early/middle ages, young PS1×APP mice displayed significantly higher levels of neuronal GSK-3β Ser-9 phosphorylation, suggesting a decreased activity of this enzyme. Also, we have observed an increased expression of the anti-apoptotic Bcl-2 protein (38) and the increase in the β-catenin protein. These data could indicate the presence of increased levels of neurotrophins in this tg model. However, except for IGF-1, which was locally increased around the Aβ plaques (although its total concentration decreased in 6- and 18-month PS1×APP mice, results not shown), none of the growth factors analyzed were modified in our transgenic model (data not shown). On the contrary, we demonstrated that soluble fractions derived from 6-month-old PS1×APP, and not from WT or PS1, activated the IGF-1R/IR-Akt pathway, phosphorylated the GSK-3β, and in

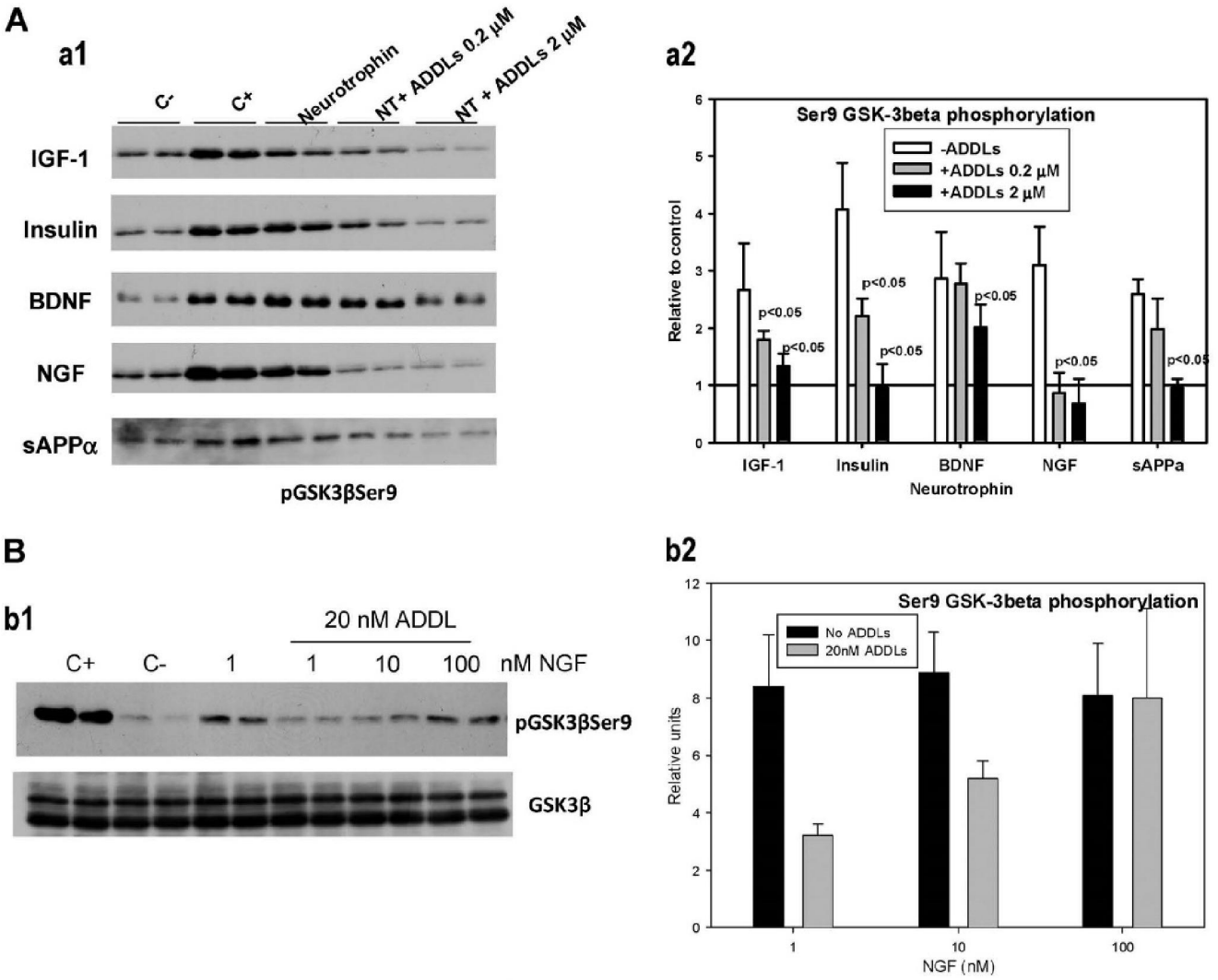

FIGURE 5. **Synthetic Aβ oligomers (ADDLs) competed with different neurotrophins for the stimulation of Ser-9 GSK-3β phosphorylation.** *A*, for competition experiments, the Ser-9 GSK-3β phosphorylation was stimulated by a fixed concentration of different neurotrophins and 0.2 or 2 μM ADDLs. After treatment, the Ser-9 GSK-3β phosphorylation was determined by Western blots (*panel a1*) and quantitatively (*panel a2*) after normalization by negative controls. *B*, inhibitory effect of ADDLs, at submaximal doses (20 nM) was reverted by increasing the concentration of different neurotrophins, such as NGF, IGF-1 or insulin. In these experiments, N2a cells were treated with different concentrations of each neurotrophin in the absence (data not shown) or presence (*panel b1*) of ADDLs. After Western blots, the GSK-3β phosphorylation was quantitatively analyzed (*panel b2*) and normalized by negative controls. *C*−, negative control; C+, positive control.

consequence, promoted the neuronal survival in primary cultures.

Within the different APP-derived fragments, both soluble APPα and -β (data not shown) were the predominant APP peptides identified in the tg-soluble fractions. Although the monomeric Aβ could also produce a similar effect (data not shown) (40), no significant amounts of monomeric Aβ were detected in 6-month-derived soluble extracts.

The implication of sAPPα in the activation of the Akt prosurvival pathway was further demonstrated *in vitro*, using synthetic sAPPα. The sAPPα produced a dose-dependent activation of the Akt-GSK-3β pathway that was inhibited by LY294002, AG1024, and picropodophyllin and mediated by the activation of, in this *in vitro* assay, IGF-1 and insulin receptors. Moreover, the effect of 6-month-old PS1×APP brain-derived fractions was completely avoided by immunodepletion experiments using 6E10. Furthermore, the estimated sAPPα concentration in the soluble fractions (~20 nM) was in the range of the calculated EC_{50} for synthetic sAPPα (2.3 nM). Interestingly, the sAPPβ fragment displayed no intrinsic activity in this *in vitro* model. To the best of our knowledge, this is the first time that the effect of sAPPα on Akt-GSK-3β pathway has been directly demonstrated.

The present data cannot demonstrate, *in vivo*, a direct cause-effect relationship between the presence of sAPPα and GSK-3β phosphorylation. However, we might postulate that, in our model, the overexpression of the tg APP produced increased amounts of sAPPα and, because of its agonist-like effect on the prosurvival receptors, could to some extent delay the Aβ pathology. In fact, although the increase in GSK-3β phosphorylation was not observed in all APP-based tg models (48, 49), all models exhibited a considerable delay between the Aβ deposi-

8. Cole, G. M., and Frautschy, S. A. (2007) *Exp. Gerontol.* **42,** 10–21
9. Moloney, A. M., Griffin, R. J., Timmons, S., O'Connor, R., Ravid, R., and O'Neill, C. (2010) *Neurobiol. Aging* **31,** 224–243
10. Hoyer, S. (1998) *J. Neural Transm.* **54,** 187–194
11. Steen, E., Terry, B. M., Rivera, E. J., Cannon, J. L., Neely, T. R., Tavares, R., Xu, X. J., Wands, J. R., and de la Monte, S. M. (2005) *J. Alzheimer Dis.* **7,** 63–80
12. Reger, M. A., Watson, G. S., Green, P. S., Wilkinson, C. W., Baker, L. D., Cholerton, B., Fishel, M. A., Plymate, S. R., Breitner, J. C., DeGroodt, W., Mehta, P., and Craft, S. (2008) *Neurology* **70,** 440–448
13. Carro, E., Trejo, J. L., Gomez-Isla, T., LeRoith, D., and Torres-Aleman, I. (2002) *Nat. Med.* **8,** 1390–1397
14. Bondy, C. A., and Cheng, C. M. (2004) *Eur. J. Pharmacol.* **490,** 25–31
15. Balaraman, Y., Limaye, A. R., Levey, A. I., and Srinivasan, S. (2006) *Cell. Mol. Life Sci.* **63,** 1226–1235
16. Lucas, J. J., Hernández, F., Gómez-Ramos, P., Morán, M. A., Hen, R., and Avila, J. (2001) *EMBO J.* **20,** 27–39
17. Peineau, S., Taghibiglou, C., Bradley, C., Wong, T. P., Liu, L., Lu, J., Lo, E., Wu, D., Saule, E., Bouschet, T., Matthews, P., Isaac, J. T., Bortolotto, Z. A., Wang, Y. T., and Collingridge, G. L. (2007) *Neuron* **53,** 703–717
18. Woodgett, J. R., and Ohashi, P. S. (2005) *Nat. Immunol.* **6,** 751–752
19. Beurel, E., and Jope, R. S. (2006) *Prog. Neurobiol.* **79,** 173–189
20. Gong, Y., Chang, L., Viola, K. L., Lacor, P. N., Lambert, M. P., Finch, C. E., Krafft, G. A., and Klein, W. L. (2003) *Proc. Natl. Acad. Sci. U.S.A.* **100,** 10417–10422
21. Lacor, P. N., Buniel, M. C., Chang, L., Fernandez, S. J., Gong, Y., Viola, K. L., Lambert, M. P., Velasco, P. T., Bigio, E. H., Finch, C. E., Krafft, G. A., and Klein, W. L. (2004) *J. Neurosci.* **24,** 10191–10200
22. De Felice, F. G., Wu, D., Lambert, M. P., Fernandez, S. J., Velasco, P. T., Lacor, P. N., Bigio, E. H., Jerecic, J., Acton, P. J., Shughrue, P. J., Chen-Dodson, E., Kinney, G. G., and Klein, W. L. (2008) *Neurobiol. Aging* **29,** 1334–1347
23. Lesné, S., Koh, M. T., Kotilinek, L., Kayed, R., Glabe, C. G., Yang, A., Gallagher, M., and Ashe, K. H. (2006) *Nature* **440,** 352–357
24. Shankar, G. M., Bloodgood, B. L., Townsend, M., Walsh, D. M., Selkoe, D. J., and Sabatini, B. L. (2007) *J. Neurosci.* **27,** 2866–2875
25. Deshpande, A., Mina, E., Glabe, C., and Busciglio, J. (2006) *J. Neurosci.* **26,** 6011–6018
26. Jimenez, S., Baglietto-Vargas, D., Caballero, C., Moreno-Gonzalez, I., Torres, M., Sanchez-Varo, R., Ruano, D., Vizuete, M., Gutierrez, A., and Vitorica, J. (2008) *J. Neurosci.* **28,** 11650–11661
27. Zhao, W. Q., De Felice, F. G., Fernandez, S., Chen, H., Lambert, M. P., Quon, M. J., Krafft, G. A., and Klein, W. L. (2008) *FASEB J.* **22,** 246–260
28. Griffin, R. J., Moloney, A., Kelliher, M., Johnston, J. A., Ravid, R., Dockery, P., O'Connor, R., and O'Neill, C. (2005) *J. Neurochem.* **93,** 105–117
29. Blanchard, V., Moussaoui, S., Czech, C., Touchet, N., Bonici, B., Planche, M., Canton, T., Jedidi, I., Gohin, M., Wirths, O., Bayer, T. A., Langui, D., Duyckaerts, C., Tremp, G., and Pradier, L. (2003) *Exp. Neurol.* **184,** 247–263
30. Ramos, B., Baglietto-Vargas, D., del Río, J. C., Moreno-Gonzalez, I., Santa-Maria, C., Jimenez, S., Caballero, C., Lopez-Tellez, J. F., Khan, Z. U., Ruano, D., Gutierrez, A., and Vitorica, J. (2006) *Neurobiol. Aging* **27,** 1658–1672
31. Caballero, C., Jimenez, S., Moreno-Gonzalez, I., Baglietto-Vargas, D., Sanchez-Varo, R., Gavilan, M. P., Ramos, B., Del Río, J. C., Vizuete, M., Gutierrez, A., Ruano, D., and Vitorica, J. (2007) *J. Neurosci. Res.* **85,** 787–797
32. Lambert, M. P., Velasco, P. T., Chang, L., Viola, K. L., Fernandez, S., Lacor, P. N., Khuon, D., Gong, Y., Bigio, E. H., Shaw, P., De Felice, F. G., Krafft, G. A., and Klein, W. L. (2007) *J. Neurochem.* **100,** 23–35
33. Kayed, R., Head, E., Thompson, J. L., McIntire, T. M., Milton, S. C., Cotman, C. W., and Glabe, C. G. (2003) *Science* **300,** 486–489
34. Araujo, F., Tan, S., Ruano, D., Schoemaker, H., Benavides, J., and Vitorica, J. (1996) *J. Biol. Chem.* **271,** 27902–27911
35. Scali, C., Caraci, F., Gianfriddo, M., Diodato, E., Roncarati, R., Pollio, G., Gaviraghi, G., Copani, A., Nicoletti, F., Terstappen, G. C., and Caricasole, A. (2006) *Neurobiol. Dis.* **24,** 254–265
36. Hongisto, V., Smeds, N., Brecht, S., Herdegen, T., Courtney, M. J., and Coffey, E. T. (2003) *Mol. Cell. Biol.* **23,** 6027–6036
37. Lonze, B. E., and Ginty, D. D. (2002) *Neuron* **35,** 605–623
38. Karlnoski, R., Wilcock, D., Dickey, C., Ronan, V., Gordon, M. N., Zhang, W., Morgan, D., and Taglialatela, G. (2007) *Neurobiol. Dis.* **25,** 179–188
39. Aberle, H., Bauer, A., Stappert, J., Kispert, A., and Kemler, R. (1997) *EMBO J.* **16,** 3797–3804
40. Giuffrida, M. L., Caraci, F., Pignataro, B., Cataldo, S., De Bona, P., Bruno, V., Molinaro, G., Pappalardo, G., Messina, A., Palmigiano, A., Garozzo, D., Nicoletti, F., Rizzarelli, E., and Copani, A. (2009) *J. Neurosci.* **29,** 10582–10587
41. Lambert, M. P., Barlow, A. K., Chromy, B. A., Edwards, C., Freed, R., Liosatos, M., Morgan, T. E., Rozovsky, I., Trommer, B., Viola, K. L., Wals, P., Zhang, C., Finch, C. E., Krafft, G. A., and Klein, W. L. (1998) *Proc. Natl. Acad. Sci. U.S.A.* **95,** 6448–6453
42. Xie, L., Helmerhorst, E., Taddei, K., Plewright, B., van Bronswijk, W., and Martins, R. (2002) *J. Neurosci.* **22,** 221RC
43. Ma, Q. L., Yang, F., Rosario, E. R., Ubeda, O. J., Beech, W., Gant, D. J., Chen, P. P., Hudspeth, B., Chen, C., Zhao, Y., Vinters, H. V., Frautschy, S. A., and Cole, G. M. (2009) *J. Neurosci.* **29,** 9078–9089
44. Engel, T., Hernández, F., Avila, J., and Lucas, J. J. (2006) *J. Neurosci.* **26,** 5083–5090
45. Su, Y., Ryder, J., Li, B., Wu, X., Fox, N., Solenberg, P., Brune, K., Paul, S., Zhou, Y., Liu, F., and Ni, B. (2004) *Biochemistry* **43,** 6899–6908
46. Rockenstein, E., Torrance, M., Adame, A., Mante, M., Bar-on, P., Rose, J. B., Crews, L., and Masliah, E. (2007) *J. Neurosci.* **27,** 1981–1991
47. Noble, W., Planel, E., Zehr, C., Olm, V., Meyerson, J., Suleman, F., Gaynor, K., Wang, L., LaFrancois, J., Feinstein, B., Burns, M., Krishnamurthy, P., Wen, Y., Bhat, R., Lewis, J., Dickson, D., and Duff, K. (2005) *Proc. Natl. Acad. Sci. U.S.A.* **102,** 6990–6995
48. Masliah, E., Westland, C. E., Rockenstein, E. M., Abraham, C. R., Mallory, M., Veinberg, I., Sheldon, E., and Mucke, L. (1997) *Neuroscience* **78,** 135–146
49. Malm, T. M., Iivonen, H., Goldsteins, G., Keksa-Goldsteine, V., Ahtoniemi, T., Kanninen, K., Salminen, A., Auriola, S., Van Groen, T., Tanila, H., and Koistinaho, J. (2007) *J. Neurosci.* **27,** 3712–3721
50. Terwel, D., Muyllaert, D., Dewachter, I., Borghgraef, P., Croes, S., Devijver, H., and Van Leuven, F. (2008) *Am. J. Pathol.* **172,** 786–798
51. Kojro, E., Postina, R., Buro, C., Meiringer, C., Gehrig-Burger, K., and Fahrenholz, F. (2006) *FASEB J.* **20,** 512–514
52. Townsend, M., Mehta, T., and Selkoe, D. J. (2007) *J. Biol. Chem.* **282,** 33305–33312
53. Zhao, W. Q., Lacor, P. N., Chen, H., Lambert, M. P., Quon, M. J., Krafft, G. A., and Klein, W. L. (2009) *J. Biol. Chem.* **284,** 18742–18753
54. Decker, H., Jürgensen, S., Adrover, M. F., Brito-Moreira, J., Bomfim, T. R., Klein, W. L., Epstein, A. L., De Felice, F. G., Jerusalinsky, D., and Ferreira, S. T. (2010) *J. Neurochem.* **115,** 1520–1529
55. Knowles, J. K., Rajadas, J., Nguyen, T. V., Yang, T., LeMieux, M. C., Vander Griend, L., Ishikawa, C., Massa, S. M., Wyss-Coray, T., and Longo, F. M. (2009) *J. Neurosci.* **29,** 10627–10637
56. Capsoni, S., Giannotta, S., and Cattaneo, A. (2002) *Mol. Cell. Neurosci.* **21,** 15–28
57. Houeland, G., Romani, A., Marchetti, C., Amato, G., Capsoni, S., Cattaneo, A., and Marie, H. (2010) *J. Neurosci.* **30,** 13089–13094
58. Braithwaite, S. P., Schmid, R. S., He, D. N., Sung, M. L., Cho, S., Resnick, L., Monaghan, M. M., Hirst, W. D., Essrich, C., Reinhart, P. H., and Lo, D. C. (2010) *Neurobiol. Dis.* **39,** 311–317
59. Baglietto-Vargas, D., Moreno-Gonzalez, I., Sanchez-Varo, R., Jimenez, S., Trujillo-Estrada, L., Sanchez-Mejias, E., Torres, M., Romero-Acebal, M., Ruano, D., Vizuete, M., Vitorica, J., and Gutierrez, A. (2010) *J. Alzheimer Dis.* **21,** 119–132
60. Moreno-Gonzalez, I., Baglietto-Vargas, D., Sanchez-Varo, R., Jimenez, S., Trujillo-Estrada, L., Sanchez-Mejias, E., Del Rio, J. C., Torres, M., Romero-Acebal, M., Ruano, D., Vizuete, M., Vitorica, J., and Gutierrez, A. (2009) *J. Alzheimer Dis.* **18,** 755–776
61. Sotthibundhu, A., Sykes, A. M., Fox, B., Underwood, C. K., Thangnipon, W., and Coulson, E. J. (2008) *J. Neurosci.* **28,** 3941–3946
62. Ruano, D., Vizuete, M., Cano, J., Machado, A., and Vitorica, J. (1992) *J. Neurochem.* **58,** 485–493

RESUMEN II

Se han desarrollado multitud de modelos transgénicos basados en mutaciones humanas encontradas sobre el gen de APP en casos de FAD. Estos modelos intentan imitar las deficiencias neurológicas observadas en EA. Ninguno de estos modelos presenta el total de la patología observada en humanos, siendo la mayor discrepancia la ausencia de ovillos neurofibrilares de Tau, y una escasa muerte neuronal. Cuando esta última se observa, sólo es a edades muy avanzadas, incluso cuando la acumulación del péptido de Ab está presente desde edades muy tempranas. Se puede pensar en un estado neuroprotector/neurotóxico que cambia con la edad y que aún no está nada claro. En nuestro trabajo, mediante el uso de experimentos *invitro* e *invivo* hemos demostrado lo siguiente:

1. El fragmento generado en el procesamiento de APP tras el corte realizado por la α-secretasa (sAPPα) actúa a través los receptores de IGF1 y de Insulina, activando la vía pro supervivencia PI3K-Akt-GSK-3β. Esto podría explicar la falta de muerte neuronal en la mayoría de los modelos transgénicos a edades tempranas.

2. La acumulación dependiente de edad de las formas oligoméricas solubles de Aβ, bloquea la acción de ciertas neurotrofinas (incluidas el sAPPα) que actúan potenciando la ruta pro supervivencia. Este bloqueo podría explicar la mayor vulnerabilidad de las neuronas a edades avanzadas.

Resultados: Capitulo III

Trujillo-Estrada *et al. Acta Neuropathologica Communications* 2013, **1**:73
http://www.actaneurocomms.org/content/1/1/73

ACTA NEUROPATHOLOGICA COMMUNICATIONS

RESEARCH Open Access

In vivo modification of Abeta plaque toxicity as a novel neuroprotective lithium-mediated therapy for Alzheimer's disease pathology

Laura Trujillo-Estrada[1,3†], Sebastian Jimenez[2,3,4†], Vanessa De Castro[1,3], Manuel Torres[2,3,4,5], David Baglietto-Vargas[1,3,6], Ines Moreno-Gonzalez[1,3,7], Victoria Navarro[2,3,4], Raquel Sanchez-Varo[1,3], Elisabeth Sanchez-Mejias[1,3], Jose Carlos Davila[1,3], Marisa Vizuete[2,3,4], Antonia Gutierrez[1,3*] and Javier Vitorica[2,3,4*]

Abstract

Background: Alzheimer's disease (AD) is characterized by the abnormal accumulation of extracellular beta-amyloid (Abeta) plaques, intracellular hyperphosphorylated tau, progressive synaptic alterations, axonal dystrophies, neuronal loss and the deterioration of cognitive capabilities of patients. However, no effective disease-modifying treatment has been yet developed. In this work we have evaluated whether chronic lithium treatment could ameliorate the neuropathology evolution of our well characterized PS1M146LxAPPSwe-London mice model.

Results: Though beneficial effects of lithium have been previously described in different AD models, here we report a novel in vivo action of this compound that efficiently ameliorated AD-like pathology progression and rescued memory impairments by reducing the toxicity of Abeta plaques. Transgenic PS1M146LxAPPSwe-London mice, treated before the pathology onset, developed smaller plaques characterized by higher Abeta compaction, reduced oligomeric-positive halo and therefore with attenuated capacity to induce neuronal damage. Importantly, neuronal loss in hippocampus and entorhinal cortex was fully prevented. Our data also demonstrated that the axonal dystrophic area associated with lithium-modified plaques was highly reduced. Moreover, a significant lower accumulation of phospho-tau, LC3-II and ubiquitinated proteins was detected in treated mice. Our study highlights that this switch of plaque quality by lithium could be mediated by astrocyte activation and the release of heat shock proteins, which concentrate in the core of the plaques.

Conclusions: Our data demonstrate that the pharmacological in vivo modulation of the extracellular Abeta plaque compaction/toxicity is indeed possible and, in addition, might constitute a novel promising and innovative approach to develop a disease-modifying therapeutic intervention against AD.

Keywords: Alzheimer, Lithium treatment, Transgenic mice, Neuronal degeneration, Axonal dystrophies, Abeta plaques, Toxicity

* Correspondence: agutierrez@uma.es; vitorica@us.es
†Equal contributors
[1]Departamento de Biologia Celular, Genetica y Fisiologia, Facultad de Ciencias, Universidad de Malaga, 29071 Malaga, Spain
[2]Departamento de Bioquímica y Biologia Molecular, Facultad de Farmacia, Universidad de Sevilla, 41012 Sevilla, Spain
Full list of author information is available at the end of the article

OBJETIVOS III

Evaluación del efecto de la ingesta crónica oral de Litio en los ratones **$PS1_{M146L}$/APP_{751SL}** modelos de la enfermedad de Alzheimer. Caracterización de cambios en la patología propia de la enfermedad.

a. Estudio de la prevención en la degeneración de las interneuronas O-LM e HIPP de hipocampo y corteza entorrinal que se da a edades tempranas en este modelo murino.

b. Evaluación de la patología del péptido Aβ tras la administración oral de Litio: estudio de los cambios en la acumulación en placas extracelulares y en la producción de formas oligoméricas solubles de Aβ.

c. Estudio de la patología asociada a Tau: evaluación de la hiperfosforilación de Tau tras la ingesta de litio, y de la formación de distrofias axonales.

d. Evaluación de las mejoras a nivel de los déficits e comportamiento/memoria propios del modelo con el tratamiento.

e. Identificación de la posible diana terapeútica del tratamiento con Litio.

Este trabajo se presenta como artículo:

Trujillo-Estrada *et al. Acta Neuropathologica Communications* 2013, **1**:73
http://www.actaneurocomms.org/content/1/1/73

ACTA NEUROPATHOLOGICA COMMUNICATIONS

RESEARCH Open Access

In vivo modification of Abeta plaque toxicity as a novel neuroprotective lithium-mediated therapy for Alzheimer's disease pathology

Laura Trujillo-Estrada[1,3†], Sebastian Jimenez[2,3,4†], Vanessa De Castro[1,3], Manuel Torres[2,3,4,5], David Baglietto-Vargas[1,3,6], Ines Moreno-Gonzalez[1,3,7], Victoria Navarro[2,3,4], Raquel Sanchez-Varo[1,3], Elisabeth Sanchez-Mejias[1,3], Jose Carlos Davila[1,3], Marisa Vizuete[2,3,4], Antonia Gutierrez[1,3*] and Javier Vitorica[2,3,4*]

Abstract

Background: Alzheimer's disease (AD) is characterized by the abnormal accumulation of extracellular beta-amyloid (Abeta) plaques, intracellular hyperphosphorylated tau, progressive synaptic alterations, axonal dystrophies, neuronal loss and the deterioration of cognitive capabilities of patients. However, no effective disease-modifying treatment has been yet developed. In this work we have evaluated whether chronic lithium treatment could ameliorate the neuropathology evolution of our well characterized PS1M146LxAPPSwe-London mice model.

Results: Though beneficial effects of lithium have been previously described in different AD models, here we report a novel in vivo action of this compound that efficiently ameliorated AD-like pathology progression and rescued memory impairments by reducing the toxicity of Abeta plaques. Transgenic PS1M146LxAPPSwe-London mice, treated before the pathology onset, developed smaller plaques characterized by higher Abeta compaction, reduced oligomeric-positive halo and therefore with attenuated capacity to induce neuronal damage. Importantly, neuronal loss in hippocampus and entorhinal cortex was fully prevented. Our data also demonstrated that the axonal dystrophic area associated with lithium-modified plaques was highly reduced. Moreover, a significant lower accumulation of phospho-tau, LC3-II and ubiquitinated proteins was detected in treated mice. Our study highlights that this switch of plaque quality by lithium could be mediated by astrocyte activation and the release of heat shock proteins, which concentrate in the core of the plaques.

Conclusions: Our data demonstrate that the pharmacological in vivo modulation of the extracellular Abeta plaque compaction/toxicity is indeed possible and, in addition, might constitute a novel promising and innovative approach to develop a disease-modifying therapeutic intervention against AD.

Keywords: Alzheimer, Lithium treatment, Transgenic mice, Neuronal degeneration, Axonal dystrophies, Abeta plaques, Toxicity

* Correspondence: agutierrez@uma.es; vitorica@us.es
†Equal contributors
[1]Departamento de Biologia Celular, Genetica y Fisiologia, Facultad de Ciencias, Universidad de Malaga, 29071 Malaga, Spain
[2]Departamento de Bioquímica y Biología Molecular, Facultad de Farmacia, Universidad de Sevilla, 41012 Sevilla, Spain
Full list of author information is available at the end of the article

Trujillo-Estrada *et al. Acta Neuropathologica Communications* 2013, 1:73
http://www.actaneurocomms.org/content/1/1/73

Background

In Alzheimer's disease (AD), the abnormal accumulation of extracellular beta-amyloid (Abeta) plaques and intracellular hyperphosphorylated tau induces progressive synaptic alterations, axonal dystrophies, neuronal loss and the deterioration of cognitive capabilities of patients [1,2]. In spite to the relatively large information about the AD pathology, no effective disease-modifying treatment has been yet developed. Within the different compounds tested, lithium, a primary drug to treat bipolar disorder, has also been suggested as a potential treatment against AD [3-6]. In fact, clinical studies indicated that lithium could be preventive in patients with MCI, whereas no beneficial effects were observed in mild to moderate AD [4]. In addition, epidemiological studies also reported a reducing risk of AD in patients with bipolar disorders treated with Li [5]. Thus, lithium may indeed constitute a useful preventive treatment for individuals at high risk of AD and/or preclinical stages of the disease.

The neuroprotective mechanisms of lithium are not completely understood. In AD models, lithium could reduce the AD pathology inhibiting (directly and/or indirectly) the activity of the tau kinase GSK-3beta. Whereas this inhibition would preclude tau phosphorylation [7,8], dystrophy formation and neuronal degeneration [9,10], the therapeutic benefits of this treatment have been questioned [11]. On the other hand, lithium also mediated the inhibition of inositol monophosphatase and the induction of mTOR-independent autophagic process [12,13]. This induction may be important in the prevention or attenuation of neurodegeneration associated with aggregated proteins. Moreover, since the accumulation of autophagic vesicles could also be implicated in the formation of axonal dystrophies in AD models [14-17], lithium should alleviate the progression of these pathological features. However, while several studies have shown beneficial effects in lowering Abeta load [18-20], others reported no effect or even increased Abeta production [11,21,22].

The origin of these controversies is currently unknown. Among other factors, the different AD models, the different protocols of lithium administration or dosage and, perhaps more relevant, the partial neuropathology displayed for most of the AD models, could explain the discrepancies between the different effects of lithium treatment in transgenic models.

In this work we have evaluated the effect of chronic oral lithium treatment using the bigenic PS1M146LxAPPSwe-London mice. This model displayed early degeneration of O-LM and HIPP interneurons (SOM/NPY-positive), in hippocampus and entorhinal cortex [23,24]. These GABAergic cells are implicated in memory/learning processes and degenerate in AD patients [25,26]. Our data demonstrated that chronic (from 3- to 9-month-old) oral lithium administration, initiated before the onset of Abeta deposits, efficiently prevented most of the early neuropathological manifestations of our PS1xAPP model. Lithium prevented the neuronal loss (at both hippocampus and entorhinal cortex), reduced the tau phosphorylation and the formation of axonal dystrophies and, in consequence, ameliorated behavioral/memory deficits observed at this age. These effects were mediated by increasing the compaction of Abeta plaques and lowering their toxic oligomeric halo. This modification on Abeta deposits toxicity is a novel disease-modifying effect of lithium, acting through the astrocytes and the release of heat shock proteins (Hsps).

Methods

Transgenic mice and lithium treatment

Generation of PS1M146LxAPP751Swe-London (PS1xAPP) mice has been reported previously [27]. Heterozygous PS1xAPP double transgenic mice (C57BL:6 background) were generated by crossing homozygous PS1 transgenic mice with heterozygous Thy1-APP751SL mice. Only male mice were used in this work.

As controls, we used age-matched non-transgenic (C57BL:6) male mice (WT) or hemizygous PS1M146L littermates (PS1). The PS1 mice displayed no apparent differences with WT mice, at the age used in this work [24] (see also Figures 1 and 2A). Only PS1xAPP mice model accumulated Abeta plaques. Thus, to specifically assess the potential therapeutic effect of lithium on the Abeta pathology, we reasoned that PS1 mice would be a better control than WT mice. An additional lithium treated PS1 group was also used as control for lithium treatment.

For lithium treatment, PS1 and PS1xAPP mice (3 month old at the beginning of treatment) were randomly divided into two groups (n = 25 each). Mice were fed, ad libitum, with standard mice diet (2014 Teklad Global 14% Protein Rodent Maintenance Diet, Harlan, Spain) or standard mice diet supplemented with lithium carbonate (1.2 g/kg 2014 diet, Harlan, Spain). The lithium group received an additional drinking bottle containing NaCl (0.7%). The treatment was continued for 6 months. The control and treated mice were weighted weekly and no significant weight loss was detected (29.20 ± 1.09 g vs 27.5 ± 2.2 g for control and Li-treated PS1xAPP mice, respectively). For the plasmatic Li content, mice were bled (100 μl) from the ocular artery. The plasmatic lithium levels were stable during the treatment and also were within the therapeutic range: 0.44 ± 0.07 mEquiv/L (n = 10) after 71 days of treatment or 0.38 ± 0.05 mEquiv/L (n = 10) at the end of treatment. This treatment was well tolerated with a low mortality during this period. (PS1 control 0%; PS1 lithium, 0%; PS1xAPP control, 20%; PS1xAPP lithium, 7.4%).

Trujillo-Estrada *et al. Acta Neuropathologica Communications* 2013, **1**:73
http://www.actaneurocomms.org/content/1/1/73

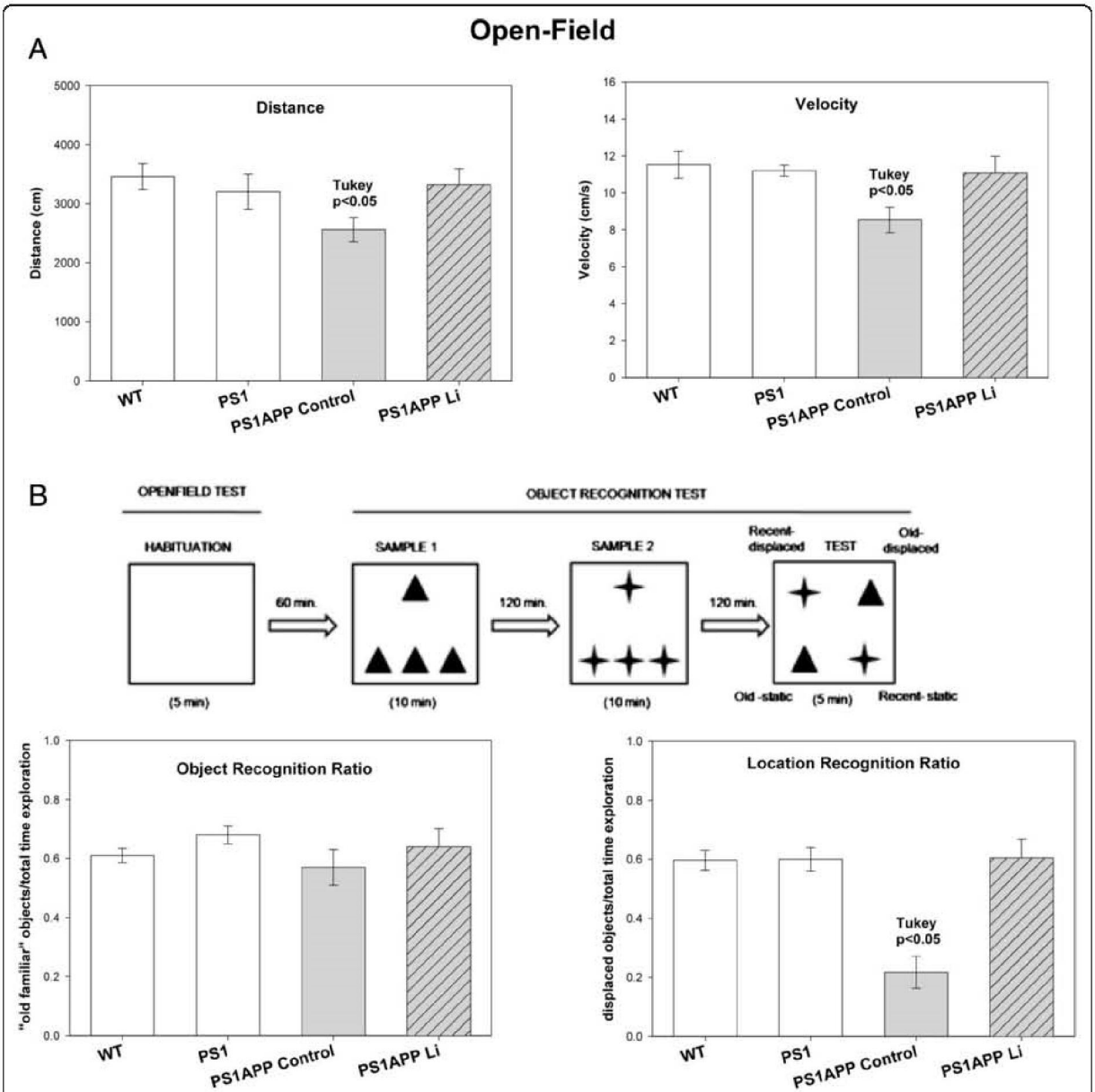

Figure 1 Lithium treatment improved the behavioral/memory deficiencies of PS1xAPP mice. (A) Open-field test. One-way ANOVA revealed significant differences between groups in both distance (F(3,24) 6.33; p 0.006) and velocity F(3,24) 8.02, p 0.002). Post-hoc analysis showed significant differences in PS1xAPP control compared with WT/PS1 and PS1xAPP lithium ($p < 0.05$). **(B)** Behavioral protocol and memory measures. Sixty min after habituation to the open-field, animals received three samples trials with 120 min inter-trial as depicted. Each symbol (triangle and star) represents one type of object. One-way ANOVA F(3,24) 21.15 p 0.0001) revealed significant differences between groups in place memory index. Post-hoc analysis showed significant difference in PS1xAPP control compared with WT/PS1 controls and PS1xAPP lithium.

After behavioral tests, control and lithium-treated mice were anesthetized with sodium pentobarbital (60 mg/kg), and transcardially perfused with 0.1 M phosphate buffered saline (PBS). Then, mice brain was quickly removed and one hemibrain dissected (cortex and hippocampus), frozen and stored at −80° C while the other hemibrain was fixed by immersion with 4% paraformaldehyde, 75 mM lysine, 10 mM sodium metaperiodate in 0.1 M phosphate buffer (PB), pH 7.4 for 5 days at 4°C. Fixed hemibrains were cryoprotected in 30% sucrose, sectioned at 40 μm thickness in the coronal plane on a freezing microtome and serially collected in wells containing cold PBS and 0.02% sodium azide.

Trujillo-Estrada *et al. Acta Neuropathologica Communications* 2013, **1**:73
http://www.actaneurocomms.org/content/1/1/73

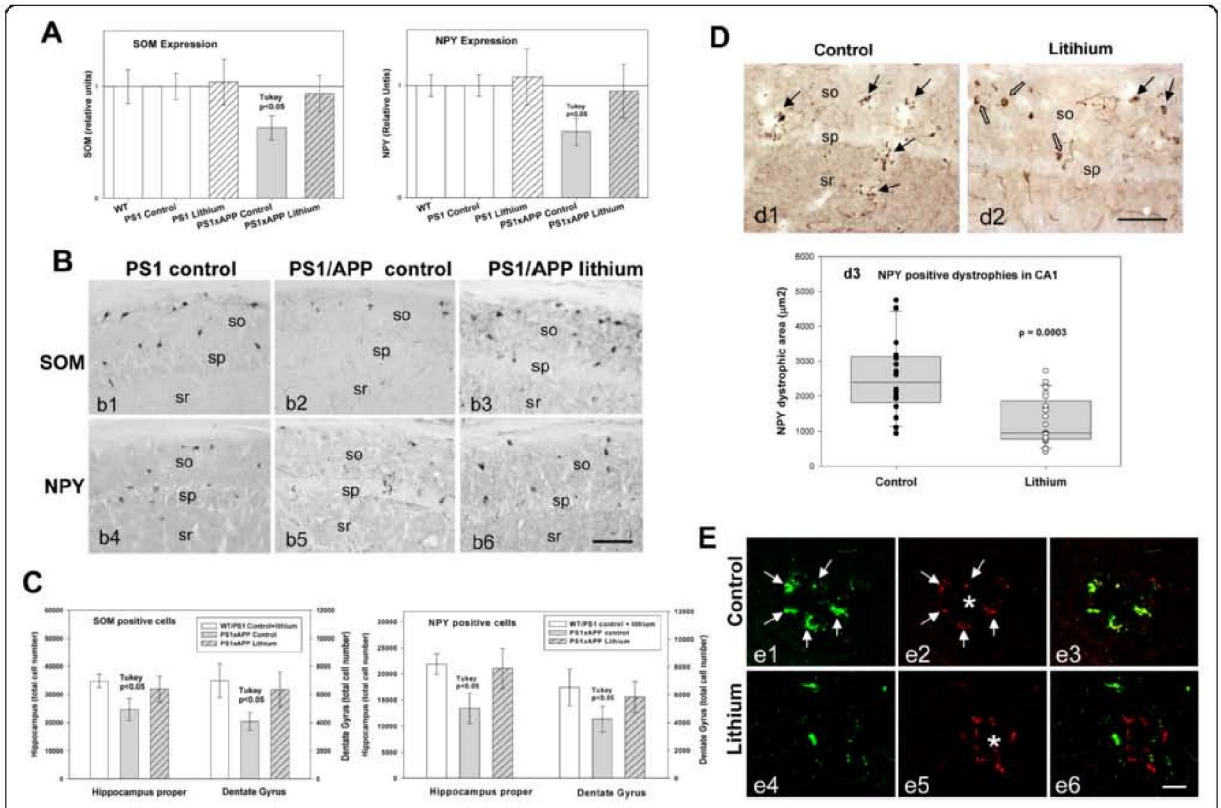

Figure 2 Lithium treatment avoided neuronal loss in the hippocampus of PS1xAPP mice. (A) The expression of SOM and NPY (n 20 mice per group) was significantly lower in PS1xAPP control group (ANOVA F(4,96) 49.63, p 0.00001. Tukey p < 0.05 or F(4,96) 27.24, p 0.0001, Tukey p < 0.05 for SOM and NPY respectively). WT, PS1 (control or lithium) and PS1xAPP lithium displayed no differences. **B)** SOM (b1-b3) or NPY (b4-b6) immunolabeled sections through CA1 subfield of PS1 control or PS1xAPP control and lithium groups. **C)** Total SOM or NPY cell number in hippocampus proper and dentate gyrus was assessed by stereology (n 5 per genotype and treatment). WT and PS1 groups displayed no differences and data were pooled. Only control PS1xAPP displayed a significant reduction in SOM (ANOVA F(2,22) 14.57, p 0.00002 or F(2.22) 11.84, p 0.0008 for hippocampus proper and dentate gyrus, respectively) and NPY (ANOVA F(2,22) 17.02, p 0.0001 or F(2,22) 6.87, p 0.008 for hippocampus proper and dentate gyrus, respectively) cell number. **D)** NPY-positive dystrophies (black arrows) in CA1 subfield of PS1xAPP control (d1) and lithium mice (d2) (open arrows: NPY cell bodies). (d3) Quantitative analysis (n 4 mice per group; 6 sections per animal) demonstrated the existence of a significant reduction of NPY-positive dystrophic area (μm2) in PS1xAPP lithium. **E)** Co-localization of SOM (green) and AT8 (red) in dystrophies assessed using confocal microscopy. In PS1xAPP control mice (e1 to e3), SOM positive dystrophies (arrows), surrounding Abeta plaque (asterisk), were positive for AT8. Lithium produced a reduction in both SOM (e4) and AT8 (e5) positive dystrophies and in the co-localization between SOM and AT8 in dystrophies (e6). Scale bars: b1-b6 100 μm; d1 and d2 100 μm; e1-e6 20 μm.

All animal experiments were performed in accordance with the animal research regulations (RD53/2013 and 2010/63/UE) from Spain and European Union, and with the approval of the Committees of Animal Research from the University of Seville (Spain) and the University of Malaga (Spain).

Behavioral studies

All experiments were conducted on age-matched male WT (n = 10), PS1 (n = 10), PS1xAPP control (n = 9) and PS1xAPP lithium-treated (n = 9) mice. Mice were tested at 9 month of age, two days previous to sacrifice. All testing were performed in the light period of the light/dark cycle and the experimenter was blind to the genotypes and treatment of mice. Animals were adapted to the experimental conditions for 6 days before behavioral testing. All mice were moved to the testing room in their home-cage and kept in the room during 1 hour to habituate to the new location; then, they were handled gently each day briefly in order to minimize non-specific stress. The behavioral experiment protocol was conducted as shown in Figure 1.

Open-field test

Besides the use of the open-field to habituate animals to the cage before the object recognition test, we examined motor function by means of spontaneous locomotor activity [28]. In this test, mice were placed in the centre of a square-shape arena (45 cm × 45 cm) and were allowed

Trujillo-Estrada *et al. Acta Neuropathologica Communications* 2013, 1:73
http://www.actaneurocomms.org/content/1/1/73

to explore the arena for 5 minutes. The arena was thoroughly cleaned with 70% ethanol solution after each trial. The locomotor activity was measured by an automated monitoring system (Ethovision, Noldus, The Netherlands). Distance travelled and velocity was quantified.

Object recognition test

The object recognition test is based in the natural tendency of rodents to explore objects (spontaneous exploratory behavior). In the present study, we used a modified protocol [29] based in the preference for the "old familiar object" over the "recent familiar object" and the preference for a novel location. Sixty minutes after habituation to the open-field, animals were first exposed to four identical objects arranged in a triangle shaped configuration and allowed to explore them for 10 minutes (Sample 1). After a delay of 2 hours, the mice received a second sample trial identical to the first, except that a novel set of four identical objects were present (Sample 2). The test trial started after 2 hours interval and lasted for 5 minutes. In the test trial, two objects from both samples 1 and 2 ("old familiar" and "recent familiar" objects, respectively) were arranged in a quadratic shape configuration, so one old object and one recent object were present in a familiar position while the other two were displaced to a new position (see Figure 1B for details). The type of object used as "old" and "recent" was counterbalanced across mice. All objects were made of plastic to prevent material preference and for an easier cleaning to prevent odor cues. The two sets of objects were different in size, form and color. The arena and objects were thoroughly cleaned with 70% ethanol solution after each trial. The time spent by the mice exploring each object was analyzed observationally. Indeed, the basic measure was the time spent by the mice exploring objects during the sample phases and during the test trial. Additionally, two discrimination indexes were calculated for the test trial: an object recognition ratio (total time exploring "old familiar" objects/total time exploration) and a location recognition ratio (total time exploring displaced objects/total time exploration). The time was recorded only when the mice touched the object with its nose or forepaws. Turning around, walking over the object, rearing above the object or resting close to the object was not deemed to be exploration. Moreover, locomotor activity was also measured with the software Ethovision XT 7.0 (Noldus, The Netherlands).

RNA and total protein extraction

Total RNA from mice hippocampi was extracted using Tripure Isolation Reagent (Roche) as described previously [23,24,30,31]. After isolation, RNA integrity was assessed by agarose gel electrophoresis. The yield of total RNA was determined by measuring the absorbance (260:280 nm) of isopropanol-precipitated aliquots of the samples. The recovery of RNA was comparable in all studied groups (1.2-1.5 μg/ mg of tissue). The protein pellets, obtained using the Tripure Isolation Reagent and isopropanol-mediated precipitation, were resuspended in 4% SDS and 8 M urea in 40 mM Tris–HCl, pH 7.4 and rotated overnight at room temperature to get complete protein solubilization.

Retrotranscription and real-time RT-PCR

Retrotranscription (RT) was performed using random hexamers, 4 μg of total RNA as template and High-Capacity cDNA Archive Kit (Applied Biosystems) following the manufacturer recommendations [24,30]. For real time RT-PCR, commercial TaqmanTM probes (Applied Biosystems) were used for amplification. PCR reactions were carried out using either ABI Prism 7000 or 7900HT sequence detector systems (Applied Biosystems). A standard curve was first constructed for every assay, using increasing amounts of cDNA. In all cases, the slope of the curves indicated optimal PCR conditions (slope 3.2-3.4). The cDNA levels of the different mice were determined using GAPDH as housekeeper. Therefore, GAPDH amplification was done in parallel with the gene to be analyzed, and this dada used to normalize target gene results.

Independently of the analyzed gene, results were always expressed using the comparative Ct method, following the Bulletin number 2 from Applied Biosystems. As a control condition, we selected 9 month-old WT mice with control diet. In consequence, the expression of all tested genes, for all ages and mice types, was referenced to the expression levels observed in this group.

Antibodies

For this study the following primary antibodies were used: anti-Neuropeptide Y (NPY) rabbit polyclonal (1:5000, Sigma); anti-Somatostatin (SOM) goat polyclonal (1:1000, Santa Cruz Biotechnology); anti-Abeta (clone 6E10) mouse monoclonal (1:5000, Signet); anti-oligomeric amyloid-beta OC rabbit polyclonal (1:5000, Millipore); anti-Abeta42 rabbit polyclonal (1:5000, Abcam); anti-phospho-tau pSer202/Thr205 mouse monoclonal (clone AT8) (1:250, Pierce); anti-microtubule-associated protein 1 light chain 3 (LC3) rabbit polyclonal (1:500, Cell Signaling); anti-GFAP rabbit polyclonal (1:10000, Dako); anti-ubiquitin rabbit polyclonal (1:5000, Dako); anti-Hsp70 rabbit polyclonal (1:5000, Neomarkers) anti-Hsp60 mouse monoclonal (1:1000, Santa Cruz, Biotechnology), anti-Hsp27 rabbit polyclonal (1:1000, Sigma).

Western blot

Western blots were performed as described [32]. Briefly, 5–20 μg of proteins from the different samples were loaded on 16%-SDS-tris-tricine-PAGE or 12%-SDS-tris-glycine-PAGE and transferred to nitrocellulose (Hybond-C

Trujillo-Estrada *et al. Acta Neuropathologica Communications* 2013, **1**:73
http://www.actaneurocomms.org/content/1/1/73

Extra; Amersham). After blocking, using 5% non-fat milk, membranes were incubated overnight, at 4°C, with the appropriate antibody Membranes were then incubated with the corresponding horseradish-peroxidase-conjugated secondary antibody (Dako, Denmark) at a dilution of 1:8000. Each blot was developed using the ECL-plus detection method (Amersham) and quantified using Image-Quant Las 4000 mini gold (GE Healthcare Bio-Sicences). For normalization purposes, proteins were first estimated by Lowry and protein loading corrected by beta-actin. In each experiment, the intensity of bands from PS1 control fed were averaged and considered as 1 relative unit. Data were always normalized by the specific signal observed in PS1 control group.

Immunohistochemistry

Serial sections from control and lithium-treated transgenic mice (n = 6 per group) were processed in parallel for immunostaining using the same batches of solutions to minimize variability in the immunohistochemical labeling conditions. Free-floating sections were first treated with 3% H2O2/10% methanol in PBS, pH 7.4 for 20 min to inhibit endogenous peroxidases, and with avidin-biotin Blocking Kit (Vector Labs, Burlingame, CA, USA) for 30 min to block endogenous avidin, biotin and biotin binding proteins. Sections were immunoreacted with the primary antibody over 24 or 48 h at room temperature. The tissue bound primary antibody was then detected by incubating for 1 h with the corresponding biotinylated secondary antibody (1:500 dilution, Vector Laboratories), and then followed by incubating for 90 min with streptavidin-conjugated horseradish peroxidase (Sigma-Aldrich) diluted 1:2000. The peroxidase reaction was visualized with 0.05% 3-3-diaminobenzidine tetrahydrochloride (DAB, Sigma-Aldrich) and 0.01% hydrogen peroxide in PBS. Except for Abeta42 immunolabeling, the chromogen solution contained 0.03% nickel ammonium sulphate for a blue reaction product. For double NPY-6E10 immunohistochemical labeling sections were first incubated with anti-NPY as described above. After the DAB-nickel reaction (dark blue end product), sections were the incubated with anti-6E10 antibody. The second immunoperoxidase reaction was developed with DAB only (brown reaction end product). After DAB, sections immunolabeled for Ubiquitin or LC3 antibodies were incubated 3 min in a solution of 20% of Congo red. Sections were then mounted on gelatin-coated slides, air dried, dehydrated in graded ethanol, cleared in xylene and coverslipped with DPX (BDH) mounting medium. Specificity of the immune reactions was controlled by omitting the primary antisera.

For double or triple immunofluorescence labelings, sections were first sequentially incubated with the indicated primaries antibodies followed by the corresponding Alexa 488/568//405 secondary antibodies (1:1000; Invitrogen). GFAP- and OC-immunolabeled sections were stained with 0.02% thioflavin-S in 50° ethanol for 5 min. Sections processed for immunofluorescence were mounted onto gelatin-coated slides, coverslipped with 0.01M PBS containing 50% glycerin and then examined under a confocal laser microscope (Leica SP5 II).

Stereological analysis

Immunopositive cells for SOM or NPY belonging to control and lithium-treated animal groups (n = 5 per group) were stereologically quantified in hippocampus proper and dentate gyrus of hippocampus according to the optical fractionator method. Briefly, the quantitative analyses were performed using an Olympus BX61 microscope interfaced with a computer and an Olympus DP71 digital camera, and the NewCAST (Computer Assisted Stereological Toolbox) software package (Olympus, Denmark). Cell counting was done through the rostrocaudal extent of the hippocampus (between −0.94 mm anterior and 3.64 mm posterior to Bregman coordinates). Neurons were quantified in every seventh section (with a distance of 280 μm), and an average of 6–7 sections was measured in each animal. CA and dentate gyrus boundaries were defined according a standard mouse stereotaxic brain atlas using a 4x objective and the number of neurons was counted using a 100×/1.35 objective. We used a counting frame of 1874.2 μm2 with step lengths of 78.93 × 78.93 μm. The total cell number was estimated using the optical fractionators formula, $N = 1/ssf \times 1/asf \times 1/hsf \times \Sigma Q^-$, where *ssf* represents the section sampling fraction, *asf* is the area sampling fraction, which is calculated by dividing the area sampled with the total area of the layer, *hsf* stands for the height sampling fraction, which is calculated by dividing the height sampled (10 μm in this study) with the section thickness, and ΣQ- is the total count of somatic profiles counted for the entire area. The precision of the individual estimations is expressed by the coefficient of error (CE) using the following formula: $CE = 1/Q \times (3A - 4B + C/12)1/2$, where $A = \Sigma Qi2$, $B = \Sigma Qi \times Qi + 1$, $C = \Sigma Qi \times Qi + 2$. The CEs ranged between 0.07 and 0.1. An investigator who was blind to the experimental conditions performed neuronal profile counting.

Plaque size

To determine the size of the plaques, anti-Abeta42 immunostained sections from control and lithium-treated mice (n = 6 per group) were analyzed using the nucleator method with isotropic probes by the NewCAST software package from Olympus stereological system. CA1 subfield was analyzed using a counting frame of 7155.3 μm2. For individual plaque measurement a 40x objective was used. Number of plaques/mm2 falling into surface categories (ranging from <200 μm2 to >2000 μm2) was calculated. Each analysis was done by a single examiner blinded to sample identities.

Trujillo-Estrada *et al. Acta Neuropathologica Communications* 2013, 1:73
http://www.actaneurocomms.org/content/1/1/73

NPY dystrophic neurites loading

NPY immunostained sections from control and lithium-treated animals were observed under a Nikon Eclipse 50i microscope using a 10x objective and CA1 images were acquired with a Nikon DS-5M high-resolution digital camera. The camera settings were adjusted at the start of the experiment and maintained for uniformity. Digital images (5 sections/mouse) from control and treated mice (n = 6 per group) were analyzed using Visilog 6.3 analysis program (Noesis, France). The area occupied by the NPY-positive dystrophic neurites was identified by level threshold which was maintained throughout the experiment for uniformity. The CA1 area in each image was manually outlined and the positive somata were removed by manual editing. The area occupied by NPY dystrophies was estimated and defined as (sum dystrophies area measured/sum CA1 area analyzed) × 100. The mean and standard deviation (SD) of the dystrophies area were determined using all the available data. Quantitative comparisons were carried out on sections processed simultaneously using same batches of solutions.

NPY dystrophies associated to plaques

The area of NPY dystrophic neurites intimately associated to plaques of different sizes (<200 μm2, 200–500 μm2, 500–2000 μm2 and >2000 μm2) was measured in double 6E10/NPY immunostained CA1 sections from control and lithium-treated animals. Images were photographed using a 20x objective with a Nikon Eclipse 50i microscope coupled to a Nikon DS-5M high-resolution digital camera. Digital images (5 sections/mouse) from control and lithium-treated animals (n = 3 per group) were analyzed using Visilog 6.3 analysis program (Noesis, Frace) to determine the NPY dystrophies area associated to each plaque size group.

Plaque compaction analysis

Abeta42 immunostained hippocamapal sections from control and lithium-treated animals were observed under a Nikon Eclipse 50i microscope and CA1 plaques were photographed using a 10x objective. Images were acquired with a Nikon DS-5M high resolution digital camera. The camera settings were adjusted at the start of the experiment and maintained for uniformity. Digital images (5 sections/mouse, n = 5 per group) were analyzed using Visilog 6.3 analysis program (Noesis, France). Abeta42 staining density was identified by bright-level threshold, the level of which was maintained throughout the experiment for uniformity. The gray-scale image was converted to a binary image for estimating the optical density which was defined as pixel units and related with the plaque size (μm2 which area was measured using the same program). Quantitative comparisons were performed on sections processed at the same time.

Oligomeric plaque halo

To analyze the oligomeric Abeta halo located at the periphery of the plaques, 40 μm floating sections were first stained with Thioflavin-S and then followed by an antibody specific to oligomers of Abeta (OC antibody; 1:5000) visualized with anti-rabbit Alexa568-conjugated secondary antibody (Invitrogen A10042; 1:1000). Images of 1,024 × 1,024 pixels were acquired by using a Leica SP5 II confocal laser microscope. A total of 15 plaques per animal were randomly photographed in CA1 subfield of control and treated animals (n = 3 per group). Laser settings were adjusted at the start of the experiment and maintained for uniformity. Images were analyzed using LAS AF Lite program (Leica). Plaque area was determined for Thioflavin-S staining (plaque core in green color) and OC immunostaining (oligomeric Abeta in red color) and the difference between the OC area and the core area was considered as the oligomeric halo surrounding plaques.

Statistical analysis

Normality of data was first assessed by using Kolmogorov-Smirnov test. Normally distributed data were expressed and represented as mean ± SD. Non-normal distributed data were represented using box-plot. For normally distributed data, means were compared using ANOVA followed by Tukey test (more than two groups) or t-test (for two group comparisons). Non-normal data were compared by Wilcoxon (for two groups) or Kruskal-Wallis tests (more than two groups). The significance was set at 95% of confidence. Fit and comparison of linear regression was done using multiple regression analysis followed by conditional sum of squares. In all cases Statgraphics plus 3.1 was used.

Results

Lithium treatment rescued behavioral/memory deficits

First, we tested whether lithium administration was able to improve the behavioral/memory deficiencies observed in the 9 month-old control PS1xAPP transgenic model. From the different tasks performed (i.e. Morris water maze), only open-field and novel object recognition showed statistical differences between PS1xAPP and WT or PS1 control mice. No differences between WT and PS1 mice were observed.

In the open-field test, control PS1xAPP mice displayed significant lower activity than either WT or PS1 mice (Figure 1A). There was a significant reduction in both total distance and velocity. No significant differences were observed in time in the periphery or center of the field, or in the immobility periods (data not shown). Also, no differences between PS1xAPP and control groups were observed in fecal boli depositions (not shown). Thus, the PS1xAPP mice were hypoactive as reported in other AD models, such as the 3xTg-AD [28]. As we shown, this mild

Trujillo-Estrada *et al. Acta Neuropathologica Communications* 2013, **1**:73
http://www.actaneurocomms.org/content/1/1/73

form of apathy in PS1xAPP mice was totally relieved after lithium treatment (Figure 1A).

We next evaluated the episodic-like memory using novel object recognition tests. These tests are based on the preference for the "old familiar object" over the "recent familiar" object and the preference for a novel location [29]. Although no differences between groups were observed in the object recognition ratio (Figure 1B), control PS1xAPP mice displayed a significant cognitive deficit in object location memory (which is hippocampus-dependent), compared with PS1/WT mice. Remarkably, full recovery of this spatial memory impairment was observed in lithium-treated PS1xAPP mice, which displayed no differences with the control groups (Figure 1B). Therefore, these data indicated that early oral lithium administration prevents the spatial memory deterioration in PS1xAPP mice.

Lithium administration prevented neuronal loss

As we have reported previously, early Abeta deposition in this PS1xAPP model is paralleled by a selective and significant decrease in the number of SOM and NPY positive GABAergic neurons in the hippocampal formation and the entorhinal cortex [23,24], (see also Figure 2A, B and C). Furthermore, SOM/NPY positive cells displayed a prominent axonal pathology (Figure 2D), with multiple dystrophies (positive also for phospho-tau) that surrounded Abeta plaques (Figure 2E). The early and extensive degenerative pathology of the GABAergic cells, including neuronal death, could be used as a surrogated marker to evaluate the neuroprotective effect of lithium at the initial stages of the disease.

We thus analyzed, at the hippocampal formation, the SOM and NPY expression by qPCR; the number of SOM or NPY immunopositive somata, by stereological quantification, and their axonal dystrophy loading. Lithium produced an effective prevention of the neurodegenerative process exhibited by this neuronal population in PS1xAPP mice (Figure 2). In fact, the mRNA expression for both neuropeptides, SOM and NPY, was virtually identical in lithium-treated PS1xAPP mice, as compared with control groups (Figure 2A). Furthermore, stereological determination of the SOM or NPY cell number (Figure 2B and C) further demonstrated the protective effect of lithium on these neurons in hippocampus proper (O-LM cells) and dentate gyrus (HIPP cells). PS1 and WT mice displayed not differences and lithium treatment of PS1 mice did not alter the expression of either SOM or NPY neuropeptides (see Figure 2A) or the number of SOM or NPY positive cells (data in Figure 2C were pooled from WT, PS1 control and lithium groups). For subsequent experiments, only PS1 control and PS1 lithium mice were included.

The same samples were used for the stereological quantification of SOM or NPY cell number at the entorhinal cortex, another early affected brain region. As previously reported [23], double transgenic mice displayed in this cortical region a significant decrease in the number of both SOM (4,207 ± 1,119 cell/mm3, n = 4, vs 8,596 ± 803 cell/mm3, n = 6, for control PS1xAPP and PS1 mice, respectively, $p < 0.05$; 52.2 ± 13.1% of reduction) and NPY (1,770 ± 227 cell/mm3, n = 4, vs 3,062 ± 363 cell/mm3, n = 6, for control PS1xAPP and PS1 mice, respectively, $p < 0.05$; 58.4 ± 7.1% of reduction) immunopositive GABAergic cells. However, after lithium treatment, the number of both neuronal populations did not differ between PS1/APP and PS1 groups (7,087 ± 1,097 cell/mm3 or 3,003 ± 423 cell/mm3, n = 4, for SOM and NPY, respectively; 17.6 ± 12.8% or 1.9 ± 13.8% of reduction).

Thus, early lithium intervention was highly effective preventing the SOM/NPY neuronal loss in both the hippocampal formation and the entorhinal cortex of PS1xAPP model.

Another prominent pathological feature of this neuronal population in our PS1xAPP mice is the extensive development of axonal dystrophies associated to Abeta plaques [15] (Figure 2D and E). Importantly, lithium treatment produced, in parallel with the prevention of the SOM/NPY cell loss, a prominent reduction of the axonal dystrophy pathology in these cells. In fact, lithium treated PS1xAPP mice displayed an obvious and highly significant decrease (−60.2%) in the NPY positive dystrophic area (Figure 2D, d1, d2 and d3). Also, there was a decrease in the AT8- and SOM-positive dystrophies (Figure 2E). Therefore, lithium avoided SOM/NPY neurodegeneration and improved the cell integrity, reducing the axonal degeneration of this highly vulnerable neuronal population.

Lithium treatment ameliorated axonal/synaptic pathology by reducing abnormal intracellular protein accumulation

PS1xAPP mice accumulated phospho-tau, LC3-II and ubiquitinated proteins in axonal dystrophies surrounding Abeta plaques (Figure 3; see also [15,16]). Thus, in agreement with the preservation of SOM/NPY neurons, lithium also reduced both the total AT8-positive phospho-tau levels, determined by western blots (Figure 3A), and the AT8-positive dystrophies, detected by immunohistochemistry (Figure 3B). Furthermore, lithium also reduced the steady-state levels of both LC3-II and ubiquitinated proteins (see Figure 3C). In fact, the steady-state levels of both LC3-II and ubiquitinated proteins were similar to those observed in the PS1 lithium group. Immunohistochemistry also demonstrated a dramatic reduction in both ubiquitin- and LC3-positive dystrophies, surrounding the Abeta plaques (Figure 3D, d2 and d4). Thus, lithium reduced the number of dystrophies and the accumulation of intracellular proteins.

This lithium-mediated reduction of the axonal dystrophic pathology could also ameliorate the synaptic degeneration. Thus, we determined (by western blots) the levels of the classic presynaptic marker synaptophysin (not shown).

Trujillo-Estrada *et al. Acta Neuropathologica Communications* 2013, 1:73
http://www.actaneurocomms.org/content/1/1/73

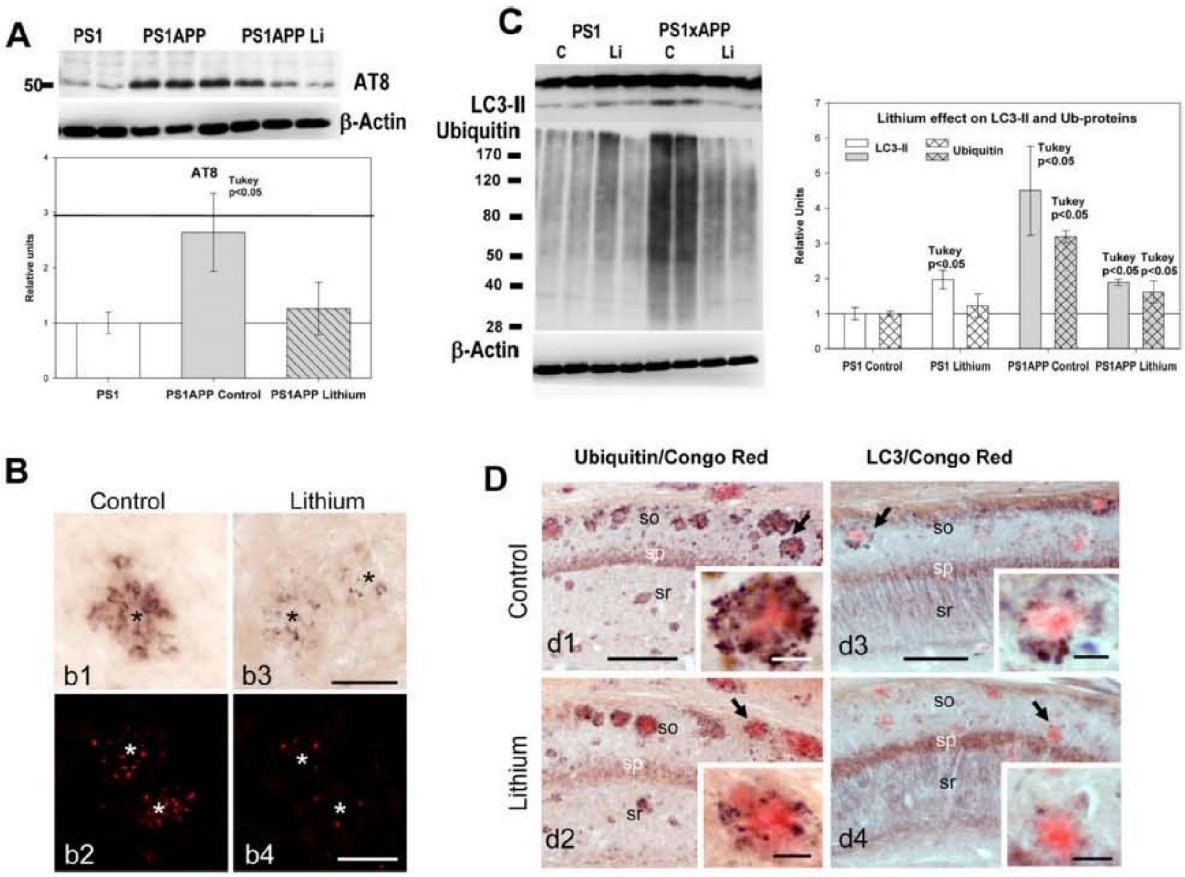

Figure 3 Lithium treatment reduced the dystrophic pathology associated to Abeta plaques. A) Representative western blot (n 7 mice per group) and quantitative analysis of phosphorylated tau, determined using AT8 clone, of total proteins from PS1 control, PS1xAPP control and PS1xAPP lithium-treated mice. For quantification, the AT8 levels were referred to PS1 control group. The AT8 levels were significantly increased in PS1xAPP control mice (ANOVA F(2,18) 22.66, p 0.0001; Tukey $p < 0.05$) whereas PS1 control and PS1xAPP lithium displayed no differences. **B)** Representative AT8 positive dystrophies surrounding Abeta plaques from control (b1 and b2) or lithium treated (b3 and b4) PS1xAPP mice. **C)** Representative western blots and quantitative analysis of steady-state levels of LC3-II and ubiquitinated proteins in PS1 and PS1xAPP control and treated mice (n 4 per genotype and treatment). A clear and significant accumulation of both LC3-II (ANOVA F(3,12) 32.52, p 0.001) and ubiquitinated proteins (ANOVA (F(3,12) 63.67, p 0.00001) was observed in PS1xAPP control mice. Lithium treatment reversed this pathology. The post-hoc analysis, using Tukey test, was indicated in the figure. **D)** Ubiquitin (d1 and d2) and LC3 (d3 and d4) immunolabeled hippocampal sections (counterstained with Congo red for Abeta plaques) of control and lithium treated PS1xAPP mice corroborated the accumulation of both markers, associated with dystrophic neurites surrounding amyloid plaques (d1 and d3) and the patent lithium reduction (d2 and d4) in the presence of ubiquitin and LC3 positive dystrophies. Inserts in d1-d4 showed higher magnification details of the dystrophies surrounding Abeta plaques. so, stratum oriens; sp, stratum pyramidale; sr, stratum radiatum. Scale bars: b1, b3 50 μm; b2, b4 100 μm; d1 to d4 200μm; inserts 25 μm.

Control PS1xAPP mice displayed a consistent and significant reduction (0.72 ± 0.12 vs 1.00 ± 0.14 for PS1xAPP and PS1 control, respectively, $n = 7$ per phenotype, Tukey $p < 0.05$) whereas a completely recovery was detected in lithium-treated PS1/APP mice (0.96 ± 0.16 for PS1xAPP lithium, $n = 9$).

Taken together, these data indicated that the chronic lithium treatment markedly reduced the plaque associated axonal dystrophy pathology, in parallel with a reduction on the abnormal intracellular accumulation of proteins and/or autophagic vesicles, in this PS1xAPP model. Furthermore, lithium also decreased the putative presynaptic degeneration observed in this transgenic mouse model.

Lithium treatment substantially modified the morphology and toxicity of the extracellular Abeta plaques

Next, we tested whether lithium treatment could alter Abeta accumulation in PS1xAPP hippocampus. Data (Table 1) indicated the absence of modifications on either i) total monomeric Abeta (quantified by western blot and 6E10 antibody), ii) soluble Abeta42 (quantified by ELISA using soluble extracts) or iii) Abeta plaque load (determined using either anti-Abeta42 or 6E10

Trujillo-Estrada *et al. Acta Neuropathologica Communications* 2013, **1**:73
http://www.actaneurocomms.org/content/1/1/73

Table 1 Abeta accumulation was not modified in the lithium treated PS1xAPP mice

		Control	Lithium
Soluble Abeta42	ELISA	27.57 ± 10.74	30.14 ± 6.47
(pg/ml)		n = 7	n = 7
Total Abeta	Western blots	1.0 ± 0.26	0.98 ± 0.60
(relative units)	6E10	n = 18	n = 25
Abeta load	Immunohistochemistry	6.83 ± 1.99	4.40 ± 1.81
(% of area)	6E10	n = 5	n = 5
Abeta42 load	Immunohistochemistry	5.09 ± 2.31	3.65 ± 1.03
(% of area)	Abeta42	n = 5	n = 5

Data are mean ± S.D.

antibodies). However, we did observe a highly significant reduction (−62.7%) in the size of the Abeta plaques in lithium-treated PS1xAPP mice, as compared with PS1xAPP control group (Figures 4A, a1, a2 and quantitatively in a3). In fact, when the distribution of the different sizes of the Abeta plaques was analyzed (Figure 4A, a4), the treated group displayed a marked increase (4 fold) in the number of small plaques (<200 μm2), with the consequent reduction in the number of medium and large size Abeta plaques.

This reduction of plaque size, in absence of a parallel reduction on the total Abeta deposition, could arise of a higher Abeta compaction. Interestingly, higher plaque compaction could reduce the Abeta pathology [33]. We thus determined the plaque compaction by quantifying the optical density of Abeta42 immunostained plaques, randomly selected by the stereological microscope (n = 800 plaques from 5 different sections and 6 different control or treated mice; see [33]). Although the plaque compaction was heterogeneous in both groups (Figure 4B), our data demonstrated the existence of a highly increase (82%) in the plaque compaction (calculated as Pixels/μm2) in the lithium treated PS1xAPP mice (Figure 4B, b5).

The increase in plaque compaction could involve a reduction of the putative toxic oligomeric Abeta that surrounded or aroused from plaques (the plaque "halo"; [34]. To quantitatively determine this possibility, the Abeta plaques were first stained with Thioflavin-S followed by immunostaining with the conformation-specific OC antibody, which recognizes fibrillar Abeta oligomers. Representative double labeled images, and the quantification of the plaque oligomeric halo, is shown in Figure 4C (c1 to c6, and c7, respectively). As expected, lithium treatment produced a significant reduction of the OC-positive plaque halo which might result in less toxic plaques.

To examine the impact of lithium treatment on the toxicity of the Abeta plaques, we quantified the NPY dystrophic area and the corresponding Abeta area in individual plaques. Using unbiased stereological counts in NPY and 6E10 double immunostained sections (Figure 5A), we first calculated the proportion of Abeta plaques devoid of NPY dystrophies. As shown, treated PS1xAPP mice displayed a small, but significant, increase in the proportion of plaques without associated NPY dystrophies (Figure 5B). More relevant, when the NPY dystrophic area was normalized by the corresponding Abeta plaque area, we observed a substantial reduction of the NPY dystrophic area per plaque in the treated PS1xAPP mice (Figure 5C). Since this reduction of the dystrophic area could just reflect the decrease in plaque size, we also plotted single NPY-dystrophic area versus the corresponding Abeta plaque area, for both control and treated PS1xAPP mice. As expected, we observed a significant positive linear correlation between both parameters in both mice groups (Figure 5D). Importantly, we also observed a significant higher dystrophic area in control PS1xAPP mice across all size of plaques, as compared with treated PS1xAPP mice. In fact, the slope of the fitted linear regression, between dystrophic area versus plaque area, presented a 3-fold decrease after lithium treatment (0.0399 ± 0.006 vs 0.0119 ± 0.0011; for control and lithium PS1xAPP mice; ANOVA $F(1,127) = 27.88$, $p = 0.00001$).

Taken together, these data demonstrated that lithium treatment modified Abeta plaques quality decreasing their toxicity measured as the capacity to induce axonal dystrophies formation.

Lithium treatment induced astrocyte activation and the incorporation of Hsps to Abeta plaques

Finally, we investigated the possible implication of astrocytes on this lithium-mediated modification of Abeta plaques. Activated astrocytes, surrounding Abeta, could highly influence the Abeta compation and plaque aggregation [35-37]. Thus, we evaluated whether lithium affected the astrocyte activation by determining the expression of GFAP by qPCR (Figure 6A) and immunohistochemistry (Figure 6B, b1 to b4). As expected, GFAP expression and astrocyte activation were increased in control PS1xAPP group (as compared with PS1 mice, Figure 6A and B). As also shown, lithium treatment produced a higher increased in GFAP expression (Figure 6A) and also in GFAP activation (compare Figures 6B, b2 and b4). In fact, in the treated PS1xAPP mice, astrocytes were more immunoreactive and clearly hypertrophic, as compared with control PS1xAPP. However, no significant lithium-dependent differences were detected on the expression of other factors, such as NGF, GDNF, NT-5, MMP9, MMP3 or ApoE, (Figure 6C). It is also noteworthy that lithium treatment has no effect on GFAP expression on non-Abeta activated astrocytes (PS1 lithium mice).

Within the different factors and/or processes that could influence Abeta compaction, it has been demonstrated that

Trujillo-Estrada *et al. Acta Neuropathologica Communications* 2013, **1**:73
http://www.actaneurocomms.org/content/1/1/73

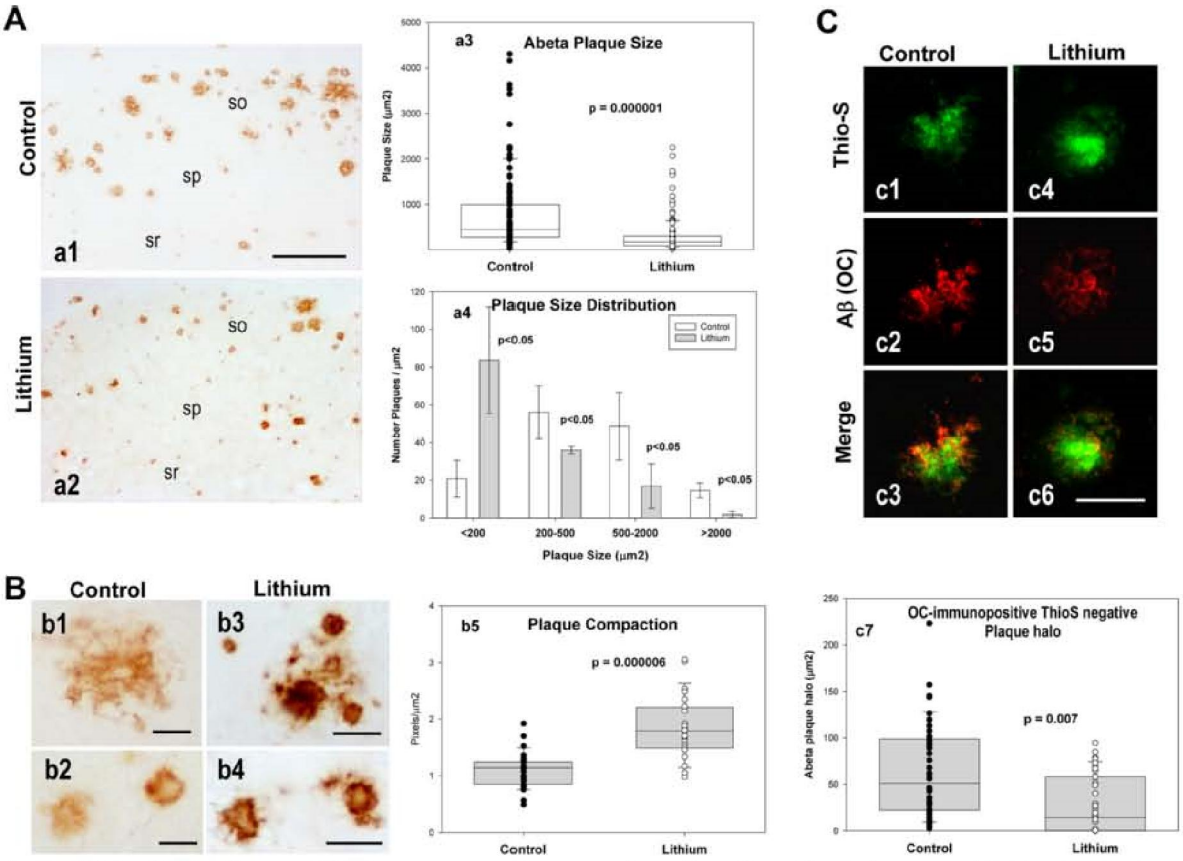

Figure 4 Lithium treatment reduced the size and increased the compaction of the extracellular Abeta plaques. A) Lithium treatment reduced the size of Abeta deposits. Plaques were immunostained with anti-Abeta42 antibody. Representative images (a1 and a2) and quantitative analysis (a3 and a4) of Abeta plaque size from the CA1 subfield of control and lithium-treated PS1xAPP mice. (a3) The individual plaque size (µm2) was quantitatively assessed from 25 sections of 6 different control or lithium treated PS1xAPP mice. (a4) The plaque size distribution was determined by calculating the number of plaques falling into distinct area categories (ranging from <200 µm2 to >2000 µm2). For each category, the difference between control and lithium was determined by t-test. so, stratum oriens; sp, stratum pyramidale; sr, stratum radiatum. **B)** Lithium treatment increased the Abeta plaque compaction. Signal density of Abeta42 immunostained plaques from control (b1, b2) and lithium-treated (b3, b4) mice were measured in the CA1 subfield of hippocampus. Optical densities (pixel/µm2) of plaques from 5 sections/mouse and 5 mice per group was represented in the graph. **C)** Plaque oligomeric halo, considered as the difference between OC- and Thio-S-stained areas was reduced by lithium. Plaques were sequentially staining with Thio-S and the OC antibody. (c1-c6) Representative images of a similar size plaque in the CA1 region of control (c1-c3) or lithium-treated (c4-c6) mice showing the plaque halo. (c7) Similar size plaques (< 200 µm2) were analyzed (15 plaques per animal, n 3 mice per group). Scale bars: a1, a2 200 µm; b1-b4 25 µm; c1-c6 20 µm.

extracellular chaperones, such as heat shock proteins (Hsps), have the capacity to reduce the Abeta toxicity by increasing the sequestration/compaction of putative toxic Abeta oligomers [36,38-41],. Furthermore, it has been also demonstrated that astrocytes could express and release different Hsps [36]. Thus, we evaluated whether lithium treatment did affect the Hsps expression. First, we determined, by western blots, the levels of Hsp27, Hsp60 and Hsp70 in PS1xAPP control and lithium treated mice. As shown in Figure 6D, we observed a consistent increase on the levels of all four proteins in the lithium group. However, no changes on expression (by qPCR) were detected (not shown). Moreover, we analyzed the in vivo localization of Hsp70 (not shown) and Hsp27 (Figure 6E) and whether lithium treatment modified their distribution. Both chaperones displayed similar immunostaining patterns. In lithium treated PS1xAPP mice (Figure 6E e1 to e5), triple labeling experiments demonstrated that anti-Hsp27 intense stained the Abeta plaque core (labeled by 6E10) and, interestingly, also activated astrocytes (GFAP-positive cells) near plaques displayed Hsp-27 immunopositive puncta. However, in control PS1xAPP mice, the core of Abeta plaques appeared weakly immunostained and low or no immunoreactivity was observed in astrocytes surrounding Abeta plaques (Figure 6E, e6-e9).

Trujillo-Estrada *et al. Acta Neuropathologica Communications* 2013, **1**:73
http://www.actaneurocomms.org/content/1/1/73

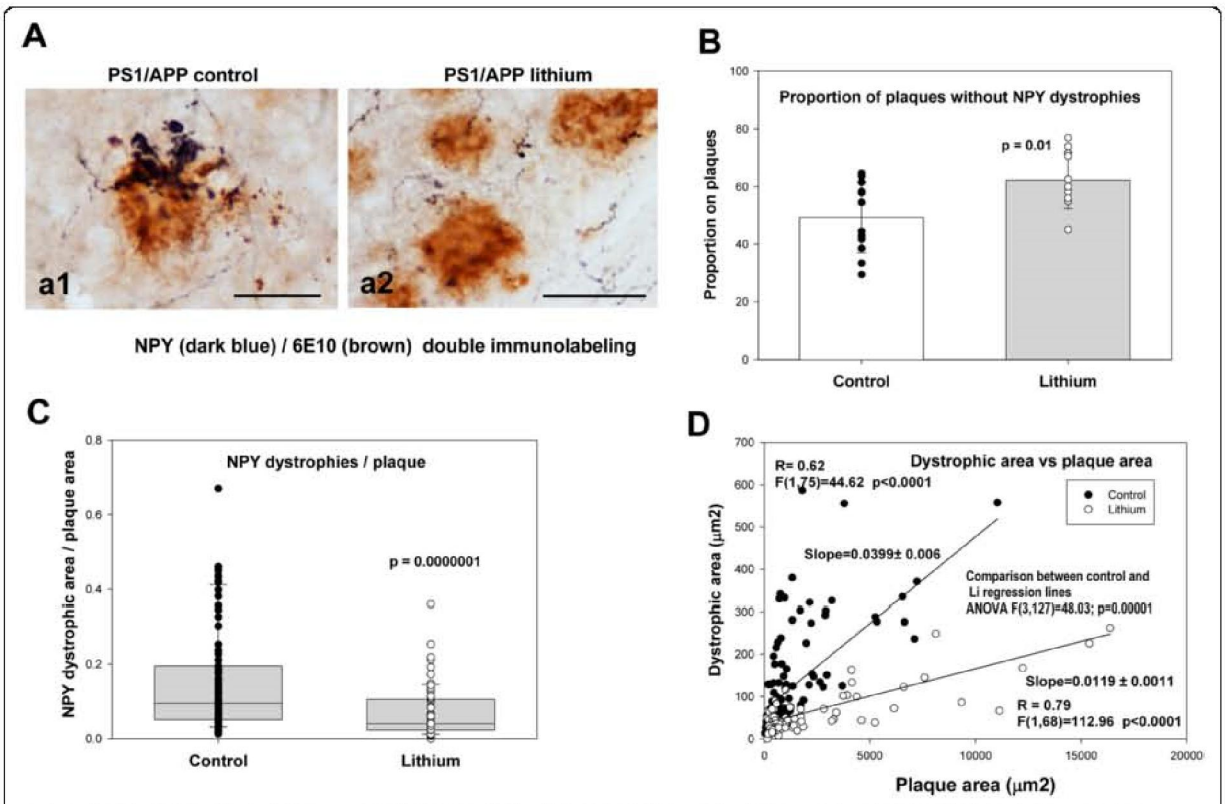

Figure 5 Lithium treatment decreased the Abeta toxicity. A) NPY-labeled dystrophic neurites, surrounding 6E10-labeled Abeta plaques, were compared in CA1 field of hippocampus from control (a1) and lithium-treated (a2) PS1xAPP mice (5 sections per mice, 3 mice per group). **B)** Lithium treatment increased the proportion of Abeta plaques displaying no apparent NPY-dystrophies. The difference between groups (indicated in the figure) was assessed using t-test. **C)** Lithium also significantly (using non-parametric Wilcoxon test) reduced the NPY dystrophic area, normalized by the corresponding plaque area. **D)** The decrease on Abeta toxicity, at all plaque sizes, was also assessed by plotting the individual NPY dystrophic area versus Abeta plaque area. The individual data from both groups were fitted to a linear model and the possible difference between groups was analyzed using Multiple Regression Analysis. As shown, both groups (control and lithium) could be fitted to a linear model and both regression lines were statistically different (ANOVA F(3,145) 38.00; p 0.00001). Furthermore, the slopes of the fitted data were also significantly different between both groups (Conditional Sum of Squares, see Results). Scale bars: a1 25 µm, a2 50 µm.

Although more experiments are clearly needed, these data indicated that lithium, modulating the production/release of Hsps by astrocytes, might decrease the toxicity of plaques by increasing the Abeta compaction.

Discussion

Here, we demonstrate that chronic oral administration of lithium, before the pathology onset, resulted in less toxic plaque formation that significantly ameliorated the degenerative processes and behavioral/memory deficits occurring during disease progression in our PS1xAPP model. Specifically, and of great relevance for AD prevention, early lithium intervention was able to arrest neuronal loss in hippocampus and entorhinal cortex of highly vulnerable populations, Beside, lithium substantially reduced the axonal dystrophic pathology, associated to amyloid plaques, by increasing the Abeta compaction. As we discuss below, these neuroprotective effects of lithium could be mediated by modifications of the plaque toxicity through the astrocytic release of heat shock proteins. On contrary to previous failed clinical studies using lithium, our results highlight the potential use of this compound as a preventive intervention to halt/slow AD pathology progression at preclinical stages.

As we reported previously, our PS1xAPP mouse displays early (6 months) neuronal loss affecting SOM/NPY GABAergic cells in the hippocampal formation and entorhinal cortex, which coincides spatiotemporally with the extracellular Abeta deposition [15,16,23,24,30,31]. In addition, another pathological feature of this AD model is the formation of abundant axonal dystrophies surrounding the Abeta plaques. Dystrophies accumulated phosphorylated tau, ubiquitinated proteins and autophagic vesicles [15,16].

Our data demonstrate that lithium administration, starting before the beginning of the neurodegenerative

Trujillo-Estrada *et al. Acta Neuropathologica Communications* 2013, 1:73
http://www.actaneurocomms.org/content/1/1/73

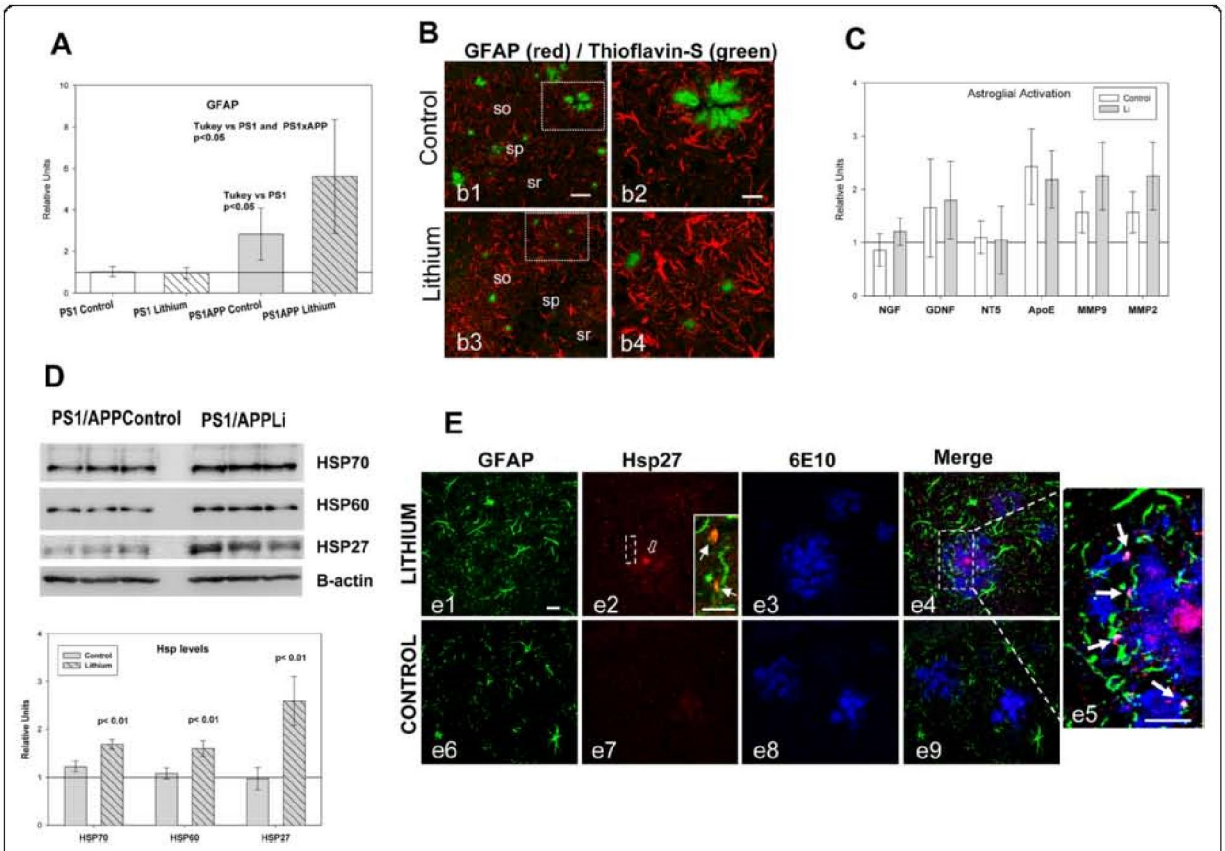

Figure 6 Lithium increased the astrocyte activation and the Hsps levels. A-B) Lithium treatment increased the astrocyte activation assessed by qPCR **(A)** and GFAP immunoreactivity **(B)**. GFAP expression **(A)** was assayed in hippocampal samples from 10 mice per group. GFAP expression increased in PS1xAPP control group and further increased in PS1xAPP lithium-treated mice. ANOVA (F(3,36) 18.82, p 0.0001). The post-hoc analysis using Tukey is presented in the graph. **B)** Representative confocal images through the CA1 field of control (b1, b2) and lithium-treated (b3, b4) mice, showing GFAP-immunoreactive astrocytes (red) and Thioflavin-stained Abeta plaques (green). As shown, GFAP immunoreactivity is clearly higher in lithium-treated mice. **C)** Lithium did not modify the expression of NGF,GDNF, NT-5, MMP9, MMP3 or ApoE, determined by qPCR (n 4 mice per group). **D)** Lithium treatment increased the levels of three Hsps (Hsp70, Hsp60 and Hsp27). Representative western blots and quantitative analysis of Hsps using protein extract from hippocampus of control and lithium-treated PS1xAPP mice (n 4 mice per group). The expression of all three Hsps was normalized using PS1 control (not shown), and the significance was determined by t-test. **E)** Confocal images through the CA1 subfield showing GFAP/Hsp27/Abeta triple immunofluorescence labeling. In lithium-treated mice (e1-e5), the core of the Abeta plaques (labeled by 6E10, in blue) is intensely stained with the anti-Hsp27 antibody (in red), as well as astrocytic puncta processes (labeled by GFAP, in green) surrounding the plaques (see insert in e2 showing double GFAP-Hsp27 labeling, and the triple labeling detail in e5). On the contrary, in control mice (e6-e9), the core of the Abeta plaques appears almost devoid of Hsp27 immunostaining and low or no immunoreactivity was observed in astrocytes surrounding the plaques. Scale bars, d1-d9 20 μm, insert in a2 10 μm.

processes, avoids the selective neuronal loss of the SOM/NPY cells in both the hippocampus and entorhinal cortex. This is the first report showing that lithium prevents neuronal loss in AD vulnerable brain regions using in vivo studies. Also, our data demonstrate that lithium ameliorates the dystrophic pathology, reducing dramatically the NPY-positive dystrophic area associated to the Abeta plaques and decreasing the levels of abnormally accumulated LC3-II, AT8 and ubiquitinated proteins. Thus, lithium clearly alleviates most of the neuropathological signs of the PS1xAPP model.

As we and others have demonstrated, the PS1xAPP mice display GSK-3beta activation and autophagy/lysosomal deficiencies [15,16,31,42,43]. Lithium could directly affect the neuronal degeneration by inhibiting the GSK-3beta activity (data not shown; [44]) and/or by activating the autophagy-mediated protein degradation [12,45,46]. These effects would reduce the accumulation of phospho-tau, LC3-II and ubiquitinated proteins and, in consequence, reduce the neurodegenerative process. However, the PS1xAPP transgenic model accumulates these proteins in axonal dystrophies surrounding the Abeta plaques. In this sense, we

and others have suggested that the formation of axonal dystrophies might be directly implicated in the neuronal degeneration during disease progression [9,15,16,47,48]. This suggestion agrees with recent data from AD patients [49]. Importantly, quantitative data demonstrate that lithium produced a prominent reduction (–60%) of the NPY-positive dystrophic area. This reduction could also be reflected by the decrease in the abnormal accumulation of phospho-tau, LC3-II and ubiquitinated proteins, associated with the dystrophic pathology, surrounding Abeta plaques.

Therefore, besides a putative direct effect either through GSK-3beta activity or autophagy/lysosomal protein degradation, the lithium-mediated amelioration of the neuropathological alterations may likely reflect the dramatic reduction in the formation of dystrophic neurites around the Abeta plaques. This effect could also reflect the lithium-dependent modifications of the Abeta plaque formation.

As we have shown here, lithium produced a prominent change in plaque morphology and quality. In fact, the Abeta plaques were smaller (see also [20]) and more compact in treated than in control PS1xAPP mice. In this context, it has been reported that the highly aggregated Abeta possesses a reduced toxicity [33,50], and therefore the observed decrease in the dystrophic area per plaque could reflect a reduction in plaque toxicity.

Regarding the plaque toxicity, it has been noted that the formation of axonal dystrophies and the synaptic degeneration seemed to be restricted to the periphery of the Abeta plaques [34,48,50]. This most periphery area (halo) of the plaques might be constituted by partially aggregated Abeta fibrillar oligomers, which could be involved on the AD pathology [51]. In this scenario, our data demonstrate that lithium produces a reduction on the fibrillar oligomeric halo (which is recognized by the conformation specific polyclonal OC antibody) of the Abeta plaques, thus diminishing the plaque toxicity.

The processes contributing in the Abeta aggregation, plaque formation or plaque compaction are actually unknown. It has been suggested that astrocytes could play a prominent role by limiting the plaque growth and the plaque-associated dystrophy formation [35,36]. Moreover, activated astrocytes may release, among different factors, Hsps [52,53], which could induce the Abeta aggregation, reducing its potential toxicity [36,38,40]. In agreement with these data, our results strongly suggest the involvement of astrocytes and extracellular Hsps as mediators of the lithium effect on plaque toxicity. In fact, we demonstrate simultaneous higher astrocyte activation with higher incorporation of Hsps in the Abeta plaques and reduced oligomeric plaque halo in lithium treated PS1xAPP mice, compared with controls. It is noteworthy the lithium-dependent increase of Hsp70 and Hsp27 in the plaque core. Although further experiments should be done, this particular localization suggests that these Hsps could be implicated in the Abeta nucleation and plaque compaction.

Conclusions

Our data demonstrate that the early chronic lithium treatment significantly ameliorates the pathological progression in this PS1xAPP AD model. Lithium could reduce neuronal/axonal degeneration by increasing the Abeta compaction and, in consequence, producing smaller Abeta plaques with lower toxic halo. Lithium could influence directly neurons but, as we have shown in this work, this compound has a novel therapeutic effect through astrocytes inducing chaperones release which have the capacity to modulate the Abeta compaction/toxicity. To the best of our knowledge, this is the first time that this therapeutic effect of lithium on Abeta plaque quality has been reported. These data reveal a novel lithium-mediated mechanism capable of altering the course of the disease in an amyloidogenic AD model. These Abeta-modifying mechanism might represent an innovative therapeutic approach to the, so far, continuing negative outcomes of AD clinical trials aimed to clear Abeta plaques once they have already formed, and to the current inability to prevent plaques from forming in the first place.

Competing of interests

The authors declare that they have no competing of interests.

Authors' contributions

MT, SJ, VN and MV carried out the molecular experiments; R S-V, L T-E, and E M-S carried out the immunohistochemical experiments; D B-V and I M-G carried the stereological experiments; V DC performed the behavioral analysis; JCD and MV participated in the design of experiment and revising the manuscript, AG and JV design the experiments, analyzed the data and wrote the manuscript. All authors read and approved the final manuscript.

Acknowledgments

This work was supported by Fondo de Investigación Sanitaria (FIS), from Instituto de Salud Carlos III of Spain, through grants PI12/01439 (to JV) and PI12/01431 (to AG), and by CIBERNED (PI2010/08) to JV and AG. SJ and VDC are the recipients of a contract from CIBERNED. VN and MT were recipients of PhD fellowships from Junta de Andalucia. LTS and ELS were recipients of PhD fellowships (FPU) from Ministerio de Educacion Cultura y Deportes. We thank Sanofi for the PS1xAPP model used in this study, and Mercedes Aneiros and Maria Luisa Gracia-Cuervo for their expert technical assistance. Antonia Gutierrez and Javier Vitorica are Co-Senior corresponding authors.

Author details

[1]Departamento de Biologia Celular, Genetica y Fisiologia, Facultad de Ciencias, Universidad de Malaga, 29071 Malaga, Spain. [2]Departamento de Bioquímica y Biología Molecular, Facultad de Farmacia, Universidad de Sevilla, 41012 Sevilla, Spain. [3]Centro de Investigación Biomédica en Red sobre Enfermedades Neurodegenerativas (CIBERNED), Madrid, Spain. [4]Instituto de Biomedicina de Sevilla (IBiS)-Hospital Universitario Virgen del Rocío/CSIC, Universidad de Sevilla, Sevilla, Spain. [5]Present addresses: Laboratory of Molecular Cell Biomedicine, University of Balearic Islands, Palma, de Mallorca, Spain. [6]Institute for Memory Impairments and Neurological Disorders, Department of Neurobiology and Behavior, University of California, Irvine, CA, USA. [7]Mitchell Center for Alzheimer's Disease and Related Brain Disorders, Department of Neurology, University of Texas Medical School at Houston, Houston, Texas, USA.

Received: 7 November 2013 Accepted: 8 November 2013
Published: 12 November 2013

References

1. Hardy J, Selkoe DJ: **The Amyloid hypothesis of Alzheimer's disease: progress and problems on the road to therapeutics.** *Science* 2002, **297**:353–356.
2. Wyss-Coray T, Rogers J: **Inflammation in Alzheimer Disease's. A Brief Review of the Basic Science and Clinical Literature.** *Cold Spring Harb Perspect Med* 2012, **2**:a006346.
3. Diniz B, Machado-Vieira R, Forlenza O: **Lithium and neuroprotection: translational evidence and implications for the treatment of neuropsychiatric disorders.** *Neuropsychiatr Dis Treat* 2013, **9**:493–500.
4. Forlenza O, Paula V, Machado-Vieira R, Diniz B, Gattaz W: **Does Lithium Prevent Alzheimer's disease?** *Drugs Aging* 2012, **29**:335–342.
5. Nunes PV, Forlenza OV, Gattaz WF: **Lithium and risk for Alzheimer's disease in elderly patients with bipolar disorder.** *B J Psychiatry* 2007, **190**:359–360.
6. Young AH: **More good news about the magic ion: lithium may prevent dementia.** *B J Psychiatry* 2011, **198**:336–337.
7. Bhat RV, Budd Haeberlein SL, Avila J: **Glycogen synthase kinase 3: a drug target for CNS therapies.** *J Neurochem* 2004, **89**:1313–1317.
8. Hernandez F, Lucas JJ, Avila J: **GSK3 and Tau: two convergence points in Alzheimer's disease.** *J Alzheime Dis* 2013, **33**:S141–S144.
9. Jin M, Shepardson N, Yang T, Chen G, Walsh D, Selkoe DJ: **Soluble amyloid beta protein dimers isolated from Alzheimer cortex directly induce Tau hyperphosphorylation and neuritic degeneration.** *Proc Natl Acad Sci USA* 2011, **108**:5819–5824.
10. Leroy K, Ando K, Laporte V, Dedecker R, Suain V, Authelet M, *et al*: **Lack of Tau proteins rescues neuronal cell death and decreases Amyloidogenic Processing of APP in APP/PS1 Mice.** *Am J Pathol* 2012, **181**:1928–1940.
11. Caccamo A, Oddo S, Tran LX, LaFerla FM: **Lithium reduces Tau Phosphorylation but not Abeta or working memory deficits in a transgenic model with both plaques and tangles.** *Am J Pathol* 2007, **170**:1669–1678.
12. Sarkar S, Floto RA, Berger Z, Imarisio S, Cordenier A, Pasco M, *et al*: **Lithium induces autophagy by inhibiting inositol monophosphatase.** *J Cell Biol* 2005, **170**:1101–1111.
13. Sarkar S, Rubinsztein DC: **Inositol and IP3 Levels Regulate Autophagy: Biology and Therapeutic Speculations.** *Autophagy* 2006, **2**:132–134.
14. Nixon RA, Wegiel J, Kumar A, Yu WH, Peterhoff C, Cataldo A, *et al*: **Extensive involvement of autophagy in Alzheimer disease: an immuno-electron microscopy study.** *J Neuropathol Exp Neurol* 2005, **64**:113–122.
15. Sanchez-Varo R, Trujillo-Estrada L, Sanchez-Mejias E, Torres M, Baglietto-Vargas D, Moreno-Gonzalez I, *et al*: **Abnormal accumulation of autophagic vesides correlates with axonal and synaptic pathology in young Alzheimer's mice hippocampus.** *Acta Neuropathol* 2012, **123**:53–70.
16. Torres M, Jimenez S, Sanchez-Varo R, Navarro V, Trujillo-Estrada L, Sanchez-Mejias E, *et al*: **Defective lysosomal proteolysis and axonal transport are early pathogenic events that worsen with age leading to increased APP metabolism and synaptic Abeta in transgenic APP/PS1 hippocampus.** *Mol Neurodegener* 2012, **7**:59.
17. Yu WH, Cuervo AM, Kumar A, Peterhoff CM, Schmidt SD, Lee JH, *et al*: **Macroautophagy–a novel beta-amyloid peptide-generating pathway activated in Alzheimer's disease.** *J Cell Biol* 2005, **171**:87–98.
18. Phiel CJ, Wilson CA, Lee VMY, Klein PS: **GSK-3[alpha] regulates production of Alzheimer's disease amyloid-[beta] peptides.** *Nature* 2003, **423**:435–439.
19. Su Y, Ryder J, Li B, Wu X, Solenberg P, Brune K, *et al*: **Lithium, a common drug for bipolar disorder treatment, regulates amyloid-beta precursor protein processing.** *Biochemistry* 2004, **43**:6899–6908.
20. Toledo EM, Inestrosa NC: **Activation of Wnt signaling by lithium and rosiglitazone reduced spatial memory impairment and neurodegeneration in brains of an APPswe/PSEN1DeltaE9 mouse model of Alzheimer's disease.** *Mol Psychiatry* 2009, **15**:272–285.
21. Feyt C, Kienlen-Campard P, Leroy K, N'Kuli F, Courtoy PJ, Brion JP, *et al*: **Lithium Chloride increases the production of Amyloid-beta Peptide independently from its inhibition of Glycogen Synthase Kinase 3.** *J Biol Chem* 2005, **280**:33220–33227.
22. Sudduth TL, Wilson JG, Everhart A, Colton CA, Wilcock DM: **Lithium treatment of APPSwDI/NOS2 (-/-) Mice Leads to Reduced Hyperphosphorylated Tau. Increased amyloid deposition and altered inflammatory phenotype.** *PLoS ONE* 2012, **7**:e31993.
23. Moreno-Gonzalez I, Baglietto-Vargas D, Sanchez-Varo R, Jimenez S, trujillo-estrada L, Sanchez-mejias E, *et al*: **Extracellular Amyloid-beta and Cytotoxic Glial Activation induce significant entorhinal neuron loss in young PS1M146L/APP751SLMice.** *J Alzheimers Dis* 2009, **18**:755–776.
24. Ramos B, Baglietto-Vargas D, Rio JC, Moreno-Gonzalez I, Santa-Maria C, Jimenez S, *et al*: **Early neuropathology of Somatostatin/NPY GABAergic cells in the hippocampus of a PS1 x APP transgenic model of Alzheimer's disease.** *Neurobiol Aging* 2006, **27**:1658–1672.
25. Chan-Palay V, Lang W, Allen YS, Haesler U, Polak JM: **Cortical neurons immunoreactive with antisera against neuropeptide Y are altered in Alzheimer's-type dementia.** *J Comp Neurol* 1985, **238**:390–400.
26. Davies P, Katzman R, Terry RD: **Reduced somatostatin-like immunoreactivity in cerebral cortex from cases of Alzheimer disease and Alzheimer senile dementa.** *Nature* 1980, **288**:279–280.
27. Blanchard V, Moussaoui S, Czech C, Touchet N, Bonici B, Planche M, *et al*: **Time sequence of maturation of dystrophic neurites associated with A [beta] deposits in APP/PS1 transgenic mice.** *ExpNeurol* 2003, **184**:247–263.
28. Filali M, Lalonde R, Theriault P, Julien C, Calon F, Planel E: **Cognitive and non-cognitive behaviors in the triple transgenic mouse model of Alzheimer's disease expressing mutated APP, PS1, and Mapt (3xTg-AD).** *Behav Brain Res* 2012, **234**:334–342.
29. Davis KE, Easton A, Eacott MJ, Gigg J: **Episodic-like memory for What-Where-Which occasion is selectively impaired in the 3xTgAD mouse model of Alzheimer's disease.** *J Alzheimer Dis* 2013, **33**:681–698.
30. Jimenez S, Baglietto-Vargas D, Caballero C, Moreno-Gonzalez I, Torres M, Sanchez-Varo R, *et al*: **Inflammatory response in the Hippocampus of PS1M146L/APP751SL mouse model of Alzheimer's disease: age-dependent switch in the microglial phenotype from alternative to classic.** *J Neurosci* 2008, **28**:11650–11661.
31. Jimenez S, Torres M, Vizuete M, Sanchez-Varo R, Sanchez-Mejias E, Trujillo-Estrada L, *et al*: **Age-dependent Accumulation of Soluble Amyloid beta (Abeta) Oligomers reverses the Neuroprotective Effect of Soluble Amyloid Precursor Protein alpha (sAPPalpha) by Modulating Phosphatidylinositol 3-Kinase (PI3K)/Akt-GSK-3beta Pathway in Alzheimer mouse model.** *J Biol Chem* 2011, **286**:18414–18425.
32. Araujo F, Tan S, Ruano D, Schoemaker H, Benavides J, Vitorica J: **Molecular and pharmacological characterization of native cortical gamma-aminobutyric acid(A) receptors containing both alpha(1) and alpha(3) subunits.** *J Biol Chem* 1998, **271**:27902–27911.
33. Cohen E, Paulsson JF, Blinder P, Burstyn-Cohen T, Du D, Estepa G, *et al*: **Reduced IGF-1 Signaling delays age-associated proteotoxicity in mice.** *Cell* 2009, **139**:1157–1169.
34. Koffie RM, Meyer-Luehmann M, Hashimoto T, Adams KW, Mielke ML, Garcia-Alloza M, *et al*: **Oligomeric amyloid-beta| associates with postsynaptic densities and correlates with excitatory synapse loss near senile plaques.** *Proc Natl Acad Sci USA* 2009, **106**:4012–4017.
35. Kraft AW, Hu X, Yoon H, Yan P, Xiao Q, Wang Y, *et al*: **Attenuating astrocyte activation accelerates plaque pathogenesis in APP/PS1 mice.** *FASEB J* 2013, **27**:187–198.
36. Ojha J, Masilamoni G, Dunlap D, Udoff RA, Cashikar AG: **Sequestration of Toxic Oligomers by HspB1 as a Cytoprotective Mechanism.** *Mol Cell Biol* 2011, **31**:3146–3157.
37. Yin KJ, Cirrito JR, Yan P, Hu X, Xiao Q, Pan X, *et al*: **Matrix Metalloproteinases expressed by astrocytes mediate extracellular Amyloid-beta peptide catabolism.** *J Neurosci* 2006, **26**:10939–10948.
38. Cascella R, Conti S, Tatini F, Evangelisti E, Scartabelli T, Casamenti F, *et al*: **Extracellular chaperones prevent Abeta-induced toxicity in rat brains.** *Biochim Biophys Acta - Molecular Basis of Disease* 1832, **2013**:1217–1226.
39. Hoshino T, Murao N, Namba T, Takehara M, Adachi H, Katsuno M, *et al*: **Suppression of Alzheimer's disease-related phenotypes by expression of heat shock protein 70 in mice.** *J Neurosci* 2011, **31**:5225–5234.
40. Mannini B, Cascella R, Zampagni M, Waarde-Verhagen M, Meehan S, Roodveldt C, *et al*: **Molecular mechanisms used by chaperones to reduce the toxicity of aberrant protein oligomers.** *Proc Natl Acad Sci USA* 2012, **109**:12479–12484.
41. Narayan P, Meehan S, Carver JA, Wilson MR, Dobson CM, Klenerman D: **Amyloid-beta Oligomers are Sequestered by both Intracellular and Extracellular Chaperones.** *Biochemistry* 2012, **51**:9270–9276.
42. Lee JH, Yu WH, Kumar A, Lee S, Mohan PS, Peterhoff CM, *et al*: **Lysosomal Proteolysis and Autophagy require Presenilin 1 and Are disrupted by Alzheimer-related PS1 mutations.** *Cell* 2010, **141**:1146–1158.
43. Yang DS, Stavrides P, Mohan PS, Kaushik S, Kumar A, Ohno M, *et al*: **Reversal of autophagy dysfunction in the TgCRND8 mouse model of**

Alzheimer's disease ameliorates amyloid pathologies and memory deficits. *Brain* 2011, 134:258–277.
44. J A, Wandosell F, Hernández F: **Role of glycogen synthase kinase-3 in Alzheimer's disease pathogenesis and glycogen synthase kinase-3 inhibitors.** *Expert Rev Neurotherapeutics* 2010, 10:703–710.
45. Heiseke A, Aguib Y, Riemer C, Baier M, Schätzl HM: **Lithium induces clearance of protease resistant prion protein in prion-infected cells by induction of autophagy.** *J Neurochem* 2009, 109:25–34.
46. Parr C, Carzaniga R, Gentleman SM, Van Leuven F, Walter J, Sastre M: **Glycogen Synthase Kinase 3 Inhibition Promotes Lysosomal Biogenesis and Autophagic Degradation of the Amyloid- + ¦ Precursor Protein.** *Mol Cell Biol* 2012, 32:4410–4418.
47. Kandalepas P, Sadleir K, Eimer W, Zhao J, Nicholson D, Vassar R: **Erratum to: The Alzheimer's beta-secretase BACE1 localizes to normal presynaptic terminals and to dystrophic presynaptic terminals surrounding amyloid plaques.** *Acta Neuropathol* 2013, 126:329–352.
48. Xie H, Hou S, Jiang J, Sekutowicz M, Kelly J, Bacskai BJ: **Rapid cell death is preceded by amyloid plaque-mediated oxidative stress.** *Proc Natl Acad Sci USA* 2013, 110:7904–7909.
49. Perez-Nievas BG, Stein TD, Tai HC, Dols-Icardo O, Scotton TC, Barroeta-Espar I, *et al*: **Dissecting phenotypic traits linked to human resilience to Alzheimer's pathology.** *Brain* 2013, 136:2510–2526.
50. Condello C, Schain A, Grutzendler J: **Multicolor time-stamp reveals the dynamics and toxicity of amyloid deposition.** *Sci Rep* 2011, 1:19.
51. Tomic JL, Pensalfini A, Head E, Glabe CG: **Soluble fibrillar oligomer levels are elevated in Alzheimer's disease brain and correlate with cognitive dysfunction.** *Neurobiol Disease* 2009, 35:352–358.
52. Renkawek K, Bosman G, de Jong W: **Expression of small heat-shock protein hsp 27 in reactive gliosis in Alzheimer disease and other types of dementia.** *Acta Neuropathol* 1994, 87:511–519.
53. Taylor AR, Robinson MB, Gifondorwa DJ, Tytell M, Milligan CE: **Regulation of heat shock protein 70 release in astrocytes: Role of signaling kinases.** *Devel Neurobiol* 2007, 67:1815–1829.

doi:10.1186/2051-5960-1-73
Cite this article as: Trujillo-Estrada *et al.*: In vivo modification of Abeta plaque toxicity as a novel neuroprotective lithium-mediated therapy for Alzheimer's disease pathology. *Acta Neuropathologica Communications* 2013 1:73.

RESUMEN III

A modo de resumen podemos decir que los principales hallazgos al respecto han sido:

1. La ingesta oral de forma crónica de Litio (de 3 a 9 meses) tratamiento iniciado antes de que se detecten las placas de Aβ, previene la mayoría de las manifestaciones neuropatológicas tempranas que presenta nuestro modelo transgénico:

    a. Previene de la pérdida neuronal observada en nuestro modelo tanto en el Hipocampo como de la corteza entorrinal.

    b. Reduce la fosforilación de Tau.

    c. Disminuye la formación de distrofias axonales.

    d. Mejora los problemas de comportamiento y memoria observados en el modelo bigénico.

2. Se observa un aumento en la compactación de las placas de Aβ y una bajada en el halo de oligómeros de Aβ que las rodea, esto podría hacerla menos tóxicas.

3. Esta mayor compactación de las placas podría estar mediada por la actuación del Litio sobre los astrocitos que potenciaría la liberación de Hsps (heat shock proteins).

Resultados: Capitulo IV.

PLOS | ONE

RESEARCH ARTICLE

Disruption of Amyloid Plaques Integrity Affects the Soluble Oligomers Content from Alzheimer Disease Brains

Sebastian Jimenez[1,2,4☯], **Victoria Navarro**[1,2,4☯], **Javier Moyano**[1,2,4], **María Sanchez-Mico**[1,2,4], **Manuel Torres**[1,2¤], **Jose Carlos Davila**[3,4], **Marisa Vizuete**[1,2,4], **Antonia Gutierrez**[3,4¶*], **Javier Vitorica**[1,2,4¶*]

1. Departamento Bioquímica y Biología Molecular, Facultad de Farmacia, Universidad de Sevilla, Sevilla, Spain, **2.** Instituto de Biomedicina de Sevilla (IBiS)-Hospital Universitario Virgen del Rocío/CSIC/Universidad de Sevilla, Sevilla, Spain, **3.** Departamento Biología Celular, Genética y Fisiología, Facultad de Ciencias, Instituto de Investigación Biomédica de Málaga (IBIMA), Universidad de Málaga, Málaga, Spain, **4.** Centro de Investigación Biomédica en Red sobre Enfermedades Neurodegenerativas (CIBERNED), Madrid, Spain

*vitorica@us.es (JV); agutierrez@uma.es (AG)

☯ These authors contributed equally to this work.

¶ AG and JV are co-senior authors on this work.

¤ Current address: Laboratory of Molecular Cell Biomedicine, University of Balearic Islands, Palma, Spain

OPEN ACCESS

Citation: Jimenez S, Navarro V, Moyano J, Sanchez-Mico M, Torres M, et al. (2014) Disruption of Amyloid Plaques Integrity Affects the Soluble Oligomers Content from Alzheimer Disease Brains. PLoS ONE 9(12): e114041. doi:10.1371/journal.pone.0114041

Editor: Ramon Trullas, IIBB/CSIC/IDIBAPS, Spain

Received: July 31, 2014

Accepted: November 3, 2014

Published: December 8, 2014

Data Availability: The authors confirm that all data underlying the findings are fully available without restriction. All relevant data are within the paper.

Funding: This work was supported by Fondo de Investigación Sanitaria (FIS), from Instituto de Salud Carlos III of Spain, through grants PI12/01431 (to AG) and PI12/01439 (to JV), by Junta de Andalucia (collaborative grant CTS-2035 to JV and AG), and by Centro de Investigacion Biomedica en Red Sobre Enfermedades Neurodegenerativas (CIBERNED) (collaborative grants PI2010/08 and PI2013/01 to JV and AG). The funders had no role in study design, data collection and analysis, decision to publish, or preparation of the manuscript.

Competing Interests: The authors confirm that the co-author Javier Vitorica is a PLOS ONE Editorial Board member. This does not alter the authors' adherence to PLOS ONE Editorial policies and criteria.

Abstract

The implication of soluble Abeta in the Alzheimer's disease (AD) pathology is currently accepted. In fact, the content of soluble extracellular Abeta species, such as monomeric and/or oligomeric Abeta, seems to correlate with the clinico-pathological dysfunction observed in AD patients. However, the nature (monomeric, dimeric or other oligomers), the relative abundance, and the origin (extra-/intraneuronal or plaque-associated), of these soluble species are actually under debate. In this work we have characterized the soluble (defined as soluble in Tris-buffered saline after ultracentrifugation) Abeta, obtained from hippocampal samples of Braak II, Braak III–IV and Braak V–VI patients. Although the content of both Abeta40 and Abeta42 peptides displayed significant increase with pathology progression, our results demonstrated the presence of low, pg/µg protein, amount of both peptides. This low content could explain the absence (or below detection limits) of soluble Abeta peptides detected by western blots or by immunoprecipitation-western blot analysis. These data were in clear contrast to those published recently by different groups. Aiming to explain the reasons that determine these substantial differences, we also investigated whether the initial homogenization could mobilize Abeta from plaques, using 12-month-old PS1xAPP cortical samples. Our data demonstrated that manual homogenization (using Dounce) preserved the integrity of Abeta plaques whereas strong homogenization

OBJETIVOS IV

Evaluación del contenido de Aβ en la fracción soluble en muestras post mortem de hipocampo de enfermos de EA y ratones transgénicos modelo de la enfermedad. Análisis de la posible repercusión, sobre el contenido de formas solubles de Aβ, del protocolo inicial de homogeneización del tejido usado en la preparación de las fracciones solubles S1. Estudio *in vitro* de estas fracciones S1 obtenidas mediante distintos protocolos de homogeneización.

a. Determinación de los niveles presentes en la fracción soluble de muestras de enfermos de EA obtenidas mediante procesos de homogeneización suaves.

b. Estudio del efecto del protocolo de homogeneización inicial del tejido sobre el contenido de las distintas especies de Aβ presentes en la fracción soluble S1.

c. Caracterización de la capacidad estimuladora y tóxica de las distintas fracciones solubles obtenidas usando diversos protocolos de homogenización sobre cultivos celulares in vitro.

Este trabajo se presenta como artículo.

PLOS | ONE

RESEARCH ARTICLE

Disruption of Amyloid Plaques Integrity Affects the Soluble Oligomers Content from Alzheimer Disease Brains

Sebastian Jimenez[1,2,4]◔, Victoria Navarro[1,2,4]◔, Javier Moyano[1,2,4], María Sanchez-Mico[1,2,4], Manuel Torres[1,2¤], Jose Carlos Davila[3,4], Marisa Vizuete[1,2,4], Antonia Gutierrez[3,4]¶*, Javier Vitorica[1,2,4]¶*

1. Departamento Bioquímica y Biología Molecular, Facultad de Farmacia, Universidad de Sevilla, Sevilla, Spain, **2.** Instituto de Biomedicina de Sevilla (IBiS)-Hospital Universitario Virgen del Rocío/CSIC/Universidad de Sevilla, Sevilla, Spain, **3.** Departamento Biología Celular, Genética y Fisiología, Facultad de Ciencias, Instituto de Investigación Biomédica de Málaga (IBIMA), Universidad de Málaga, Málaga, Spain, **4.** Centro de Investigación Biomédica en Red sobre Enfermedades Neurodegenerativas (CIBERNED), Madrid, Spain

*vitorica@us.es (JV); agutierrez@uma.es (AG)

◔ These authors contributed equally to this work.

¶ AG and JV are co-senior authors on this work.

¤ Current address: Laboratory of Molecular Cell Biomedicine, University of Balearic Islands, Palma, Spain

OPEN ACCESS

Citation: Jimenez S, Navarro V, Moyano J, Sanchez-Mico M, Torres M, et al. (2014) Disruption of Amyloid Plaques Integrity Affects the Soluble Oligomers Content from Alzheimer Disease Brains. PLoS ONE 9(12): e114041. doi:10.1371/journal.pone.0114041

Editor: Ramon Trullas, IIBB/CSIC/IDIBAPS, Spain

Received: July 31, 2014

Accepted: November 3, 2014

Published: December 8, 2014

Data Availability: The authors confirm that all data underlying the findings are fully available without restriction. All relevant data are within the paper.

Funding: This work was supported by Fondo de Investigación Sanitaria (FIS), from Instituto de Salud Carlos III of Spain, through grants PI12/01431 (to AG) and PI12/01439 (to JV), by Junta de Andalucia (collaborative grant CTS-2035 to JV and AG), and by Centro de Investigacion Biomedica en Red Sobre Enfermedades Neurodegenerativas (CIBERNED) (collaborative grants PI2010/08 and PI2013/01 to JV and AG). The funders had no role in study design, data collection and analysis, decision to publish, or preparation of the manuscript.

Competing Interests: The authors confirm that the co-author Javier Vitorica is a PLOS ONE Editorial Board member. This does not alter the authors' adherence to PLOS ONE Editorial policies and criteria.

Abstract

The implication of soluble Abeta in the Alzheimer's disease (AD) pathology is currently accepted. In fact, the content of soluble extracellular Abeta species, such as monomeric and/or oligomeric Abeta, seems to correlate with the clinico-pathological dysfunction observed in AD patients. However, the nature (monomeric, dimeric or other oligomers), the relative abundance, and the origin (extra-/intraneuronal or plaque-associated), of these soluble species are actually under debate. In this work we have characterized the soluble (defined as soluble in Tris-buffered saline after ultracentrifugation) Abeta, obtained from hippocampal samples of Braak II, Braak III–IV and Braak V–VI patients. Although the content of both Abeta40 and Abeta42 peptides displayed significant increase with pathology progression, our results demonstrated the presence of low, pg/μg protein, amount of both peptides. This low content could explain the absence (or below detection limits) of soluble Abeta peptides detected by western blots or by immunoprecipitation-western blot analysis. These data were in clear contrast to those published recently by different groups. Aiming to explain the reasons that determine these substantial differences, we also investigated whether the initial homogenization could mobilize Abeta from plaques, using 12-month-old PS1xAPP cortical samples. Our data demonstrated that manual homogenization (using Dounce) preserved the integrity of Abeta plaques whereas strong homogenization

procedures (such as sonication) produced a vast redistribution of the Abeta species in all soluble and insoluble fractions. This artifact could explain the dissimilar and somehow controversial data between different groups analyzing human AD samples.

Introduction

Progressive aggregation and accumulation of extracellular amyloid-β (Abeta) peptides is central to Alzheimer's disease (AD) pathogenesis [6]. Multiple Abeta oligomers, ranging from low-molecular weight oligomers to protofibrils and fibrils, apparently coexist in the brain tissue. However, the exact nature of these toxic aggregated Abeta peptides and their origin (intra- or extraneuronal or even plaque-derived) remains speculative. After the initial investigation by Podlisny et al. [15], a growing number of evidences strongly indicate that soluble Abeta forms, rather than insoluble species, including amyloid plaques, are the main toxic species associated with AD (see [1] and [5], for recent reviews). Subsequent studies by different independent groups, in an attempt to identify the precise soluble form that best correlated with cognitive impairment, have in fact reported a remarkable diversity of soluble aggregates in the interstitial fluid of human AD and transgenic model brains. Based on *in vitro*, using synthetic Abeta peptides, or "*in vivo*" experiments, different soluble Abeta oligomers, ranging from dimers to high-molecular weight aggregates (such as 12-mer, 24-mer, 32-mer, 150-mer) have been identified as the putative neurotoxic agents, disturbing the neurotransmission and causing neuronal death (see table 1 from [1]). The reasons for this apparent heterogeneity are not known but could derive from the different aggregation protocols of synthetic Abeta (for instance see [2] and [11]), the different transgenic models used or the different brain regions characterized. In this sense, it is particularly intriguing the quantitative and qualitative differences between soluble Abeta isolated by microdialysis and by homogenization-centrifugation approaches, reported even by the same group [24].

Perhaps more relevant is the fact that, using brain samples from Alzheimer patients, a great disparity in the nature and quantities of soluble Abeta has been observed. For instance, relatively large amounts of monomeric and dimeric soluble Abeta (identified by western blots) have been reported by some groups [3, 12, 13, 17, 23, 24] whereas others found small amounts (pg range, detected by dot blots or sensitive oligomeric specific ELISA assays) of soluble Abeta [4, 21]. Among multiple causes, these differences between groups could reflect the absence of a unified isolation protocol for the extraction and characterization of soluble Abeta. In fact, many different homogenization (from manual to sonication) and centrifugation protocols have been used to isolate a theoretically similar extracellular soluble fraction. Considering that Abeta plaques constitute a large reservoir of different Abeta species, and that their number increased with the

Table 1. Human samples.

mean Age ± SD	Sex	Delay post-mortem mean h ± SD	BRAAK
84.0±5.47	7 male - 4 female	6.2±4.5	II
78.1±11.99	4 male - 3 female	5.76±5.44	III–IV
80.4±10.21	4 male - 8 female	11.2±4.0	V–VI

doi:10.1371/journal.pone.0114041.t001

pathology, strong homogenization protocols could indeed disturb the stability of plaques, and cause the release of different Abeta species. However, few (if any) control experiments were carried out to determine the extent of plaque disruption due to the isolation procedure.

In the present study, we analysed the Abeta content in the soluble fractions of the hippocampus from human AD autopsy samples and transgenic models in order to investigate the possible repercussion of the homogenization protocols in the soluble fraction preparation. For that, we have directly compared the effect of homogenization using gentle conditions with sonication at different intensities. We concluded that strong homogenization, such as sonication, produced the release of Abeta peptides from Abeta plaques to soluble fractions.

Materials and Methods

Antibodies

82E1 and anti-soluble APPalpha antibodies were purchased from Immuno Biological Laboratories (IBL). 6E10 antibody was provided by Signet Laboratories. Anti-LC3B and anti-ATP synthase-beta were purchased from Cell Signaling Laboratories and BD Transduction Laboratories, respectively. Anti-mouse or anti-rabbit horseradish-peroxidase-conjugated secondary antibodies were purchased from Dako Denmark.

Human samples

The study was performed using 30 cases obtained from the BTIN-Tissue Bank for Neurological Research (Madrid, Spain) and from the Neurological Tissue Bank of IDIBELL-Hospital of Bellvitge (Barcelona, Spain), approved by the committee for human and animal use for research at Seville and Malaga Universities, Spain. The cases were scored for Braak stage for neurofibrillary tangles (II–VI). In Table 1 are detailed the age, Braak stage, sex and the delay post-mortem before the extraction of the samples.

Preparation of human brain lysates

Soluble (S1) fractions were prepared as described previously [9, 10, 19, 22]. Briefly, frozen human hippocampal tissue was homogenized (1/5 w/v) using a manual Dounce homogenizer (10 strokes using pestle A (large clearance:

0.114 ± 0.025 mm) and 10 strokes using pestle B (small clearance: 0.05 ± 0.025 mm), in Tris-buffered saline (TBS; 20 mM Tris-HCl, 140 mM NaCl, pH 7.5) containing protease and phosphatase inhibitors (Roche). Homogenates were then ultracentrifuged (4℃ during 60 min) at 100,000 × g (TLA110 rotor, Optima MAX Preparative Ultracentrifuge, Beckman Coulter). The supernatant, which constitutes the S1 fractions, was collected, aliquoted and stored at −80℃ for further use. The remaining pellet (P1) was stored at −80℃ until needed.

Sequential protein extraction

For sequential extraction experiments, the P1 fraction was first resuspended (by Dounce homogenization; 10 strokes using pestle B) in RIPA buffer (1% CHAPS, 1% deoxycholate, 0.2% SDS, 140 mM NaCl, 10 mM Tris-HCl, pH 7.4, containing protease and phosphatase inhibitors), incubated for 30 min at 4℃ with agitation, and centrifuged at 30,000 × g for 30 min at 4℃. The supernatant constituted the S2 fraction. The pellet from this centrifugation was sequentially extracted (by incubating during 30 min, 4℃ followed by centrifugation 30,000 × g for 30 min) using buffered-SDS 2% (2% SDS in 20 mM Tris-HCl, pH 7.4, 140 mM NaCl) (S3 fraction) and 4% SDS plus 8 M urea (P3 fraction). All isolated fractions were aliquoted and stored at −80℃ until use.

Abeta quantification by sandwich ELISA

The amount of soluble Abetax-40 or Abetax-42 peptides was determined in human soluble S1 fractions, using commercial sandwich ELISA (Human Abx-40 ELISA Kit, Invitrogen; Amyloid beta x-42 ELISA, DRG) following the manufacturer recommendations. For these experiments equivalent amount of proteins, from the different S1 fractions isolated from Braak II to Braak V–VI samples, were pooled. For each assay, 25 μg of protein from the pooled-soluble fractions was used. The ELISA experiments were repeated four times, in independent experiments, using duplicate or triplicate replicas.

For oligomeric ELISA, we used 6E10-6E10 antibody pairs in conjunction with the Alpha-Lisa technology, developed by Perkin Elmer. This assay recognized synthetic Abeta dimer, used as standards, whereas synthetic monomeric Abeta42 produced no signal over the background. The lower limit sensitivity of this assay was 0.02 pg/μl.

Preparation of PS1delta9xAPPswe cortical fractions

All animal experiments were performed in accordance with the guidelines of the Committee of Animal Research of the University of Seville (Spain), University of Malaga (Spain) and the European Union Regulations.

B6.Cg-Tg(APPswe,PSEN1dE9)85Dbo/J (PS1xAPP) transgenic model was maintained in C57BL/6 genetic background for several generations (F10). Cortical samples from 12 months PS1xAPP transgenic mice were homogenized in TBS (1/10 w/v) containing protease and phosphatase inhibitor-cocktail (Roche), using

PLOS | ONE

two different approaches: a) manual Dounce homogenizer (10 strokes with pestle A and 10 strokes with pestle B) or b) sonication (100 W ultrasonic processor UP100 H, Hielscher) for x4 or x8, 15 sec pulses at 4℃.

After homogenization, the different fractions were isolated as described in [17]. Briefly, homogenates were first centrifuged at 14,000 × g (30 min, 4℃). The supernatant (containing soluble and microsomal fraction) was then ultracentrifuged at 100,000 × g (60 min, 4℃) using a TLA110 rotor (Optima MAX Preparative Ultracentrifuge, Beckman Coulter). The supernatant of this ultracentrifugation constituted the TBS soluble fraction. The pellet, that constituted the microsomal fraction, was resuspended in TBS.

On the other hand, pellets from the first centrifugation (membranes plus Abeta plaques) were sequentially solubilized using 2% buffered-SDS followed by SDS-Urea (4% SDS plus 8 M urea).

PS1xAPP sequential protein extraction

For these experiments, 12-month-old PS1xAPP cortical tissue was used. The TBS soluble fraction was isolated by ultracentrifugation as described above. For the sequential detergent-based extraction, the ultracentrifugation pellets were sequentially extracted using 2% CHAPS (in TBS), RIPA buffer, 2% SDS and finally 4% SDS-8 M urea. For each detergent treatment pellets were resuspended in the appropriate media, incubated for 30 min at 4℃ and centrifuged at 30,000 × g (30 min, 4℃). All fractions were stored at −80℃ for further use.

Western blots

Western blots were performed as described previously [9, 10, 19, 22]. Briefly, for Abeta peptides, 10–20 μg (unless stated in text) of protein from the different samples were loaded on 16% SDS-Tris-Tricine-PAGE and transferred to PVDF (Immobilon-P Transfer Membrane, Millipore). For sAPPalpha, LC3 and ATPsynthase, 12% SDS-Tris-Glicine-PAGE was used and transferred to nitrocellulose (Optitran, GE Healthcare Life Sciences).

Membranes were then blocked using 2% low-fat milk in TPBS (0.1% Tween-20, 137 mM NaCl, 2.7 mM KCl, 10 mM phosphate buffer, pH 7.4) and incubated overnight, at 4℃, with the appropriate antibody. The membranes were then incubated with anti-mouse or anti-rabbit horseradish-peroxidase-conjugated secondary antibody (Dako) at a dilution of 1/10,000. The blots were developed using the Pierce ECL 2 Western Blotting Substrate detection method (0.5 pg, lower limit sensitivity; Thermo Scientific). The images were obtained with the luminescent image analyzer Image Quant LAS4000 mini (GE Healthcare Life Sciences) and then analyzed using PCBAS program.

RNA extraction, retrotranscription and real-time RT-PCR

Total RNA was extracted from cells (line N13) using Tripure Isolation Reagent (Roche). After isolation the RNA integrity was determined, by agarose gel

PLOS | ONE

electrophoresis, resulting comparable in all samples. Total RNA was determined by spectrophotometric measures.

Retrotranscription (RT) was performed using 4 μg of total RNA as template and High-Capacity cDNA Archive Kit (Ref.4368813, Applied Biosystems) following the manufacturer recommendations. For real time RT-PCR, 40 ng of cDNA were mixed with 2x Taqman Universal Master Mix (Ref.4369016, Applied Biosystems) and 20x Taqman Gene Expression assay probes (TNFalpha, Mm00443258_m1; IL1beta, Mm00434228_m1; IL6 Mm00446190_m1; GAPDH, Mm99999915_g1; 18s, Mm03928990; beta-actin, Mm00607939_s1; Applied Biosystems). PCR reactions were carried out in 96 well plates using either ABI Prism 7000 or 7900HT sequence detector systems (Applied Biosystems). The RT-PCR conditions included two initial steps of 2 min at 50℃ to activate the polymerase followed by 10 min at 95℃, and the subsequent 40 cycles of denaturation (95℃, 15 sec) and annealing (60℃, 1 min). The cDNA levels of the different samples were determined using GAPDH as housekeeper. Similar results were obtained using beta-actin or 18s rRNA (not shown). The amplification of the housekeeper was done in parallel with the gene to be analyzed, showing a similar amount of cDNA in all tested samples. All our data are expressed as the mean of at least three different measures [9], [10], [19], [22].

Amyloid plaque isolation

Beta-amyloid plaques were isolated as described [18]. PS1xAPP (12 months of age) cortical samples were homogenized using Dounce as above and centrifuged at 2,000 × g for 30 min (4℃). The supernatant was further centrifuged for 1 hour at 20,000 × g to collect the pellet, enriched in amyloid beta plaques. This pellet was resuspended in PBS, layered over a discontinuous sucrose gradient (0.4 ml of 1.0 M; 0.4 ml of 1.2, 0.8 ml of 1.4 and 0.4 ml of 2.0 M sucrose in PBS, pH 7.4) and centrifuged at 100,000 × g (Optima MAX Preparative Ultracentrifuge, Beckman Coulter) for 1 h at 4℃ using a TLS-55 swing rotor. Then, fractions (from top) were removed and the 1.4–2.0 M sucrose interphase (enriched in amyloid plaques) was collected and diluted in PBS. The enriched amyloid fraction was centrifuged at 100,000 × g for 1 h at 4℃, and the pellet was collected and resuspended in PBS pH 7.4. The sample was separated in two aliquots, one was Dounce homogenated and the other one was subjected to sonication (8 pulses of 15 seconds). The two samples were centrifuged at 100,000 × g for 1 h at 4℃, and the supernatant and pellet were collected.

N2a cultures and cell survival

N2a cells were plated at 25,000 cells/cm2 and cultured in high glucose DMEM (Biowest)/OptiMEM (Gibco) (50–50%) supplemented with 2 mM glutamine (Biowest) and 5% (v/v) foetal bovine serum (Biowest) in the presence of penicillin (Biowest) and streptomycin (Biowest) (100 units/ml and 0.01 mg/ml, respectively) at 37℃ and 5% CO2. For survival experiments, the medium was changed

to high glucose DMEM and serum-deprived. The cells were then treated with different amounts of TBS fractions, from Dounce or sonication homogenization, during 24 hours. The cells survival was assayed by Flow Cytometry using the apoptosis detection kit ANNEXIN V-FITC (Immunostep).

N13 culture and stimulation

The N13 microglial cells were plated at 15,000 cells/cm2 and cultured in RPMI 1640 (Biowest) supplemented with 2 mM glutamine (Biowest) and 5% (v/v) foetal bovine serum (Biowest), in the presence of 100 U/ml penicillin and 100 µg/ml streptomycin (Biowest) at 37℃ and 5% CO2. Cells were treated with different amounts of TBS soluble fractions, from Dounce or sonication, during 3 hours. Then, they were collected to isolate RNA. As controls, N13 cells were treated with equivalent volume of PBS.

Statistical analysis

Normality of data was first assessed by using Kolmogorov-Smirnov test. Normally distributed data were expressed and represented as mean ± SD. For normally distributed data, means were compared using ANOVA followed by Tukey test (more than two groups) or t-test (for two group comparisons).

Results

Low content of soluble Abeta oligomeric in AD patients hippocampal formation

We have first analyzed the Abeta content of soluble fractions prepared from the hippocampal formation (hippocampus proper, subiculum and entorhinal cortex), using Dounce homogenization and ultracentrifugation (see also [9, 10, 19, 22]), of AD (Braak stage V–VI) and non-demented control (Braak stages II to IV) age-matched autopsy samples.

Quantitative analysis, using Abetax-42 or Abetax-40 sandwich ELISA (Fig. 1A), demonstrated the presence of very small amounts (pg/µg of protein) of soluble Abeta40-42 peptides in both AD and non-AD samples (see also [4] and [24]). In fact, Braak II samples displayed low levels of Abeta40 whereas Abeta42 was practically undetectable. As shown (Fig. 1A, a1 and a2), we observed a gradual and significant increase in both soluble species, Abeta42 and Abeta40, although more pronounced in the Abeta42 peptide, along the disease progression (3.1-fold in Braak III–IV and 12.5-fold in Braak V–VI). In consequence, the soluble Abeta42 peptide became equimolar with Abeta40 in demented patients (Fig. 1A, a3). Using the Abeta40 plus Abeta42 peptide to estimate the total soluble Abeta species, our soluble samples from AD brains contained approx 4 ng/g tissue of soluble Abeta40-42 peptides. This value was clearly lower to that reported by others [13].

PLOS ONE | Soluble Abeta Peptides in AD Brain

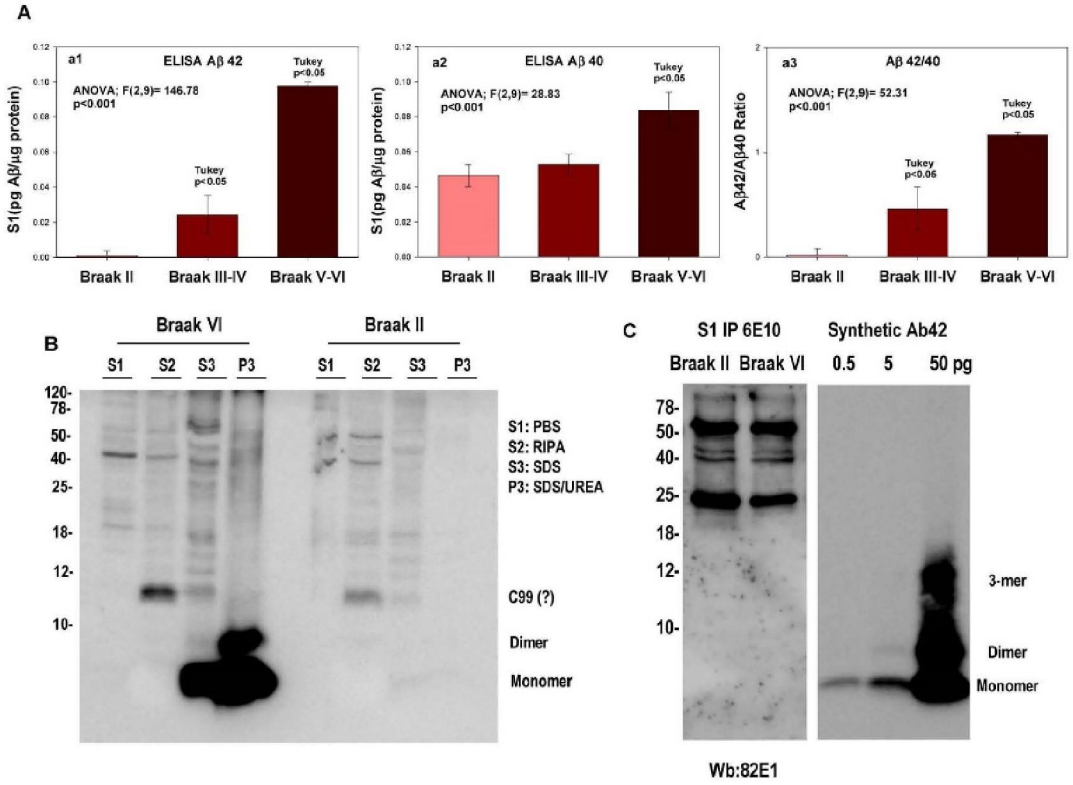

Figure 1. Low soluble Abeta levels were identified in hippocampal samples from age-matched controls (Braak II and III–IV) and demented patients (Braak V–VI). A: Soluble fractions from 11 Braak II, 7 Braak III–IV or 12 Braak V–VI samples were pooled and the Abeta x-42(a1) or x-40(a2) quantified by sandwich ELISA. Each assay was repeated 4 times in triplicate replicas (n=4 per Braak stage). Although the level of Abeta species from all samples was low (pg/µg protein), there was a significant (showed in the figure) increased in Abetax-42 and Abetax-40 in Braak V–VI. In consequence, there was also an increase in Abeta42/40 ratio (a3) from Braak II to Braak V–VI. B: Western blots of soluble (S1) or detergent-based extracted proteins showed the absence, or below detection limits, of Abeta monomers or oligomers in soluble fractions. Hippocampal samples from Braak VI or Braak II individuals were sequentially extracted in parallel. No Abeta bands were detected in S1 or CHAPS fractions. Monomeric, dimeric and other oligomeric species were clearly identified in 2% SDS and 4% SDS/8M urea samples. C: (left panel) One hundred micrograms of proteins from pooled soluble (S1) Braak II or Braak V–VI fractions were subjected to immunoprecipitation using 6E10 antibody. The immunopellets were analyzed by western blots using 6E10 (not shown) or 82E1. No specific bands, by comparison between Braak II and V–VI, were observed. Control experiments (right panel) demonstrated that 0.5 pg of synthetic Abeta42 could clearly be observed by our western blot system.

doi:10.1371/journal.pone.0114041.g001

We next attempted to characterize the Abeta species using western blots. Importantly, neither monomeric/dimeric Abeta nor other oligomeric Abeta species could be detected in soluble (S1, Fig. 1B) or in vesiculated (S2, Fig. 1B) Braak VI fractions, as compared with Braak II samples. However, the monomeric-dimeric Abeta (and probably other oligomeric forms) were clearly visible when Abeta plaques were solubilized using 2% SDS (S3) and especially using 4% SDS/8M urea (P3) (Fig. 1B). Furthermore, even using a large amount of proteins (100 µg of soluble fraction, S1) in 6E10 immunoprecipitation assays (Fig. 1C), we were unable to detect any distinctive Abeta specie in Braak V–VI, compared with Braak II.

Taken together, these data are consistent with the existence of low levels of soluble Abeta (pg levels), and the virtual absence of monomeric Abeta in the

PLOS | ONE

soluble fraction of AD samples. We cannot discard the presence of minute amounts of monomeric Abeta (below the detection limits of our western blots, 0.5 pg, see Fig. 1C) or small quantities of oligomeric Abeta, not detected by our assays. In any case, these data are in clear contrast with those reported recently [13, 14, 16, 17, 23].

The homogenization procedure largely determined the content of Abeta species in the soluble fraction

While multiple reasons could explain the different levels of soluble Abeta reported in human AD samples, the initial homogenization of the tissue could be crucial to maintain the integrity of the Abeta plaques. A strong (aggressive) treatment of the tissue could disrupt the aggregated Abeta from plaques and, in consequence, contaminate all fractions with artifactual, plaque-derived, soluble Abeta species. To evaluate this possibility, we have directly compared the effect of homogenization using manual Dounce (see Methods) with sonication at different intensities. As a natural rich source of human Abeta, we have used 12 month-old cerebral cortex from PS1xAPP double transgenic mice. At this age, this model displayed the presence of abundant Abeta plaques in the cerebral cortex (not shown).

After homogenization, the TBS soluble fraction (equivalent to S1, see above) and the microsomal (equivalent to the dispersible fraction reported by [16, 17]) fractions were isolated by ultracentrifugation (see Methods). The Abeta from plaques were then extracted by sequential solubilization using 2% SDS and 4% SDS plus 8 M urea (following [16, 17] protocol). As expected from our previous work [10, 19, 22] (see Fig. 2A), the monomeric and oligomeric Abeta were preferentially observed in membrane/plaque associated fractions, extracted with 2% SDS and 4% SDS/8M urea. These fractions released a relatively large amount of monomers, dimers and other oligomeric Abeta species. However, as also reported previously [10, 19, 22], in 6–12 months old PS1xAPP mice, these species were absent (or below the detection limit of our western blots) in the TBS soluble fraction or in the microsomal fraction (see Fig. 2A). The lack of oligomeric Abeta in the TBS fraction was also probed by using a 6E10-6E10 oligomeric ELISA (AlphaLisa, Perkin Elmer) assay (Fig. 2B). On the contrary, when the same cortical tissue was subjected to sonication, a pulse-dependent redistribution of Abeta in all soluble fractions was observed. As shown, the TBS soluble fraction was contaminated with relatively high levels of monomeric Abeta (Fig. 2A). Furthermore, we also observed the presence of different putative Abeta oligomers, such as dimers, trimers, and low molecular weight-Abeta in these contaminated soluble fractions (the presence of such oligomers was really high after 8 pulses of sonication, see Fig. 2A). These Abeta oligomers were also clearly detected by 6E10-6E10 oligomeric Abeta ELISA (Fig. 2B). Similarly, the microsomal fractions were also highly contaminated with different Abeta species. Concomitantly, we also observed a decrease in the Abeta content from plaque rich fractions (2% SDS and 4% SDS/8M urea extracted pellets). Therefore, sonication (even using low

PLOS | ONE

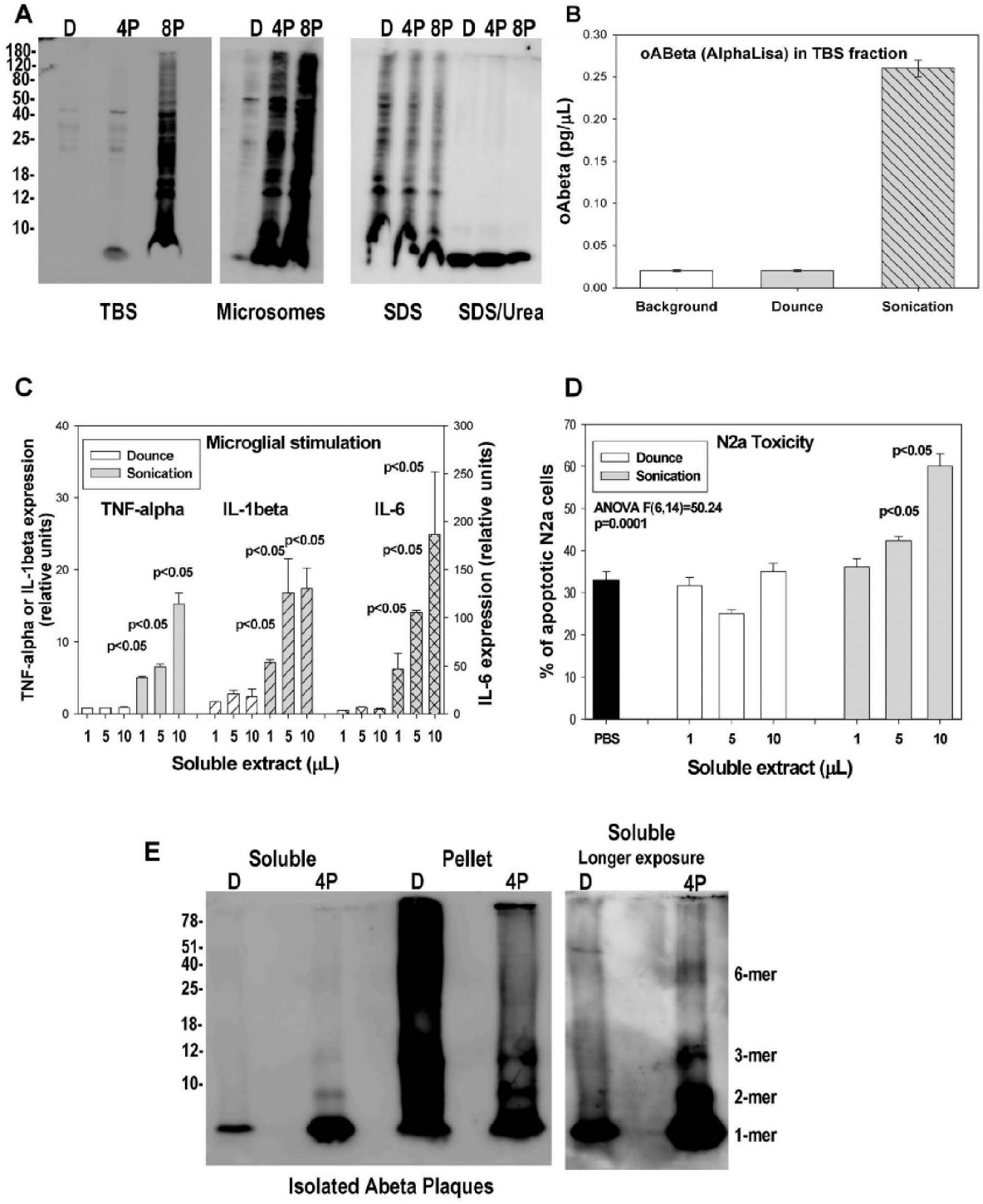

Figure 2. The homogenization procedure has high impact on the integrity of Abeta plaques with the consequent solubilization and redistribution of Abeta in different fractions. A: Western blots, using 82E1, demonstrated the redistribution of monomeric/oligomeric Abeta species in soluble TBS or microsomal fractions (left and middle panel) after homogenization using 4 (4P) or 8 (8P) pulses of sonication (100 watts) as compared with Dounce. This

increment was paralleled by a decrease on the Abeta content from 2% SDS or 4% SDS/8M urea extracted samples (right panel). This experiment was repeated four times with similar results. B: The oligomeric Abeta content of TBS soluble fractions was also assayed using an oligomeric (6E10-6E10) specific ELISA assay. No oligomeric Abeta was detected in Dounce prepared TBS fractions, whereas 0.28±0.01 pg/μl of Abeta was detected after sonication of the same cortical tissue. C–D: In vitro experiments demonstrating the stimulation of microglial cultures (C) or the toxic effect (D) of TBS soluble fractions prepared by either Dounce or sonication. A clear dose-dependent stimulation of N13 cells (C) or increase in apoptotic N2a cells (D) was observed exclusively on sonicated samples. E: Sonication could release Abeta from isolated Abeta plaques. Isolated Abeta plaques were homogenized by either Dounce or sonication (4 pulses) and the soluble Abeta release, after ultracentrifugation, was assayed by western blots. As shown, sonication solubilized and released predominantly monomeric and dimeric Abeta. After longer exposures (right panel), other Abeta oligomers, such as trimers or hexamers, could be also identified.

doi:10.1371/journal.pone.0114041.g002

doses) produced the redistribution of Abeta species from plaques to more soluble fractions.

Since the oligomeric Abeta could act as either, a pro-inflammatory agent, activating microglial cells and producing a classic immunological response [9], or as a cytotoxic agent, producing cell death [10], we next evaluated whether the redistribution of soluble Abeta species, due to the homogenization procedure, was also able to modify the stimulatory and toxic properties of the soluble TBS fractions. As shown in Fig. 2C, different amounts of Dounce-derived soluble fractions induced absolutely no microglial response, as determined by the expression of TNF-alpha, IL-6 and IL-1beta. However, stimulation with the TBS soluble fraction after sonication (4 pulses) produced strong microglial activation, characterized by the induction of the expression of all classic factors assayed. Furthermore, we have also tested the toxicity of the soluble fractions using N2a cells. As expected from previous work [9], the Dounce-derived TBS fraction from 12 month-old PS1xAPP produced no toxicity to N2a cells, whereas sonication-derived fractions produced a clear toxic effect (Fig. 2D).

It could be argued that sonication was indeed releasing highly compartmentalized Abeta, rather than mobilizing Abeta from plaques. Thus, we next directly tested the effect of sonication on isolated Abeta plaques. For these experiments, plaques were isolated by ultracentrifugation on sucrose gradients and homogenized by Dounce or sonication. As shown, mild (Dounce) homogenization released a limited amount of monomeric Abeta from plaques (<1% from total). However, sonication disrupted the Abeta plaques producing (after centrifugation) soluble monomers and, in minor extent, dimeric, trimeric and hexameric Abeta (see Fig. 2E, longer exposure). It is noteworthy the presence of high levels of Abeta oligomers after 4% SDS/8M urea extraction of intact plaques. However, these oligomers were drastically reduced after sonication. Thus, sonication seemed to induce the disaggregation and solubilization of highly aggregated Abeta from plaques. Taken together, these data demonstrated that the homogenization procedure was critical to maintain the integrity of Abeta plaques, and to avoid the contamination of the different fractions with soluble Abeta species.

Next, we evaluated our isolation protocol using (in addition to anti-Abeta) anti-soluble APPalpha antibody (as a marker of the extracellular compartment), anti-ATPsynthase Beta (mitochondria), LC3-I (cytosol) and LC3-II (as marker for autophagic vesicles). First, we determined the distribution of APP-derived soluble peptides (sAPPalpha and Abeta) after serial ultracentrifugation and detergent-

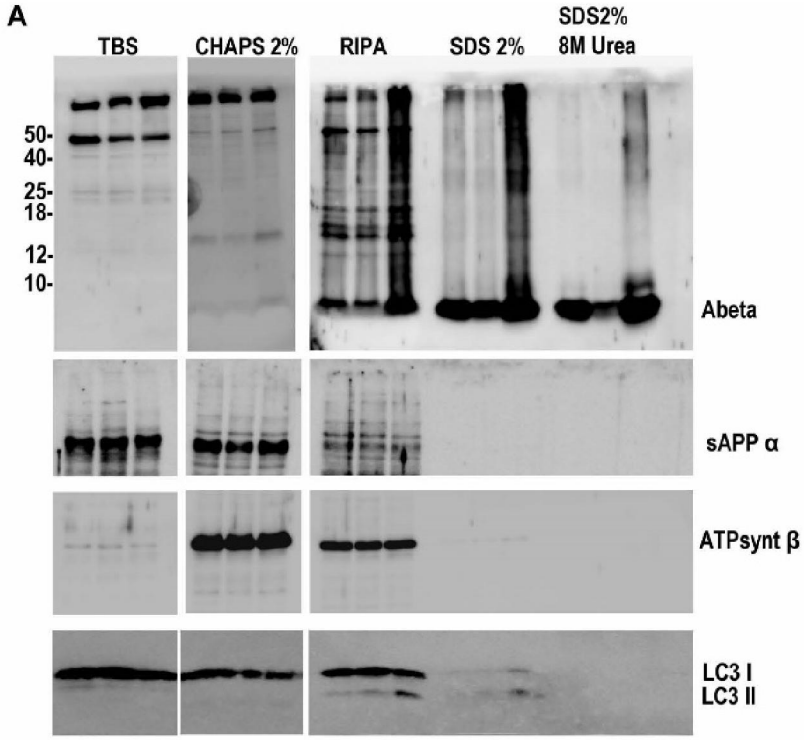
A
TBS
CHAPS 2%
RIPA
SDS 2%
SDS2%
8M Urea
50-
40-
25-
18-
12-
10-
Abeta
sAPP α
ATPsynt β
LC3 I
LC3 II

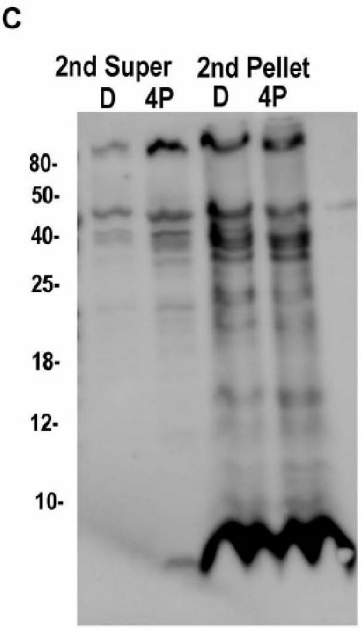
C
2nd Super
2nd Pellet
D
4P
D
4P
80-
50-
40-
25-
18-
12-
10-

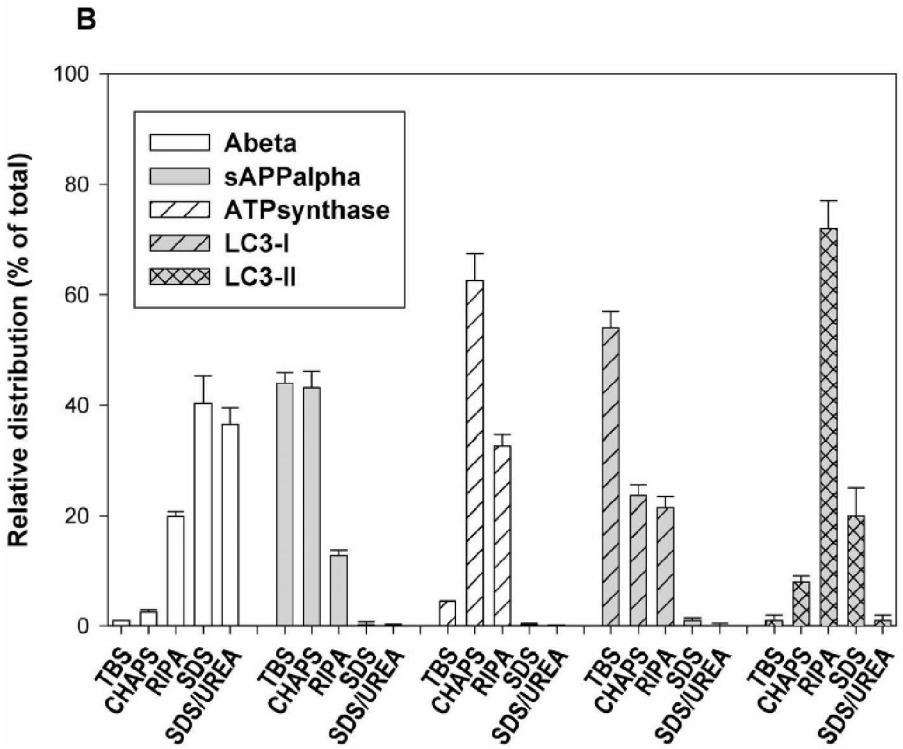
B
Relative distribution (% of total)
100
80
60
40
20
0
Abeta
sAPPalpha
ATPsynthase
LC3-I
LC3-II
TBS
CHAPS
RIPA
SDS
SDS/UREA

Figure 3. A–B: Biochemical analysis of the Dounce-derived soluble fractions. The presence of APP derived fragments, such as Abeta (6E10) and soluble APPalpha (extracellular), together with LC3-I (cytosolic), ATPsynthase-beta (mitochondrial) and LC3-II (autophagic vesicles) was tested by western blots. A representative western blot (A) or quantitative analysis of three experiments (B) is shown. Although contaminated with cytosolic proteins (LC3-I), the TBS soluble fraction was enriched in extracellular soluble APP-alpha and lacked monomeric Abeta. The monomeric Abeta was predominantly concentrated in vesiculated, LC3-II positive, and plaque associated fractions. **C: Dounce homogenization preserved the integrity of Abeta plaques.** After a first homogenization and centrifugation, pellets containing Abeta plaques were re-homogenized using Dounce or sonication (4 pulses) and the soluble Abeta content assayed using western blots and 6E10. Monomeric Abeta was exclusively observed after sonication.

doi:10.1371/journal.pone.0114041.g003

based extraction. As expected from previous data, the TBS soluble fraction was enriched on soluble APPalpha and no Abeta was detected (see Fig. 3A and B for quantification). However, this TBS-soluble fraction seemed to be contaminated with cytosolic proteins (detected using LC3-I) and presented low mitochondrial contamination (ATPsynthase). On the other hand, the Abeta species were principally accumulated into the intracellular, vesiculated, LC3-II positive fraction (probably autophagic vesicles, extracted after RIPA treatment) and in plaque enriched fractions (2% SDS and 4% SDS/8M urea releasable fraction). Thus, these data demonstrated that the TBS soluble fractions contained extracellular and cytosolic proteins with low contamination of Abeta plaques.

We have also evaluated to which extent our approach, Dounce homogenization, could release the plaque-associated Abeta from tissue. For this experiment, PS1xAPP cortical samples (12 months of age) were first homogenized, using Dounce, and ultracentrifuged in order to eliminate all putative soluble Abeta. The remaining pellets (containing plaques) were subjected to a second round of homogenization using either Dounce or sonication. Theoretically, all soluble Abeta species release from this second homogenization should derive from intracellular vesicles and/or Abeta plaques. As shown in Fig. 3C, Dounce homogenization did not produce the release of monomeric Abeta whereas monomeric, dimeric and probably trimeric Abeta were clearly observed after sonication of the samples.

Discussion

In this work, we demonstrate that different conditions of sample homogenization profoundly affect the Abeta content in the soluble fractions, probably by inducing artefactual mobilization of Abeta species from Abeta plaques. We show that using a mild homogenization protocol (manual Dounce), which is the routine procedure in our lab, the soluble fractions from both AD brain samples and PS1xAPP mouse brain tissue contain very small amounts of oligomeric Abeta. In contrast, when using stronger homogenization methods, such as sonication, large amounts of Abeta oligomers were found in the soluble fractions.

We first characterized the soluble Abeta content in hippocampal samples obtained from age-matched non-demented (Braak II, III and IV) and demented (Braak V and VI) human autopsies. The soluble fractions were prepared using mild homogenization conditions, followed by ultracentrifugation, as reported previously [9, 10, 19, 22]. Our data demonstrated the presence of limited amounts

of Abeta (pg/μg protein) in the soluble fractions, although we were unable to identify the nature of the Abeta peptides by either western blots or in immunoprecipitation assays using 6E10 or OC (not shown) antibodies. Overall, these data are similar to those reported by some authors [21, 4], but differ from many others reporting the presence of large amounts of different soluble Abeta species, specially in human AD samples [3, 13, 14, 16, 17, 24, 23].

These differences could derive, at least in part, from the different brain regions analyzed and the relative abundance of diffuse versus neuritic Abeta plaques (hippocampal formation with low or non diffuse plaques, unpublished results, versus different cortical areas with relatively high proportion of diffuse plaques; see [13]). However, these conflicting observations could also derive from the different protocols used in the soluble fraction preparation. This observation prompted us to investigate the possible effect of the homogenization protocol in the preparation of soluble fractions and plaque integrity. For this purpose, we directly compared two approaches broadly used for homogenization and isolation of soluble Abeta species, manual Dounce homogenization [9, 4, 21] versus sonication [17, 16]. Using 12-month-old PS1xAPP cortical samples as a source of abundant Abeta plaques, we demonstrate that Dounce homogenization mostly preserves the integrity of Abeta plaques and, in consequence, minimizes the level of contaminating Abeta in soluble fractions, whereas sonication (and probably other strong homogenization approaches) mechanically disrupts Abeta plaques, determining a redistribution of monomeric/oligormeric Abeta in all fractions analyzed. It is particularly relevant the presence of large amounts of Abeta in the soluble TBS fraction and in the microsomal fractions. These two fractions were virtually devoid of Abeta when using manual Dounce homogenization (see also [19]).

A direct consequence of the homogenization method used, is the presence of varying amounts of oligomeric Abeta which strongly influence the pro-inflammatory and toxic effects of the soluble fractions, assayed "*in vitro*". As we demonstrate in this work, the scarce soluble Abeta, extracted using mild homogenization, produces no microglial stimulation and no degeneration in "*in vitro*" assays. On the contrary, the presence of high levels of monomeric and/or oligomeric species, extracted using sonication, produces clear microglial stimulation and neuronal degeneration. Thus, as a consequence of a strong initial tissue homogenization, the soluble TBS fraction could artifactually become pro-inflammatory and neurotoxic.

It could be argued that the absence of Abeta in the Dounce-homogenized soluble fractions is due to an incomplete disruption of the tissue and that sonication could better mobilize the soluble Abeta pool. Although it is possible that a fraction of the soluble Abeta might indeed remain unextracted in the Dounce-treated tissue, the redistribution observed after sonication most probably reflects the disaggregation of the Abeta plaques. This suggestion is based on: i) the soluble Abeta42 is detected predominantly in samples from demented individuals (Braak V–VI), whereas similar Abeta40 levels are clearly observed in samples with few or no Abeta plaques (Braak II), moderate Abeta pathology (Braak III–IV) and

high pathology (Braak V–VI); ii) as showed (see Fig. 2A), sonication produced a redistribution of Abeta from 2% SDS or 4% SDS/8M urea fractions (mostly Abeta plaques) to soluble fractions; iii) we observed a strong effect of sonication treatment on the integrity of biochemically isolated Abeta plaques. In fact, after sonication, the Abeta initially forming SDS-resistant aggregates, sedimentable by ultracentrifugation, is solubilized and redistributed into the TBS fraction. Taken together, these data demonstrate that isolation of soluble Abeta species is highly dependent on Abeta plaque preservation, and that the homogenization procedure is a critical step.

The existence of low levels of Abeta species (below the detection limits of our assays) in TBS soluble fractions is in agreement with data obtained by others using microdialysis [7, 8, 20]. In fact, when the brain tissue is not manipulated, the Abeta levels in the interstitial fluid (ISF) are much lower than that obtained in the TBS extractable fractions [7, 8]. As we have demonstrated in this work, if the integrity of Abeta plaques is preserved during homogenization, the levels of soluble Abeta are very low, below the detection limits of most common approaches. However, when the Abeta plaques are disturbed, more soluble Abeta is clearly detected. Thus, the plaques constituted a very large pool of Abeta (either monomeric or oligomeric) than could be released not only by treatment using detergents or formic acid but mechanically during homogenization using strong conditions (such as sonication).

Based on the above data, it could be argued that soluble fractions isolated using mild (possible low recovery) or strong (partial plaque solubilization) homogenization approaches are not representative of the real Abeta content in the interstitial fluids (see also [8]), and that only microdialysis, using large cutoff membranes, may better represent the actual Abeta equilibrium in the ISF (see [20]). However, taken into account that microdialysis is an "*in vivo*" procedure, the isolation of soluble fractions is the only approach to analyze postmortem human tissue. Thus, to characterize the soluble Abeta species from human samples, special care must be taken in the initial tissue homogenization since, due to the Abeta plaque instability, a strong homogenization procedure could produce a vast redistribution of the Abeta species in all soluble and insoluble fractions. This artifact could explain the dissimilar and somehow controversial data between different groups analyzing human AD samples.

Acknowledgments

SJ is recipient of a contract from CIBERNED. VN is recipient of PhD fellowships from Junta de Andalucia. FJM is recipient of PhD fellowships (FPU) from Ministerio de Educacion Cultura y Deportes. We thank Maria Luisa Garcia-Cuervo for their expert technical assistance.

Author Contributions

Conceived and designed the experiments: JV AG MV JCD. Performed the experiments: SJ VN MT MSM JM. Analyzed the data: JV AG MV JCD. Contributed reagents/materials/analysis tools: JV AG. Contributed to the writing of the manuscript: JV MV AG JCD.

References

1. **Benilova I, Karran E, De Strooper B** (2012) The toxic A[beta] oligomer and Alzheimer's disease: an emperor in need of clothes. Nat Neurosci 15: 349–357.
2. **Chromy BA, Nowak RJ, Lambert MP, Viola KL, Chang L, et al.** (2003) Self-Assembly of Abeta1-42 into Globular Neurotoxins. Biochemistry 42: 12749–12760.
3. **Dohler F, Sepulveda-Falla D, Krasemann S, Altmeppen H, Schluter H, et al.** (2014) High molecular mass assemblies of amyloid-beta oligomers bind prion protein in patients with Alzheimer's disease. Brain 137: 873–886.
4. **Esparza TJ, Zhao H, Cirrito JR, Cairns NJ, Bateman RJ, et al.** (2013) Amyloid-beta oligomerization in Alzheimer dementia versus high-pathology controls. Ann Neurol 73: 104–119.
5. **Gilbert BJ** (2013) The role of amyloid beta in the pathogenesis of Alzheimer's disease. J Clin Pathol 66: 362–366.
6. **Hardy J, Selkoe DJ** (2002) The Amyloid Hypothesis of Alzheimer's Disease: Progress and Problems on the Road to Therapeutics. Science 297: 353–356.
7. **Hong S, Ostaszewski B, Yang T, O'Malley T, Jin M, et al.** (2014) Soluble Abeta Oligomers Are Rapidly Sequestered from Brain ISF In-Vivo and Bind GM1 Ganglioside on Cellular Membranes. Neuron 82: 308–319.
8. **Hong S, Quintero-Monzon O, Ostaszewski BL, Podlisny DR, Cavanaugh WT, et al.** (2011) Dynamic Analysis of Amyloid beta-Protein in Behaving Mice Reveals Opposing Changes in ISF versus Parenchymal Abeta during Age-Related Plaque Formation. J Neurosci 31: 15861–15869.
9. **Jimenez S, Baglietto-Vargas D, Caballero C, Moreno-Gonzalez I, Torres M, et al.** (2008) Inflammatory Response in the Hippocampus of PS1M146L/APP751SL Mouse Model of Alzheimer's Disease: Age-Dependent Switch in the Microglial Phenotype from Alternative to Classic. J Neurosci 28: 11650–11661.
10. **Jimenez S, Torres M, Vizuete M, Sanchez-Varo R, Sanchez-Mejias E, et al.** (2011) Age-dependent Accumulation of Soluble Amyloid beta (Abeta) Oligomers Reverses the Neuroprotective Effect of Soluble Amyloid Precursor Protein-alpha (sAPPalpha) by Modulating Phosphatidylinositol 3-Kinase (PI3K)/Akt-GSK-3beta Pathway in Alzheimer Mouse Model. J Biol Chem 286: 18414–18425.
11. **Kayed R, Head E, Thompson JL, McIntire TM, Milton SC, et al.** (2003) Common Structure of Soluble Amyloid Oligomers Implies Common Mechanism of Pathogenesis. Science 300: 486–489.
12. **Lesne SE, Sherman MA, Grant M, Kuskowski M, Schneider JA, et al.** (2013) Brain amyloid-beta oligomers in ageing and Alzheimer's disease. Brain 136: 1383–1398.
13. **Mc Donald JM, Savva GM, Brayne C, Welzel AT, Forster G, et al.** (2010) The presence of sodium dodecyl sulphate-stable Abeta dimers is strongly associated with Alzheimer-type dementia. Brain 133: 1328–1341.
14. **Perez-Nievas BG, Stein TD, Tai HC, Dols-Icardo O, Scotton TC, et al.** (2013) Dissecting phenotypic traits linked to human resilience to Alzheimer's pathology. Brain 136: 2510–2526.
15. **Podlisny MB, Ostaszewski BL, Squazzo SL, Koo EH, Rydell RE, et al.** (1995) Aggregation of Secreted Amyloid -Protein into Sodium Dodecyl Sulfate-stable Oligomers in Cell Culture. J Biol Chem 270: 9564–9570.
16. **Rijal Upadhaya A, Capetillo-Zarate E, Kosterin I, Abramowski D, Kumar S, et al.** (2012) Dispersible amyloid beta-protein oligomers, protofibrils, and fibrils represent diffusible but not soluble aggregates: their role in neurodegeneration in amyloid precursor protein (APP) transgenic mice. Neurobiol Aging 33: 2641–2660.

17. **Rijal Upadhaya A, Kosterin I, Kumar S, von Arnim CAF, Yamaguchi H, et al.** (2014) Biochemical stages of amyloid-beta peptide aggregation and accumulation in the human brain and their association with symptomatic and pathologically preclinical Alzheimer's disease. Brain 137: 887–903.

18. **Rostagno A, Ghiso J** (2001) Isolation and Biochemical Characterization of Amyloid Plaques and Paired Helical Filaments. In: Current Protocols in Cell Biology. John Wiley & Sons, Inc.

19. **Sanchez-Varo R, Trujillo-Estrada L, Sanchez-Mejias E, Torres M, Baglietto-Vargas D, et al.** (2012) Abnormal accumulation of autophagic vesicles correlates with axonal and synaptic pathology in young Alzheimer's mice hippocampus. Acta Neuropathol 123: 53–70.

20. **Takeda S, Hashimoto T, Roe AD, Hori Y, Spires-Jones TL, et al.** (2013) Brain interstitial oligomeric amyloid beta increases with age and is resistant to clearance from brain in a mouse model of Alzheimer's disease. FASEB J 27: 3239–3248.

21. **Tomic JL, Pensalfini A, Head E, Glabe CG** (2009) Soluble fibrillar oligomer levels are elevated in Alzheimer's disease brain and correlate with cognitive dysfunction. Neurobiol Disease 35: 352–358.

22. **Torres M, Jimenez S, Sanchez-Varo R, Navarro V, Trujillo-Estrada L, et al.** (2012) Defective lysosomal proteolysis and axonal transport are early pathogenic events that worsen with age leading to increased APP metabolism and synaptic Abeta in transgenic APP/PS1 hippocampus. Mol Neurodeg 7: 59.

23. **Watt A, Perez K, Rembach A, Sherrat N, Hung L, et al.** (2013) Oligomers, fact or artefact? SDS-PAGE induces dimerization of beta-amyloid in human brain samples. Acta Neuropathol 125: 549–564.

24. **Yang T, Hong S, O'Malley T, Sperling RA, Walsh DM, et al.** (2013) New ELISAs with high specificity for soluble oligomers of amyloid beta-protein detect natural Abeta oligomers in human brain but not CSF. Alzheimer's & Dementia 9: 99–112.

RESUMEN IV

A modo de resumen podemos decir que:

Al comparar el efecto sobre la cantidad de especies de Aβ presentes en las fracciones solubles usando condiciones suaves (manualmente con Dounce) en comparación con homogeneizaciones más agresivas (sonicación a distintas intensidades) concluimos que:

1. Las técnicas más agresivas producen la liberación de péptidos Aβ a partir de las placas de extracelulares. Esta liberación pueden generar artefactos, ya que producirían un paso de Aβ de la placa hasta la fracción soluble, generando un artefacto experimental que nada tiene que ver con las condiciones fisiológicas *in vivo.*

2. Estas fracciones solubles obtenidas con protocolos que pueden afectar a la integridad de la placa son capaces de producir la estimulación de respuesta inflamatoria clásica y muerte neuronal en experimentos *in vitro*, mientras que las obtenidas mediantes métodos suaves no.

d. Discusión

1. Respuesta inflamatoria en SNC en los ratones transgénicos PS1xAPP modelo de la enfermedad de Alzheimer a los 6 y 18 meses de edad.

En los cerebros de pacientes de EA se produce un incremento de células microgliales activas alrededor de las placas de Abeta, así como un aumento en los niveles de citoquinas pro-inflamatorias, por lo que muchos los autores proponen que la inflamación contribuye a la patogénesis inicial de dicha patología. Aunque los resultados no son concluyentes, existen diversos estudios que muestran una correlación negativa entre las alteraciones en la función cognitiva y la activación de la microglía en la EA (Edison y col., 2008; Yokokura y col., 2011, Varnum e Ikezu, 2012). Apoyando esta hipótesis, estudios en pacientes que toman antiinflamatorios de forma habitual han mostrado una menor incidencia de la enfermedad de Alzheimer en estos pacientes(Morales y col., 2014)..Sin embargo otros estudios no corroboran los mismos resultados (pon biblio) Por lo tanto resulta de vital importancia determinar si la función microglial juega un papel beneficioso o perjudicial en el inicio y la progresión de la EA, a fin de poder proponer mecanismos de regulación de su actividad como posible diana terapéutica de dicha patologia (Condello y col., 2015).

En el primer trabajo presentado en este manuscrito, hemos realizado la caracterización del estado de activación de la microglía en el modelo transgénico **$PS1_{M146L}$/APP_{751SL}**, detectando un claro paralelismo, tanto espacial como temporal, entre la deposición de Aβ en placas extracelulares y la activación de la microglía (Simard y col., 2006).

1.1. La microglía en contacto directo con las placas extracelulares del péptido Aβ se activa a un fenotipo alternativo M2 (independientemente de la edad del animal) mientras que la microglía entre placas se activa a un fenotipo clásico M1 sólo a edades avanzadas.

A edades tempranas, la microglía activa se concentra EXCLUSIVAMENTE rodeando e infiltrando a estas placas, y se mantiene en estado de reposo en las regiones interplacas. En este sentido, experimentos *in vivo* mediante microscopia multifoton, han revelado que la formación de placas está seguida de una rápida activación y reclutamiento de la microglia a la misma (Meyer-Luehmann y col., 2008). Además, recientemente se ha demostrado que las placas de Abeta son capaces de atraer y estimular a la microglía al poseer en su superficie diversos receptores que reconocen al péptido Aβ (Yu y Ye, 2015).

Nuestros resultados muestran que la microglía asociada a placas se activa a un estado alternativo M2, caracterizada por la expresión de marcadores alternativos como YM-1 y la ausencia de factores cito-tóxicos (TNF-α, TRAIL, FASL e iNOS), datos que concuerdan con los obtenidos por otros autores (Imai y col., 2007; Chhor y col., 2013). A edades avanzadas (18 meses), la microglía activa que rodea a la placa continúa siendo YM-1 positivas y TNF-α negativas. Por tanto concluimos que en el modelo animal PS1xAPP las células microgliales en contacto directo con las placas de Abeta presentan un estado de activación alternativo independientemente de la edad del animal. Este fenotipo de activación microglial M2 se manifiesta además por un incremento en la expresión de IL-4, citoquina liberada por los linfocitos Th2 y astrocitos activados, y que participa en la activación microglial a un fenotipo M2 (Iribarnen y col., 2005; Butovsky y col., 2005; Ponomarev y col., 2007; Lyons y col., 2007 a,b.).

Hay que destacar que, a edades tempranas, en el modelo PS1xAPP la expresión de IL-4 está limitada a los astrocitos activos que rodean a la placa, mientras que a edades avanzadas la expresan además los linfocitos T CD3+ que concentrados alrededor de las placas. En conjunto, estos resultados parecen indicar que la IL-4 producida por los astrocitos, y por las células CD3+ en animales viejos, podrían controlar la activación de la microglía hacia el fenotipo alternativo no inflamatorio, sin llegar a descartar que la placa por si sola fuese capaz de realizar dicho efecto. El factor o factores que produce la activación de los astrocitos están aún por determinar.

Desde un punto de vista fisiológico la activación alternativa M2 parece ejercer una función neuro-protectora (Cherry y col., 2014, y otros artículos, pon unos cuantos mas). En presencia de IL-4 la microglía produce factores tróficos, como IGF-1 (Butovsky y col., 2006; Zhao y col., 2006; Chhor y col., 2013); además, reduce la toxicidad del péptido Aβ tanto *in vitro* como *in vivo* (Iribarnen y col., 2005; Butovsky y col., 2005, 2006; Lyons y col., 2007a,b) y potencia su fagocitosis (Koenigsknecht-Talboo y Landreth, 2005; Mandrekar y col., 2009). En nuestro trabajo hemos observado un aumento tanto en la expresión de IGF-1 alrededor de las placas de Aβ, como en la fagocitosis del péptido Abeta por la microglía activa que rodea las placas. Dichos resultados son apoyados por Bolmon y col. (2008), que demuestran que la microglía activa participa activamente en la internalización del Aβ de las placas influyendo de esta manera en el mantenimiento del tamaño de las mismas. Apoyando esta idea se ha demostrado en distintos modelos transgénicos de EA que la ablación de distinto genes implicados en el reclutamiento de células microgliales (como los genes del receptor TLR2, o de CCR2) producen un incremento en los niveles de Aβ42, acelerando los daños en la memoria e incrementando la patología vascular amiloide (ElKhoury y col., 2007; Richard y col.,2008). Además existen diversos estudios que correlacionan ciertas variaciones

genéticas en TREM2 (Triggering receptor expressed on myeloid cells 2, proteína reguladora de la fagocitosis en microglía y macrófagos), con un mayor riesgo de padecer la EA (Guerreiro y col., 2013; Jonsson y col., 2013).

Nosotros proponemos que la activación alternativa de la microglía asociada a la placa podría actuar limitando la toxicidad del Aβ mediante varios mecanismos posibles:

- generando una barrera física, ya que se ha demostrado que las áreas de placas no cubiertas por microglía son menos compactas y están asociadas con una distrofia axonal más severa (Condello y col., 2015).

- y/o ayudando a mantener niveles bajos de Aβ extracelular debido a su capacidad fagocítica (Simard y col., 2006; Mandrekar y col., 2009),.

Esta función neuro-protectora microglial podría estar mediada por el aumento en la expresión de IGF-1. Apoyando esta hipótesis, se ha demostrado que la vacunación con acetato de glatirámero, fármaco utilizado para el tratamiento de la esclerosis múltiple que potencia la respuesta Th2, produce un aumento en la expresión de IL-4 y reduce las placas de Aβ (Butovsky y col., 2006).

1.2. **Efecto de las formas oligoméricas solubles del péptido β-amiloide sobre la microglía interplaca.**

Cuando estudiamos la respuesta microglial en el modelo PS1xAPP a los 18 meses de edad, además de la activación M2 alrededor de la placa, se produce una activación de la microglía interplaca con un fenotipo Th1 caracterizado por un aumento en la expresión de TNF-α (y posiblemente de otros factores inflamatorios relacionados con TNF-α). Por tanto, a edades avanzadas coexisten dos poblaciones de células microgliales activas, lo que posiblemente esté reflejando la existencia de distintos activadores microgliales; Por un lado, las placas, que de forma directa o indirecta a través de IL-4, podrían estimular la microglía hacia un fenotipo M2 no citotóxico. Y por otro lado, un agente, posiblemente difusible, responsable de la activación generalizada interplaca con carácter citotóxico tipo M1 (Cherry y col., 2014), y que podría corresponder a las formas solubles tóxicas de Aβ oligomérico como ha sido propuesto por diversos autores (Haass y Selkoe, 2007; Benilova y col., 2012; Viola y Klein, 2015). De hecho nuestros resultados a edades tempranas muestran niveles muy bajos de Aβ42 soluble y de formas oligoméricas que aumentan significativamente a los 18 meses de edad. Esta activación microglial interplaca podría estar reflejando una respuesta

Th1/Th17 mediada por la infiltración de linfocitos T CD3+ en el parénquima cerebral. Teniendo en cuenta trabajos anteriores realizados en enfermos de EA y en modelos animales de la enfermedad (Itagaki y col. 1988;Togo y col.,2002; Stalder y col., 2005), buscamos y encontramos células CD3+ en el hipocampo de nuestro modelo PS1APP a los 18 meses. Sin embargo, y a pesar de dicha infiltración no encontramos cambios en la expresión de IL-12, IL-17 e IL-23 (citoquinas que polarizan hacia una respuesta Th1), y sí un aumento en la expresión de IL-4 e IL-10. Ya que las células CD3+ infiltradas expresan IL-4, podríamos sugerir que están polarizadas a un estado Th2 y/o Treg, siendo muy poco probable que la activación generalizada Th1 sea debido a su infiltración. De hecho parece ocurrir lo contrario, ya que la presencia de estas células Th2/Treg antiinflamatorias podría estar limitando el efecto neurotóxico de la activación generalizada de la microglía, y de esta manera explicar la ausencia de síntomas de encefalitis en los modelos de EA (Stalder y col., 2005).

Existen muchas evidencias que sugieren que las formas oligoméricas solubles de Aβ (ADDLs) son los agentes tóxicos en la EA (Lambert y col., 1998; Haass y Selkoe, 2007). Estos ADDLs sólo existen en enfermos de EA (Gong y col., 2003; Lacor y col., 2004) y en modelos animales de la enfermedad, y su contenido aumenta a medida que progresa la patologia (Lambert y col., 2007). En el modelo PS1xAPP estas formas solubles de Aβ42 se detectan exclusivamente (mediante los anticuerpos Nu-1 y A11) a los 18 meses de edad y no a edades más tempranas.

Dichos oligómeros difusibles podrían ser los causantes de la activación microglial generalizada observada a edades avanzadas. Hemos demostrado nuestra hipótesis realizando cultivos microgliales que tratamos con monómeros y oligómeros de Aβ42: mientras que las formas monoméricas no tienen ningún efecto sobre el cultivo, las formas oligoméricas producen un gran aumento en la expresión de TNF-α, Además, y aun más relevante es que la fracción soluble extracelular S1 de ratones WT de 6 y 18 meses y de ratones PS1xAPP de 6 meses, carentes, todos de formas oligoméricas, no modifican la expresión de TNF-α de estos cultivos., mientras que las fracciones S1 de animales PS1xAPP de 18 meses producen una fuerte estimulación en la expresión de TNF-α. Al inmunodepletar el Aβ presente en las fracciones S1 de 18 meses usando los anticuerpos 6e10 o A11, se pierde totalmente la capacidad estimuladora de estas fracciones S1, demostrando de esta manera que las formas oligoméricas solubles de Abeta son las responsables de la respuesta inflamatoria Th1 de la microglía interplaca.

Por tanto proponemos que la activación generalizada, con fenotipo clásico y potencialmente tóxico que se observa a los 18 meses en el modelo PS1xAPP podría

ser debido a la acumulación de las formas solubles oligoméricas de Aβ en el parénquima cerebral.

Se ha reportado que el envejecimiento y el Aβ podrían disminuir la expresión neuronal de ciertos inhibidores microgliales tales como CD200, fractalkina o algunos neurotransmisores como acetilcolina o noradrenalina (Cardona y col., 2006; Chitnis y col., 2007; Heneka y O'Banion, 2007; Lyons y col., 2007a; Duan y col., 2008). Además la neuronas dañadas podrían liberar estimulantes microgliales como ATP, UDP o CCL21 (de Jong y col., 2005; Inoue y col., 2007). De hecho es posible, que la activación clásica observada en nuestro modelo esté reflejando un efecto sinérgico del efecto directo del Aβ oligomérico soluble sobre la microglía, y de un efecto indirecto generado por los fallos en la correcta comunicación neurona-microglía.

Aunque el papel de la activación clásica de la microglía no está completamente dilucidado, sí ha sido ampliamente demostrado el efecto tóxico del TNF-α y de otros factores relacionados con TNFα e iNOS ((Cantarella y col., 2003; Lee y col., 2004; Li y col., 2004; Medeiros y coll., 2007; Uberti y col., 2007). En nuestro trabajo, al igual que en otros modelos animales (Schmitz y col., 2004), hemos observado, coincidiendo con la activación clásica microglial, una disminución significativa en el número de neuronas piramidales hipocampales. Estos resultados no nos permiten establecer una relación causal directa entre ambos eventos, pero es muy probable que la producción de TNFα, TRAIL, FASL y derivados de NO, junto con la presencia de formas oligoméricas solubles de Aβ, y otros componentes presentes en estas fracciones solubles, contribuyan a la degeneración piramidal de forma directa.

2. La fracción soluble extracelular S1 de los ratones PS1xAPP produce efectos antagónicos sobre la ruta de señalización pro-supervivencia PI3K/AKT a los 6 y 18 meses de edad.

Cada vez existen más evidencias de que la vía de señalización PI3K/Akt/GSK-3β se encuentra alterada en enfermos de EA probablemente debido a su interacción con Aβ (Bondy y col., 2004). La hipótesis GSK3 de la EA propone que la sobreactivación de esta vía podría estar implicada en dististas manifestaciones patológicas de la enfermedad y participar de forma activa en la hiperfosforilación de Tau (De Felipe y col., 2008), la inhibición de la LTP, las alteraciones en la memoria y pérdida de sinápsis (Lesné y col., 2006), la muerte neuronal (Shankar y col., 2007; Deshpande y col., 2006), así como en la respuesta inflamatoria citotóxica (Jiménez y col., 2008). Apoyendo esta hipótesis se ha demostrado que la sobreexpresión de GSK3B en un modelo condicional

transgénico produce la hiperfosforilación de Tau y la muerte neuronal (Lucas y col, 2001; Engel y col., 2006), mientras que su inhibición farmacológica con litio disminuye la producción de Aβ y su acumulación en placas extracelulares (Su y col., 2004), produciendo mejoras en la memoria, preservando la estructura de las dendritas y reduciendo la patología de Tau en modelos transgénicos de EA (Noble y col., 2005; Rockenstein y col., 2007). De hecho, el efecto de las formas oligoméricas solubles de Aβ podría realizarse a través de la interaccion con dicha via (Gong y col., 2003; Lacor y col., 2004),

La actividad GSK3beta además está implicada en el procesamiento de APP y la producción de Abeta. Por ello estudiamos el nivel de fosforilación de GSK3b en Ser9 en el hipocampo de animales PS1xAPP de 6 meses de edad (sin muerte de neuronas piramidales) y de 18 meses,(cuando la degeneración de neuronas piramidales es evidente) (Jiménez y col., 2008).Nuestros resultados muestran que los ratones jóvenes tienen altos niveles de fosforilación de GSK3b-Ser9, sugiriendo una menor actividad de esta enzima y coincidiendo con un incremento en la expresión de la proteína anti-apoptótica BCL-2 (Karlnoski y col., 2007) y un incremento de la proteína β-catenina. Estos datos podrían indicar que se están produciendo niveles altos de neurotrofinas. Sin embargo en nuestro modelo transgénico PS1APP, a excepción de IGF-1, que se concentra alrededor de las placas de Abeta, pero cuyos niveles totales están disminuidos tanto a los 6 como 18 meses, ninguno de los factores tróficos estudiados presenta cambios.Sin embargo, nuestros resultados demuestran que las fracciones solubles S1 de ratones PS1xAPP de 6 meses, actuando a través de receptores IGF-1, activa la vía PI3K/Akt fosforilando a GSK3b en su residuo Ser9, y en consecuencia posee actividad neuroprotectora, que se manifiesta promoviendo la supervivencia neuronal en cultivos de células N2A. Esto no ocurre con las fracciones S1 obtenidas de WT o el modelo transgénico monogénico PS1 de la misma edad.

Los fragmentos derivados del procesamiento de APP mayoritarios en las fracciones S1 de los animales PS1xAPP a 6 meses de edad son el sAPPα y sAPPβ. El Aβ monomérico, que podría tener un efecto similar a estos fragmentos (Giuffrida y col., 2009) está ausente en dichas fracciones. En nuestro trabajo hemos usado sAPPα sintético en cultivos de células N2A y hemos demostrado que dicho fragmento soluble produce una activación dosis dependiente de la ruta Akt-GSK3b, que es inhibida por LY294002, AG1024 y picropodofilina, indicando que la activación de esta vía está mediada por los receptores de IGF-1 e Insulina. Dicho efecto desaparece tras la inmunodepleción de la fracción S1 con el anticuerpo 6e10. Además, hay que tener en cuenta que la concentración de sAPPα en estas fracciones S1 es aproximadamente de 20nM, del mismo rango que la EC_{50} para el sAPPα sintético (2.3 nM).

Por el contrario, el fragmento sAPPβ no presenta ningún tipo de efecto en nuestro modelo *in vitro*.

Estos datos demuestran por primera vez el efecto directo del sAPPα sobre la vía Akt-GSK-3β *in vitro*, y, aunque no pueden probar dicha relación *in vivo*, sí nos permiten postular que, en nuestro modelo PS1xAPP, el sAPPα actuando a través de los R de IGF-1/insulina y la vía pro-supervivencia Akt-GSK-3β podrían provocar un retraso en la patología asociada a Aβ.

De hecho, aunque el incremento en la fosforilación de GSK-3β no se observa en todos los modelos transgénicos basados en APP (Masliah y col., 1997; Malm y col., 2007), todos ellos presentan un considerable retraso entre la acumulación de Aβ y la patología neuronal. Por lo tanto nuestros resultados muestran una nueva conexión entre el metabolismo de APP y la regulación de GSK3β que podría explicar la lenta progresión en la patología observada en los modelos transgénicos, así como la disminución en la patología de Tau y el aumento de la supervivencia neuronal en algunos modelos APP-Tau (Terwel y col., 2008). Se podría pensar en la activación de la actividad α-secretasa como una posible diana terapéutica en EA (Kojro y col., 2006).

Además hemos demostrado el efecto inhibitorio de las formas oligoméricas solubles de Aβ sobre la vía Akt-GSK-3β. Hemos identificado 5 especies oligoméricas solubles (resistentes a SDS) de 24, 47, 57, 90 y 96 kDa en las fracciones S1 de los ratones PS1APP de 18 meses. El tratamiento de cultivos de la línea neuronal N2a con estos S1 de 18 meses dan lugar a una clara inhibición en la fosforilación de Akt (Townsend y col., 2007). Esta inhibición parece estar mediada por un efecto directo sobre los receptores tróficos, ya que al menos, los receptores de IGF-1 e insulina son inhibidos por dichas fracciones S1 de 18 meses. Esta inhibición está mediada por los oligómeros de Aβ, ya que su eliminación mediante inmunodeplición con el anticuerpo A11 revierte completamente el efecto inhibitorio de la fracción S1 sobre la vía Akt-GSK-3β.

Por lo tanto, podemos concluir a este respecto que, la aparición de Aβ oligomérico extracelular parece inhibir la vía pro supervivencia Akt-GSK-3β. Este efecto es consistente con la disminución observada en la fosforilación del residuo Ser9 de GSK-3β, el aumento en la fosforilación de Tau (no mostrado), y con la hiperfosforilación y degradación de β-catenina observada en las muestras de hipocampo de ratones PS1APP de 18 meses. Además, como hemos comentadoen el apartado 1 de esta discusión, la presencia de estos oligómeros extracelulares determinan la activación potencialmente neurotóxica de la microglía coincidiendo con la perdida de las neuronas piramidales de CA1 (Jimenez y col., 2008). Teniendo en cuenta todas estas evidencias, podemos decir que la acumulación de los oligómeros de Aβ extracelulares producen la inhibición de las rutas pro supervivencia coincidiendo con una activación de la respuesta

inflamatoria neurotóxica, y generando en su conjunto un ambiente apropiado para inducir la muerte neuronal.

Nuestros resultados también podrían indicar que estas formas oligoméricas solubles que aparecen a los 18 meses de edad podrían ejercer su acción inhibitoria por efecto directo sobre distintos receptores tróficos. Para ello nos basamos en nuestros resultados que demuestran:

a. La mayor selectividad de los oligómeros de abeta por los receptores de NGF que por los de BDNF.
b. La reversión de los efectos inhibitorios de los oligómeros de abeta al aumentar la concentración de distintas neurotrofinas como NGF, insulina o IGF-1.

Varios autores han sugerido también un posible efecto directo de los oligómeros de Aβ sobre los receptores de Insulina (Zhao y col., 2008; Xie y col., 2002), aunque no se puede descartar que estas especies solubles de Aβ puedan realizar su efecto inhibitorio por otros mecanismos. Así, podrían actuar a nivel de otros receptores como los de NMDA o p75NTR (Zhao y col., 2009; Decker y col., 2010; Knowles y col., 2009), e incluso reduciendo o inhibiendo la respuesta a insulina (Zhao y col., 2008; Ma y col., 2009) a través de la fosforilación de Akt473 que no activa la vía. En nuestros experimentos *in vitro* la fosforilación de Akt473 siempre ha sido paralela a la fosforilación de Akt308 y GSK-3β Ser9 en los cultivos neuronales primarios.

Aunque no conocemos exactamente la causa de tal discrepancia en nuestros resultados, hay que tener en cuenta que los tratamientos *in vitro* realizado han sido muy cortos (20-30 minutos) para minimizar la muerte celular.

Respecto a la relevancia fisiológica de nuestros hallazgos, podríamos concluir que una bajada crónica en las vías de señalización tróficas podría estar implicada en el desarrollo de la EA (Capsoni y col., 2002, 2010; Houeland y col., 2010). En este sentido el efecto inhibitorio de los oligómeros de Aβ sobre los receptores tróficos podría contribuir a la inhibición de las rutas prosupervivencia, y en consecuencia, estar implicados en la vulnerabilidad mayor del sistema colinérgico observado en EA.

El Aβ oligomérico también podría unirse directamente al receptor p75NTR (Knowles y col., 2009; Braithwaite y col., 2010) permitiendo la formación de neuritas distróficas (también observada en nuestro modelo) (Ramos y col., 2006; Baglietto-Vargas y col., 2010; Moreno-Gonzalez y col., 2009), la activación de la casacada de muerte celular mediada por c-Jun (Sotthibundh y col., 2008).

3. Efecto del tratamiento crónico oral de litio sobre la patología relacionada con la EA en ratones PS1xAPP

A pesar de la vasta información que existe sobre las alteraciones patológicas acaecidas en el desarrollo y progresión de la EA, aún no se ha desarrollado ningún tratamiento efectivo que palie los síntomas de la misma y modifique el curso natural de la enfermedad. El litio, fármaco de elección para en el trastorno bipolar, ha sido sugerido por diversos autores como un tratamiento potencial contra la EA (ver revisiones Diniz B y col., 2013; Forlenza y col., 2012; Nunes y col., 2007; Young y col., 2007). Existen estudios clínicos que indican que el litio podría ser preventivo en pacientes con MCI, mientras que no produce mejora en EA moderado. Además estudios epidemiológicos muestran que pacientes con trastorno bipolar tratados con litio tienen menor riesgo de sufrir EA (ver revisión Nunes y col., 2007). Por todo esto se ha propuesto el uso del litio como un posible tratamiento preventivo en individuos con riesgo de sufrir EA o que se encuentren en estados preclínicos de la enfermedad. Por ello decidimos someter a los animales PS1xAPP a una ingesta crónica con litio antes de que comience el desarrollo de la patologia.

Nuestros resultados muestran que el tratamiento con litio desde edades tempranas (antes de que aparezcan los primeros acúmulos de péptido Aβ) tiene como consecuencia la formación de placas menos tóxicas, y previene, en cierto grado, los déficits de comportamiento y memoria que tienen lugar en el modelo PS1xAPP, disminuyendo a la vez la muerte neuronal.

El efecto neuroprotector del Litio podría estar relacionado con la modificación de la toxicidad de la placa de Aβ por la acción de las HSPs (*heat shock proteins*) liberadas por los astrocitos. De forma que, a diferencia de otros tratamientos clínicos usando Litio, nuestro trabajo indica que este tratamiento puede ser usado como una intervención preventiva para mejorar la progresión de la EA desde estados preclínicos.

Como hemos comentado con anterioridad nuestro ratón transgénico PS1xAPP presenta perdida neuronal desde edades tempranas (6 meses). Esta neurodegeneración afecta a las células GABAérgicas SOM/NPY positivas de la formación hipocampal y la corteza entorrinal, las cuales coinciden en espacio y tiempo con la acumulación extracelular de Aβ (Sanchez-Varo y col., 2012; Torres M y col., 2012; Moreno-Gonzalez I y col., 2009; Ramos B. y col., 2006; Jimenez S. y col., 2008; Jimenez S. y col., 2011). Otra caractervstica patolσgica de este modelo de EA es la formaciσn de distrofias axonales rodeando las placas de Aβ, distrofias que acumulan tau

fosforilada, proteínas ubiquitinadas y vesículas autofágicas (Sanchez-Varo y col., 2012; Torres M y col., 2012;).

A este respecto nuestros datos demuestran que la ingesta de litio, cuando comienza antes del inicio de los procesos neurodegenerativos, impide que se produzca esta pérdida neuronal selectiva para las SOM/NPY tanto de hipocampo como en la corteza entorrinal. Este es el primer estudio que muestra que el litio previene de la muerte neuronal de estas zonas especialmente vulnerables durante EA en un estudio *in vivo*. El efecto del Litio no queda aquí, ya que también mejora las distrofias y con esto produce una disminución drástica en las áreas distróficas NPY-positivas que están asociadas a las placas (en torno al 60%), en la acumulación anormal de LC3-II y de las proteínas ubiquitinadas. Por ello decimos que el litio mejora la mayoría de las marcas neuropatológicas que presenta el modelo PS1xAPP.

Se ha descrito, por nuestro grupo y otros, que el ratón PS1APP presenta activación de GSK-3β y deficiencias a nivel del sistema autofagia/lisosoma (Sanchez-Varo y col., 2012; Torres M y col., 2012; Jimenez S. y col., 2001; Lee JH. y col., 2010; Yang DS. y col., 2011). El litio podría estar protegiendo la neurodegeneración de forma directa por la inhibición de la actividad de GSK-3β (datos no mostrados; (JA. y col., 2010)) y/o por la activación de la degradación de proteínas a través de la autofagia (Sarkar S. y col., 2005, Heiseke y col., 2009; Parr C. y col., 2012). Estos efectos podrían reducir la acumulación de tau fosforilada, proteínas ubiquitinadas y LC3-II, y en consecuencia reducir los procesos neuro-degenerativos. Además en el modelo PS1APP estas proteínas se acumulan en las distrofias axonales que rodean las placas de Aβ. Por ello nosotros sugerimos que la formación de estas distrofias axonales podrían estar implicadas en la degeneración neuronal que se produce durante la progresión de la enfermedad (Jin M. y col., 2011; Sanchez-Varo R. y col., 2012; Torres M. y col., 2012; Kandalepas P. y col., 2013; Xie H. y col., 2013), basándonos en resultados recientemente descritos en enfermos de EA (Perez-Nievas BG. y col., 2013).

Por otro lado, el litio, además de afectar la actividad de GSK3-β y del sistema autofágico/lisosomal, también podría estar actuando sobre la formación de la placa, modificando tanto la forma como la calidad de las mismas. De hecho las placas en los ratones tratados con litio son más pequeñas (Toledo EM. y col., 2009) y más compactas que en el grupo PS1APP control. A este respecto se ha reportado que un mayor nivel de compactación del Aβ disminuye su efecto tóxico (Cohen E. y col., 2009; Condello C. y col., 2012); además la bajada en el área ocupada por distrofias por placa podría reflejar una disminución en la toxicidad de las mismas. Parece la que la formación de distrofias y la degeneración sináptica está restringida a la periferia de la placa (halo) (Koffie RM. Y col., 2009; Xie H. y col., 2013; Condello C. y col., 2011). Dichas zonas periféricas

podrían contener Aβ oligomérico fibrilar parcialmente agregado, que podrían estar implicados en el desarrollo de la patología de EA (Tomic JL. Y col., 2009). Y en efecto, nuestros resultados muestran que el litio produce una reducción del halo oligomérico (reconocido por el anticuerpo específico de esta conformación OC) que rodea la placa de Aβ, disminuyendo así la toxicidad de la placa.

El proceso implicado en la agregación de Aβ, la formación de la placa o su compactación son desconocidos. Se ha sugerido un papel importante de los astrocitos en el control del crecimiento de la placa y en la formación de las distrofias asociadas a las mismas (Kraft AW. y col., 2013; Ojha J. y col., 2011). Además los astrocitos activos pueden liberar una gran cantidad de factores, entre los que se encuentran las HSPs (Renkawek k. y col., 1994; Taylor AR. y col., 2007), que podrían aumentar la agregación/compactación de Aβ, reduciendo así su toxicidad potencial (Ojha J. y col., 2011 Cascella R. y col., 2013; Mannini B. y col., 2012). Nuestros resultados apoyan la posible implicación de los astrocitos y las HSPs extracelulares como posibles mediadores del efecto del litio sobre la toxicidad de la placa. De hecho demostramos que, en los animales tratados con litio, existe una mayor activación de los astrocitos coincidiendo con una mayor incorporación de HSPs en las placas y una reducción del halo oligomérico que rodea a las mismas. Aunque son necesarios más experimentos que corroboren estos resultados, podemos decir que en animales tratados con litio se produce un aumento de Hsp70 y Hsp27 en el centro de la placa, lo que podría estar indicando que estas HSPs están implicadas en la nucleación del péptido Aβ y de la compactación de la placa.

4. **Influencia del protocolo de homogeneización usado para generar la fracción S1 sobre el contenido de formas solubles del péptido Aβ.**

Con todos los resultados expuestos hasta el moemento podemos proponer que las formas solubles oligoméricas de Aβ juegan un papel importante en el desarrollo y la progresión de la enfermedad de Alzheimer, por lo que la caracterización de las mismas es de vital importancia. La obtención de estas fracciones solubles a partir de tejidos siempre se tratará de una aproximación experimental, nos dará una idea del contenido de las mismas que puede poseer el parénquima cerebral, pero nunca será al 100% como sus niveles fisiológicos *in vivo*. En nuestro laboratorio hemos demostrado que las distintas condiciones a la hora de homogeneizar la muestra para obtener estas fracciones S1 pueden afectar al contenido de Aβ de las fracciones solubles, probablemente al inducir la movilización de las placas de Aβ que pueden pasar al medio soluble generando un artefacto del procedimiento.

Mostramos que usando un protocolo suave de homogeneización (mediante Dounce manual), que es nuestro procedimiento de rutina, las fracciones S1, tanto las que provienen de muestras de enfermos de EA, como de muestras del modelo doble transgénico PS1xAPP contienen pequeñas cantidades de especies oligoméricas de Aβ. Por el contrario, cuando usamos métodos más agresivos, tales como la sonicación, se encuentran en estas fracciones solubles grandes cantidades de oligómeros de Aβ.

Primero hemos caracterizado el contenido de Aβ soluble en muestras de hipocampo humanas de individuos no dementes (con estadios Braak II, III y IV) e individuos dementes (Braak V y VI). Estas fracciones solubles fueron preparadas usando una homogeneización suave seguida de ultra centrifugación (Jimenez S. y col., 2008, 2011; Sanchez-Varo R. y col., 2012; Torres M. y col., 2012). Nuestros datos muestran unos niveles muy limitados de Aβ (pg/µg proteína) en las fracciones S1, y nos fue imposible identificar la naturaleza de estos péptidos de Aβ mediante western blot o inmunoprecipitación usando los anticuerpos 6e10 u OC (datos no mostrados). Estos datos coinciden con los expuestos por otros autores (Tomic JL. Y col., 2009; Esparza TJ. Y col., 2013), mientras que difieren de otros que reportan la presencia de grandes cantidades de especies solubles de Aβ, especialmente en las muestras humanas (Dohler F. y col., 2014, Mc Donald JM. Y col., 2010; Perez-Nievas BG. y col., 2013; Rijal Upadhaya A. y col., 2012, 2014, Watt A. y col., 2013; Yang T. y col., 2013).

Estas diferencias pueden venir, al menos en parte, de la distintas regiones del cerebro analizadas y de la relativa abundancia de placas difusas o placas neuríticas de Aβ (la formación hipocampal apenas presenta placas difusas, datos no mostrados, mientras que las distintas áreas corticales contienen una mayor proporción de éstas; ver (Mc Donald JM. Y col., 2010)).

Pero también pueden venir de los distintos protocolos que se usan para generar la fracción soluble. Este hecho nos hizo evaluar el efecto de la homogeneización inicial del tejido sobre la fracción soluble y la integridad de la placa. Para tal propósito hemos comparado dos procedimientos ampliamente usados para el aislamiento de especies solubles de Aβ:

1. La homogeneización manual con el uso de Dounce (Jimenez S. y col., 2008; Esparza TJ. Y col., 2013; Tomic JL., 2009), es considerado un método suave de rotura tisular.
2. Sonicación (Rijal Upadhaya A. y col., 2012, 2014), es considerado un método más agresivo de rotura tisular.

Usando cortezas de ratones $PS1_{delta9}xAPP_{swe}$ de 12 meses como fuente de placas de Aβ, demostramos que la homogeneización con Dounce preserva la integridad de la placa y, en consecuencia, minimiza el nivel de contaminación de Aβ en las fracciones solubles. Por otro lado la sonicación (y probablemente otros procedimientos iguales de agresivos) produce una rotura mecánica de la placa de Aβ, dando lugar a una redistribución de monómeros y oligómeros de Aβ en todas las fracciones estudiadas. Es especialmente relevante la presencia de grandes cantidades de Aβ en la fracción soluble TBS y en la fracción microsomal. Estas dos fracciones no poseen Aβ cuando se usa la homogeneización manual con el Dounce (ver Sanchez-Varo R. y col., 2012).

Una consecuencia directa del método usado, es la presencia de cantidades variables de Aβ oligomérico que están implicados en el efecto pro inflamatorio y tóxico de las fracciones solubles in vitro. Como demostramos en este trabajo, el escaso Aβ soluble que se obtiene con la homogeneización suave de los tejidos, no produce ni estimulación microglial ni muerte neuronal en nuestros experimentos in vitro. Por el contrario, la fracción soluble genera tras sonicación, con sus altos niveles de Aβ monomérico y oligomérico produce una clara estimulación microglial y degeneración neuronal en los mismos experimentos *in vitro*. Así, como consecuencia de un mecanismo de homogeneización agresivo, la fracción soluble TBS se podría convertir en pro inflamatoria y neurotóxica de forma artefactual.

Se puede argumentar que la ausencia de Aβ en la fracción S1 tras la homogeneización con el Dounce se puede deber a una incompleta rotura del tejido y que la sonicación podría movilizar el pool de Aβ soluble. Podría ocurrir pero pensamos que es más probable que la redistribución después de la sonicación refleje la disgregación de la placa de Aβ más que la recuperación total de las formas solubles de Aβ. Nos basamos en las siguientes pruebas:

1. El Aβ42 soluble es detectado de forma predominante en muestras de indiviudos dementes (Braak V-VI), mientras que niveles similares de $Aβ_{40}$ se han observado en todos los estadios; Braak II (con pocas o ninguna placa de Aβ), Braak III-IV (con una patología moderada de Aβ) y Braak V-VI (con una fuerte patología).

2. La sonicación produce una redistribución de Aβ desde las fracciones 2%SDS y 4%SDS/8M Urea (que contienen las placas de Aβ) hasta la fracción soluble.

3. Se ha observado un fuerte efecto del tratamiento de sonicado sobre las placas de Aβ aisladas.

De hecho después de la sonicación, el Aβ que inicialmente se encuentra formando agregados resistentes a SDS que son sedimentables por ultra centrifugación se solubiliza y se redistribuye a la fracción TBS. Si tomamos en conjunto todos estos datos podemos afirmar que el aislamiento de las especies solubles de Aβ depende del mantenimiento de la integridad de la placa y por lo tanto la homogeneización del tejido es un paso vital.

La existencia de bajos niveles de especies solubles de Aβ (por debajo de los límites detectables de nuestro experimento) en la fracción soluble TBS coincide con los datos obtenidos por otros laboratorios usando micro diálisis (Hong S. y col., 2011, 2014; Takeda S. y col., 2013). De hecho, cuando el tejido no se manipula, los niveles de Aβ en el fluido intersticial (ISF) son mucho menor que el obtenido en las fracciones TBS (Hong S. y col., 2011, 2014). Si la integridad se mantiene durante la homogeneización los niveles de Ab soluble son muy bajos, por debajo de los límites de detección de la mayoría de técnicas. Sin embargo, cuando la placa de Ab se rompe, mucha más cantidad de Ab soluble es detectada. Es evidente que la placa de Aβ constituye una potente fuente de péptido Aβ (tanto monomérico como oligomérico), que podrían liberarse no sólo mediante el uso de detergentes o ácido fórmico, sino también durante la homogeneización mecánica usando condiciones agresivas (tales como la sonicación).

Si no basamos en estos datos podemos afirmar que las fracciones solubles que se generan por homogeneización suave (pueden tener una recuperación de formas solubles baja) o por métodos de homogeneización agresivos (que pueden solubilizar parte de la placa) no son representativos del contenido real de Aβ en el líquido intersticial (Hong S. y col., 2011), y que sólo la micro diálisis, usando membranas con poros de gran tamaño de corte, puede darnos una idea del equilibrio de Aβ en el ISF (Takeda S. y col., 2013). Teniendo en cuenta que la micro diálisis es un procedimiento *in vivo*, que no podemos usar para analizar los tejidos postmortem de enfermos, sólo nos queda la generación de estas fracciones solubles S1 para hacernos una idea de qué contiene el ISF. Así que para caracterizar estas especies solubles de Aβ en muestras humanas hay que tener un especial cuidado en la homogeneización inicial de los tejidos debido a la inestabilidad de la placa de Aβ. Una homogeneización agresiva podría producir una redistribución de las especies de Aβ tanto en las fracciones solubles como insolubles. Estos artefactos podrían explicar la variabilidad de datos que podemos encontrar entre los distintos grupos que analizan muestras de enfermo de EA.

e. Conclusiones

1. A edades tempranas, en nuestro modelo transgénico, la aparición de placas determina la activación de la microglía hacia un fenotipo alternativo, aparentemente, con un papel neuro protector. La activación microglial está limitada a las células en contacto directo con las placas de Aβ. Mientras que a edades mayores (18 meses) coincidiendo con la acumulación de Aβ oligomérico soluble extracelular, se produce una activación generalizada de la microglía hacia un fenotipo clásico caracterizado por la producción de factores citotoxicos.

2. En ratones jóvenes PS1APP el sAPPα presente en las fracciones soluble extracelulares actúa al menos a través del receptor de IGF-1 y del receptor de Insulina produciendo la activación de la vía Akt-GSK-3β. La activación de esta vía, clásicamente considerada como una vía pro superviviencia. A edades tardías (18 meses) la presencia de múltiples formas oligoméricas solubles de Aβ produce la inhibición de la actividad de ciertas neurotrofinas (incluido el efecto beneficioso de sAPPα) este efecto podría estar mediado por la interacción con sus respectivos receptores.

3. El tratamiento desde edades tempranas (antes de que empiecen la acumulación de péptido Aβ) y crónico con la ingesta oral de litio disminuye de forma significativa la progresión patológica observada en este modelo PS1xAPP murino de la EA.

4. El litio podría aumentar la compactación de las placas de Aβ, generando placas de menor tamaño y con menor halo oligomérico tóxico a su alrededor. Disminuyendo la degeneración neuronal y axonal.

5. El litio podría actuar directamente sobre las neuronas, pero nosotros mostramos el efecto sobre los astrocitos y la liberación por parte de estos de chaperonas que pueden afectar a la compactación y toxicidad de las placas.

6. El contenido de Aβ42 soluble en las muestras humanas de enfermo de EA es muy limitado (pg/µg proteína). Por debajo de los niveles de detección de la mayoría de técnicas, cuando se usan protocolos de homogeneización suaves de los tejidos.

7. Los mecanismos usados en la homogeneización inicial de los tejidos determinan pueden influenciar sobre el contenido de las distintas especies de Aβ en la fracción soluble. De forma que los mecanismos más agresivos como la sonicación pueden extraer de la placa estas especies de Aβ hacia la fracción soluble al afectar la integridad de la placa.

8. Los mecanismos agresivos de homogeneización generan fracciones solubles con capacidad para inducir una respuesta inflamatoria tóxica y muerte neuronal *in vitro*.

9. Todos los métodos *in vitro* para generar estas fracciones solubles S1 a partir de muestras post mortem generan artefactos que pueden infravalorar o supervalorar las especies de Aβ presentes *in vivo* en el líquido intersticial. .

References

1. **Benilova I, Karran E, De Strooper B** (2012) The toxic A[beta] oligomer and Alzheimer's disease: an emperor in need of clothes. Nat Neurosci 15: 349–357.
2. **Chromy BA, Nowak RJ, Lambert MP, Viola KL, Chang L, et al.** (2003) Self-Assembly of Abeta1-42 into Globular Neurotoxins. Biochemistry 42: 12749–12760.
3. **Dohler F, Sepulveda-Falla D, Krasemann S, Altmeppen H, Schluter H, et al.** (2014) High molecular mass assemblies of amyloid-beta oligomers bind prion protein in patients with Alzheimer's disease. Brain 137: 873–886.
4. **Esparza TJ, Zhao H, Cirrito JR, Cairns NJ, Bateman RJ, et al.** (2013) Amyloid-beta oligomerization in Alzheimer dementia versus high-pathology controls. Ann Neurol 73: 104–119.
5. **Gilbert BJ** (2013) The role of amyloid beta in the pathogenesis of Alzheimer's disease. J Clin Pathol 66: 362–366.
6. **Hardy J, Selkoe DJ** (2002) The Amyloid Hypothesis of Alzheimer's Disease: Progress and Problems on the Road to Therapeutics. Science 297: 353–356.
7. **Hong S, Ostaszewski B, Yang T, O'Malley T, Jin M, et al.** (2014) Soluble Abeta Oligomers Are Rapidly Sequestered from Brain ISF In-Vivo and Bind GM1 Ganglioside on Cellular Membranes. Neuron 82: 308–319.
8. **Hong S, Quintero-Monzon O, Ostaszewski BL, Podlisny DR, Cavanaugh WT, et al.** (2011) Dynamic Analysis of Amyloid beta-Protein in Behaving Mice Reveals Opposing Changes in ISF versus Parenchymal Abeta during Age-Related Plaque Formation. J Neurosci 31: 15861–15869.
9. **Jimenez S, Baglietto-Vargas D, Caballero C, Moreno-Gonzalez I, Torres M, et al.** (2008) Inflammatory Response in the Hippocampus of PS1M146L/APP751SL Mouse Model of Alzheimer's Disease: Age-Dependent Switch in the Microglial Phenotype from Alternative to Classic. J Neurosci 28: 11650–11661.
10. **Jimenez S, Torres M, Vizuete M, Sanchez-Varo R, Sanchez-Mejias E, et al.** (2011) Age-dependent Accumulation of Soluble Amyloid beta (Abeta) Oligomers Reverses the Neuroprotective Effect of Soluble Amyloid Precursor Protein-alpha (sAPPalpha) by Modulating Phosphatidylinositol 3-Kinase (PI3K)/Akt-GSK-3beta Pathway in Alzheimer Mouse Model. J Biol Chem 286: 18414–18425.
11. **Kayed R, Head E, Thompson JL, McIntire TM, Milton SC, et al.** (2003) Common Structure of Soluble Amyloid Oligomers Implies Common Mechanism of Pathogenesis. Science 300: 486–489.
12. **Lesne SE, Sherman MA, Grant M, Kuskowski M, Schneider JA, et al.** (2013) Brain amyloid-beta oligomers in ageing and Alzheimer's disease. Brain 136: 1383–1398.
13. **Mc Donald JM, Savva GM, Brayne C, Welzel AT, Forster G, et al.** (2010) The presence of sodium dodecyl sulphate-stable Abeta dimers is strongly associated with Alzheimer-type dementia. Brain 133: 1328–1341.
14. **Perez-Nievas BG, Stein TD, Tai HC, Dols-Icardo O, Scotton TC, et al.** (2013) Dissecting phenotypic traits linked to human resilience to Alzheimer's pathology. Brain 136: 2510–2526.
15. **Podlisny MB, Ostaszewski BL, Squazzo SL, Koo EH, Rydell RE, et al.** (1995) Aggregation of Secreted Amyloid Beta-Protein into Sodium Dodecyl Sulfate-stable Oligomers in Cell Culture. J Biol Chem

f. Bibliografía

Abramov E, Dolev I, Fogel H, Ciccotosto GD, Ruff E, Slutsky I. (2009). Amyloid-β as a positive endogenous regulator of reléase probability at hippocampal synapses. *Nat Neurosci*., 12(12):1567-1576.

Arendt T, Bigl V, Tennstedt A, Arendt A. (1985) Neuronal loss in different parts of the nucleus basalis is related to neuritic plaque formation in cortical target areas in Alzheimer's disease. *Neuroscience*. 14: 1-14.

Armstrong RA. (2006). Plaques and tangles and the pathogenesis of Alzheimer's disease. *Folia Neuropathol.*, 44(1):1-11.

Ashe KH, Zahs KR. (2010).Probing the biology of Alzheimer's disease in mice. *Neuron*,66:631-645.

Avila-Muñoz E, Arias C. (2014) When astrocytes become harmful: Functional and inflammatory responses that contribute to Alzheimer's disease. *Ageing Res Rev*. 18:29-40.

Baglietto-Vargas D, Moreno-Gonzalez I, Sanchez-Varo R, Jimenez S, Trujillo-Estrada L, Sanchez-Mejias E, Torres M, Romero- Acebal M, Ruano D, Vizuete M, Vitorica J, Gutierrez A. (2010). Calretinin interneurons are early targets of extracellular amyloid-beta pathology in PS1/APP Alzheimer mice hippocampus. *J Alzheimers Dis.*, 21(1):119-132.

Baron R, Babcock AA, Nemirovsky A, Finsen B, Monsonego A. (2014). Accelerated microglial pathology is associated with Ab plaques in mouse models of Alzheimer's disease. *Aging Cell*, 13:584-595.

Bartus RT. (2000). On neurodegenerative diseases, models, and treatment strategies: lessons learned and lessons forgotten a generation following the cholinergic hypothesis. *Exp Neurol,*163 (2):495-529.

Bayer TA, Wirths O. (2010). Intracellular accumulation of amyloid-beta –a predictor for synaptic dysfunction and neuron loss in Alzheimer's disease. *FNAGI*, 2(8):1-10.

Beckmann N, Schuler A, Mueggler T, Meyer EP, Wiederhold KH, Staufenbiel M, Krucher T. (2003). Age-dependent cerebrovascular abnormalities and blood flow disturbances in APP23 mice modeling Alzheimer's disease. *J Neurosci*., 23(24):8453-8459.

Benilova I, Karran E, De Strooper B. (2012). The toxic Aβ oligomer and Alzheimer's disease: an emperor in need of clothes. *Nat Neurosci*., 15(3):349-357.

Bi X, Gall CM, Zhou J, Lynch G. (2002). Uptake and pathogenic effects of amyloid β peptide 1-42 are enhanced by integrin antagonists and blocked by NMDA receptor antagonists. *Neuroscience*, 112:827-840.

Bilkei-Gorzo A. (2014). Genetic mouse models of brain ageing and Alzheimer's disease. *Pharmacol Ther*., 142(2):244-257.

Billings LM, Oddo S, Green KN, McGaugh JL, LaFerla FM. (2005). Intraneuronal Abeta causes the onset of early Alzheimer's disease-related cognitive deficits in transgenic mice. *Neuron*, 45(5):675-688.

Blanchard V, Moussaoui S, Czech C, Touchet N, Bonici B, Planche M, Canton T, Jedidi I, Gohin M, Wirths O, Bayer TA, Langui D, Duyckaerts C, Tremp G, Pradier L. (2003). Time sequence of maturation of dystrophic neuritis associated with Abeta deposits in APP/PS1 transgenic mice. *Exp Neurol.*, 184(1):247-263.

Blurton-Jones M, LaFerla F. (2006). Pathways by which Aβ facilites tau pathology. *Curr Alzheimer Res.*, 3:437-448.

Boche D, Perry VH, Nicoll JA. (2013) Review: activation patterns of microglia and their identification in the human brain. *Neuropathol Appl Neurobiol.* 39(1):3-18.

Bolmont T, Haaiss F, Eicke D, Radde R, Mathis C, Klunk WE, Kohsaka S, Jucker M, Calhoun ME. (2008). Dynamics of the microglial/amyloid interaction indicate a role in plaque maintenance. *J Neurosci.*, 28(16):4283-4292.

Bondolfi L, Calhoun M, Ermini F, Kuhn HG, Wiederhold KH, Walker L, Staufenbiel M, Jucker M. (2002). Amyloid associated neuron loss and gliogenesis in the neocortex of amyloid precursor protein transgenic mice. *J Neurosci*., 22(2):515-522.

Bondy CA, Cheng CM.(2004) Signaling by insulin-like growth factor 1 in brain. *Eur J Pharmacol.* 19;490(1-3):25-31. Review

Borchelt DR, Thinakara G, Eckman CB, Lee MK, Davenport F, Ratovitsky T, Prada CM, Kim G, Seekins S, Yager D, Slunt HH, Wangc R, Seeger M, Levev AI, Gandy SE, Copeland NG, Jenkins NA, Price DL, Younkin SG, Sisodia SS. (1996). Familial Alzheimer's disease-linked presenilin 1 variants elevate Abeta1-42/1-40 ratio in vitro and in vivo. *Neuron*, 17(5):1005-1013.

Borchelt DR, Ratovitski T, van Lare J, Lee MK, Gonzales V, Jenkins NA, Copeland NG, Price DL, Sisodia SS. (1997). Accelerated amyloid deposition in the brains of transgenic mice coexpressing mutant presenilin 1 and amyloid precursor proteins. *Neuron*, 19(4):393-345.

Bornemann KD, Wiederhold KH, Pauli C, Ermini F, Stalder M, Schnell L, Sommer B, Jucker M, Staufenbiel M. (2001). Abeta induced inflammatory processes in microglia cells of APP23 transgenic mice. *Am J Pathol.*, 158(1):63-73.

Boutajangout A, Authelet M, Blanchard V, Touchet N, Tremp G, Pradier L, Brion JP. (2004). Characterisation of cytoskeletal abnormalities in mice transgenic wild-type human tau an falimilial Alzheimer's disease mutants of APP and presenilin-1. *Neurobiol Dis.*, 15(19):47-60.

Braithwaite SP, Schmid RS, He DN, Sung ML, Cho S, Resnick L, Monaghan MM, Hirst WD, Essrich C, Reinhart PH, Lo DC. (2010). Inhibition of c-Jun kinase provides neuroprotection in a model of Alzheimer's disease. *Neurobiol Dis.* 39(3):311-7.

Brunden KR, Trojanowski JQ and Lee VM. (2009) Advances in tau-focused drug discovery for Alzheimer's disease and related tauopathies. *Nat Rev Drug Discov*. 8: 783-793.

Butovsky O, Koronyo-Hamaoui M, Kunis G, Ophir E, Landa G, Cohen H, Schwartz M. (2006). Glatiramer acetate fights against Alzheimer's disease by inducing dendritic-like microglia expressing insulin-like growth factor 1. *Proc Natl Acad Sci USA*, 103(31):11784-11789.

Butovsky O, Talpalar AE, Ben-Yaakov K, Schwartz M. (2005) Activation of microglia by aggregated β-amyloid or lipopolysaccharide impairs MHC-II expression and renders them cytotoxic whereas IFN-gamma and IL-4 render them protective. Mol Cell Neurosci. 29(3):381-93.

Cabezas R, Avila M, Gonzalez J, El-Bachá RS, Báez E, García-Segura LM, Jurado Coronel JC, Capani F, Cardona-Gomez GP, Barreto GE. (2014) Astrocytic modulation of blood brain barrier: perspectives on Parkinson's disease. *Front Cell Neurosci*. 8:211.

Cantarella G, Uberti D, Carsana T, Lombardo G, Bernardini R, Memo M. (2003) Neutralization of TRAIL death pathway protects human neuronal cell line from beta-amyloid toxicity. *Cell Death Differ* 10:134–141.

Capsoni S, Giannotta S, Cattaneo A. (2002) Nerve growthfactor and galantamine ameliorate early signs of neurodegeneration in anti-nerve growth factor mice. *PNAS* 99: 12432-12437.

Capsoni S, Tiveron C, Vignone D, Amato G, Cattaneo A. (2010) Dissecting the involvement of tropomyosinrelated kinase A and p75 neurotrophin receptor signaling in NGF deficit-induced neurodegeneration. *PNAS* 107: 12299-12304.

Cardona AE, Pioro EP, Sasse ME, Kostenko V, Cardona SM, Dijkstra IM, Huang D, Kidd G, Dombrowski S , Dutta R, Lee JC, Cook DN, Jung S, Lira SA, Littman DR, Ransohoff RM. (2006). Control of microglial neurotoxicity by the fractalkine receptor. *Nat Neurosci* 9:917–924.

Cascella R, Conti S, Tatini F, Evangelisti E, Scartabelli T, Casamenti F. (2013) Extracellular chaperones prevent Abeta-induced toxicity in rat brains. *Biochim Biophys Acta - Molecular Basis of Disease* 1832,2013:1217–1226.

Chan-Palay V, Lang W, Allen YS, Haesler U, Polak JM. (1985). Cortical neurons immunoreactive with antisera against neuropeptide Y are altered in Alzheimer's-type dementia. *J Comp Neurol*., 238:390–400.

Chen YR, Glabe CG. (2006) Distinct Early Folding and Aggregation Properties of Alzheimer Amyloid-β Peptides Aβ40 and Aβ42. *J Biol Chem.* 281: 24414-24422.

Cherry JD, Olschowka JA, O'Banion MK. (2014). Neuroinflammation and M2 microglia: the good, the bad, and the inflamed. *J Neuroinflammation*., 11:98.

Chhor V, Le Charpentier T, Lebon S, Oré MV, Celador IL, Josserand J, Degos V, Jacotot E, Hagberg H, Sävman K, Mallard C, Gressens P, Fleiss B. (2013) Characterization of phenotype markers and neuronotoxic potential of polarised primary microglia in vitro. *Brain Behav Immun*. 32:70-85.

Chitnis T, Imitola J, Wang Y, Elyaman W, Chawla P, Sharuk M, Raddassi K, Bronson RT, Khoury SJ. (2007). Elevated neuronal expression of CD200 protects Wlds mice from inflammation-mediated neurodegeneration. *Am J Pathol*., 170:1695–1712.

Cho SH, Sun B, Zhou Y, Kauppinen TM, Halabisky B, Wes P, Ransohoff RM, Gan L. (2011). CX3CR1 protein signaling modulates microglial activation and protects against plaque independent cognitive deficits in a mouse model of Alzheimer disease. *J Biol Chem.,* 286(37):32713-32722.

Chui DH, Tanahashi H, Ozawa K, Ikeda S, Checler F, Ueda O, Suzuki H, Araki W, Inoue H, Shirotani K, Takahashi K,Gallyas F, Tabira T. (1999). Transgenic mice with Alzheimer presenilin 1 mutations show accelerated neurodegeneration without amyloid plaque formation. *Nat Med., 5(5):560-564.*

Cohen E, Paulsson JF, Blinder P, Burstyn-Cohen T, Du D, Estepa G. (2009). Reduced IGF-1 Signaling delays age-associated proteotoxicity in mice. *Cell*, 139:1157–1169

Colton CA, Mott RT, Sharpe H, Xu Q, Van Nostrand WE, Vitek MP. (2006). Expression profiles for macrophage alternative activation genes in AD and in mouse models of AD. *J Neuroinflammation*, 3(27):1-12.

Condello C, Schain A, Grutzendler J. (2011). Multicolor time-stamp reveals the dynamics and toxicity of amyloid deposition. *Sci Rep*., 2011,1:19.

Condello C, Yuan P, Schain A, Grutzendler J. (2015). Microglia constitute a barrier that prevents neurotoxic protofibrillar Aβ42 hotspots around plaques. *Nat Commun*., 6:6176.

Corbo CP, Alonso A del C. (2011). Therapeutic targets in Alzheimer's disease and related tauopathies. *Prog Mol Biol Transl Sci*., 98: 47–83.

Coyle JT, Price DL, DeLong MR. (1983). Alzheimer's disease: a disorder of cortical cholinergic innervation. *Science,* 219 (4589): 1184-1190.

Craig LA, Hong NS, McDonald RJ. (2011). Revisiting the cholinergic hypothesis in the development of Alzheimer's disease. *Neurosci Biobehav Rev*., 35:1397-1409.

Crews L, Masliah E. (2010). Molecular mechanisms of neurodegeneration in Alzheimer's disease. *Hum Mol Genet.,* 19(R1):R12-20.

Cribbs DH, Berchtold NC, Perreau V, Coleman PD, Rogers J, Tenner AJ, Cotman CW. (2012). Extensive innate immune gene activation accompanies brain aging, increasing vulnerability to cognitive decline and neurodegeneration: a microarray study. *J Neuroinflammation.* 9:179.

Crimins JL, Pooler A, Polydoro M, Luebke JI, Spires-Jones TL. (2013). The intersection of amyloid β and tau in glutamatergic synaptic dysfunction and collapse in Alzheimer's disease. *Ageing Res Rev*., 12:757-63.

Crowther DC, Kinghorn KJ, Page R, Lomas DA. (2004). Therapeutic targets from a Drosophila model of Alzheimer's disease. *Curr Opin Pharmacol.*, 4:513-516.

Cruts M, Theuns J, Van Broeckhoven C. (2012). Locus-specific mutation databases for neurodegenerative brain diseases. *Hum Mutat.* 33(9):1340-4.

Cummings BJ, Head E, Ruehl W, Milgram NW, Cotman CW. (1996). The canine as an animal model of human aging and dementia. *Neurobiol Aging,* 17, 259–268.

Czech C, Tremp G, Pradier L. (2000). Presenilins and Alzheimer's disease: biological functions and pathogenic mechanisms. Prog Neurobiol., 60(4):363-84. Review.

Davies CA, Mann DM, Sumpter PQ and Yates PO. (1987). A quantitative morphometric analysis of the neuronal and synaptic content of the frontal and temporal cortex in patients with Alzheimer's disease. *JNeurol Sci.,* 78(2):151-164.

Davies P, Katzman R, Terry RD. (1980). Reduced somatostatin-like immunoreactivity in cerebral cortex from cases of Alzheimer disease and Alzheimer senile dementa. *Nature*, 288:279–280.

Deane R, Zlokovic BV. (2007). Role of the blood-brain barrier in the pathogenesis of Alzheimer's disease. *Curr Alzheimer Res*., 4(2):191-7. Review.

Decker H, Lo KY, Unger SM, Ferreira ST, Silverman MA. (2010) Amyloid-β peptide oligomers disrupt axonal transport through an NMDA receptor-dependent mechanism that is mediated by Glycogen Synthase Kinase 3β in primary cultured hippocampal neurons. The Journal of Neuroscience, 30: 9166-9171.

De Felice FG, Velasco PT, Lambert MP, Viola K, Fernandez SJ, Ferreira ST, Klein WL. (2007). Abeta oligomers induce neuronal oxidative stress through an N-methyl-D-aspartate receptor-dependent mechanism tha tis blocked by the Alzheimer drug memantine. *J Biol Chem.,* 282:11590–11601**.**

De Jong EK, Dijkstra IM, Hensens M, Brouwer N, van Amerongen M, Liem RS, Boddeke HW, Biber K. (2005). Vesicle-mediated transport and reléase of CCL21 in endangered neurons: a posible explanation fo rmicroglia activation remote from a primary lesion. *J Neurosci.,* 25:7548–7557.

De la Torre JC. (2011). Three postulates to help identify the cause of Alzheimer's disease. *J Alzheimers Dis.*, 24(4):657-668.

DeKosky ST, Scheff SW. (1990). Synapse loss in frontal cortex biopsies in Alzheimer's disease: correlation with cognitive severity. *Ann Neurol*., 27, 457-464.

Deschaintre Y, Richard F, Leys D, Pasquier F. (2009). Treatment of vascular risk factors is associated with slower decline in Alzheimer disease. *Neurology,* 73(9):674-680.

De Strooper B. (2003). Aph-1, Pen-2, and nicastrin with presenilin generate an active γ-secretase complex. *Neuron*, 38:9–12.

De Strooper B. (2010). Proteases and proteolysis in Alzheimer Disease: A multifactorial view on the disease process. *Physiol Rev*., 90:465-494.

Devi L, Ohno M. (2010). Genetic reductions of beta-site amyloid precursor protein-cleaving enzyme 1 and amyloid-beta ameliorate impairment of conditioned taste aversión memory in 5XFAD Alzheimer's disease model mice. *Eur J Neurosci.,* 31:110–118.

Dewachter I, Ris L, Croes S, Borghgraef P, Devijer H, Voets T, Nilius B, Godaux E, Van Leuven F. (2008). Modulation of synaptic plasticity and Tau phosphorylation by wild-type and mutant presenilin1. *Neurobiol Aging*, 26:639-652.

Dickson DW. (1997). The pathogenesis of senile plaques. *J Neuropathol Exp Neurol*., 56(4):321-339.

Diniz B, Machado-Vieira R, Forlenza O. (2013). Lithium and neuroprotection: translational evidence and implications for the treatment of neuropsychiatric disorders. *Neuropsychiatr Dis Treat*., 9:493–500

Dohler F, Sepulveda-Falla D, Krasemann S, Altmeppen H, Schluter H. (2014). High molecular mass assemblies of amyloid-β oligomers bind prion protein in patients with Alzheimer's disease. *Brain*, 137: 873–886.

Duan RS, Yang X, Chen ZG, Lu MO, Morris C, Winbland B, Zhu J. (2008). Decreased fractalkine and increased IP-10 expression in aged brain of APPswe transgenic mice. *Neurochem Res.,* 33:1085–1089.

Dudai Y, Morris RG. (2013). Memorable trends. *Neuron,* 80(3):742-50.

Duyckaerts C, Potier MC, Delatour B. (2008). Alzheimer disease models and human neuropathology: similarities and differences. *Acta Neuropathol.*, 115(1):5-38.

Duyckaerts C, Delatour B, Potier MC. (2009). Classification and basic pathology of Alzheimer disease. *Acta Neuropathol*., 118:5-36.

Eckman EA, Adams SK, Troendle FJ, Stodola BA, Kahn MA, Fauq AH. (2006). Regulation of steady-state β-amyloid levels in the brain by neprilysin and endothelin-converting enzyme but not angiotensin-converting enzyme. *J Biol Chem*., 281:30471–30478.

Eckman EA, Reed DK, Eckman CB. (2001). Degradation of the Alzheimer's amyloid β peptide by endothelin-converting enzyme. *J Biol Chem.,* 276:24540–24548.

Eckman EA, Watson M, Marlow L, Sambamurti K, Eckman CB. (2003). Alzheimer's disease β-amyloid peptide is increased in mice deficient in endothelin-converting enzyme. *J Biol Chem*., 278:2081–2084.

Edbauer D, Winkler E, Regula JT, Pesold B, Steiner H, Haass C. (2003). Reconstitution of gamma-secretase activity. *Nat Cell Biol*., 5(5):486-8.

Edison P, Archer HA, Gerhard A, Hinz R, Pavese N, Turkheimer FE, Hammers A, Tai YF, Fox N, Kennedy A, Rossor M, Brooks DJ. (2008). Microglia, amyloid, and cognition in Alzheimer's disease: An [11C](R)PK11195-PET and [11C]PIB-PET study. *Neurobiol Dis.,* 32(3):412- 419.

Eikelenboom P, Veerhuis R, Scheper W, Rozemuller AJ, van Gool WA, Hoozemans JJ. (2006). The significance of neuroinflammation in understanding Alzheimer's disease. *J Neural Transm.,* 113(11):1685-95. Review

Eisenstein M. (2011) Genetics: finding risk factors. *Nature,* 475: S20-22.

Elder GA, Gama Sosa MA, De Gasperi R, Dickstein DL, Hof PR. (2010a). Presenilin transgenic mice as models of Alzheimer's disease. *Brain Struct Funct*., 214:127-143.

Elder GA, Gama Sosa MA, De Gasperi R. (2010b). Transgenic mouse models of Alzheimer's disease. *Mt Sinai J Med*., 77:69-81.

El Khoury J, Toft M, Hickman SE, Means TK, Terada K, Geula C, Luster AD. (2007). Ccr2 deficiency impairs microglial accumulation and accelerates progression of Alzheimer-like disease. *Nat Med.,* 13(4):432-438.

Engel T, Hernandez F, Avila J, Lucas JJ. (2006). Full reversal of Alzheimer's disease-like phenotype in a mouse model with conditional overexpression of Glycogen Synthase Kinase-3. *Journal of Neuroscience.,* 26: 5083-5090.

Esparza TJ, Zhao H, Cirrito JR, Cairns NJ, Bateman RJ. (2013). Amyloid-beta oligomerization in Alzheimer dementia versus high-pathology controls. *Ann Neuro.,I* 73: 104–119.

Evin G, Weidemann A. (2002). Biogenesis and metabolism of Alzheimer's disease Aβ amyloid peptides. *Peptides*, 23(7):1285-1297.

Farrer LA, Cupples LA, Haines JL, Hyman B, Kukull WA, Mayeux R, Myers RH, PericakVance MA, Risch N and van Duijn CM. (1997). Effects of age, sex, and ethnicity on the association between apolipoprotein E genotype and Alzheimer disease. A metaanalysis. APOE and Alzheimer Disease Meta Analysis Consortium. *JAMA*. 278: 1349-1356.

Farris W, Schütz SG, Cirrito JR, Shankar GM, Sun X, George A, Leissring MA, Walsh DM, Qiu WQ, Holtzman DM, Selkoe DJ. (2007). Loss of neprilysin function promotes amyloid plaque formation and causes cerebral amyloid angiopathy. The American Journal of Pathology, *Am J Pathol.,* 171(1):241-251.

Forlenza O, Paula V, Machado-Vieira R, Diniz B, Gattaz W. (2012). Does Lithium Prevent Alzheimer's disease? *Drugs Aging*, 29:335–342

Frautschy SA, Cole GM, Baird A. (1992). Phagocytosis and deposition of vascular β-amyloid in rat brains injected with Alzheimer β-amyloid. *Am J Pathol.*, 140(6):1389-1399.

Friedman LG, Qureshi YH, Yu WH. (2015). Promoting autophagic clearance: viable therapeutic targets in Alzheimer's disease. *Neurotherapeutics,* 12:94-108.

Fu W, Jhamandas JH. (2014). Role of astrocytic glycolytic metabolism in Alzheimer's disease pathogenesis. *Biogerontology*, 15(6):579-586.

Fuhrmann M, Bittner T, Jung CKE, Burgold S, Page RM, Mitteregger G, Haass C, LaFerla FM, Krestzschmar H, Herms J. (2010). Microglial Cx3cr1 knockout prevents neuron loss in a mouse model of Alzheimer's disease. *Nat Neurosci.*, 13(4):411-413.

Funalot B, Ouimet T, Claperon A, Fallet C, Delacourte A, Epelbaum J, Subkowski T, Léonard N, Codron V, David JP, Amouyel P, Schwartz JC, Helbecque N. (2004). Endothelin-converting enzyme-1 is expressed in human cerebral cortex and protects against Alzheimer's disease. *Mol Psychiatry,* 9:1122-8.

Gendron TF, Petrucelli L. (2009). The role of tau in neurodegeneration. *Mol Neurodegener.,* 4:13.

German DC, Manaye KF, White CL, Woodward DJ, McIntire DD, Smith WK Kalaria RN, Mann DM. (1992). Diseasespecific patterns of locus coeruleus cell loss. *Ann Neurol.*, 32(5):667 676.

Giannakopoulos P, Herrmann FR, Bussière T, Bouras C, Kövari E, Perl DP, Morrison JH, Gold G, Hof PR. (2003). Tangle and neuron numbers, but not amyloid load, predict cognitive status in Alzheimer's disease. *Neurology*, 13;60(9):1495-500.

Giannakopoulos P, Hof PR, Bouras C. (1998). Selective vulnerability of neocortical association areas in Alzheimer's disease. *Microsc Res Tech.,* 43(1):16-23.

Ginhoux F, Greter M, Leboeuf M, Nandi S, See P, Gokhan S, Mehler MF, Conway SJ, Ng LG, Stanley ER, Samokhvalov IM, Merad M. (2010). Fate mapping analysis reveals that adult microglia derive from primitive macrophages. *Science,* 330:841–845.

Girão da Cruz MT, Jordão J, Dasilva KA, Ayala-Grosso CA, Ypsilanti A, Weng YQ, Laferla FM, McLaurin J, Aubert I. (2012). Early increases in soluble amyloid-β levels coincide with cholinergic degeneration in 3xTg-AD mice. *J Alzheimers Dis*., 32(2):267-72.

Giuffrida ML, Caraci F, Pignataro B, Cataldo S, De Bona P, Bruno V, Molinaro G, Pappalardo G, Messina A, Palmigiano A, Garozzo D, Nicoletti F, Rizzarelli E, Copani A. (2009). Beta-amyloid monomers are neuroprotective. *J Neurosci.*, 29(34):10582-10587.

Glass C, Saijo K, Winner B, Marchetto MC, Gage FH. (2010). Mechanisms underlying inflammation in neurodegeneration. *Cell*, 140(6):918-934.

Glenner GG, Wong CW. (1984). Alzheimer's disease: initial report of the purification and characterization of a novel cerebrovascular amyloid protein. *Biochem Biophys Res Commun.,* 120: 885-890.

Glezer I, Simard AR, Rivest S. (2007) Neuroprotective role of the innate immune system by microglia. *Neuroscience*, 147(4):867-83. Review.

Goldsbury C, Frey P, Olivieri V, Aebi U, Muller SA. (2005). Multiple assembly pathways underlie amyloid- fibril polymorphisms. *J Mol Biol.,* 352:282-298.

Gómez-Isla T, Price JL, McKeel J, Morris JC, G rowdon JH, Hyman BT. (1996). Profound loss of layer II entorhinal cortex neurons occurs in very mild Alzheimer's disease. *J Neurosci*., 16: 4491-4500

Gomez-Isla T, Spires T, De Calignon A, Hyman BT. (2008). Neuropathology of Alzheimer's disease. *Handb Clin Neurol*., 89:233-243.

Gomez-Nicola D, Perry VH. (2015). Microglial dynamics and role in the healthy and diseased brain: a paradigm of functional plasticity. *Neuroscientist*, 21(2):169-184.

Gong Y, Chang L, Viola KL, Lacor PN, Lambert MP, Finch CE, Krafft GA, Klein WL. (2003). Alzheimer's disease-affected brain: presence of oligomeric Aβ ligands (ADDLs) suggests a molecular basis for reversible memory loss. *Proc Natl Acad Sci U S A.,* 100:10417–10422.

Götz J. (2001). Tau and transgenic animal models. *Brain Res Rev.*, 35(3):266-286.

Gralle M, Ferreira ST. (2007). Structure and functions of the human amyloid precursor protein: the whole is more than the sum of its parts. *Prog Neurobiol*., 82(1):11-32.

Greenfield JP, Tsai J, Gouras GK, Hai B, Thinakaran G, Checler F, Sisodia SS, Greengard P, Xu H. (1999). Endoplasmic reticulum and trans-Golgi network generate distinct populations of Alzheimer β-amyloid peptides. *Proc Natl Acad Sci USA*., 96(2):742-747.

Guerreiro R, Wojtas A, Bras J, Carrasquillo M, Rogaeva E, Majouine E, Cruchaga C, Sassi C, Kauwe JS, Younkin S, Hazrati L, Collinge J, Pocock J, Lashley T, Williams J, Lambert JC, Amouyel P, Goate A, Rademakers R, Morgan K, Powell J, St George-Hyslop P, Singleton A, Hardy J. (2013). TREM2 variants in Alzheimer's disease. *N Engl J Med*., 268:117-127.

Haass C, Hung AY, Selkoe DJ. (1991). Processing of β-amyloid precursor protein in microglia and astrocytes favors an internal localization over constitutive secretion. *The Journal of Neuroscience.* 11: 3783-3793

Haass C, Selkoe DJ. (2007). Soluble protein oligomers in neurodegeneration: lessons from the Alzheimer's amyloid beta-peptide. *Nat Rev Mol Cell Biol.*, 8(2):101-112.

Hans Kretzschmar. (2009) Brain banking: opportunities, challenges and meaning for the future. *Nature Reviews NeuroscienceE,* **10,** 70-78.

Hardy JA, Higgins GA. (1992). Alzheimer's disease: the amyloid cascade hypothesis. *Science*, 256(5054):184-185.

Hardy J, Selkoe DJ. (2002). The amyloid hypothesis of Alzheimer's disease: Progress and problems on the road to therapeutics. *Science,* 297:353-356.

Heiseke A, Aguib Y, Riemer C, Baier M, Schtzl HM. (2009). Lithium induces clearance of protease resistant prion protein in prion-infected cells by induction of autophagy. *J Neurochem*.,109:25–34.

Heneka MT, Ramanathan M, Jacobs AH, Dumitrscu-Ozimek L, Bilkei-Gorzo A, DebeirT, Sastre M, Galldiks N, Zimmer A, Hoehn M, Heiss WD, Klockgether T, Staufenbiel M. (2006). Locus coeruleus degeneration promotes Alzheimer pathogenesis in amyloid precursor protein 23 transgenic mice. *J Neurosci*., 26(5):1343-1354.

Heneka MT, O'Banion MK. (2007). Inflammatory processes in Alzheimer's disease. *J Neuroimmunol.*, 184(1-2):69-91.

Heneka MT, Golenbock DT, Latz E. (2015a).Innate immunity in Alzheimer's disease. *Nat Immunol*., 16(3):229-236.

Heppner FL, Ransohoff RM, Becher B. (2015). Immune attack: the role of inflammation in Alzheimer disease. *Nat Rev Neurosci*., 16(6):358-372.

Herrup K. (2015). The case for rejecting the amyloid cascade hypothesis. *Nat Neurosci*., 18(6):794-799.

Hiltunen M, van Groen T, Jolkkonen J. (2009). Functional roles of amyloid-beta protein precursor and amyloid-beta peptides: evidence from experimental studies. *J Alzheimers Dis.,* 18(2):401-412.

Hong S, Ostaszewski B, Yang T, O'Malley T, Jin M. (2014). Soluble Aβ oligomers are rapidly sequestered from brain ISF In-vivo and bind GM1 ganglioside on cellular membranes. *Neuron*, 82: 308–319.

Hong S, Quintero-Monzon O, Ostaszewski BL, Podlisny DR, Cavanaugh WT. (2011). Dynamic analysis of amyloid β-protein in behaving mice reveals opposing changes in ISF versus parenchymal Aβ during age-related plaque formation. *J Neurosci.,* 31: 15861–15869.

Houeland G, Romani A, Marchetti C, Amato G, Capsoni S,Cattaneo A, Marie H. (2010). Transgenic mice with chronic NGF deprivation and Alzheimer's disease-like pathology display hippocampal region-specific impairments in Short- and Long-Term plasticities. *The Journal of Neuroscience*, 30: 13089-13094.

Hunt CE, Turner AJ. (2009). Cell biology, regulation and inhibition of β-secretase (BACE-1). *FEBS J*., 276(7):1845-59.

Iadecola C. (2004). Neurovascular regulation in the normal brain and in Alzheimer's disease. *Nat Rev Neurosci.*, 5(5):347-360.

Imahori K, Uchida T. (1997). Physiology and pathology of tau protein kinase in relation to Alzheimer´s disease. *J Biochem*., 121(2):179-88. Review

Imai F, Suzuki H, Oda J, Ninomiya T, Ono K, Sano H, Sawada M. (2007) Neuroprotective effect of exogenous microglia in global brain ischemia. *J. Cereb Blood Flow Metab*. 27:488–500.

Ingelsson M, Fukumoto H, Newell KL, Growdon JH, Hedley-Whyte ET, Frosch MP, Albert MS, Hyman BT, Irizarry MC. (2004). Early Abeta accumulation and progressive synaptic loss, gliosis, and tangle formation in AD brain. Neurology., 23;62(6):925-31.

Inoue K, Koizumi S, Tsuda M. (2007). The role of nucleotides in the neuron-glia communication responsible for the brain functions. *J Neurochem*., 102:1447–1458.

Iqbal K, Grundke-Iqbal I. (2008). Alzheimer neurofibrillary degeneration: significance, ethiopathogenesis, therapeutics and prevention. *J Cell Mol Med*., 12(1):38-55.

Iribarren P, Chen K, Hu J, Zhang X, Gong W, Wang JM. (2005). IL-4inhibits the expression of mouse formyl peptide receptor 2, a recepto rfor amyloid β 1–42, in TNF-alpha-activated microglia. J Immunol., 175:6100–6106.

Itagaki S, McGreer PL, Akiyama H. (1988). Presence of T-cytotoxic suppressor and leucocyte common antigen positive cells in Alzheimer's disease brain tissue. *Neurosci Lett*., 91:259–264.

Ittner LM, Ke YD, Delerue F, Bi M, Gladbach A, van Eersel J, Wolfing H, Chieng BC, Christie MJ, Napier IA, Eckert A, Staufenbiel M, Hardeman E, Gotz J. (2010). Dendritic function of tau mediates amyloid-β toxicity in Alzheimer's disease mouse models. *Cell.* 142:387–397.

J A, Wandosell F, Hernández F. (2010).:Role of glycogen synthase kinase-3 in Alzheimer's disease pathogenesis and glycogen synthase kinase-3 inhibitors. *Expert Rev Neurotherapeutics*. 10:703–710

Jankowsky JL, Slunt HH, Ratovitski T, Jenkins NA, Copeland NG, Borchelt DR. (2001). Coexpression of multiple transgenes in mouse CNS: a comparison of strategies. *Biomol Eng.,* 17:157–165.

Jankowsky JL, Younkin LH, Gonzales V, Fadale DJ, Slunt HH, Lester HA, Younkin SG, Borchelt DR. (2007). Rodent A beta modulates the solubility and distribution of amyloid deposits intransgenic mice. *J Biol Chem*., 282(31):22707-22720.

Jiang ZJ, Richardson JS, Yu PH. (2008). The contribution of cerebral vascular semicarbazidesensitive amine oxidase to cerebral amyloid angiopathy in Alzheimer's disease. *Neuropathol Appl Neurobiol.*, 34(2):194-204.

Jimenez S, Baglietto-Vargas D, Caballero C, Moreno-Gonzalez I, Torres M, Sanchez-Varo R, Ruano D, Vizuete M, Gutierrez A, Vitorica J. (2008). Inflammatory response in the hippocampus of PS1M146L/APP751SL mouse model of Alzheimer's disease: age-dependent switch in the microglial phenotype from alternative to classic. *J Neurosci.,* 28(45):11650-61.

Jimenez S, Torres M, Vizuete M, Sanchez-Varo R, Sanchez-Mejias E, Trujillo-Estrada L, et al. (2011). Age-dependent accumulation of soluble amyloid beta (Aβ) oligomers reverses the neuroprotective effect of soluble amyloid precursor protein alpha (sAPPalpha) by modulating phosphatidylinositol 3-Kinase (PI3K)/Akt-GSK-3beta pathway in Alzheimer mouse model.J Biol Chem., 286:18414–18425.

Jin M, Shepardson N, Yang T, Chen G, Walsh D, Selkoe DJ. (2011). Soluble amyloid β protein dimers isolated from Alzheimer cortex directly induce Tau hyperphosphorylation and neuritic degeneration. *Proc Natl Acad Sci USA*.,108:5819–5824.

Johnstone M, Gearing AJ, Miller KM. (1999). A central role for astrocytes in the inflammatory response to beta-amyloid; chemokines, cytokines and reactive oxygen species are produced. *J Neuroimmunol.,* 93(1-2):182-193.

Jonsson T, Stefansson H, Steinberg S, Jonsdottir I, Jonsson PV, Snaedal J, Bjornsson S, Huttenlocher J, Levey AI, Lah JJ, Rujescu D, Hampel H, Giegling I, Andreassen OA, Engedal K, Ulstein I, Djurovic S, Ibrahim- Verbaas C, Hofman A, Ikram MA, van Duijn CM, Thorsteinsdottir U, Kong A, Stefansson K. (2013). Variant of TREM2 associated with the risk of Alzheimer's disease. *N Engl J Med.*, 368(2):107-116.

Kalaria RN. (1999). The blood-brain barrier and cerebrovascular pathology in Alzheimer's disease. *Ann NY Acad Sci.,* 893: 113–125.

Kalaria RN. (2000) The role of cerebral ischemia in Alzheimer's disease. *Neurobiol Aging,* 21: 321–330.

Kalaria R. (2002). Similarities between Alzheimer's disease and vascular dementia. *J Neurol Sci.,* 203-204:29-34.

Kalinin S, Polak PE, Lin SX, Sakharkar AJ, Pandey SC, Feinstein DL. (2012). The noradrenaline precursor L-DOPS reduces pathology in a mouse model of Alzheimer's disease. *Neurobiol Aging,* 33(8):1651-1663.

Kandalepas P, Sadleir K, Eimer W, Zhao J, Nicholson D, Vassar R. (2013). Erratum to: The Alzheimer's beta-secretase BACE1 localizes to normal presynaptic terminals and to dystrophic presynaptic terminals surrounding amyloid plaques.Acta Neuropathol.,126:329–352.

Kanemitsu H, Tomiyama T, Mori H. (2003). Human neprilysin is capable of degrading amyloid β peptide not only in the monomeric form but also the pathological oligomeric form. *Neuroscience Letters.* 350: 113-116.

Karlnoski R, Wilcock D, Dickey C, Ronan V, Gordon MN, Zhang W, Morgan D, Taglialatela G. (2007). Upregulation of Bcl-2 in APP transgenic mice is associated with neuroprotection. **Neurobiology of Disease**, 25: 179-188.

Karran E, Mercken M, De Strooper B. (2011). The amyloid cascade hypothesis for Alzheimer's disease: an appraisal for the development of therapeutics. *Nat Rev Drug Discov*.,10(9):698-712.

Kausahl A, Wani WY, Anand R, Gill KD. (2013). Spontaneous and induced nontransgenic animal model of AD: modeling AD using combinatorial approach. *Am J Alzheimer Dis Other Demen*., 28(4):318-326.

Kettenmann H, Kirchhoff F, Verkhratsky A. (2013). Microglia: new roles for the synaptic stripper. *Neuron,* 77(1):10-8.

Kielian T. (2006) Toll-like receptors in central nervous system glial inflammation and homeostasis. *J Neurosci Res*., 83:711-30. Review.

Kimura T, Ishiguro K, Hisanaga S. (2014). Physiological and pathological phosphorylation of tau by Cdk5. *Front Mol Neurosci*., 7:65.

Knowles JK, Rajadas J, Nguyen TV, Yang T, LeMieux MC, Vander Griend L, Ishikawa C, Massa SM, WyssCoray T, Longo FM. (2009). The p75 neurotrophin receptor promotes Amyloid-β(1-42)-induced neuritic dystrophy in vitro and in vivo. *The Journal of Neuroscience*, 29: 10627-10637.

Koenigsknecht-Talboo J, Landreth GE. (2005) Microglial phagocytosis induced by fibrillar beta-amyloid and IgGs are differentially regulated by proinflammatory cytokines. *J Neurosci.,* 25:8240–8249.

Koffie RM, Meyer-Luehmann M, Hashimoto T, Adams KW, Mielke ML, Garcia-Alloza M,et al. (2009). Oligomeric amyloid-beta¦ associates with postsynaptic densities and correlates with excitatory synapse loss near senile plaques. *Proc Natl Acad Sci USA.*,106:4012–4017

Kojro E, Postina R, Buro C, Meiringer C, Gehrig-Burger K, Fahrenholz F. (2006). The neuropeptide PACAP promotes [alpha]-secretase pathway for processing Alzheimer amyloid precursor protein*. FASEB J*., 20 (3): 512-514.

Kraft AW, Hu X, Yoon H, Yan P, Xiao Q, Wang Y, Gil SC, Brown J, Wilhelmsson U, Restivo JL, Cirrito JR, Holtzman DM, Kim J, Pekny M, Lee JM. (2013). Attenuating astrocyte activation accelerates plaque pathogenesis in APP/PS1 mice. *FASEB J.,* 27(1):187-198.

Kraft-Terry SD, Buch SJ, Fox HS, Gendelman HE. (2009). A coat of many colors: neuroimmune crosstalk in human immunodeficiency virus infection. *Neuron,* 64(1):133-45. Review.

Kurt MA, Davies DC, Kidd M, Duff K, Howlett DR. (2003). Hyperphosphorylated tau and paired helical filament-like structures in the brains of mice carrying mutant amyloid precursor protein and mutant presenilin-1 transgenes. *Neurobiol Dis*., 14(1):89-97.

Lacor PN, Buniel MC, Chang L, Fernandez SJ, Gong Y, Viola KL, Lambert MP, Velasco PT, Bigio EH, Finch CE, Krafft GA, Klein WL. (2004). Synaptic targeting b yAlzheimer's-related amyloid β oligomers. *JNeurosci*., 24:10191–10200.

LaFerla FM, Green KN, Oddo S. (2007). Intracellular amyloid-β in Alzheimer's disease. *Nat Rev Neurosci*., 8:499-509.

Lalonde R, Kim HD, Maxwell JA, Fukuchi K. (2005). Exploratory activity and spatial learning in 12-month-old APP(695)SWE/co+PS1/DeltaE9 mice with amyloid plaques*. Neurosci Lett.,* 390(2):87-92.

Lambert MP, Barlow AK, Chromy BA, Edwards C, Freed R, Liosatos M, Morgan TE, Rozovsky I, Trommer B, Viola KL, Wals P, Zhang C, Finch CE, Krafft GA, Klein WL. (1998). Diffusible, nonfibrillar ligands derived from Abeta1-42 are potent central nervous system neurotoxins. *Proc Natl Acad Sci USA.*, 95(11):6448-6453.

Lambert MP, Velasco PT, Chang L, Viola KL, Fernandez S, Lacor PN, Khuon D, Gong Y, Bigio EH, Shaw P, De Felice FG, Krafft GA, Klein WL. (2007) Monoclonal antibodies that target pathological assemblies of Abeta. *J Neurochem.,* 100:23–35.

Latta CH, Brothers HM, Wilcock DM. (2014). Neuroinflammation in Alzheimer's disease; a source of heterogeneity and target for personalized therapy. *Neuroscience*, S0306-4522(14)00820-3.

Lazarov O, Peterson LD, Peterson DA, Sisodia SS. (2006). Expression of familial Alzheimer's disease-linked presenilina-1 variant enhances perforant pathway lesion-induced neuronal loss in the entorhinal cortex. *JNeurosci.*, 26(2):429-434.

Lee VMY, Goedert M, Trojanowki Q. (2001). Neurodegenerative taupathies. *Ann Rev Neurosci.*, 24:1121-1159.

Lee DCY, Landreth GE. (2010). The role of microglia in amyloid clearance from AD brain. *J Neural Transm.,* 117:949-960.

Lee SM, Yune TY, Kim SJ, Kim YC, Oh YJ, Markelonis GJ, Oh TH. (2004) Minocycline inhibits apoptotic cell death via attenuation of TNF-alpha expression following iNOS/NO induction by lipopolysaccharide in neuron/glia co-cultures. *J Neurochem*., 91:568–578.

Lesné S, Koh MT, Kotilinek L, Kayed R, Glabe CG, Yang A, Gallagher M, Ashe KH. (2006). A specific amyloid-beta protein assembly in the brain impairs memory. *Nature*, 440(7082):284-285.

Li M, Chen L, Hon Seng Lee D, Yu LC, Zhang Y. (2009b). The role of intracellular amyloid Aβ in Alzheimer's disease. *Prog Neurobiol.*,83:131-139.

Li R, Yang L, Lindholm K, Konishi Y, Yue X, Hampel H, Zhang D, Shen Y. (2004). Tumor necrosis factor death receptor signaling cascade is required for amyloid-beta protein-induced neuron death. *J Neurosci*., 24:1760–1771.

Lim D, Ronco V, Grolla AA, Verkhratsky A, Genazzani AA. (2014) Glial Calcium Signalling in Alzheimer's Disease. Rev Physiol Biochem Pharmacol., 167:45-65.

Liu C, Götz J. (2013). How it all started: tau and protein phosphatase 2A. *J Alzheimers Dis*., 37(3):483-94. Review.

Liu Z, Condello C, Schain A, Harb R, Grutzendler J. (2010). CX3CR1 in microglia regulates brain amyloid deposition through selective protofibrillar amyloid-β phagocytosis. *J Neurosci.,* 30(50):17091-17101.

Lucas JJ, Hernandez F, Gomez-Ramos P, Moran MA, Hen R, Avila J. (2001) Decreased nuclear [beta]-catenin, tau hyperphosphorylation and neurodegeneration in GSK-3β conditional transgenic mice. *EMBO J.,* 20: 27-39.

Luna-Muñoz J, Charles R. Harrington, Claude M. Wischik, Paola Flores-Rodríguez, Jesús Avila, Sergio R. Zamudio, Fidel De la Cruz, Raúl Mena, Marco A. Meraz-Ríos and Benjamin Floran-Garduño. (2013). Phosphorylation of Tau protein associated as a protective mechanism in the presence of toxic, C-Terminally truncated Tau in Alzheimer's disease. Understanding Alzheimer's disease. ISBN: 978-953-51-1009-5.

Lyons A, Downer EJ, Crotty S, Nolan YM, Mills KH, Lynch MA. (2007a). CD200 Ligand receptor interaction modulates microglial activation in vivo and in vitro: a role for IL-4. *J Neurosci*., 27:8309–8313.

Lyons A, Griffin RJ, Costelloe CE, Clarke RM, Lynch MA. (2007b). IL-4 attenuates the neuroinflammation induced by amyloid-β in vivo and in vitro. *J Neurochem.,* 101:771–781.

Malm TM, Koistinaho M, Parepalo M, Vatanen T, Ooka A, Karlsson S, Koistinaho J. (2005). Bone-marrow-derived cells contribute to the recruitment of microglial cells in response to β-amyloid deposition in APP/PS1 double transgenic Alzheimer mice. *Neurobiol Dis.*, 18(1):134-142.

Malm TM, Iivonen H, Goldsteins G, Keksa-Goldsteine V, Ahtoniemi T, Kanninen K, Salminen A, Auriola S, van Groen T, Tanila H, Koistinaho J. (2007) Pyrrolidine Dithiocarbamate activates Akt and improves spatial learning in APP/PS1 mice without affecting β-Amyloid Burden. *Journal of Neuroscience,* 27: 3712-3721.

Manaye KF, Mouton PR, Xu G, Drew A, Lei DL, Sharma Y, Rebeck GW, Turner S. (2013). Age-related loss of noradrenergic neurons in the brains of triple transgenic mice. *Age (Dordr),* 35(1):139-147.

Mandrekar S, Jiang Q, Lee CY, Koenigsknecht- Talboo J, Holtzman DM, Landreth GE. (2009). Microglia mediate the clearance of soluble Abeta through fluid phase macropinocytosis. *J Neurosci.,* 29(13):4252- 4262.

Mannini B, Cascella R, Zampagni M, Waarde-Verhagen M, Meehan S, Roodveldt C., et al. (2012). Molecular mechanisms used by chaperones to reduce the toxicity of aberrant protein oligomers.Proc Natl Acad Sci USA., 109:12479–12484.

Masliah E, Westland CE, Rockenstein EM, Abraham CR, Mallory M, Veinberg I, Sheldon E, Mucke L. (1997). Amyloid precursor proteins protect neurons of transgenic mice against acute and chronic excitotoxic injuries in vivo. Neuroscience 78: 135-146.

Masters CL, Simms G, Weinman NA, Multhaup G, McDonald BL, Beyreuther K. (1985). Amyloid plaque core protein in Alzheimer disease and Down syndrome. *PNAS*, 82: 4245-4249.

Mastrangelo MA, Bowers WJ. (2008). Detailed immunohistochemical characterization of temporal and spatial progression of Alzheimer's disease-related pathologies in male triple transgenic mice. *BMC Neurosci.,* 9:81.

Matarin M, Salih DA, Yasvoina M, Cummings DM, Guelfi S, Liu W, Nahaboo Solim MA, Moens TG, Paublete RM, Ali SS, Perona M, Desai R, Smith KJ, Latcham J, Fulleylove M, Richardson JC, Hardy J, Edwards FA. (2015). A Genome-wide Gene-Expression Analysis and Database in Transgenic Mice during Development of Amyloid or TauPathology. *Cell Rep*., 10(4):633-644.

Matsuo ES, Shin RW, Billingsley ML, Van deVoorde A, O'Connor M, Trojanowski JQ and Lee VM. (1994). Biopsy-derived adult human brain tau is phosphorylated at many of the same sites as Alzheimer's disease paired helical filament tau. *Neuron*, 13: 989-1002

McDonald CR, Gharapetian L, McEvoy LK, Fennema-Notestine C, Hagler DJ Jr, Holland D, Dale AM, Alzheimer's Disaese Neuroimaging Initiative. (2012). Relationship between regional atrophy rates and cognitive decline in mild cognitive impairment. *Neurobiol Aging,* 33:242-253.

Mc Donald JM, Savva GM, Brayne C, Welzel AT, Forster G, et al. (2010) The presence of sodium dodecyl sulphate-stable Abeta dimers is strongly associated with Alzheimer-type dementia. *Brain*, 133:1328–1341.

McDonald RJ. (2002). Multiple combinations of co-factors produce variants of age-related cognitive decline: a theory. *Can J Exp Psychol.,* 56(3):221-239.

McGeer EG, McGeer PL. (2010). Neuroinflammation in Alzheimer's disease and mild cognitive impairment: a field in its infancy. *J Alzheimers Dis.,* 19(1):355-361.

McNaull BBA, Todd S, McGuinness B, Passmore AP. (2010). Inflammation and Anti-Inflammatory strategies for Alzheimers's disease - A mini-review. *Gerontology*, 56:3-14.

Medeiros R, Prediger RD, Passos GF, Pandolfo P,Duarte FS ,Franco JL, Dafre AL, Di Giunta G,Figueiredo CP, Takahashi RN, Campos MM, Calixto JB. (2007). ConnectingTNF-α signaling.pathways.to.iNOS.expression in a Mouse Model of Alzheimer's Disease: Relevance for the Behavioral and Synaptic Deficits Induced by Amyloid- β Protein. *J Neurosci.,* 27:5394–5404.

Mena MA, Garcia de Yebenes J. (2008). Glial cells as players in parkinsonism: the "good," the "bad," and the "mysterious" glia. *The Neuroscientist*, 14(6):544-560.

Meyer-Luehmann M, Spires-Jones TL, Prada C, Garcia-Alloza M, de Calignon A, Rozkalne A, Koenigsknecht-Talboo J, Holtzman DM, Bacskai BJ, Hyman BT. (2008). Rapid appearance and local toxicity of amyloid-β plaques in a mouse model of Alzheimer's disease. *Nature*, 451(7179):720-724.

Miners JS, Palmer JC, Tayler H, Palmer LE, Ashby E, Kehoe PG, Love S. (2014). Aβ degradation or cerebral perfusion? Divergent effects of multifunctional enzymes. *Front Aging Neurosci.,* 6:238

Mittelbronn M, Dietz K, Schluesener HJ, Meyermann R. (2001). Local distribution of microglia in the normal adult human central nervous system differs by up to one order of magnitude. *Acta Neuropathol*., 101(3):249-55.

Mizushima N, Komatsu M. (2011). Autophagy: renovation of cells and tissues. *Cell,* 147(4):728-741.

Moore S, Evans LD, Andersson T, Portelius E, Smith J, Dias TB, Saurat N, McGlade A, Kirwan P, Blennow K, Hardy J, Zetterberg H, Livesey FJ. (2015). APP Metabolism Regulates Tau Proteostasis in Human Cerebral Cortex Neurons. *Cell Rep*., 11(5):689-696.

Morales I, Guzmán-Martínez L, Cerda-Troncoso C, Farías GA, Maccioni RB. (2014). Neuroinflammation in the pathogenesis of Alzheimer's disease. A rational framework for the search of novel therapeutic approaches. *Front Cell Neurosci.,* 8:112.

.**Moreno-Gonzalez I, Baglietto-Vargas D, Sanchez-Varo R, Jimenez S, Trujillo-Estrada L, Sanchez-Mejias E, del Rio JC, Torres M, Romero-Acebal M, Ruano D, Vizuete M, Vitorica J, Gutiérrez A.** (2009). Extracellular Amyloid-β and cytotoxic glial activation induce significant entorhinal neuron loss in Young PS1M146L/APP751SL mice. *J Alzheimers Dis.*, 18:755-776.

Morishima-Kawashima M, Ihara Y. (2002). Alzheimer's disease: β-Amyloid protein and tau. *J Neurosci Res.,* 70(3):392-401.

Morley JE, Farr SA, Banks WA, Johnson SN, Yamada KA, Xu LA. (2010). Physiological role for amyloid-β protein: enhancement of learning and memory. *J Alzheimers Dis.*, 19(2):441-449.

Morris M, Maeda S, Vossel K and Mucke L. (2011). The many faces of tau. Neuron. 70:410–426.

Mosser DM, Edwards JP. (2008). Exploring the full spectrum of macrophage activation. *Nat Rev Immunol.* 8:958–969.

Mosher KI, Wyss-Coray T. (2014). Microglial dysfunction in brain aging and Alzheimer's disease. *Biochem Pharmacol*., 88:594-604.

Mrak RE, Griffin ST. (2005). Glia and their cytokines in progression of neurodegeneration. *Neurobiol Aging*, 26(3):349-354.

Mucke L, Masliah M, Yu GQ, Mallory M, Rockenstein EM, Tatsuno G, Hu K, Kholodenko D, Johnson-Wood K, McConlogue L. (2000). High-level neuronal expression of Aβ1-42 in wild-type human amyloid protein precursor transgenic mice: synaptotoxicity without plaque formation. *J Neurosci*., 20(11):4050-4058.

Mueller-Steiner S, Zhou Y, Arai H, Roberson ED, Sun B, Chen J, Wang X, Yu G, Esposito L, Mucke L, Gan L. (2006). Anti amyloidogenic and neuroprotective functions of cathepsin B: implications for Alzheimer's disease. *Neuron,* 51(6):703-714.

Musiek ES, Holtzman DM. (2015). Three dimensions of the amyloid hypothesis: time, space and wingmen'. *Nat Neurosci*., 18(6):800- 806.

Nagele RG, D'Andrea MR, Lee H, Venkataraman V, Wang HY. (2003). Astrocytes accumulate Aβ 42 and give rise to astrocytic amyloid plaques in Alzheimer disease brains. *Brain Res.*, 971(2):197-209.

Nedergaard M. (2013). Garbage truck of the brain. *Science*, 340(6140):1529-1530.

Neha, Sodhi RK, Jaggi AS, Singh N. (2014). Animal models of dementia and cognitive dysfunction. *Life Sci.,* 109(2):73-86.

Neve RL, Harris P, Kosik KS, Kurnit DM, Donlon TA. (1986). Identification of Cdna clones for the human microtubule-associated protein tau and chromosomal localization of the genes for tau and microtubule-associated protein 2. *Brain Res.,* 387(3):271-280.

Newman M, Ebrahimie E, Lardelli M. (2014). Using the zebrafish model for Alzheimer's disease research. *Front Genet*., 5:189.

Nixon RA. (2007). Autophagy, amyloidogenesis and Alzheimer disease. *J Cell Sci.,* 120:4081-4091.

Nixon RA, Yang DS. (2011). Autophagy failure in Alzheimer's disease-locating the primary defect. *Neurobiol Dis*., 43(1):38-45.

Noble W, Planel E, Zehr C, Olm V, Meyerson J, Suleman F, Gaynor K, Wang L, LaFrancois J, Feinstein B, Burns M, Krishnamurthy P, Wen Y, Bhat R, Lewis J, Dickson D, Duff K. (2005). Inhibition of glycogen synthase kinase-3 by lithium correlates with reduced tauopathy and degeneration in vivo. *Proc Natl Acad Sci U S A*., 10;102(19):6990-5.

Noguchi A, Matsumura S, Dezawa M, Tada M, Yanazawa M, Ito A, Akioka M, Kikuchi S, Sato M, Ideno S, Noda M, Fukunari A, MUramatsu SI, Itokazu Y, Sato K, Takahashi H, Teplow DB, Nabeshima YI, Kakita A, Imahori K, Hoshi M. (2009). Isolation and characterization of patient-derived, toxic, high mass amyloid-β protein assembly from Alzheimer disease brains. *J Biol Chem.,* 284:32895-32905.

Nunes PV, Forlenza OV, Gattaz WF. (2007).Lithium and risk for Alzheimer's disease in elderly patients with bipolar disorder. B J Psychiatry, 190:359–360.

Nuzzo D, Picone P, Caruana L, Vasto S, Barera A, Caruso C, Di Carlo M. (2014). Inflammatory mediators as biomarkers in brain disorders*. Inflammation*, 37:639-48.

Oakley H, Cole SL, Logan S, Maus E, Shao P, Craft J, Guillozet-Bongaarts A, Ohno M, Disterhoft J, Van Eldik L, Berry R, Vassar R. (2006). Intraneuronal β-amyloid aggregates, neurodegeneration, and neuron loss in transgenic mice with five familial Alzheimer's disease mutations: potential factors in amyloid plaque formation. *J Neurosci*., 26(40):10129-10140.

O'Brien RJ, Wong PC. (2011). Amyloid precursor protein processing and Alzheimer's disease. *Annu Rev Neurosci*., 34:185-204.

Oberheim NA, Goldman SA, Nedergaard M. (2012). Heterogeneity of astrocytic form and function. *Methods Mol Biol.,* 814:23-45. Review.

Oddo S, Caccamo A, Shepherd JD, Murphy MP, Golde TE, Kayed R, Metherate R, Mattson MP, Akbari Y, LaFerla FM. (2003). Tripletransgenic model of Alzheimer's disease with synaptic dysfunction. *Neuron,* 39(3):409-421.

Oddo S, Caccamo A, Cheng D, Jouleh B, Torp R, LaFerla FM. (2007). Genetically augmenting tau levels does not modulate the onset or progression of Abeta pathology in transgenic mice. *J Neurochem*., 102(4):1053-1063.

Ohno M, Chang L, Tseng W, Oakley H, Citron M, Klein WL, Vassar R, Disterhoft JF. (2006). Temporal memory deficits in Alzheimer's mouse models: rescue by genetic deletion of BACE1. *Eur J Neurosci*., 23(1):251-260.

Ojha J, Masilamoni G, Dunlap D, Udoff RA, Cashikar AG. (2011). Sequestration of Toxic Oligomers by HspB1 as a Cytoprotective Mechanism. Mol Cell Biol., 31:3146–3157.

O'Neil JN, Mouton PR, Tizabi Y, Ottinger MA, Lei DL, Ingram DK, Manaye KF. (2007). Catecholaminergic neuronal loss in locus coeruleus of aged female dtg APP/PS1 mice. *J Chem Neuroanat.,* 34(3-4):102-107.

Ota Y, Zanetti AT, Hallock RM. (2013). The role of astrocytes in the regulation of synaptic plasticity and memory formation. Neural Plast., 185463.

Overk CR, Masliah E. (2014). Pathogenesis of synaptic degeneration in Alzheimer's disease and Lewy body disease. *Biochem Pharmacol*., 88(4):508-516.

Padurariu M, Ciobica A, Lefter R, Serban IL, Stefanescu C, Chirita R. (2013). The oxidative stress hypothesis in Alzheimer's disease. *Psychiatr Danub*., 25(4):401-409.

Palop JJ, Mucke L. (2010). Amyloid-β-induced neuronal dysfunction in Alzheimer's disease: from synapses toward neuronal networks. *Nat Neurosci.*, 13(7):812-818.

Parent AT, Thinakaran G. (2010). Modeling presenilin-dependent familial Alzheimer's disease: emphasis on presenilin substrate-mediated signaling and synaptic function. *Int J Alzheimers Dis*., 825918.

Park KW, Yoon HJ, Kang DY, Kim BC, Kim S, Kim JW. (2011) Regional cere-bral blood flow differences in patients with mild cognitive impairment between those who did and did not develop Alzheimer's disease. *Psychiatry Res*., 203:201–206.

Parkhurst CN, Yang G, Ninan I, Savas JN, Yates JR 3rd, Lafaille JJ, Hempstead BL, Littman DR, Gan WB. (2013). Microglia promote learning-dependent synapse formation through brain-derived neurotrophic factor. *Cell,* 155(7):1596-1609.

Parr C, Carzaniga R, Gentleman SM, Van Leuven F, Walter J, Sastre M. (2012). Glycogen Synthase Kinase 3 inhibition promotes lysosomal biogénesis and autophagic degradation of the amyloid-β Precursor Protein. Mol Cell Biol., 32:4410–4418.

Perez-Nievas BG, Stein TD, Tai HC, Dols-Icardo O, Scotton TC, Barroeta-Espar I, Fernandez- Carballo L, de Munain EL, Perez J, Marquie M, Serrano-Pozo A, Frosch MP, Lowe V, Parisi JE, Petersen RC, Ikonomovic MD, López OL, Klunk W, Hyman BT, Gómez-Isla T. (2013). Dissecting phenotypic traits linked to human resilience to Alzheimer's pathology. *Brain,* 136(Pt 8):2510-2526.

Perl DP. (2010). Neuropathology of Alzheimer's disease. *Mt Sinai J Med.*, 77:32-42.

Perry VH, Nicoll JAR, Holmes C. (2010). Microglia in neurodegenerative disease. *Nat RevNeurol.*, 6:193-201.

Pertusa M, Garcia-Matas S, Rodriguez-Farre E, Sanfeliu C, Cristofol R. (2007). Astrocytes aged in vitro show a decreased neuroprotective capacity. *J Neurochem.*, 101(3):794-805.

Ponomarev ED, Maresz K, Tan Y, Dittel BN. (2007). CNS-derived interleukin 4 is essential for the regulation of autoinmune inflammation and induces a state of alternative activation in microglial cells.JNeurosci., 27:10714–10721.

Popović M, Caballero-Bleda M, Kadish I, Van Groen T. (2008). Subfield and layer-specific depletion in calbindin-D28K, calretinin and parvalbumin immunoreactivity in the dentate gyrus of amyloid precursor protein/presenilin 1 transgenic mice. *Neuroscience, 155(1):182-191*.

Priller C, Dewachter I, Vassallo N, Paluch S, Pace C, Kretzschmar HA, Van Leuven F, Herms J. (2007). Mutant presenilin 1 alters synaptic transmission in cultured hippocampal neurons. *J Biol Chem*., 282(2):1119-1127.

Prut L, Abramowski D, Krucker T, Levy CL, Roberts AJ, Staufenbiel M; Wiessner C. (2007). Aged APP23 mice show a delay in switching to the use of a strategy in the Barnes maze. *Behav Brain Res*., 179(1):107-110.

Puzzo D, Privitera L, Leznik E, Fà M, Staniszewski A, Palmeri A, Arancio O. (2008). Picomolar amyloid-beta positively modulates synaptic plasticity and memory in hippocampus. *J Neurosci*., 28(53):14537-14545.

Querfurth HW, LaFerla FM. (2010). Alzheimer's disease. *N Engl J Med*., 362(4):329-344.

Rajendran L, Annaert W. (2012). Membrane trafficking pathways in Alzheimer's Disease. *Traffic*, 13(6):759-770.

Ramos B, Baglietto-Vargas D, del Río JC, Moreno-González I, Santa-María C, Jiménez S, Caballero C, Lopez-Tellez JF, Khan ZU, Ruano D, Gutierrez A, Vitorica J. (2006). Early neuripathology of somatostatin/NPY GABAergic cells in the hippocampus of a PS1xAPP transgenic model of Alzheimer's disease. *Neurobiol Aging,* 27(11):1658-1672.

Renkawek K, Bosman G, de Jong W. (1994). Expression of small heat-shock protein hsp 27 in reactive gliosis in Alzheimer disease and other types of dementia. Acta Neuropathol., 87:511–519

Richard KL, Filali M, Pre´fontaine P, Rivest S. (2008). Toll-like receptor 2 acts as a natural innate immune receptor to clear amyloid beta 1–42 and delay the cognitive decline in a mouse model of Alzheimer's disease. *JNeurosc*i., 28:5784–5793.

Rijal Upadhaya A, Capetillo-Zarate E, Kosterin I, Abramowski D, Kumar S, et al. (2012) Dispersible amyloid β-protein oligomers, protofibrils, and fibrils represent diffusible but not soluble aggregates: their role in neurodegeneration in amyloid precursor protein (APP) transgenic mice. *Neurobiol Aging*, 33: 2641–2660.

Rijal Upadhaya A, Kosterin I, Kumar S, von Arnim CAF, Yamaguchi H, et al. (2014). Biochemical stages of amyloid-beta peptide aggregation and accumulation in the human brain and their association with symptomatic and pathologically preclinical Alzheimer's disease. *Brain,* 137: 887–903

Roberson ED, Halabisky B, Yoo JW, Yao J, Chin J, Yan F, Wu T, Hamto P, Devidze N, Yu GQ, Palop JJ, Noebels JL, Mucke L. (2011). Amyloid-β/Fyn-induced synaptic, network, and cognitive impairments depend on tau levels in multiple mouse models of Alzheimer's disease. *J Neurosci*., 31:700–711.

.

Rockenstein E, Torrance M, Adame A, Mante M, Baron P, Rose JB, Crews L, Masliah. (2007). Neuroprotective effects of regulators of the glycogen synthase kinase-3beta signalling pathway in a transgenic model of Alzheimer's disease are associated with reduced amyloid precursor protein phosphorylation. *J Neurosci*., 27:1981-1991.

Rogers J, Mastroeni D, Leonard B, Joyce J, Grover A. (2007). Neuroinflammation in Alzheimer's disease and Parkinson's disease: are microglia pathogenic in either disorder? Int Rev Neurobiol., 82:235-46. Review.

Rothwell NJ, Luheshi GN. (2000). Interleukin 1 in the brain: biology, pathology and therapeutic target. *Trends Neurosci*., 23(12):618-25. Review.

Rovelet-Lecrux A, Hanneguin D, Raux G, Le Meur N, Laquerrière A, Vital A, Dumanchin C, Feuillete S, Brice A, Vercelletto M, Dubas F, Frebourg T, Campion D. (2006). APP locus duplication causes autosomal dominant early onset Alzheimer disease with cerebral amyloid angiopathy. *Nat Genet.*, 38(1):24-26.

Ruan L, Kang Z, Pei G, Le Y. (2009). Amyloid deposition and inflammation in APPswe/PS1dE9 mouse model of Alzheimer's disease. *Curr Alzheimer Res.,* 6:531-540.

Rutten BP, Van der Kolk NM, Schafer S, van Zandvoort MA, Bayer TA, Steinbusch HW, Schmitz C. (2005). Age-related loss of synaptophysin immunoreactive presynaptic boutons within the hippocampus of APP751SL, PS1M146L, and APP751SL/PS1M146L transgenic mice. *Am J Pathol.,* 167(1):161-173.

Sakono M, Zako T. (2010). Amyloid oligomers: formation and toxicity of Aβ oligomers. *FEBS Journal,* 277:1348-1358.

Sanchez-Varo R, Trujillo-Estrada L, Sanchez-Mejias E, Torres M, Baglietto-Vargas D, Moreno-Gonzalez I,et al. (2012). Abnormal accumulation of autophagic vesicles correlates with axonal andsynaptic pathology in young Alzheimer's mice hippocampus.Acta Neuropathol., 123:53–70

Sarkar S, Floto RA, Berger Z, Imarisio S, Cordenier A, Pasco M,et al. (2005). Lithium induces autophagy by inhibiting inositol monophosphatase. J Cell Biol., 170:1101–1111.

Sastre M, Klockgether T, Heneka MT. (2006). Contribution of inflammatory processes to Alzheimer's disease: molecular mechanisms. *Int J Dev Neurosci*., 24(2-3):167-76. Review.

Saunders AM, Strittmatter WJ, Schmechel D, George-Hyslop PH, Pericak-Vance MA, Joo SH, Rosi BL, Gusella JF, Crapper-MacLachlan DR, Alberts MJ, et al. (1993). Association of apolipoprotein E allele epsilon 4 with late-onset familial and sporadic Alzheimer's disease. *Neurol*., 43:1467-72.

Schmitz C, Rutten BP, Pielen A, Schafer S, Wirths O, Tremp G, Czech C, Blanchard V, Multhaup G, Rezaie P, Korr H, Steinbusch HW, Pradier L, Bayer TA. (2004). Hippocampal neuron loss exceeds amyloid plaque load in a transgenic mouse model of Alzheimer's disease. *Am J Pathol.*, 164(4):1143- 1146.

Scholz T, Mandelkow E. (2014). Transport and diffusion of Tau protein in neurons. *Cell Mol Life Sci.*, 71:3139-3150.

Scuderi C, Esposito G, Blasio A, Valenza M, Arietti P, Steardo L Jr, Carnuccio R, De Filippis D, Petrosino S, Iuvone T, Di Marzo V, Steardo L. (2011) Palmitoyl ethanolamide counter acts reactive astrogliosis induced by β-amyloid peptide. J Cell Mol Med., 15: 2664–2674.

Selkoe DJ. (2001). Alzheimer's disease: genes, proteins, and therapy. *Physiol Rev.*, 81(2):741-766.

Selkoe DJ. (2004). Cell biology of protein misfolding: The examples of Alzheimer's and Parkinson's diseases. *Nat Cell Biol*., 6(11):1054-1061.

Selkoe DJ. (2008). Biochemistry and molecular biology of amyloid β-protein and the mechanism of Alzheimer's Disease. *Handb Clin Neurol*., 89:245-260.

Shankar GM, Li S, Mehta TH, Garcia-Munoz A, Shepardson NE, Smith I, Brett FM, Farrell MA, Rowan MJ,Lemere CA, Regan CM, Walsh DM, Sabatini BL, Selkoe DJ. (2008). Amyloid-β protein dimers isolated directly from Alzheimer's brains impair synaptic plasticity and memory. *Nat Med.,* 14(8):837-842.

Shie FS, Woltjer RL. (2007) Manipulation of microglial activation as a therapeutic strategy in Alzheimer's disease. Curr Med Chem., 14(27):2865-71. Review.

Simard AR, Soulet D, Gowing G, Julien JP, Rivest S. (2006). Bone marrow-derived microglia play a critical role in restricting senile plaque formation in Alzheimer's disease. *Neuron*, 49(4):489-502.

Simic G, Lucassen PJ, Krsnik Z, Kostovic I, Windblad B, Bogdanovic N. (2000). nNOS expression in reactive astrocytes correlates with increased cell death related DNA damage in the hippocampus and entorhinal cortex in Alzheimer's disease. *Exp Neurol.*, 165(1):12-26.

Small DH. (2008). Network dysfunction in Alzheimer's disease: does synaptic scaling drive disease progression? *Trends in Molecular Medicine*, 14(3):103-108.

Small DH. (2009). Dysregulation of calcium homeostasis in Alzheimer's disease. *Neurochem Res*., 34:1824-1829.

Sofroniew MV and Vinters HV. (2010) Astrocytes: biology and pathology. *Acta Neuropathol*., 119: 7–35.

Sokolowski JD, Mandell JW. (2011). Phagocytic clearance in neurodegeneration. *Am J Pathol.,* 178(4):1416-1428.

Sotthibundhu A, Sykes AM, Fox B, Underwood CK, Thangnipon W, Coulson EJ. (2008). β-Amyloid 1-42 induces neuronal death through the p75 neurotrophin receptor. *Journal of Neuroscience,* 28: 3941-3946.

Spillantini MG, Goedert M. (2013). Tau pathology and neurodegeneration. *Lancet Neurol*., 12(6):609-22. Review

Spires-Jones TL, Hyman BT. (2014). The intersection of amyloid-β and tau at synapses in Alzheimer's disease. *Neuron*, 82(4):756-771.

Spires-Jones TL, Stoothoff WH, de Calignon A, Jones PB, Hyman BT. (2009). Tau pathophysiology in neurodegeneration: a tangled issue. Trends in Neurosciences, 32:150-159.

StalderAK, Ermin iF, Bondolfi L, Krenger W, Burbach GJ, Deller T, Coomaraswamy J, Staufenbiel M, Landmann R, Jucker M. (2005). Invasion of hematopoietic cells into the brain of amyloid precursor protein transgenic mice. *J Neurosci*., 25:11125–11132.

Streit WJ. (2005). Microglia and neuroprotection: implications for Alzheimer's disease. *Brain Res Rev.*, 48(2):234-239.

Streit WJ, Xue QS, Tischer J, Bechmann I. (2014). Microglial pathology. *Acta Neuropathol Commun*., 2(1):142.

Sturchler-Pierrat C, Abramowski D, Duke M, Wiederhold KH, Mistl C, Rothacher S, Ledermann B, Bürki K, Frey P, Paganetti PA, Waridel C, Calhoun ME, Jucker M, Probst A,

Staufenbiel M, Sommer B. (1997). Two amyloid precursor protein transgenic mouse models with Alzheimer disease-like pathology. *Proc Nat Acad Sci USA.,* 94(24):13287-13292.

Sturchler-Pierrat C, Staufenbiel M. (2000). Pathogenic mechanisms of Alzheimer's disease analyzed in the APP23 transgenic mouse model. *Ann N Y Acad Sci*., 920:134–139.

Su Y, Ryder J, Li B, Wu X, Fox N, Solenberg P, Brune K, Paul S, Zhou Y, Liu F, Ni B. (2004). Lithium, a common drug for bipolar disorder treatment, regulates amyloid-β precursor protein processing. Biochemistry, 8; 43(22):6899-908.

Takahashi RH, Milner TA, Li F, Nam EE, Edgar MA, Yamaguchi H, Beal MF, Xu H, Greengard P, Gouras GK. (2002). Intraneuronal Alzheimer Aβ42 accumulates in multivesicular bodies and is associated with synaptic pathology. *Am J Pathol*., 161:869-1879.

Takasugi N, Tomita T, Hayashi I, Tsuruoka M, Niimura M, Takahashi Y, Thinakaran G, Iwatsubo T. (2003). The role of presenilin cofactors in the gamma-secretase complex. Nature. 422: 438-441.

Takeda S, Hashimoto T, Roe AD, Hori Y, Spires-Jones TL, et al. (2013). Brain interstitial oligomeric amyloid-β increases with age and is resistant to clearance from brain in a mouse model of Alzheimer's disease. *FASEB J.,* 27: 3239–3248

Tampellini D, Gouras GK. (2010). Synapses, synaptic activity and intraneuronal Aβ in Alzheimer's disease. *Front Aging Neurosci.,* 21;2. pii: 13.

Tanemura K, Chui DH, Fukuda T, Murayama M, Park JM, Akagi T, Tatebayashi Y, Miayaska T, Kimura T, Hashikawa T, Nakano Y, Kudo T, Takeda M, Takashima A. (2006). Formation of tau inclusions in knock-in mice with familial Alzheimer disease (FAD) mutation of presenilin 1 (PS1). *J Biol Chem.,* 281(8):5037-5041.

Tang Z, Pi X, Chen F, Shi L, Gong H, Fu H, Qu Z. (2012). Fifty percent reduced-dose cerebral CT perfusion imaging of Alzheimer's disease: regional blood flow abnormalities. *Am J Alzheimers Dis Other Demen.,* 27:267–274.

Takami M, Nagashima Y, Sano Y, Ishihara S, Morishima-Kawashima M, Funamoto S, Ihara Y. (2009) γ-Secretase: successive tripeptide and tetrapeptide release from the Transmembrane Domain of β-Carboxyl Terminal Fragment. *Journal of Neuroscience.,* 29: 13042-13052.

Tanzi RE, McClatchey AI, Lamperti ED, VillaKomaroff L, Gusella JF, Neve RL. (1988). Protease inhibitor domain encoded by an amyloid protein precurosr mRNA associated with Alzheimer's disease. *Nature*, 331(6156):528-530.

Taylor AR, Robinson MB, Gifondorwa DJ, Tytell M, Milligan CE. (2007). Regulation of heat shock protein 70 release in astrocytes: Role of signaling kinases. Devel Neurobiol., 67:1815–1829

Terry RD, Masliah E, Salmon DP, Butters N, DeTeresa R, Hill R, Hansen LA and Katzman R. (1991). Physical basis of cognitive alterations in Alzheimer's disease: synapse loss is the major correlate of cognitive impairment. *Ann Neurol.,* 30(4):572–580.

Terwel D, Muyllaert D, Dewachter I, Borghgraef P, Croes S, Devijver H, Van Leuven F. (2008). Amyloid activates GSK-3β to aggravate neuronal tauopathy in bigenic mice. Am J Pathol., 172(3):786-98.

Thal DR, Capetillo-Zarate E, Del Tredici K, Braak H. (2006). The development of amyloid-β protein deposits in the aged brain. *Sci Aging Knowledge Environ*., 6:re1.

Thinakaran G, Koo EH. (2008). Amyloid precursor protein trafficking, processing, and function. *J Biol Chem.*, 283(44):29615-29619.

Thompson PM, Hayashi KM, de Zubicaray G, Janke AL, Rose SE, Semple J, Herman D, Hong MS, Dittmer SS, Doddrell DM, Toga AW. (2003). Dynamics of Gray Matter Loss in Alzheimer's Disease. *The Journal of Neuroscience*, 23: 994-1005

Togo T, Akiyama H, Iseki E, Kondo H, Ikeda K, Kato M, Oda T, Tsuchiya K, Kosaka K. (2002). Occurrence of T cells in the brain of Alzheimer's disease and other neurological diseases. *J Neuroimmunol.*, 124:83–92.

Toledo EM, Inestrosa NC. (2009). Activation of Wnt signaling by lithium and rosiglitazone reduced spatial memory impairment and neurodegeneration in brains of an APPswe/PSEN1DeltaE9 mouse model of Alzheimer's disease. Mol Psychiatry, 15:272–285.

Tomic JL, Pensalfini A, Head E, Glabe CG. (2009). Soluble fibrillar oligomer levels are elevated in Alzheimer's disease brain and correlate with cognitive dysfunction. Neurobiol Disease, 35:352–358.

Torres M, Jimenez S, Sanchez-Varo R, Navarro V, Trujillo-Estrada L, Sanchez-Mejias E,et al. (2012). Defective lysosomal proteolysis and axonal transport are early pathogenic events that worsen with age leading to increased APP metabolism and synaptic Abeta in transgenic APP/PS1 hippocampus.*Mol Neurodegener*., 7:59

Townsend M, Mehta T, Selkoe DJ. (2007). Soluble Aβ inhibits specific signal transduction cascades common to the insulin receptor pathway. Journal of Biological Chemistry 282: 33305-33312.

Tuppo EE, Arias HG. (2005). The role of the inflammation in Alzheimer's disease. *Int J Biochem Cell Biol.*, 37(2):289-305.

Uberti D, Ferrari-Toninelli G, Bonini SA, Sarnico I, Benarese M, Pizzi M, Benussi L, Ghidoni R, Binetti G, Spano P, Facchetti F, Memo M. (2007). Blockade of the tumor necrosis factor-related apoptosis inducing ligand death receptor DR5 prevents β-amyloid neurotoxicity. *Neuro psycho ph*armacology 32:872–880.

Van Gassen G, Annaert W. (2003). Amyloid, presenilins, and Alzheimer's disease. Neuroscientist., 9(2):117-26. Review.

Varnum MM, Ikezu T. (2012). The classification of microglial activation phenotypes on neurodegeneration and regeneration in Alzheimer's disease brain. *Arch Immunol Ther Exp*., 60:251–266.

Vassar R, Kovacs DM, Yan R, Wong PC. (2009). The β-secretase enzyme BACE in health and Alzheimer's disease: regulation, cell biology, function, and therapeutic potential. *J Neurosci*., 29(41):12787-12794.

Verkhratsky A, Olabarria M, Noristani HN, Yeh CY, Rodriguez JJ. (2010). Astrocytes in Alzheimer's disease. *Neurotherapeutics,* 7(4):399-412.

Vermeer SE, Prins ND, den Heijer T, Hofman A, Koudstaal PJ, Breteler MM. (2003). Silent brain infarcts and the risk of dementia and cognitive decline. *N Engl J Med*., 348:1215–1222

Viola KL, Klein WL. (2015). Amyloid β oligomers in Alzheimer's disease pathogenesis, treatment, and diagnosis. *Acta Neuropathol.,* 129:183-206.

Von Gunten A, Kövari E, Bussière T, Rivara CB, Gold G, Bouras C, Hof PR, Giannakopoulos P. (2006) Cognitive impact of neuronal pathology in the entorhinal cortex and CA1 field in Alzheimer's disease. *Neurobiology of Aging*, 27:270–277.

Voytko ML, Tinkler GP. (2004). Cognitive function and its neural mechanisms in nonhuman primate models of aging, Alzheimer disease, and menopause. *Front Biosci*., 9:1899–1914.

Wakabayashi T, De Strooper B. (2008) Presenilins: members of the gamma-secretase quartets, but part-time soloists too. *Physiology (Bethesda).* 23:194-204.

Walsh DM, Lomakin A, Benedek GB, Maggio JE, Condron MM, Teplow DB. (1997). Amyloid β- protein fibrillogenesis: Detection of a protofibrillar intermediate. *J Biol Chem.*, 272(35):22364-22374.

Walsh DM, Selkoe DJ. (2007). Aβ oligomers – a decade of discovery.*JNeurochem.,*101(5):1172-84.

Walter J, Grunberg J, Capell A, Pesold B, Schindzielorz A, Citron M, Mendla K, George Hyslop PS, Multhaup G, Selkoe DJ, Haass C. (1997). Proteolytic processing of the Alzheimer disease-associated presenilin-1 generates an in vivo substrate for protein kinase C. *PNAS*. 94: 5349-5354.

Wang HY, Lee DH, D'Andrea MR, Peterson PA, Shank RP, Reitz AB. (2000). B-amyloid (1-42) bind to alpha7nicotinic acetylcholine receptor with high affinity.Implications for Alzheimer's disease pathology. *J Biol Chem.*, 275(8):5626-5632.

Wang JZ, Xia YY, Grundke-Iqbal I, Iqbal K. (2013). Abnormal hyperphosphorylation of Tau: sites, regulation, and molecular mechanism of neurofibrillary degeneration. *J Alzheimers Dis*., 33:S123-S139.

Watt A, Perez K, Rembach A, Sherrat N, Hung L, et al. (2013). Oligomers, fact or artefact? SDS-PAGE induces dimerization of beta-amyloid in human brain samples. *Acta Neuropathol*., 125: 549–564.

Webster SJ, Bachstetter AD, Nelson PT, Schmitt FA, Van Eldik LJ. (2014). Using mice to model Alzheimer's dementia: an overview of the clinical disease and the preclinical behavioral changes in 10 mouse models. *Front Genet*., 5(88):1-23.

Weekman EM, Sudduth TL, Abner EL, Popa GJ, Mendenhall MD, Brothers HM,BraunK, Greenstein A, Wilcock DM. (2014). Transition from an M1 to a mixed neuroinflammatory phenotype increases amyloid deposition in APP/PS1 transgenic mice. J Neuroinflammation, 11:127.

West MJ, Coleman PD, Flood DG, Troncoso JC. (1994). Differences in the pattern of hippocampal neuronal loss in normal ageing and Alzheimer's disease. *Lancet*, 344(8925):769-772.

Whitehouse PJ, Price DL, Clark AW, Coyle JT, DeLong MR. (1981). Alzheimer disease: evidence for selective loss of cholinergic neurons in the nucleus basalis. *Ann Neurol.,* 10(2):122-126.

Whitehouse PJ, Price DL, Struble RG, Clark AW, Coyle JT, Delon MR. (1982). Alzheimer's disease and senile dementia: loss of neurons in the basal forebrain. *Science,* 215(4537):1237-39.

Wolfe MS. (2007). When loss is gain: reduced presenilin proteolytic function leads to increased Aβ42/Aβ40. Talking Point on the role of presenilin mutations in Alzheimer disease. *EMBO Rep.* 8(2):136-40. Review

Wolfe MS, Kopan R. (2004). Intramembrane proteolysis: theme and variations. *Science*, 305(5687):1119-1123.

Wyss-Coray T, Loike JD, Brionne TC, Lu E, Anankov R, Yan F, Silverstein SC, Husemann J. (2003). Adult mouse astrocytes degrade amyloid-beta in vitro and in situ. *Nat Med.*, 9(4):453-457.

Wyss-Coray T. (2006). Inlfammation in Alzheimer disease: driving force, bystander o beneficial response? *Nat Med.*, 12(9):1005-1015.

Xie H, Hou S, Jiang J, Sekutowicz M, Kelly J, Bacskai BJ. (2013). Rapid cell death is preceded by amyloid plaque-mediated oxidative stress. *Proc Natl Acad Sci USA*., 110:7904–7909

Xie L, Helmerhorst E, Taddei K, Plewright B, van Bronswijk W, Martins R. (2002). Alzheimer's β-Amyloid Peptides Compete for Insulin Binding to the Insulin Receptor. *The Journal of Neuroscience* 22: RC221.

Yamada K, Nabeshima T. (2000). Animal models of Alzheimer's disease and evaluation of antidementia drugs. *Pharmacol Ther*., 88:93-113.

Yamashima T. (2013). Reconsider Alzheimer's disease by the "calpain-cathepsin hypothesis" A perspective review. *Prog Neurobiol*., 105:1-23.

Yang CN, Shiao YJ, Shie FS, Guo BS, Chen PH, Cho CY, Chen YJ, Huang FL, Tsay HJ. (2011). Mechanism mediating oligomeric Aβ clearance by naïve primary microglia. *Neurobiol Dis.*, 42(3):221-230.

Yang DS, Stavrides P, Mohan PS, Kaushik S, Kumar A, Ohno M., et al. (2011). Reversal of autophagy dysfunction in the TgCRND8 mouse model of Alzheimer's disease ameliorates amyloid pathologies and memory deficits.Brain, 134:258–277.

Yang T, Hong S, O'Malley T, Sperling RA, Walsh DM, et al. (2013). New ELISAs with high specificity for soluble oligomers of amyloid beta-protein detect natural Abeta oligomers in human brain but not CSF. *Alzheimer's & Dementia,* 9: 99–112.

Yokokura M, Mori N, Yagi S, Yoshikawa E, Kikuchi M, Yoshihara M, Wakuda T, Sugihara G, Takebayashi K, Suda Si, Iwata Y, Ueki T, Tsuchiya KJ, Suzuki K, Nakamura K, Ouchi Y. (2011). In vivo changes in microglial activation and amyloid deposits in brain regions with hypometabolism in Alzheimer's disease. *Eur J Nucl Med Mol Imaging,* 38(2):343-351.

Young AH. (2011). More good news about the magic ion: lithium may prevent dementia.B J Psychiatry, 198:336–337

Yu Y, Ye RD. (2015). Microglial Aβ receptors in Alzheimer's disease. *Cell Mol Neurobiol.,* 35(1):71-83.

ZhaoW, Xie W, Xiao Q, Beers DR, Appel SH. (2006). Protective effects of an anti-inflammatory cytokine, interleukin-4, on moto neuron toxicity induced by activated microglia. *J Neurochem.,* 99:1176–1187.

Zerbinatti CV, Wahrle SE, Kim H, Cam JA, Bales K, Paul SM, Holtzman DM, Bu G. (2006). Apolipoprotein E and low density lipoprotein receptor-related protein facilitate intraneuronal Aβ42 accumulation in amyloid model mice. *J Biol Chem*., 281(47):36180-86.

Zhang D, Hu X, Qian L, O'Callaghan JP and Hong JS. (2010) Astrogliosis in CNS pathologies: is there a role for microglia? *Mol. Neurobiol.,* 41: 232–241.

Zhang YW, Thompson R, Zhang H, Xu H. (2011). APP processing in Alzheimer's disease. *Mol Brain*, 4:3.

Zhao WQ, De Felice FG, Fernandez S, Chen H, LambertMP, Quon MJ, Krafft GA, Klein WL. (2008). Amyloid-β oligomers induce impairment of neuronal insulin receptors. *FASEB J.,* 22: 246-260.

Zhao WQ, Lacor PN, Chen H, Lambert MP, Quon MJ, Krafft GA, Klein WL. (2009). Insulin receptor dysfunction impairs cellular clearance of neurotoxic oligomeric Aβ. *Journal of Biological Chemistry,* 284: 18742-18753

Zolezzi JM, Bastías-Candia S, Santos MJ, Inestrosa NC. (2014). Alzheimer's disease: relevant molecular and physiopathological events affecting amyloid-β brain balance and the putative role of PPARs. *Front Aging Neurosci*. 6:176.